ASTR 511: ASTRONOMICAL TECHNIQUES

Fall 2003

Syllabus   **Announcements**   **Schedule**

Lectures

Problem Sets   **Labs**   **Obs. Calendar**

USNO Data   **Weather**   **Web Links**

IDL Resources

ASTR 511 IDL Tutorial

Course Contacts

		Office	E-mail
Instructor	Robert O'Connell	Astronomy 251B	rwo
TA	Peter Frinchaboy	Astronomy 220	pmf8b
40-in Imaging Support	David McDavid	Astronomy 210	dam3ma
40-in Spectroscopy Support	Jeff Crane	Astronomy 222	jdc2k

Department Phone:	924-7494
LMO Phone:	924-7080
Fan 40-in Phone:	979-0685
Fan Computer Phone:	979-0686
121/130 Observing Message:	924-7238

Last modified **August 2003** *by* rwo

Astronomy 511 Lecture Materials

Fall 2003

Web pages, viewgraphs, and supporting material used in the lectures are posted here. Most are in the form of HTML or PDF files. You can download PDF readers from Adobe Systems.

Click here for a consolidated PDF file of all lecture notes (86 MB)
(note: links are inoperative)

- **Introduction: Observing Projects in the Context of ASTR 511** (HTML)

- **1. Observations in Astronomy** (HTML)

  - 1-A. Non-EM Channels

  - 1-B. Tips for Success (HTML)

- **2. The Electromagnetic Spectrum**

  - 2-A. EM Spectrum: Discovery & Diagnostics (HTML)

  - 2-B. Major Facilities (All Bands) (HTML)

- - 16-B. LBT Construction Images (HTML)

- **17. Astronomical Polarimetry (David McDavid, guest lecture)** (HTML)

- **18. Infrared Astronomy (Mike Skrutskie, guest lecture)** (HTML)

- **19. Ultraviolet (& Space) Astronomy** (HTML)

- **20. UIT and the Astro Missions** (HTML)

- **21. Atmospheric Degradation & Compensation** (HTML)

Return to ASTR 511 Home Page

ASTRONOMICAL OBSERVING PROJECTS IN CONTEXT OF ASTR 511

OBSERVING PROJECT	ASTR 511 TOPICS
## 1. THE PROPOSAL[*] **Award of observing time on major astronomical facilities is a competitive process, in which proposals for observing projects are reviewed and ranked by a Time Allocation Committee (TAC).** **For almost all public, national facilities, competition is tough.** **Ratio of requested to available time about 2:1 to >5:1.** **A compelling proposal must be clearly, persuasively, and consisely written and must demonstrate:** • **An important/interesting problem/question** • **Technical feasibility** • **Provides definitive answer to question posed** ## 2. OBSERVING RUN PREPARATION **Instrument documentation**	**EM bands & phenomena** **UVOIR capabilities** **Nature of astrophysical sources** **ROMPS & SWAGS** **Optics**

Exposure estimation

Target selection: coordinates & key properties

Calibration planning, select calibrators

Finding charts

Instrument configuration files

Observing strategy & sequences

3. MAKING OBSERVATIONS

Prime & secondary targets

Calibration

On-line assessment

Assessment of sky & other interfering conditions

Documentation of observations

4. DATA REDUCTION

Removal of instrumental signatures

Correction for Earth's atmosphere, IS dust

Calibration

Conversion to fluxes, colors, positions, spectra, line strengths, etc.

5. DATA ANALYSIS & INTERPRETATION*

Extract scientifically meaningful information from reduced data

Answer the questions you posed

Available telescopes & instruments

Exposure Time Calculators (ETCs)

Sky surveys

Databasing

Detectors

   Emphasis: CCD's

Imaging

Spectroscopy

Flux calibration

Statistics of observations

Interactive computing

Image processing

Effects of IS dust

Effects of Earth's atmosphere

Multicolor analysis

Place in larger context

Be alert: anything new, unexpected?

6. PUBLICATION

7. PUBLIC RELATIONS

---

[*]**Most challenging phases**

⬆ **Lecture Index**　　➡ **Next Lecture**

Last modified August 2003 by *rwo*

1: INTRODUCTION TO UVOIR ASTRONOMY

Southern Milky Way from CTIO

I. WHY UVOIR?

A. Definition

UVOIR = the "UV, Optical, Near-Infrared" region of EM spectrum

- Shortest wavelength: 912 Å (91.2 nm) --- Lyman edge of H I; interstellar medium is
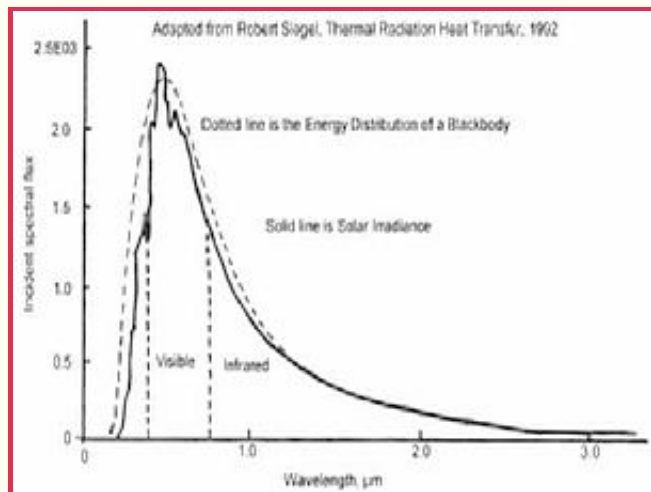
opaque for hundreds of Å below here

  ○ **Longest wavelength: ~3 μ (3000 nm) --- serious H_2O absorption in <u>Earth's atmosphere</u> above here**
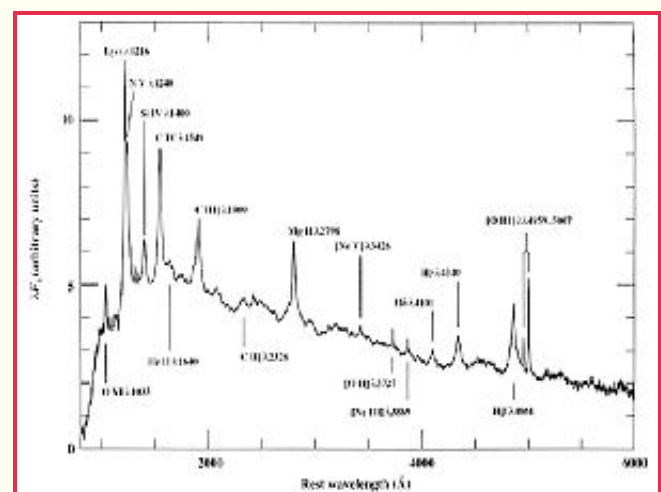
B. Uniqueness

- **Best developed instrumentation; best understood astrophysically**
- **<u>Highest density</u> of astrophysical information**
- **Provides prime diagnostics on the <u>two most important physical tracers</u>:**

<div align="center">
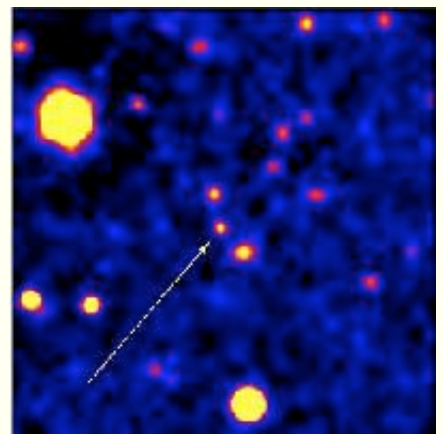
<u>STARS</u>   <u>PLASMAS (to 10^5K)</u>

</div>

<div align="center">

> **===> UVOIR observations/identifications are almost always <u>prerequisites</u> to a thorough understanding of cosmic sources in other EM bands.**

</div>

  ○ **Stars are the basic building blocks of the universe (even if not the most important by mass)**

  ○ **For instance, stars establish fundamental cosmic <u>age</u> and <u>distance</u> scales**

    ▪ **Ages: e.g. star cluster <u>turnoff temperatures/luminosities</u>**

    ▪ **Distances: e.g. Cepheid variations, supernovae**

  ○ **Example: Gamma Ray Burst sources first detected in 1970's, but only physically interpreted after optical ID's in 1997.**

First optical ID of a GRB.
Click for info.

II. KINDS OF UVOIR OBSERVATIONS

- <u>Imaging</u>: distribution of EM energy on celestial sphere
- <u>Astrometry</u> : a sub-class of imaging: precision measures of positions & motions
- <u>Spectral Energy Distributions (SEDs)</u>: distribution of EM energy with frequency
  - Photometry (low resolution)
  - Spectroscopy (higher resolution)
- <u>Variability</u>
- <u>Polarimetry</u>

III. PRIORITY OF OBSERVATIONS IN ASTRONOMY

Astronomy is driven more by <u>new observational discoveries</u> than by fundamental interpretive insights (i.e. theory). Direction of field shaped by observations in about 3/4 of instances.

Few important astronomical discoveries were predicted; many were actually <u>accidental</u>

Examples: (technique/original motivation in *parentheses*)

- **Uranus** (*visual telescopic sky-scan*)
- **Expanding universe** (*faint galaxy spectroscopic survey*)
- **Pulsars** (*radio scintillation observations*)
- **Supermassive black holes/AGN's** (*radio surveys, optical spectroscopic surveys*)
  Although nuclear activity had been recognized since the 1940's (Seyfert), its prevalence and significance was not understood until radio observations in the 1950's-60's, especially of the compact Quasi Stellar Objects.
- **Large scale structure** (*redshift surveys aimed at measuring galaxy luminosity function*)
- **Dark matter in spiral galaxies**: <u>flat rotation curves</u> (*optical/radio spectroscopy*)
- **X-ray emitting gas in clusters of galaxies** (*early X-ray surveys*)
- <u>Gamma ray bursts</u> (*military satellites looking for clandestine nuclear tests*)
- **Extra-solar planets** (*optical spectroscopic monitoring*)
  There was a general expectation that these existed, based on the Copernican Principle, for example. But theoreticians predicted that massive planets could exist only at large distances from parent stars, implying 5-year or longer survey periods.
- <u>High redshift evolution of galaxies</u>: "Butcher-Oemler effect" & <u>"faint blue galaxies"</u> (*deep optical imaging*)
  HST contributions were actually hindered by theoretical prejudice. A deep pencil-beam survey was delayed by 5 years.

Counterexamples: theory-driven discoveries

- **Neptune**
- **General relativistic distortion of space-time near Sun**
- **21 cm line of HI**
- **Helioseismology**

- **Cosmic microwave background**
  - Predicted 1948. Actual discovery 16 years later was accidental, but a second team was preparing a deliberate search and would have been successful.

Priority of observations means that all astronomers, observers or not, must know how to <u>interpret and critically evaluate</u> them and must stay alert for the <u>new opportunities</u> they present.

> **What's meaningful? What's not? What's real vs. what's noise? How big are systematic errors? What's interesting? What's right?**

> > **<u>Example 1</u>: what is this? how was it made? what do the colors mean?**
> > **<u>Example 2</u>: what does this diagram test? what important physical implications?**
> > **<u>Example 3</u>: what causes the scatter in this diagram?**
> > **<u>Example 4</u>: is there a statistically meaningful result here? what is it?**
> > **<u>Example 5</u>: classic example of systematic error**
> > **<u>Example 6</u>: discovery of the year or statistical fluke?**

NB: Champion "discoverer" of 20th century was <u>Fritz Zwicky</u>. Discovered dark matter; inaugurated research on <u>supernovae</u> & clusters of galaxies; predicted neutron stars & gravitational lenses.

IV. HISTORICAL LESSON: TECHNOLOGY DRIVES DISCOVERY

Most groundbreaking discoveries are enabled by <u>NEW observational capabilities</u>.

- **Local example: HEMT detectors from NRAO CDL enabled current generation of CMB experiments**

Key <u>technology development</u> for UVOIR astronomy:

- **17th century: telescopes**

- **19th century: spectroscopy, photography, quality lens making, large structure engineering**

- **20th century: large mirror fabrication, electronic detectors, digital computers, space astronomy**

- **Since 1980: array detectors**

Mt. Wilson 100-in. Discovered external galaxies, expanding universe.
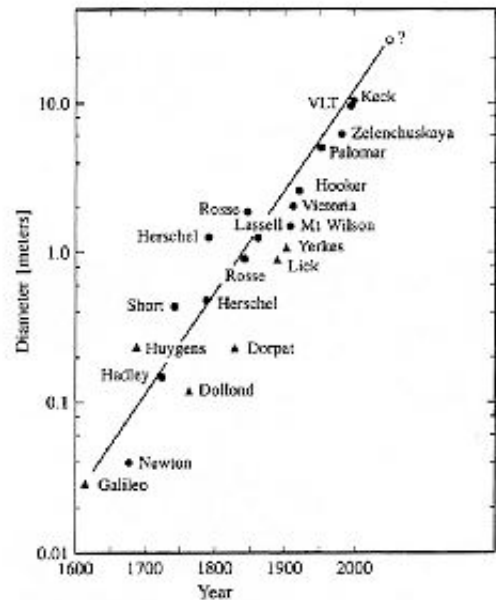
UVOIR <u>telescope size</u>: determines ultimate sensitivity

- **Diameter doubling time ~45 years**

- **Largest scopes now 8-10m diam**

  Collecting area of 10-m is 4×10^{6} that of the dark-adapted eye

- **In planning: 15-m to 40-m**

- **For a given technology, cost $\sim D^{2.6}$**

  Cost is roughly proportional to mass. Even using new technologies, next generation of large ground-based telescopes will cross the $1 billion threshold.

Other key developments:

- <u>**Sky surveys**</u>

  - **First: Hipparchus, 130 BC. Thousands since.**

  - **Two most important in 20th century:**

    - **Henry Draper Catalog [HD] (all-sky, stellar spectra) ===> stellar astrophysics.**

    - **Palomar 48-in Schmidt Sky Survey [POSS] & southern counterparts (all-sky, deep imaging) ===> source for identification of all types of stars, clusters, nebulae, and extragalactic systems. Online version: Digitized Sky Survey.**

  - **Large format, 2-D array detectors are driving current explosion in imaging/spectroscopic sky surveys (e.g. 2dF, SDSS, 2MASS, and many others, often with cutie-pie names)**

- <u>**Classification systems**</u> **(e.g. HD stellar spectral classification, ca. 1890; Hubble galaxy classification, ca. 1920)**

V. FLUX MEASUREMENTS IN ASTRONOMY

A. Signal-to-Noise Ratio

"Sensitivity"---i.e. the faintest source measurable---is not simply a matter of the size of the photon collector.

It is instead a <u>signal-to-noise</u> issue:

- **SNR (or "S/N") = value measured / uncertainty in measure**

- **Depends on structure of source (point vs. extended), nature of luminous background & surroundings, foreground absorption, telescope & instrument throughput, characteristics of detectors (quantum efficiency, noise)**

- **Fundamental limits from <u>photon statistics</u>**

    - $SNR < \sqrt{N}$, **where N is number of detected source photons**

B. Typical SNR's in Astronomy:

- **Some things are known exactly (SNR is infinite)**

    - **Sun is a star**
    - **Only one star interior to Earth's orbit**
    - **No new elements possible lighter than Uranium**

- **High precision measures: e.g. length of AU; period of pulsars. SNR > 10^7.**

- **Measures of astronomical EM fluxes:**

    - **Best precision: SNR ~ 1000 (0.1% error)**

        - <u>**Low**</u> **by lab standards! Problems: difficulty of calibration; faintness of interesting sources.**

    - **Typical "good" measures: SNR ~ 20-30**

    - **Threshold detections: SNR ~ 5-10**

C. The Magnitude System: see <u>Lecture 2.</u>

D. Backgrounds

- **Even when source fluxes are appreciable, detection can be inhibited by luminous backgrounds, which reduce SNR. Become important when:**

    (background flux)$_{resol\text{-}element}$ ~ (source flux)$_{resol\text{-}element}$

- **Diffuse backgrounds, e.g.:**

    <u>**UVOIR**</u>**: artificial light pollution + Earth's atmosphere + ecliptic scattered sunlight + scattered Galactic light**

    Far IR: <u>interstellar "cirrus"</u> = warm dust

    Radio: Cosmic Microwave Background

- **Discrete source backgrounds, e.g.:**

    Exclusion zone around bright stars caused by scattered light within instrument

    Source "confusion" caused by diffractive blending of multiple faint sources

VI. LIMITS OF OBSERVATIONAL CAPABILITY

A. <u>EM Wavelength Coverage</u>

- <u>Rapid expansion since 1950</u>**: click on link for breadth of EM coverage**
- **Most of "feasible" spectrum now accessible**

B. <u>Point Source Sensitivity</u>

Faintest UVOIR point source detected:

- **Naked eye: 5-6 mag**
- **Galileo telescope (1610):   8-9 mag**
- **Palomar 5-m (1948):   21-22 mag (pg),**
                                         25-26 mag (CCD)
- **Keck 10-m (1992):   27-28 mag**
- **HST (2.4-m in space, 1990):   29-30 mag**

NB: current optical detectors have ~ 100% quantum efficiency. Therefore, we can't improve sensitivity via detector development. In UV, IR there is room for detector improvement.

C. <u>Spatial Resolution</u>

- **Fundamental limit governed by <u>diffraction</u> in telescope/instruments: minimum image diameter is given by:**

$$\theta_{min} \sim 2.5\lambda/D \quad \text{radians}$$

    where D is the diameter of the telescope aperture

- **At 5500 Å, $\theta_{min} \sim 28''/D_{cm}$**
- **Inside Earth's atmosphere, <u>turbulence</u> strongly affects image diameter.**

    Resulting image blur & motion is called "seeing", and typically yields:

$$\theta_{atm} \sim 0.5 - 2''$$

... i.e. spatial resolution in most instances is governed by the <u>atmosphere</u>, not the telescope. (Much effort is now aimed at turbulence control near telescopes.)

- **Best UVOIR images: HST, ~ 0.06" (~ a quarter at 90 km)**

  - **Best overall: VLBA (~ 0.001")---but limited to very high surface brightness radio sources (rare)**

- **Anticipated ground-based (8-m) single-aperture "adaptive optics" systems: 0.05" over limited fields (in NIR, but probably not for < 1μ)**

- **Anticipated UVOIR interferometers: 0.001"**

D. Spectral Resolution
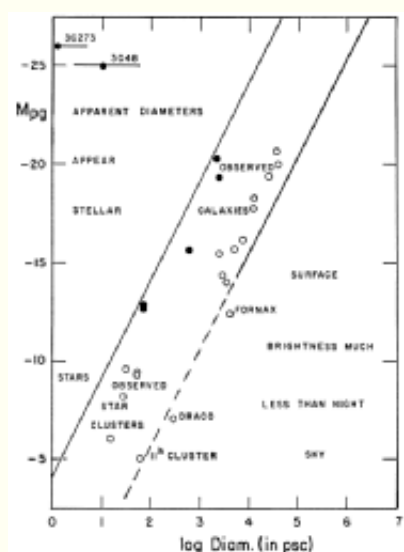
- **Theoretical maximum governed by diffraction in optical components, but practical limit set by photon rates. High resolution devices are typically <u>photon-starved</u> (except for Sun).**

- **ID's, surveys, classification at <u>low resolution</u> (10-5000 Å)**

- **Physical analysis at <u>moderate-to-high</u> resolution (0.01-10 Å)**

- **Highest to date: ~ 0.001 Å**

E. Other Properties : e.g. polarization, variability
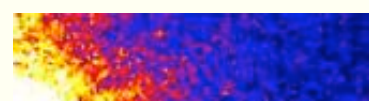
F. Examples of Background-Induced Selection Effects

Galaxy surface-brightness selection, shown in the "Arp Diagram" (Arp 1965):
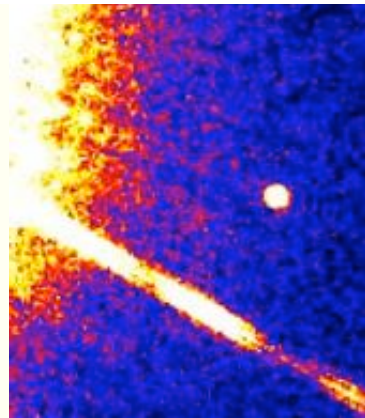
- **Diagram shows that identified galaxies occupy a relatively small range of parameter space, bounded by the night sky surface brightness on one side and the spatial resolution of survey telescopes on the other.**

- **Example of a previously-concealed class of galaxies: "ultracompact dwarf galaxies" (Drinkwater et al. 2003)**

Brown dwarf companions to bright stars

Brown dwarf companions can be 10^3 to 10^6 times fainter than their primary stars. Scattered light from primary inhibits searches. For detection by direct imaging, require a scattered light suppression technique. Same problem, much worse, affects search for Earthlike planets in orbit around nearby stars.

VII. NON-EM CONVEYORS OF COSMIC INFORMATION

Most astrophysical information is derived from the study of electromagnetic waves propagating over significant distances. However, there are several niches where important information is, or could be, conveyed by other means. For a list, click here.

Related pages:

Non-EM channels for astrophysical information

Tips for success in observational astronomy

References:

- **LLM, Chapter 1**

- **Harwit, *Cosmic Discovery* [QB43.2.H37]**

- **"99 Things About the Last 100 Years of Astronomy," V. Trimble, Mercury, Nov-Dec 99, p. 17.**

Lecture Index   Next Lecture

Last modified August 2003 by rwo

NON-EM CONVEYORS OF COSMIC INFORMATION
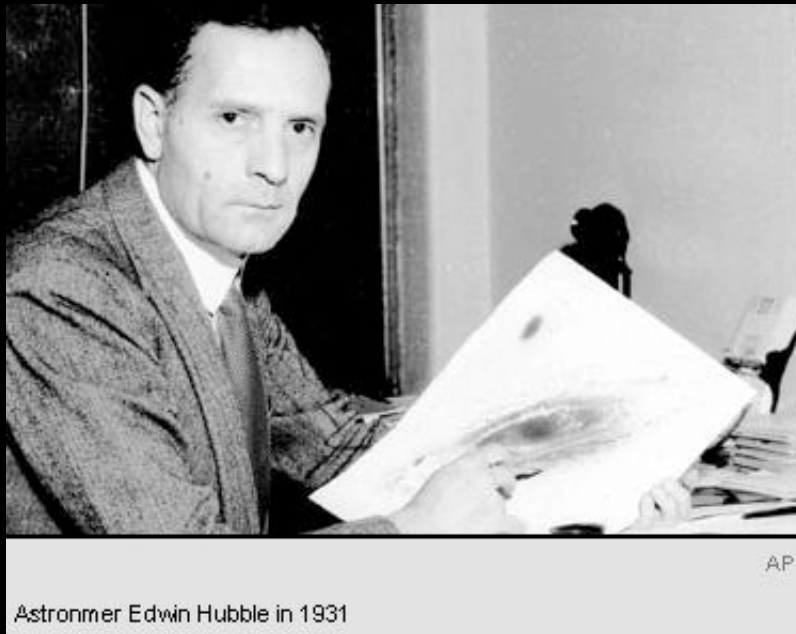
Channels which do <u>not</u> involve long-range propagation of EM signals from sources:

- o **Interplanetary spacecraft for in-situ sampling**

- o **Meteorites (including from Mars & the Moon)**

- o **Terrestrial isotopic abundances**

- o **Interplanetary/interstellar dust grains**

    [Dust deposition on Earth: $\sim$150 tons/day]

- o **Cosmic rays**

- o **Solar wind**

- o **Geophysical evidence: $L_\odot(t)$; SN irradiation?; impact craters**

- o **Neutrinos**

- o **Tides**

- o **Gravitational waves?**

- o **Dark matter particles??**

TIPS FOR SUCCESS IN OBSERVATIONAL ASTRONOMY

Astronmer Edwin Hubble in 1931

Your aim by PhD time should be to become one of the <u>leading authorities</u> on some area of significant current interest. It is expected that this area will usually be of modest scope, but when conference organizers are picking the most knowledgeable younger speakers for review talks, you want your name to be on the short list.

A. Ask the <u>right questions</u>.

- **Learn to <u>rank</u> issues for overall importance to the field and for novelty.**

B. Learn to assess <u>solvability</u>: which problems are ripe for progress?

- **Solvability is a function both of state of current knowledge and available**

instrumentation.

- Many "interesting" problems are <u>not</u> ripe for solution.

- Evaluate SNR issues

- Also assess the interests & strengths of <u>competing groups</u> & their potential for beating you to a result.

C. Plan to take quick advantage of <u>new observational capabilities</u>.

- These are often the source of important new discoveries.

- A "new capability" can be as simple as a new type of imaging filter.

D. Develop a healthily <u>skeptical</u> outlook.

- *Cultivated skepticism* is the cornerstone of science:

    "He believed in the primacy of doubt, not as a blemish upon our ability to know but as the essence of knowing."
    ----- J. Gleick, writing about physicist Richard Feynman.

- Apply to: established results, new results, <u>your</u> results

    <u>Be self-critical</u>: make "reality check" your mantra

E. <u>Know the background</u> thoroughly:

- Learn to <u>critically dissect the literature</u>, based on original, not secondary, sources.

    Read the more important papers from hardcopy; annotate them or make written summaries of key findings, strengths & weaknesses. It helps to keep copies of related papers together in a binder.

- For longer term projects (e.g. a thesis) it is important to learn the entire history of your field. Among other benefits, there are many excellent insights that remain unexploited in the older literature

- It is just as important to become familiar with the <u>wrong</u> ideas and why they were wrong as it is to know the currently accepted "right" ideas. There are many more wrong ideas than right ones.

- Beware of the "emperor's new clothes."

F. Develop skill with <u>ROMPs & SWAGs</u>

- Simple exploratory calculations are the best way to shape any research program.

G. Understand your <u>instruments</u> well

- This will take a minimum of 2-3 observing runs with a given instrument.

- **Learn their limits and how to push the envelope**

H. Understand <u>analysis techniques</u> well

- **It is doubtful that your early reductions/analysis for a given problem will be acceptable in the long run.**

- **<u>Test</u> techniques on synthetic data sets where you know the answer.**

I. Track your own <u>progress</u>

- **Set milestones and regularly review your progress towards them; are you converging towards answering the main questions?**

- **Keep a regular journal of your ideas (good & bad)**

J. Dealing with computers

- **Computers are tools, <u>not science</u>**

- **Despite appearances, computers have <u>not</u> increased the capacity of the human brain to absorb and process information**

- **Don't trust and <u>always verify</u>**

- **If it's important, read it from <u>paper</u>**

K. Dealing with advisors

- **Most advice comes from long experience; don't disregard it lightly. In troublesome areas, seek advice from more than one senior person.**

- **Look at any research project as an opportunity to grow as a scientist beyond the nominal boundaries. You may well have new insights or see new avenues to exploit that your overloaded advisor has missed or ignored.**

- **In the course of a PhD project, you are expected to become nearly independent of your advisor and at least as knowledgeable as he/she is on that subject.**

L. Dealing with groups

A glance at the ApJ will demonstrate the growing dominance of group science

- **Bring a unique strength, skill**

- **Produce**

- **Think for yourself**

- **Lead by example**

- **Be sure you develop a reputation/expertise that <u>distinguishes</u> you from other group members.**

- Consult history of "big physics" (accelerators, etc) for sociology.

    - E.g.: larger groups breed institutional imperatives for publicizing results, which is why the media often mistake incremental results for fundamental ones.

M. Publishing

- A good goal by PhD time is to have published in the major journals one paper for every year you've been in graduate school. You should be lead author of some of these.

- Learn to write good, clear, concise scientific prose. Most entering graduate students cannot do this.

    - Consult style guides for tips, e.g. the **Guide to Science Writing** from the Journal of Young Investigators and *The Elements of Style* by Strunk & White.

    - Write up several page summaries of interim results in full journal style. These serve as good writing practice, as drafts for polished versions or presentations, and to place your accomplishments in the context of the main issues you are trying to address.

- Be aware of the ``reader pyramid'': few people will read the whole paper; more will read the introduction and conclusion; many more will skim/read the abstract.

    - Be sure the abstract contains all the key points.

    - Be sure the Intro/Conclusion are clear and complete; the conclusion should emphasize what is new or unique about the work.

- Set high standards for yourself (and your co-authors) in writing. Reputations are based on the number of good papers one produces, not the total number of papers.

N. Presentations

- Learn to give interesting and effective presentations on all time scales from 5 minutes to an hour. Analyze and emulate others who do this well. Real-time rehearsals are the only way to prepare well for your early ventures in this arena.

- Unfortunately, you will need to learn PowerPoint or the equivalent. Just keep in mind that PowerPoint is the messenger, not the message.

O. Observing Proposals

- A compelling proposal must be clearly, persuasively, and concisely written and must demonstrate:

    1. that the questions you are asking are important/interesting;
    2. that the program is technically feasible;
    3. that it will provide a definitive answer to the questions posed.

- Write for harried TAC members who have only a few minutes to read each proposal

and who are looking for <u>reasons to reject</u>

- Write for people who are generally well informed but who are not specialists in the field. Clearly explain the main issues. Place in the larger context. Make sure claims for importance/uniqueness are defensible; don't exaggerate.

- Keep it short and clear: use subheadings, short paragraphs, topic sentences, large fonts; don't crowd text

- Put key points up front

- Don't waffle: where ambiguities exist, state clearcut choices and how you intend to resolve the issues involved

- Illustrations add interest and can substitute for lengthy text

- Essential: proofread line-by-line from <u>paper</u>, not a computer screen; always spell-check.

[↑] Lecture Index **[→] Next Lecture**

Last modified June 2007 by <u>rwo</u>

ASTROPHYSICAL INFORMATION
DERIVED FROM THE EM SPECTRUM

Position

Radial Velocity

Transverse Velocity

Distance

Luminosity

Temperature(s)

Chemical Composition

Mass

Size

Pressure

Density

Magnetic Fields

Rotation

Turbulence

Variability

....etc

THE ELECTROMAGNETIC SPECTRUM

- **References: LLM: 1, 2.2, 3.2.1, 3.3**

- **Regions of the EM spectrum: see chart, next page**

  o Nomenclature

  o Wavelength, frequency, energy units

  > **Convenient working units in any band typically yield numerical values in the range 1–10000 $\rightarrow$ heterogenous!**

  > > **Radio: cm, GHz, or MHz**
  > > **Far-IR/Sub-mm: μ or mm**
  > > **IR: μ**
  > > **UVOIR: Å, μ, or nm**
  > > **EUV: eV or Å**
  > > **X-Ray: keV**
  > > **Gamma Ray: MeV**

  o Windows in Earth's atmosphere

  o History of astronomical coverage: see Lecture 1

  o Modern detection limits: see chart

  o Major discoveries: see 2.A

  o Important observatories: see 2.B

EM SPECTRUM (continued)

Here is a convenient summary of the EM spectrum from Menzel, Whipple & de Vaucouleurs (1970). (Detector listing out of date.)
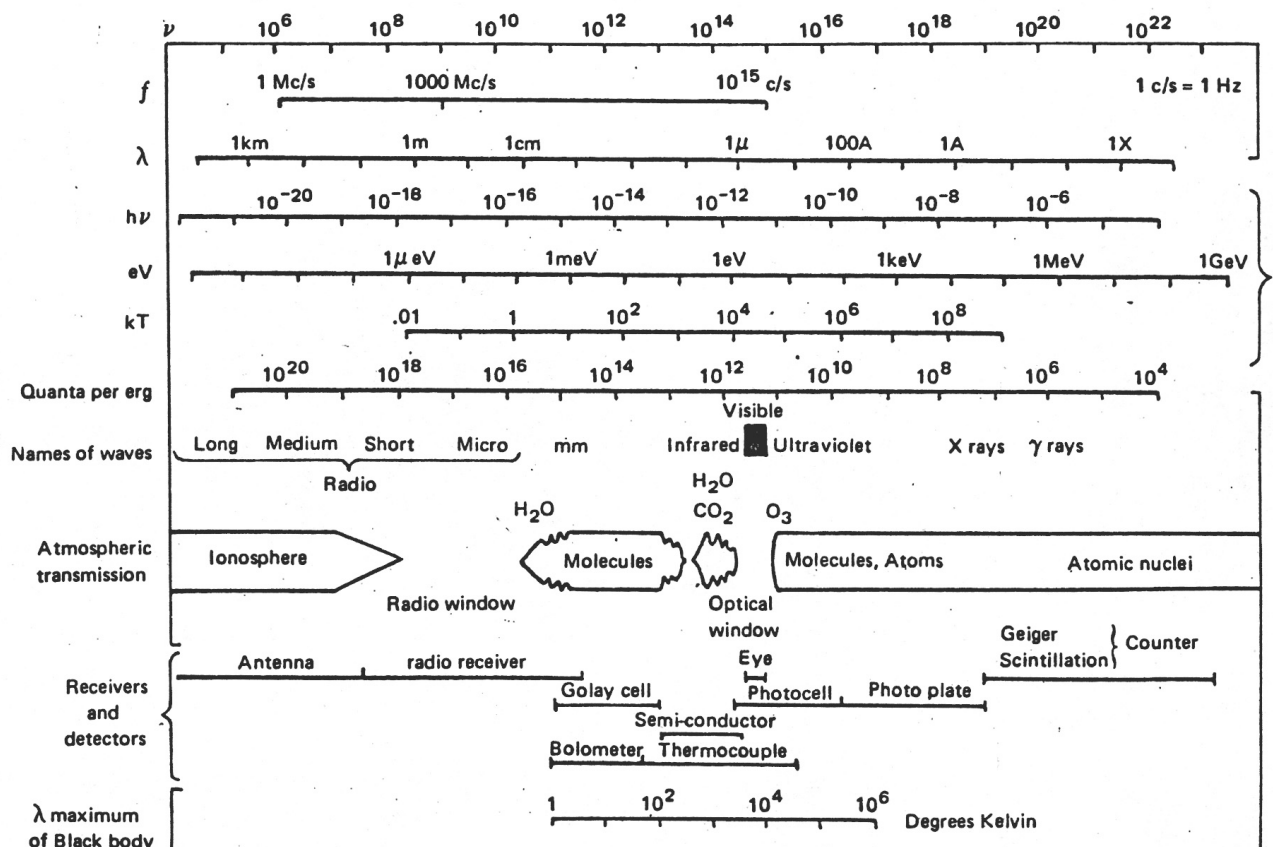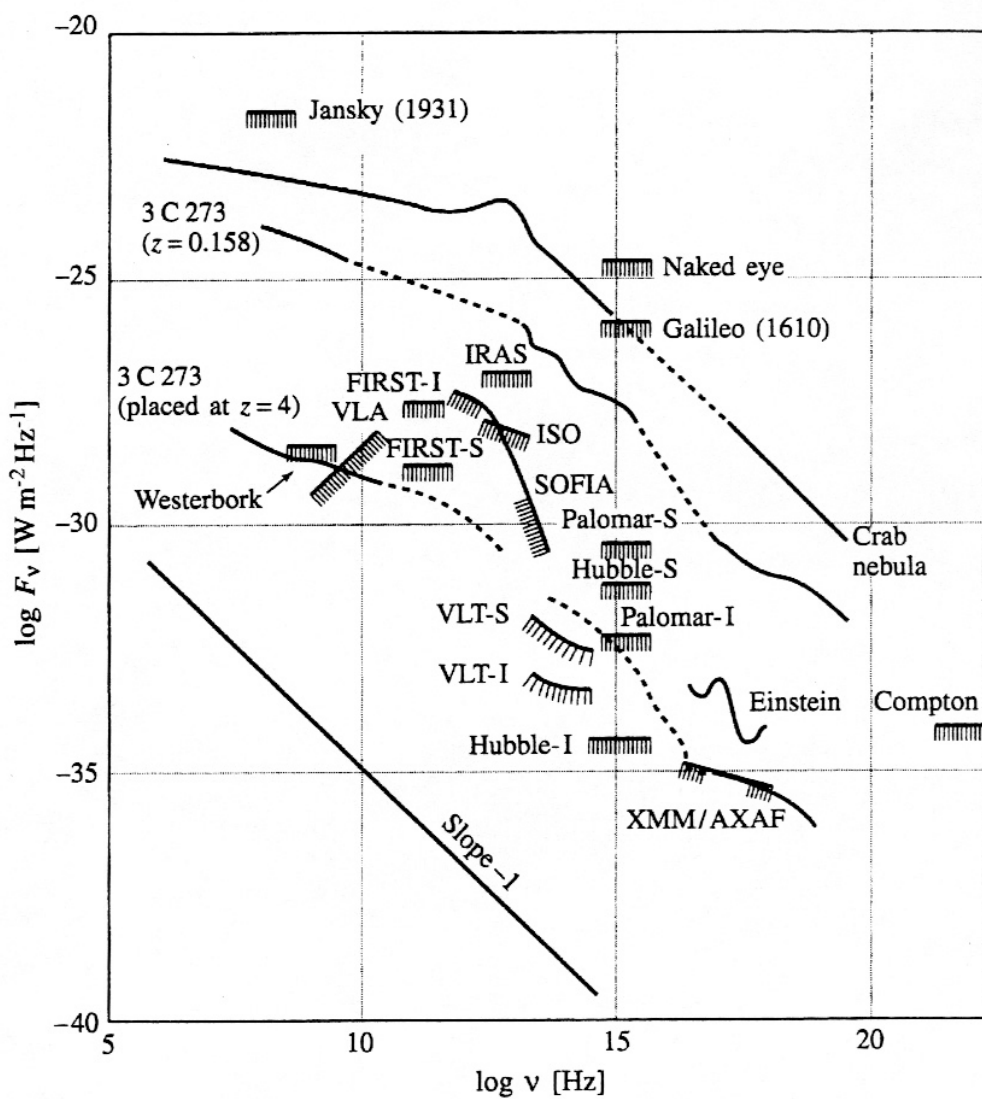
FIGURE 8-1

The electromagnetic spectrum and detectors. Symbols: ν, frequency in cycles/sec or Hertz, Hz; f, frequency in 10^6 Hz or Mc/s; λ, wavelength; $h\nu$, energy of a quantum in ergs; eV, energy of a quantum in electron volts (1 eV $= 1.59 \times 10^{-12}$ erg); kT, thermal energy in °K.

EM SPECTRUM (continued)

Modern detection limits. **The envelope with a slope of -1 corresponds to $\nu F_\nu = const$ and implies constant energy per decade in EM spectrum.**

EM DETECTOR TYPES

Bolometers

- **Most basic detector type: a simple absorber**

- **Temperature responds to total EM energy deposited by all mechanisms during thermal time-scale**

- **Electrical properties change with temperature**

- **Broad-band (unselective); slow response**

- **Primarily far infrared, sub-millimeter (but also high energy thermal pulse detectors)**

Coherent Detectors

- **Multiparticle detection of electric field amplitude of incident EM wave**

- **Phase information preserved**

- **Frequency band generally narrow but tunable**

- **Heterodyne technique mixes incident wave with local oscillator**

- **Response proportional to instantaneous power collected in band**

- **Primarily radio, millimeter wave, but some IR systems with laser LO's**

EM DETECTORS (continued)

Photon Detectors

- **Respond to individual photon interaction with electron(s)**

- **Phase not preserved**

- **Broad-band above threshold frequency**

- **Instantaneous response proportional to collected photon rate (not energy deposition)**

- **Many devices are integrating (store photoelectrons prior to readout stage)**

- **UVOIR, X-ray, Gamma-ray**

  o **Photoexcitation devices: photon absorption changes distribution of electrons over states. E.g.: CCD's, photography**

  o **Photoemission devices: photon absorption causes ejection of photoelectron. E.g.: photocathodes and dynodes in photomultiplier tubes.**

  o **High energy cascade devices: X- or gamma-ray ionization, Compton scattering, pair-production produces multiparticle pulse. E.g. gas proportional counters, scintillators**

USEFUL EM SPECTRUM CONVERSIONS

21 cm = 1420 MHz [Hyperfine line, HI]

1 cm = 30 GHz

1 mm = 300 GHz = 1000μ

1 μ = 10^4 Å = 1000 nm

5500 Å = 5.5×10^{14} Hz [V band center]

1 nm = 10 Å

1 Å = 10^{-8} cm

1 eV = 1.60×10^{-12} erg = 12400 Å

13.6 eV = 912 Å [Lyman limit = IP of HI]

1 keV = 12.4 Å = 2.4×10^{17} Hz

$m_e c^2$ = 511 keV

EM SPECTRUM MEASUREMENTS

Basic observed quantity: FLUX

> **Flux is the energy incident per unit time per unit area within a defined EM band:**
>
> $$f \equiv E_{in\,band}/A\,t$$
>
> > **(or power per unit area)**
>
> **Usually quoted at top of Earth's atmosphere**

Band definitions for flux:

- o **"Bolometric": all frequencies**

- o **Finite bands (typically 1-20%) defined by, e.g., filters such as U,B,V,K**

- o **"Monochromatic": infinitesimal band, $\nu \rightarrow \nu + d\nu$**

  > **Also called "spectral flux density"**
  >
  > **Denoted: f_ν or f_λ**
  >
  > **Note conversion: since $f_\nu d\nu = f_\lambda d\lambda$ and $\nu = c/\lambda$,**
  >
  > > $$\rightarrow \nu f_\nu = \lambda f_\lambda$$
  >
  > **Not observed directly. Rather, inferred from observations made with finite bands:**
  >
  > > $$< f_\lambda > = \int T(\lambda) f_\lambda d\lambda \,/\, \int T(\lambda) d\lambda,$$
  >
  > > **...where T is the system response function.**

EM MEASUREMENTS (continued)

Units for astronomical fluxes: Note <u>not MKS</u>

o Standard UVOIR Units:

$$[f_\nu] = \mathrm{erg}\ \mathrm{s}^{-1}\ \mathrm{cm}^{-2}\ \mathrm{Hz}^{-1}$$

$$[f_\lambda] = \mathrm{erg}\ \mathrm{s}^{-1}\ \mathrm{cm}^{-2}\ \mathrm{\mathring{A}}^{-1}$$

o All-band unit (from radio "flux unit"): Jansky

$$\mathbf{1\ Jy} = 10^{-26}\ \mathrm{w}\ \mathrm{m}^{-2}\ \mathrm{Hz}^{-1}$$

$$= 10^{-23}\ \mathrm{erg}\ \mathrm{s}^{-1}\ \mathrm{cm}^{-2}\ \mathrm{Hz}^{-1}$$

THE UVOIR MAGNITUDE SYSTEM, BRIEFLY

An ancient and arcane, but compact and by now unchangeable, way of expressing brightnesses of astronomical sources.

Magnitudes are a logarithmic measure of <u>spectral flux density</u> (<u>not</u> flux!)

- **Monochromatic Apparent Magnitudes**

  o $m_\lambda \equiv -2.5 \log_{10} f_\lambda - 21.1$,

  　　where f_λ is in units of $\mathrm{erg\ s^{-1}\ cm^{-2}\ \mathring{A}^{-1}}$

  o **This system of "monochromatic magnitudes per unit wavelength" is also known as the "STMAG" system, because it is widely used by HST observers.**

  o **Normalization is chosen to coincide with the zero point of the widely-used "visual" or standard "broad-band" V magnitude system:**

  　　i.e. $m_\lambda(5500\,\mathring{A}) = V$

  o **Zero Point: fluxes at 5500 Å corresponding to $m_\lambda(5500\mathring{A}) = 0$, are (Bessell 1998)**

  　　$f_\lambda^0 = 3.63 \times 10^{-9}\,\mathrm{erg\ s^{-1}\ cm^{-2}\,\mathring{A}^{-1}}$, **or**

  　　$f_\nu^0 = 3.63 \times 10^{-20}\,\mathrm{erg\ s^{-1}\ cm^{-2}\,Hz^{-1}}$, **or**

  　　$f_\nu^0 = 3630\ \mathrm{Janskys}$

  　　$\phi_\lambda^0 = f_\lambda^0/h\nu = 1005\ \mathrm{photons\ cm^{-2}\,s^{-1}\,\mathring{A}^{-1}}$
  　　is the corresponding photon rate per unit wavelength

THE MAGNITUDE SYSTEM (continued)

● **Surface Brightnesses (extended objects):**

o $\mu_\lambda \equiv m_\lambda + 2.5 \log_{10} \Omega$

where m_λ **is the integrated magnitude of the source and** Ω **is the angular area of the source in units of arcsec^2.**
1 arcsec$^2 = 2.35 \times 10^{-11}$ steradians.

o μ **is the magnitude corresponding to the mean flux in one arcsec^2 of the source. Units of** μ **are quoted, misleadingly, as "magnitudes per square arcsecond."**

● **Absolute Magnitudes**

o $M \equiv m - 5 \log_{10}(D/10)$**, where D is the distance to the source in parsecs**

o M **is the apparent magnitude the source would have if it were placed at a distance of 10 pc.**

o M **is an** <u>intrinsic</u> **property of a source**

o **For the Sun,** $M_V = $ **4.83**

[A more complete discussion of magnitudes & colors will be given later.]

SPECTRAL ENERGY DISTRIBUTIONS

The spectral energy distribution (SED) is $f_\nu(\nu)$ or $f_\lambda(\lambda)$ — i.e. the distribution of spectral flux density over wavelength or frequency.

o For a given SED, the total flux in a finite band is then:

$$F_b = \int\limits_{\nu_1}^{\nu_2} f_\nu \, d\nu$$

$$= \ln 10 \int\limits_{\nu_1}^{\nu_2} \nu f_\nu \, d\log_{10}(\nu)$$

This implies that $\nu f_\nu = \lambda f_\lambda \sim$ the power per unit area per decade in the SED.

Most astronomical sources are <u>broad-band</u> emitters, over at least several decades. Multiband observations of the SED permit dissection of source physics.

o It is tempting to approximate multiband SED data with simple functions, like power laws or Planck functions. But this is almost always misleading. See "3C 273 and the Power Law Myth," Perry et al. MNRAS, 228, 623, 1987 and the plots on the next page.

o Lesson: coordinates used for representation of an SED can influence one's impression of source energetics, emission mechanism, source structure, importance of given EM domain, etc. Plotting style chosen often depends on funding agency!
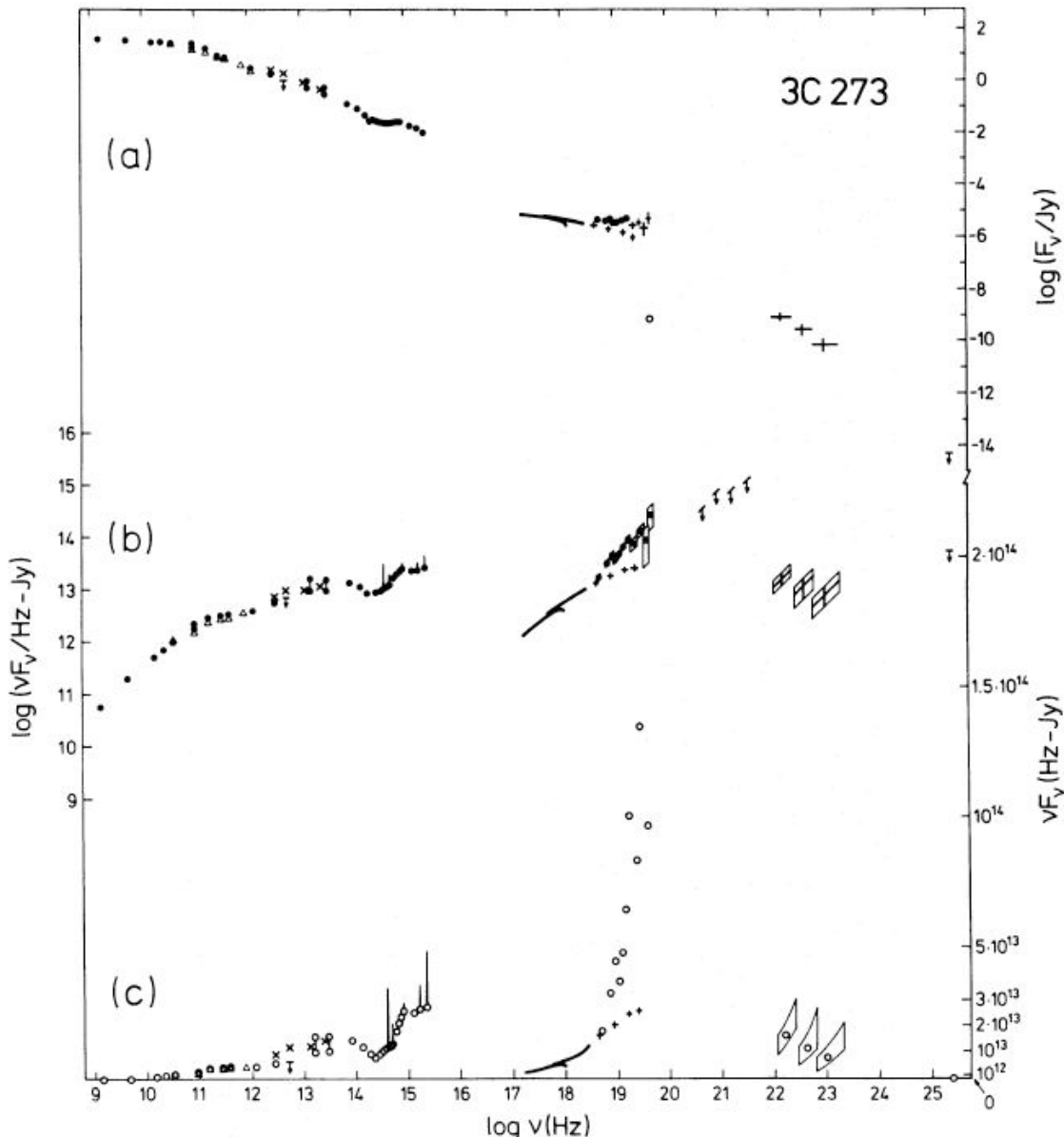
626   *J. J. Perry, M. J. Ward and M. Jones*

Figure 1. The spectrum of 3C 273: (a) the log of the observed flux density plotted against the log of the frequency; (b) log ($v \times$ flux density) plotted against log frequency; this represented peaks where the emitted energy peaks; (c) linear representation of frequency $\times$ flux density plotted against log frequency; the area under the curve is proportional to the emitted energy per frequency bandwidth at the frequency shown. It is clear from (c) that the energy is not emitted uniformly over all frequencies.

CHARACTERIZATION OF EM SOURCES

- **Luminosity (L)**

  o <u>Power</u> (energy/sec) radiated by source into 4π sterad

  o Units: egs s^{-1}

- **Flux (f)**

  o Power from source crossing normal to <u>unit area</u> at specified location a distance D from source

  o $f = L/4\pi D^2$ if source isotropic, no absorption

  o Units: egs s^{-1} cm^{-2}

- **Specific Intensity (or "surface brightness") (I)**

  o Power from source crossing unit area at specified location and moving into <u>unit solid angle</u> about a specified direction

  o Units: egs s^{-1} cm^{-2} sterad^{-1}

  o Relation to flux: if $\hat{r}$ is a unit direction vector at the surface, which has a normal vector $\hat{z}$, then:

  $$f = \int\limits_{4\pi} I(\hat{r}) \ \hat{z} \cdot \hat{r} \ d\Omega$$

  where the element of solid angle in spherical coordinates is $d\Omega = \sin\theta \, d\theta d\phi$.

  o So: $f \sim \langle I \rangle \, \Delta\Omega$

  o I is <u>independent of distance</u> if there is no absorption or emission along path <u>and</u> source remains resolved

EM CHARACTERIZATION (continued)

- **As for flux, symbols like L_ν, I_ν, I_λ denote monochromatic versions of these quantities.**

- **<u>Warning</u>: this nomenclature is ubiquitous among astronomers but is <u>not</u> widely used outside of astronomy. In radiometry, for instance, "irradiance" is used for flux, "radiance" is used for specific intensity, "flux" is used for luminosity, and so forth. Symbols are also different. Beware!**

THE PLANCK FUNCTION

The Planck function is both a useful fiducial energy distribution <u>and</u> an important diagnostic of source astrophysics. It describes the EM energy distribution of a source in thermal equilibrium ($=$ a "black body"). Assumptions about source:

- Strictly homogeneous: T constant, unchanging everywhere.
- Strong coupling between radiation field and matter; optically thick
- All microscopic processes in balance; number in states given by Boltzman distribution

Under these conditions, the specific intensity (I) is independent of the source's density, chemical composition, shape, etc., and is given by:

$$B_\nu(\nu, T) = \frac{2h\nu^3}{c^2} \frac{1}{e^{h\nu/kT} - 1}$$

$$B_\lambda(\lambda, T) = \frac{2hc^2}{\lambda^5} \frac{1}{e^{hc/kT\lambda} - 1}$$
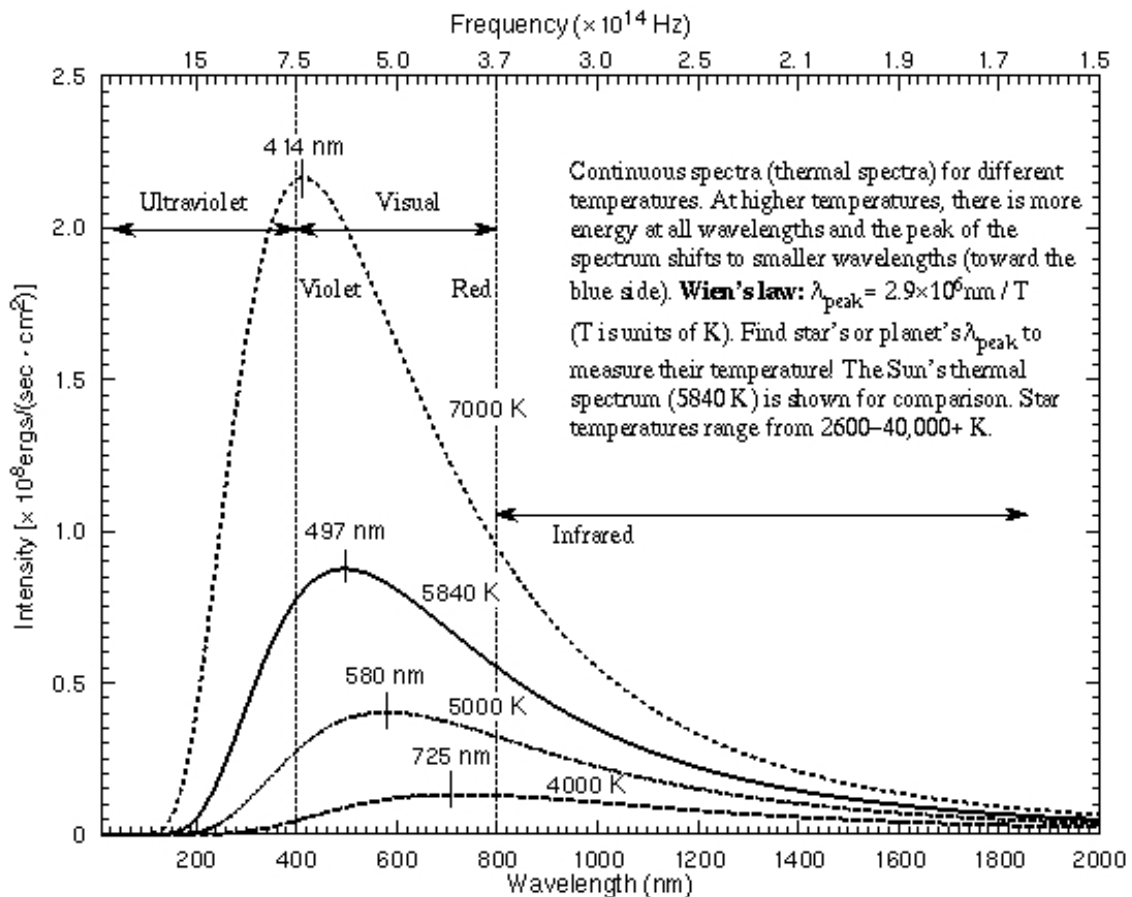
Units: $\mathrm{erg\ s^{-1}\ cm^{-2}\ [Hz\ or\ cm]^{-1}\ sterad^{-1}}$

Bolometric integral:

$$\int\limits_0^\infty B_\nu(\nu, T)d\nu = \int\limits_0^\infty B_\lambda(\lambda, T)d\lambda = \sigma_0 T^4/\pi,$$

where σ_0 is the Stefan-Boltzmann constant

$\left(5.67 \times 10^{-5}\,\mathrm{erg\ s^{-1}\ cm^{-2}\ deg^{-4}}\right)$

THE PLANCK FUNCTION (continued)

Planck Function Spectra (©Nick Strobel)
Plotted is πB_λ in units of $10^8 \, \mathrm{erg} \, \mathrm{s}^{-1} \, \mathrm{cm}^{-2} \, \mathrm{nm}^{-1}$

THE PLANCK FUNCTION (continued)

Limiting forms:

$$h\nu/kT << 1 \rightarrow B_\nu(T) = 2kT/\lambda^2 \quad \text{("Rayleigh-Jeans")}$$

$$B_\lambda(T) = 2ckT/\lambda^4 \quad \text{(See next page)}$$

$$h\nu/kT >> 1 \rightarrow B_\nu(T) = 2h\nu^3\, e^{-h\nu/kT}/c^2 \ \text{("Wien")}$$

Limit on SED Slope:

Note that $d\log B_\nu/d\log\nu \le 2$ for all ν and T.
A steeper continuum slope might occur in the case of nonthermal sources, etc., but is a warning to do a reality check.
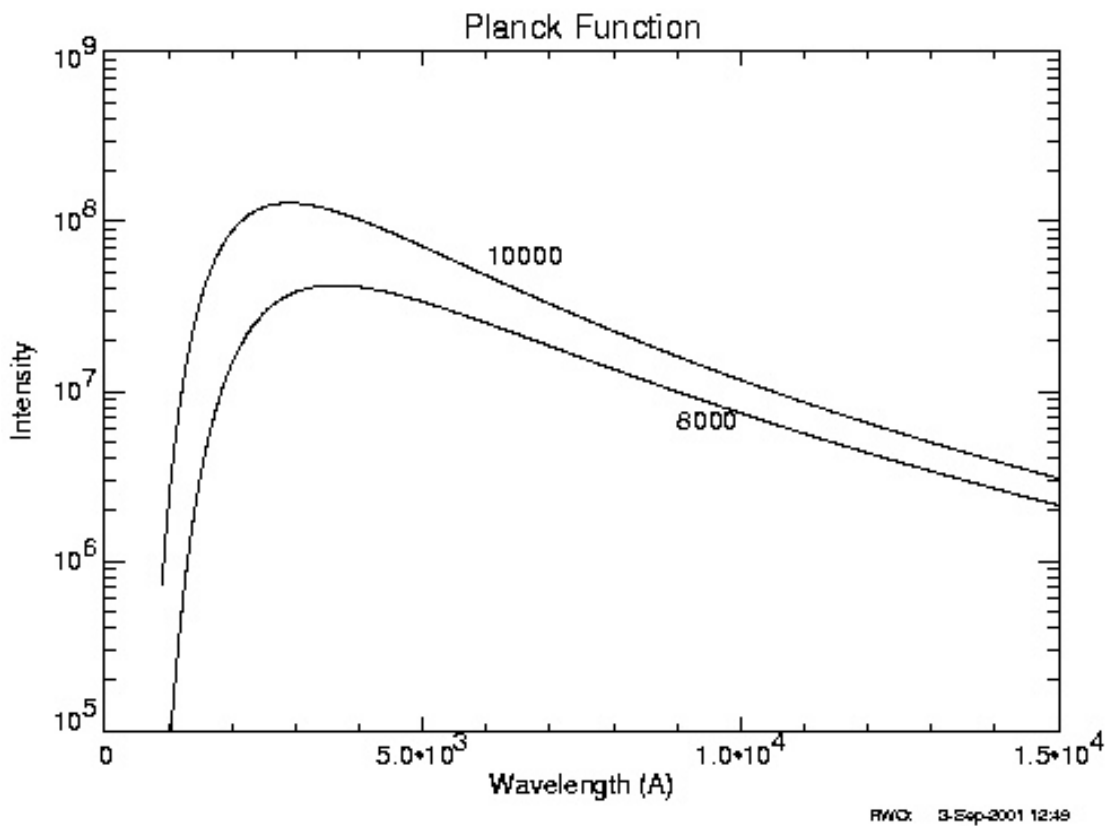
Wien's Displacement Law: maximum in Planck function occurs at

$$\lambda_{max} = 0.51T^{-1} \ \text{cm for } B_\nu$$
$$\lambda_{max} = 0.29T^{-1} \ \text{cm for } B_\lambda$$

Cf. plot on previous page. Useful for defining the "characteristic temperature" of a given EM domain

THE PLANCK FUNCTION (continued)

Planck function plotted in log (flux) to show Rayleigh-Jeans asymptote ($B_\lambda \sim \lambda^{-4}$) at long wavelengths.
Plotted is πB_λ in units of $\mathrm{erg}\ \mathrm{s}^{-1}\ \mathrm{cm}^{-2}\ \text{Å}^{-1}$.
Curves labeled with temperature.

EM SPECTRUM:
DISCOVERY & DIAGNOSTICS

EM REGION	RELATIVE WAVELENGTH	NEW PHENOMENA	KEY DIAGNOSTIC FOR
RADIO	10^6	AGN, jets, CMB, Pulsars	Neutral ISM, Molecular ISM
IR	100	Protostars	Dust, Cold ISM, Shrouded Starbursts, z > 3 Galaxies
OPTICAL	1.0	Planets, Stars, Galaxies, The Universe	Almost all
UV	0.1	Intergalactic Medium	Massive Stars, Hot & Cold ISM, AGN
X-RAY	10^{-4}	XR Binaries, Hot ICM	Hot ISM, AGN
GAMMA RAY	10^{-6}	GR Bursters	

Perspective question: *what would we know about the universe today if Earth had an atmosphere which was optically thick in the UVOIR? Would science other than astronomy be as well developed as now?*

MAJOR FACILITIES BY EM BAND 1990-2010
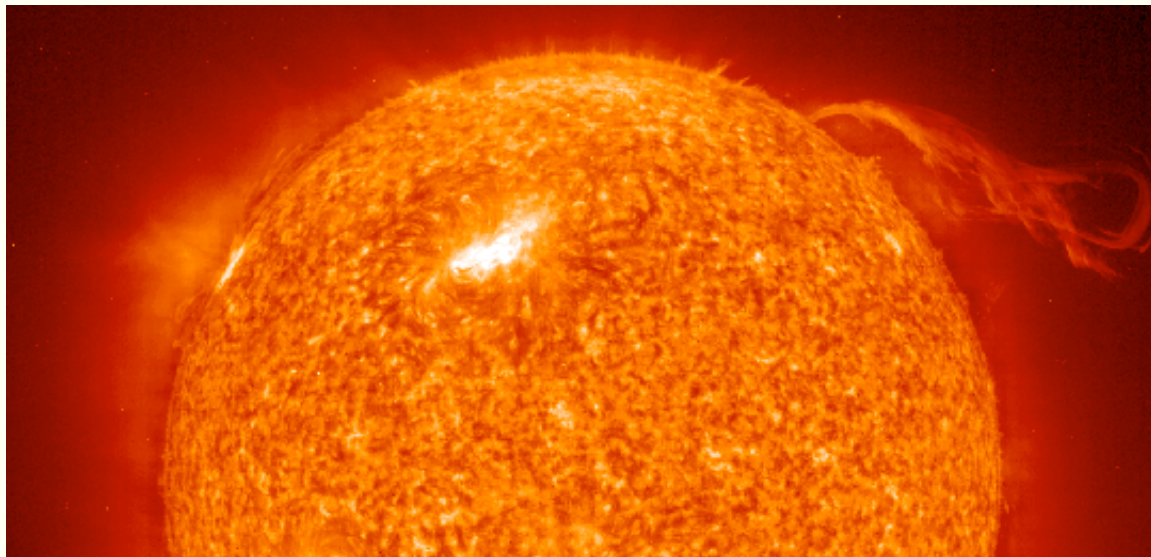
EM REGION	RELATIVE WAVELENGTH	FACILITIES	SURVEYS
RADIO	10^6	VLA, GBT, Arecibo MPIfR 100-m, AT, VLBA, Merlin, BIMA, IRAM, Nobeyama, JCMT, OVRO, CSO, ALMA	VLA/NVSS, VLA/FIRST COBE, WMAP
IR	100	IRTF, UKIRT, ISO, SIRTF, SOFIA	2MASS
OPTICAL	1.0	HST VLT, Keck, GTC, LBT, HET, SALT, Subaru, Gemini, Magellan, MMT, Palomar	POSS II, ESO/SERC-SSS, SDSS, Hipparcos
UV	0.1	IUE, HST, EUVE, FUSE, GALEX	GALEX
X-RAY	10^{-4}	ASCA, ROSAT, RXTE, BeppoSAX,Chandra, XMM	ROSAT
GAMMA RAY	10^{-6}	CGRO, HETE, INTEGRAL, SWIFT, GLAST	

Entries in green are space-based.

You can find links to most of these facilities at one of the following sites:

- SEDS Large Optical Telescopes Links
- SEDS Orbital Telescopes Links
- Large Telescope FAQ

3. ASTROPHYSICAL SOURCES

*Sun in H-alpha showing active regions
and a flame-like "prominence."*

I. INTRODUCTION

There are many distinct types of astrophysical sources: stars, AGNs, planets, H II regions, synchrotron jets, hot intracluster gas, shocked gas (SNRs), etc

Main issues:

1. **Generation of photons**
2. **Transfer of photons to observer = *radiative transfer***
3. **Deduction of physical properties from emergent spectrum**

(1) Photon generation:

- **Many different mechanisms**

- **Usually several types important in given source**

- **Mechanisms usually broad-band, but often dominate distinct bands**

- **"Thermal" vs "non-thermal"**

  - **Thermal: emitters/absorbers close to Boltzmann distribution ("thermal equilibrium" or TEQ)**

    - **In many, not all, cases, radiation field is close to B_ν, the Planck function**

  - **Non-Thermal: emitters/absorbers/radiation far from TEQ**

    - **Best example: synchrotron sources = continuum radiation from relativistic electrons with non-Maxwellian energy distribution moving in magnetic fields. If e-energy distribution is a power law, so is emitted radiation.**

- **The underlying complexity of typical sources is emphasized by the image of the Sun at the top of the page. We are aware of the many different physical environments on the Sun's surface only by virtue of its proximity.**

(2) <u>Radiative Transfer</u>:

- **Transfer is characterized by the <u>optical depth</u>, $\tau(\nu)$**

- **Probability of escape from a given location in the source is $\sim e^{-\tau(\nu)}$**

- **$\tau << 1$: "optically thin". See <u>directly</u> to sources of photons.**

- **$\tau \gtrsim 1$: "optically thick". Observed photon distribution has been <u>transformed</u> in ν, direction, and/or intensity.**

  - **NB: "Thick" does <u>not</u> mean "dark." (The Sun is optically thick!) Rather, observable photons escape only from outermost ~ 1 optical depth of source.**

- **Propagation of photon energy is described by <u>the "equation of transfer"</u>**

(3) <u>Deduction of Physical Properties</u>

- **How to relate observables to source physics?**

II. COMPARISON OF TWO CANONICAL SOURCE TYPES

In this section, we discuss two canonical types of astrophysical sources: STARS & AGNs and compare them in the following characteristics:

- Structures
- Spectra: Continua
- Spectra: "Lines" (fine structure)
- Information carried by their spectra

STRUCTURES

STARS:

- **<u>Dense spheres</u>, r ~ $10^{11\text{-}13}$ cm**

- **Stars are dynamically stable, apart from convection and surface phenomena, throughout most of their lifetimes**

- **$\sim$ Isotropic radiators.**

- **Nuclear reactions maintain high-temperature (>10^7 K) core.**

- **XR and GR radiation transferred slowly through high optical depth envelope. Degraded to UVOIR band.**

- **Observed radiation escapes from a <u>very thin</u> (300 km in Sun) layer = "photosphere"**

    NB: photospheres ($\sim 10^{17}$ particles/cm^3 in the Sun) are DENSE by the standards of AGN emitting regions

- **Subsidiary processes (e.g. driven by magnetic fields) radiate small amounts in non-UVOIR bands.**

AGNs ("Active Galactic Nuclei"):

- **Supermassive black hole (M ~ $10^{7\text{-}9}$ M$_{sun}$; R$_{Schw}$ ~ 3 x 10^{13} M$_8$ cm) at center of an <u>*accretion disk*</u> with r $\gtrsim 10^{16}$ cm.**

- **Accretion disk is fed by infalling material; matter is continuously transported through disk**

- **Dissipation and magnetic processes near center of disk generate relativistic particles, $\gamma \sim 10^3$. These can generate relativistic jets.**

- **Observed radiation emerges from a <u>large volume</u> with nonuniform properties**

- **Relativistic jets and disk confinement produce <u>anisotropic</u> radiation.**

- **Relativistic particles produce broad-band non-thermal synchrotron radiation, directly observed at radio wavelengths.**

- **Direct thermal radiation from denser, hot inner disk (UV).**

- **Photon boosting of low-energy photons by inverse Compton scattering to UV/XR bands.**

    Compton boost: $\nu_2 \sim \nu_1 \gamma^2$

- **Hard radiation field produces strong ionization of gas in a large, low-density volume around disk, ===> UVOIR, XR emission lines.**

- **Strong heating of surrounding dust grains ===> IR continuum & emission lines (3-500μ). (But grains vaporized near center.)**

- **Star-formation regions often associated with AGN in disk galaxies (chicken or egg?).**

CONTINUUM SPECTRA

STARS

- **Primary component is UVOIR radiation from photosphere.**

    - **Thermal source; emergent spectrum $\sim$ Planck function**

    - **Small spread of T around characteristic effective T_e of photosphere, approximately depth where $\tau \sim 1$ at any wavelength.**

    - F_λ **peak at** $\sim 2900/T_4$ **Å.**

    - **Photospheric temperatures $\sim$ 1000-100000 K.**

    - **Strong time variation only in minority of cases**

- <u>**Strong concentration to UVOIR**</u>**, with rise $\nu f_\nu \sim \nu^3$ to peak, then dropoff.**

- **Spectral slope at higher ν allows estimate of mean T_e.**

- **Major <u>absorption discontinuities</u> from ionization edges of abundant ions (e.g. H: Lyman edge 912 Å, Balmer edge 3646 Å).**

- Low level radiation in other bands from high temperature corona, synchrotron radiation, etc.

AGNs:

- Primary component is <u>very broad-band, nonthermal radiation</u> extending from radio to XR.

- Shape: <u>no simple parameterization</u>.

- Thermal components in IR (dust grains) & UV ("UV bump" from inner accretion disk).

- Continuum spectrum <u>depends on viewing angle</u> because of thick obscuring tori

- Strong time variation common

LINE SPECTRA

STARS:

- Complex, narrow, <u>absorption</u> lines

  - Produced by transitions in those atoms, ions, and molecules which are prevalent at characteristic T_e and pressure.

  - From thin layers of <u>cooler gas projected against higher T continuum</u> of inner photosphere.

- Doppler widths small (thermal), ~ few km s^{-1}

- Line spectrum reflects physical state (composition, temperature, pressure) of photosphere

- Lines and local continuum usually coupled (imply ~ same T)

AGNs:

- <u>Emission</u> lines since generally <u>not viewed against continuum source</u>.

- Wide range of ionizations (e.g. neutral to Fe XIV)

- **Wide range of Doppler widths in different galaxies, to >10^4 km s^{-1}**

- **Lines and local continuum <u>decoupled</u> since originate in different volumes**

- **Doppler widths reflect kinematic motions of gas clouds**

    - **"Broad" lines from $r \lesssim$ 1 pc**

    - **"Narrow" lines to $\gtrsim$ 100 pc from BH**

- **Line spectrum depends on <u>viewing angle</u> (inner regions concealed by thick tori, dust clouds). Polarization.**

DEDUCTIONS FROM OBSERVATIONS

STARS:

- **Continuum slope & structure: T**

- **Ionization edge discontinuities: pressure/gravity**

- **Line widths: <u>pressure/gravity</u>, rotation, outflows**

- **Line strengths: T, pressure/gravity, chemical abundances. E.g.:**

    - **Classic <u>"spectral-type"</u> sequence is a <u>T-sequence</u>**

    - **<u>Abundances</u>: selected species easy to measure: e.g. Ca/H, Mg/H, Fe/H. He/H (hot stars only)**

    - **Light element (e.g. C,N,O) abundances more difficult: C IV (UV) in hot stars; various atomic lines in cool stars require high spec resol; molecules in cool stars (CH, CN, NH, etc)**

    - **Ionization decreases with increasing gas pressure: e.g. use Mg I 5175 Å strength as <u>dwarf/giant discriminant</u> for Galactic structure studies**

    - **NB: Derived abundances are sensitive to proper T,P estimation**

- **Integrated light of stars allows inferences concerning ages, abundances of distant stellar populations. "Population synthesis":**

    - **Fit full energy distribution with combinations of <u>single generation models</u> to determine star formation history & abundances**

- Use selected lines for <u>age-abundance separation</u>, e.g. $H\beta$, Mg,Fe for old pops

AGNs:

- **Slope & structure of continuum related to energy distribution of electrons, importance of Compton scattering, accretion disk structure, dust emission/absorption, etc.**
    - Less definitive interpretation than stellar continua because of multiple components, complex generation mechanisms, absence of near-TEQ.
    - One test for a <u>nonthermal source</u>: polarization. Another: compare its mean surface brightness to the Planck function and derive corresponding T:

$$B_\nu(T) = f_\nu/\Omega$$

   where f is the flux, B is Planck function and Ω is the angular area (or upper limit) of the source. Is T "unphysically" high?

- **(Emission) line strengths yield electron temperature & gas density;**

- <u>Line ionization level</u> **constrains far-UV continuum ("hardness" of ionizing radiation).**

- <u>Line widths</u>, **positions probe kinematics of turbulent gas near BH, outflows, etc.**

- **Line strengths yield abundances**
    - ...although of <u>different</u> species than in stars: e.g. O, N, He, S, Fe (uncommon)...but not Ca, Mg (unless UV access), etc.

- **ID's, Surveys: strong emission line sources (photons concentrated to narrow bands) easier to detect than pure continuum sources**

References:

- **Properties of stars: D. F. Gray (1992) "Observation & Analysis of Stellar Photospheres"**

- **Properties of AGNs: B. M. Peterson (1997) "An Introduction to Active Galactic Nuclei"**

- **Spectroscopy: LLM, Sec. 5.1**

Last modified September 2003 by rwo

SIMPLE RADIATIVE TRANSFER

The <u>theory of radiative transfer</u> provides the means for determining the emergent EM spectrum of a cosmic source and also for describing the effects of media through which the radiation passes on its way to final detection.

References:

LLM, Section 5.1

Gray (1992) "Observation & Analysis of Stellar Photospheres"

Kourganoff (1963) "Basic Methods in Transfer Problems"

Mihalas (1978) "Stellar Atmospheres"
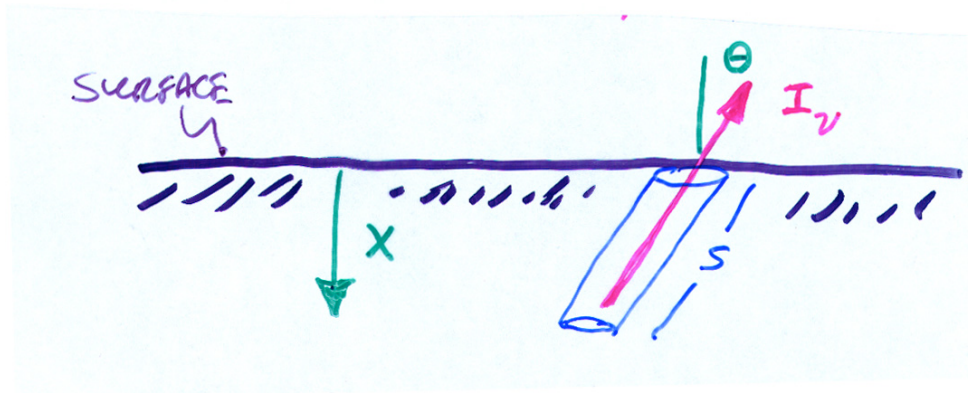
Shu (1991) "The Physics of Astrophysics: Vol. 1 Radiation"

Zeldovich & Raizer (1966) "Physics of Shock Waves & High Temperature Hydrodynamic Phenomena"

Only simple discussion here, for plane-parallel, 2D case

Details: ASTR 543-4

**THE EQUATION OF TRANSFER: describes the change in
<u>specific intensity</u> for photons traveling a distance s in a specific
direction at a given position x in a source**

$$dI_\nu(x, \nu, \theta) = -\kappa(x, \nu) I_\nu \, ds + j(x, \nu, \theta) \, ds$$

The EOT contains destruction (κI) and creation (j) terms

κ: Absorption coefficient. Units: cm^{-1}

**j: Emission coefficient. Units:
$\mathrm{ergs\ s^{-1}\, cm^{-3}\, Hz^{-1}\, sterad^{-1}}$**

Relation to quantities per particle:

**$\kappa = \sum_i n_i \alpha_i(\nu)$, where α is the radiative cross section
(cm^2) per particle at ν**

**$j = \sum_i n_i \epsilon_i(\nu, \theta)$, where ϵ is the emission coefficient
(intensity units) per particle at ν**

. . . and n_i is the density of particles of type i (units cm^{-3})

**NB: both κ and j include effects of photon <u>scattering</u>—i.e. redirection
of photons in θ**

Solution of EOT

Define: $\mu = \cos\theta$, **and**

$$\text{"optical depth"} \quad \tau(\nu) = \int\limits_{0}^{x} \kappa(x,\nu)\, dx$$

(recall x measures physical depth into source)

Then rewrite EOT as

$$\mu\frac{dI_\nu}{d\tau} = I_\nu - S_\nu$$

...where $S_\nu \equiv \dfrac{j(\nu)}{\kappa(\nu)}$ **is the "source function"**
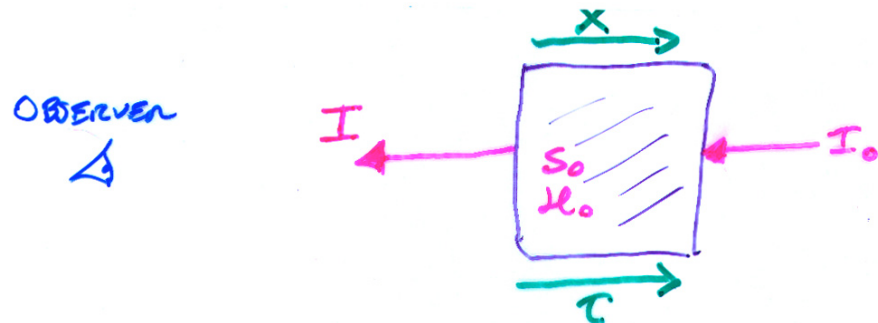
Formal solution, for I **at given** ν **(and** $\theta = 0$**) at surface of plane-parallel slab with optical depth** τ_1**:**

$$I_\nu = I_\nu(\tau_1)\, e^{-\tau_1} + \int\limits_{0}^{\tau_1} S_\nu(t)\, e^{-t} dt$$

The emergent intensity is the integral of the source function at a given optical depth in the layer weighted by $e^{-\tau}$ plus the fraction of the incident intensity which escapes absorption in the source (given by $e^{-\tau_1}$).

The integral is straightforward if S **is known in advance. But if the radiation field is important in determining the distribution of matter over states, then** S **will** <u>depend on</u> I **(over all** ν**), so that one must solve an** <u>integral equation</u>**. Techniques for doing this are in the references & ASTR 543-4.**

Application to a Uniform "Slab" Source

- **Plane-parallel, <u>homogeneous</u> source, intensity I_o incident on back side; no photon scattering**

- **For given ν, source function, emission, absorption coefficients are constant: j_o, κ_o, $S_o = j_o/\kappa_o$,**

- **Total physical depth $x_o \rightarrow$ optical depth $\tau_o = \kappa_o x_o$**

- **Then solution to EOT is**

$$I = S_o(1 - e^{-\tau_o}) + I_o e^{-\tau_o}$$

- **Limiting cases**

  - **<u>Optically thick</u>: $\tau_o(\nu) >> 1$: $I = S_o$**

    Interpretation: see into source a distance $\sim$ one optical depth, or $x_1 \sim 1/\kappa_o \rightarrow I \sim j_o x_1$
    Incident radiation totally extinguished

  - **<u>Optically thin</u>: $\tau_o(\nu) << 1$: $I = \tau_o S_o + I_o(1 - \tau_o)$**
    $$= j_o x_o + I_o(1 - \tau_o)$$

    Interpretation: see all photons generated in observer direction by slab; see all but fraction τ_o of incident photons

LTE

Kirchoff's Law:

- **In strict thermodynamic EQ at temperature T,**
$$I_\nu = B_\nu(T) \text{ and } dI/d\tau = 0$$
- **The EOT then requires that**
$$I_\nu = B_\nu(T) = S_\nu = j(\nu)/\kappa(\nu)$$
- **$\rightarrow$ Kirchoff's Law: $j(\nu)/\kappa(\nu) = B_\nu(T)$ in TEQ**

Local Thermodynamic Equilibrium:

- **If $S_\nu = j(\nu)/\kappa(\nu) \sim B_\nu(T)$ even if $I_\nu \neq B_\nu$, this is "LTE"**
- **Occurs where local collisions govern distribution over states and radiation is relatively weakly coupled to local matter**
- **A <u>remarkable simplification</u>, considering complexity of interactions & number of microstates affecting j and κ**
- **Often applies to dense astrophysical sources: e.g. <u>stellar atmospheres</u>.**

- **LTE slab: $I_\nu \sim B_\nu(T)(1 - e^{-\tau_o}) + I_0\, e^{-\tau_o}$, where T is a characteristic temperature**

APPLICATION TO STELLAR PHOTOSPHERES

Combining relations above, the emergent intensity from a stellar atmosphere in LTE will be (for $\theta = 0$)

$$I_\nu(\nu) = \int\limits_0^\infty B_\nu(\nu, T(\tau))\, e^{-\tau} d\tau$$

where τ is the optical depth at ν.

Basic computational problem: determine the $\underline{T(\tau)\ \text{function}}$. This requires solving a set of simultaneous integral equations.

• "Grey" Atmosphere: $\kappa = const$, independent of ν

τ is the same for all ν at a given physical depth x

Solve by various approximation techniques (see references). Solution is:
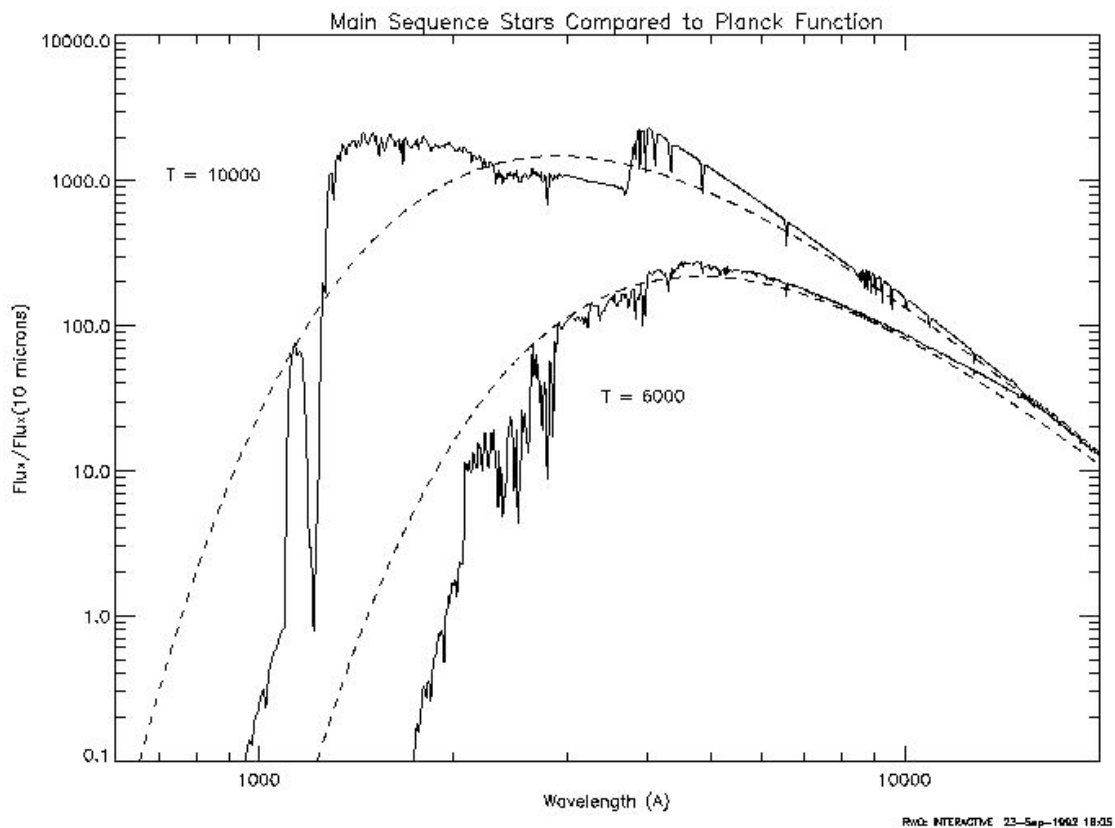
$$T^4(\tau) \sim \frac{3}{4}\,(\tau + \frac{2}{3})T_e^4$$

... where the "effective temperature" is defined by $T_e^4 \equiv F_0/\sigma_0$, and F_0 is the emergent bolometric flux at the top of the atmosphere

PHOTOSPHERES (continued)

- **The grey solution is a slowly varying function of wavelength, and $I_\nu \sim B_\nu(T_e)$.**

- **Useful approximation for various ROM applications.**

- **Departures from the grey solution occur because the real opacity can be a strong function of wavelength—e.g. in spectral "features" (absorption lines or continuum discontinuities) or in continuous opacity sources (e.g. H$^-$ in solar-type stars).**

- **For ν's where opacity is large, radiation emerges from layers closer to surface. These have <u>lower</u> temperatures, so the SED there falls below the grey approximation.**

- **But the energy absorbed where opacity is high must emerge elsewhere in the spectrum to conserve overall energy in the radiation flow; there output exceeds the grey approximation. See plots next page.**

PHOTOSPHERES (continued)

Comparison between true emergent spectrum from stellar photosphere and Planck functions

SOME UVOIR OBSERVING APPLICATIONS
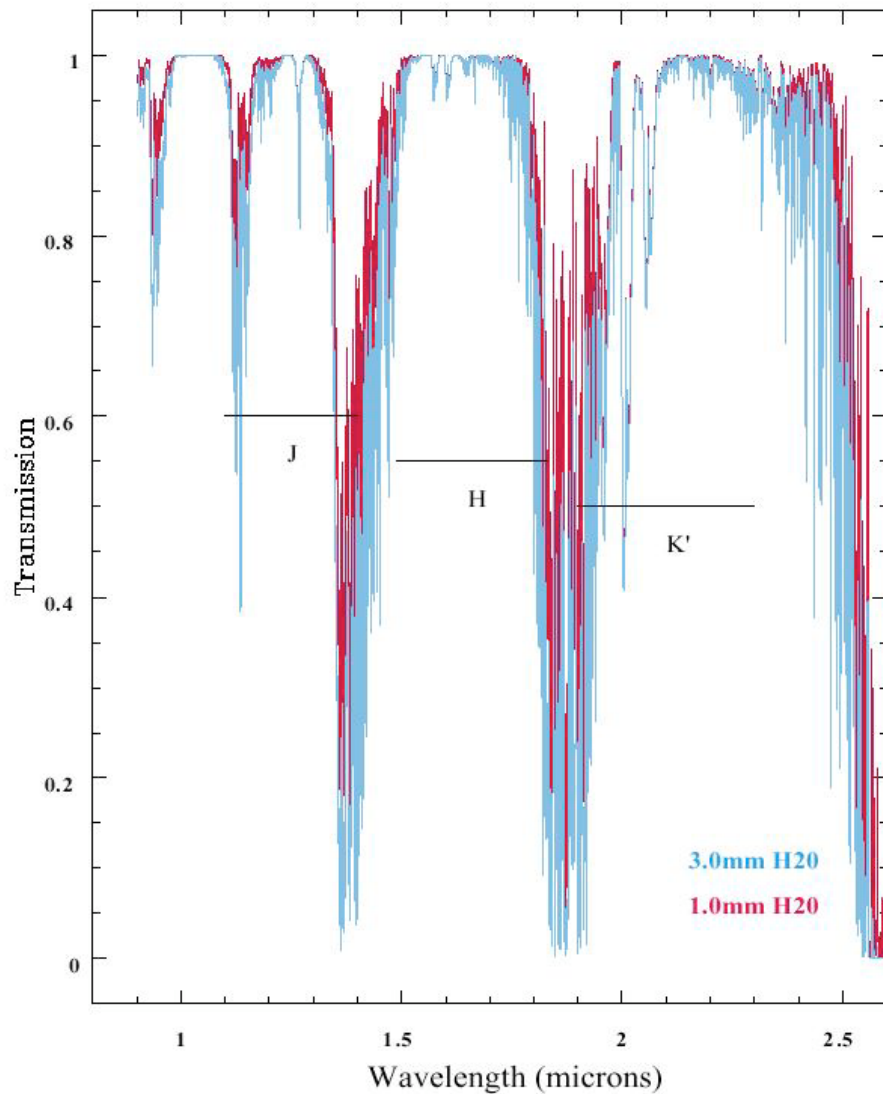
A. TRANSFER THROUGH EARTH'S ATMOSPHERE

- **Treat as LTE slab:** $I_\nu \sim B_\nu(T)(1 - e^{-\tau_o}) + I_0\, e^{-\tau_o}$
  ($\theta = 0$ assumed)

- **Molecular absorptive opacity (e.g. from H_2O) is important in the IR. Slab solution shows that absorption must be accompanied by <u>thermal</u> <u>emission</u>.**

- **Knowing $\tau(\nu)$ in a given band, can estimate effects of both absorption and emission of atmosphere by putting $T \sim$ 270 K into LTE slab solution.**

- **Note that the peak of B_ν at 270 K is at $\sim 20\mu$**

- **Combined absorption and contaminating emission seriously affect observations where τ is finite and $B_\nu(T)$ is large (mostly $\lambda > 1.5\mu$)**

- **Where B_ν at 270 K is small (e.g. $\lambda < 1\mu$), the atmosphere produces <u>"extinction"</u> given by $e^{-\tau_o(\nu)}$ term <u>without</u> re-emission.**

- **So, in optical bands, $I = I_0\, e^{-\tau_o(\nu)}$, and the extinction in magnitudes is**

$$\Delta m \equiv -2.5 \log_{10}(I/I_0) = 2.5\, \tau_o(\nu) \log_{10} e = 1.086\, \tau_o(\nu)$$
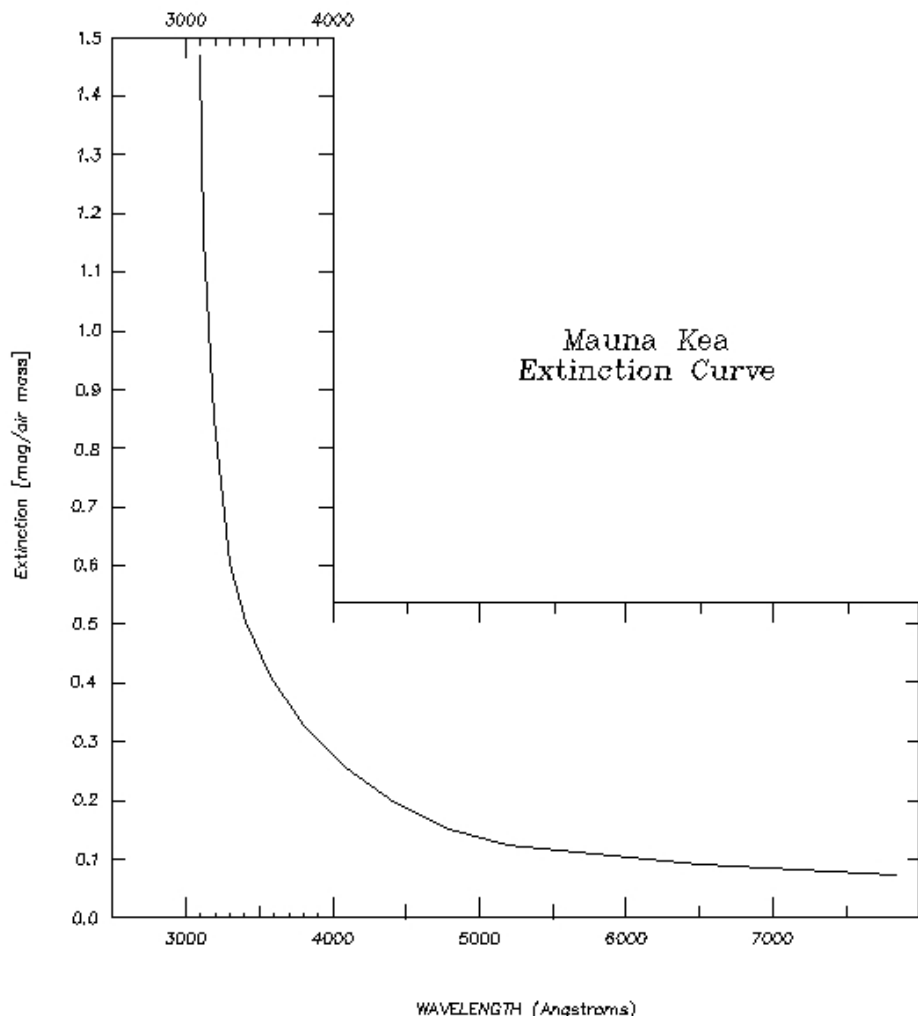
- **Several components contribute to $\tau(\nu)$ in Earth's atmosphere, with different ν dependence and altitude distributions. Extinction effects are illustrated on the next pages.**

TRANSFER IN THE ATMOSPHERE (continued)

Transmission of the Earth's atmosphere in the near-infrared. Absorption here is dominated by strong H_2O bands. Lines show the definitions of the J, H, and K' photometric bands, which lie in relatively clean regions.

TRANSFER IN THE ATMOSPHERE (continued)

Optical-band atmospheric extinction curve (in magnitudes per unit air mass) for Mauna Kea showing the strong increase to short wavelengths. Only the continuous component of extinction is shown.

B. INTERSTELLAR EXTINCTION

- **<u>Interstellar dust</u> is the main source of opacity in the interstellar medium at UVOIR wavelengths.**

- **Dust temperature is so low (usually < 100K) that re-emission in these bands is ~ 0, so $I = I_0 \, e^{-\tau_o(\nu)}$.**

- **Dust grains range in size from macromolecules to particles ~ 3000Å diameter.**

- **The grains responsible for UVOIR extinction consist mainly of silicates and graphite (carbon) and produce primarily continuous opacity.**

- **Typical radii and densities for such grains are $r \sim 0.05\mu = 500$ Å and $\rho \sim 3$ gr cm^{-3}.**

- **Optical depth for grains of a given type:**

  $$\tau(\nu) = n_g \, \pi r^2 \, Q(\nu) \, L$$

  ...where n_g is the density of grains per unit volume in the ISM, r is the grain radius, Q is the "extinction efficiency," and L is the pathlength

  Q includes both absorption and scattering effects
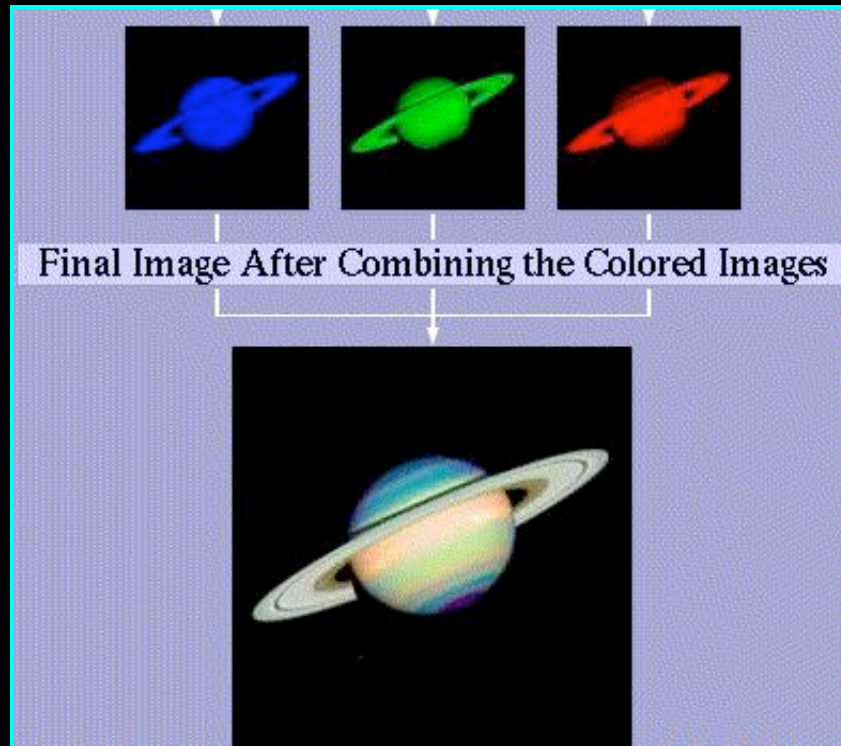
- **Must sum up over all types and sizes of grains**

- **For bands ~ 0.3–2.5μ, find empirically that extinction is**

  $$\Delta m(\nu) = 1.086 \, \tau(\nu) \sim K \, L \, (a + b \, \nu)$$

  ...where K, a, and b are constants

- **Typical extinction in the V-band is about 1 mag per 2×10^{21} gas atoms cm^{-2} in our Galaxy**

- **Any UVOIR photon energy absorbed is <u>re-radiated</u> by the grains at far-IR wavelengths ($> 50\mu$).**

INTERACTIVE COMPUTING AND IMAGE PROCESSING

Final Image After Combining the Colored Images

I. INTRODUCTION

Everyone knows that the science that can be done at a given time is circumscribed by the available resources. In astronomy, we often regard <u>telescopes</u> **as the essential infrastructure.**

But data taking and analysis resources are just as important, often more so, in determining what we can do. The development of astronomy over the last 50 years has been shaped by the capabilities of computers to a much larger extent than is often recognized.

II. HISTORY OF COMPUTERS IN ASTRONOMY

- **1800-1920: Women**

- **1920's-50's: Mechanical calculators (arithmetic)**

- **1960's:**

What is this picture?

    Mainframe computers (e.g. IBM 704, 360; CDC)
        Batch processing only (i.e. no interactive control)
        Hollerith punch card programming
        Data storage: punch cards or magnetic tape
        Fortran is dominant language
        VICAR: JPL planetary imaging reduction system
        CITRAN (Caltech), JOSS (MIT): experimental interactive time-sharing systems, running on mainframes; printer terminal I/O

- **1970-75:**

    Minicomputers (e.g. PDP) used in data acquisition
    HP & TI hand calculators appear (full function/programmable)
    Interactive data analysis using Tektronix graphics terminals
        E.g. NRAO, KPNO spectroscopy packages
        1-bit plots but no greyscale images

- **1975-80:**

    Fortran 77
    PC's appear, but little used professionally
    Early systems for interactive 2-D astronomical image processing:
        IRAF (KPNO), AIPS (NRAO), IDL (NASA)
        Use stand-alone greyscale (256 level) or multiframe (color) TV monitors

- **1980-85:**

    DEC VAX Minicomputers widely used
        Virtual memory allows processing of large images
        VAX's offer multiple shared terminal access; cards eliminated
        Greyscale/color terminals
    Standardized transportable astronomical data formats (FITS)
    File exchange protocols (e.g. FTP) developed
    Email available on limited-access networks (government)
    STScI develops STSDAS (IRAF-based) to reduce HST data
    IBM PC's used as desktop terminals; limited graphics
    X-windows software developed (MIT)
    Supercomputers (e.g. Cray) are specialized, expensive systems

- **1985-90:**

Mainframe computers/operating systems begin to fade
  1988: UVa Cyber mainframe allows maximum of 64 files per user(!) in disk storage
SUN, Silicon Graphics microcomputers gain popularity
  Desktop workstations include full graphics/image displays
  High capacity disk drives begin to drop rapidly in price
VAX/VMS operating system cedes ground to UNIX
TeX typesetting software invented by Donald Knuth
DAOPHOT (stand-alone Fortran program for stellar photometry)

- **1990-99:**

  UNIX systems dominate in astronomy
  LINUX (PC-based UNIX) appears
  Fortran 90/95 modernize the standard computational language
  Networked workstations/PC's linked to form supercomputers
  Microsoft Windows operating system appears
  Portable laptop computers become popular
  Graphical User Interfaces (GUI's) become widespread in applications software
  C, C++ in wide use
    (Note that the Baroque programming style of these languages is totally unsuited to the earlier punch-card environment.)
  Internet transforms computer communications
    Email becomes universal
    World Wide Web protocols established (led by physical scientists)
    Efficient browsers, search engines (e.g. Google)
    Astronomical public internet data centers established (e.g. CDS, NED, ADC)
    Public literature databases established (e.g. ADS, astro-ph)
    Internet data transfer rivals or replaces transfer by magnetic tape
  IRAF, STSDAS, AIPS, IDL become more sophisticated & robust
  CIAO (Chandra X-ray data reduction)

- **2000-- :**

  Search engines & literature databases become essential to routine work
  Electronic presentations become standard (Powerpoint, PDF)
  LINUX takes lead over UNIX for research systems
    Apple adopts LINUX for Macintosh OS-X
    Outlook poor for Windows in research
  Large databases established:
    Sky surveys (e.g. SDSS, 2MASS, POSS, NVSS)
    Telescope archives (e.g. STScI/MAST, Chandra, NOAO, NRAO)
  Plans for new facilities push envelope of computing power (e.g. ALMA, LSST)
  International virtual observatory planned

III. WIDELY-USED CURRENT SYSTEMS IN ASTRONOMY

A. Operating Systems

UNIX
LINUX and Apple OS-X
Windows
      Mainly for communications, text, presentations

B. Languages

General purpose: Fortran, C, C++, IDL
Scripting: Perl, Python

C. Multipurpose Interactive Astronomical Data Reduction Packages

UVOIR: IRAF, STSDAS, MIDAS
Radio: AIPS, AIPS++
X-ray: CIAO, TARA

D. Special Purpose Software (interactive and not)

Image Display: SAOImage, DS9, ATV
Point Source Photometry: DAOPHOT, DOPHOT
Plotting: SuperMongo, PGPLOT
Source ID/Classification: FOCAS, SExtractor
X-ray Model Spectra: XSPEC
Math/Statistics: Numerical Recipes (C, C++, Fortran)

E. Interactive Mathematical Packages

Mathematica, Maple, MATLAB

Recent evolution:

Dramatic improvements in computer hardware and software have made it possible to manipulate very large amounts of data rapidly and efficiently. However, the critical qualitative change in the conduct of astronomy has come about through access to powerful <u>interactive computation and display</u>, which permits understanding of numerical data in ways that were possible only for analytic functions 20 years ago.

> **===> In the last 20 years, interactive computing has produced a fundamental transformation in the conduct and scope of astronomical research.**

Choices?

If you become an observational astronomer, you have essentially <u>no choice</u> but to become familiar with IRAF/STSDAS (UVOIR), AIPS (radio), CIAO (X-ray), etc. because these provide the primary standardized data reduction procedures. The main decision, therefore, is what <u>other</u> systems are most profitable to learn.

IV. IDL

The "Interactive Data Language" is distributed by <u>Research Systems, Inc.</u>

Unique status as a fully interactive, high-level language with a large library of astronomer-written utilities.

Nearest thing to a <u>"universal" astronomical data system</u> because:

1. It is currently <u>used across the entire EM spectrum from gamma ray to radio wavelengths</u>. This is unlike most other astronomical software, which is usually confined to one wavelength regime.

2. It potentially duplicates the functionality of almost any other astronomical software, from simple arithmetic computations and graphics to full-blown GUI-based data analysis packages.

    Don't be misled: the capability is there, but <u>you</u> may have put in the effort to make it work, depending on the application.

Places to look for a quick introduction:

For introduction and applications to astronomical image processing, see the <u>Guide to IDL for Astronomers</u>

<u>Sample list of library software</u>

Key advantages over Fortran, C, etc:

Fully interactive with embedded graphics and I/O device drivers
Dynamic memory allocation
Accelerated computation on arrays
Large number of built-in interactive functions & utilities
Large body of public, easily-implemented astronomical utilities
Writing code with interactive programming/iteration greatly
    enhances efficiency & reliability
Pre-compilation not required

Key advantages over MATLAB, etc:

Full high-level programming features
Oriented toward image processing
Large suite of astronomical-oriented utilities (e.g. FITS file I/O,
    coordinate systems, astrometry, databasing, etc)

Key advantages over IRAF, etc:

Full high-level programming features; not simply a package of
    pre-defined, specialized programs

Intended for user customization, adaptation, extension
Active data stored in RAM, not as files
    (minimizes use of cumbersome file names and
    greatly facilitates computations)
Greater versatility, transparency, and user control
Journaling, command recall/edit, & other convenience features
    for increased efficiency
Source code for applications routines available and modifiable on demand
Writing code with interactive programming/iteration greatly
    enhances efficiency & reliability
Pre-compilation not required

Key disadvantages:

IDL is an <u>interpreted</u> rather than <u>compiled</u> language:
    Compiled languages execute more rapidly and use memory more efficiently. The
    differences will be invisible for most computations up to moderate scale. But for
    large-scale computing, Fortran and C are a better choice.
No equation-solving capability (use Mathematica/Maple there).

V. THE ROLE OF IDL

- **Data <u>analysis</u> and <u>visualization</u> (as opposed to reduction)**

    - **IDL is <u>not</u> a recommended alternative for routine data reduction tasks (e.g. for CCD mosaics) where IRAF, AIPS, etc., offer powerful, reliable, and convenient packages. These have gone through many iterations, and most user needs have been accommodated.**

    - **But the multitude of specialized analysis procedures needed following data reduction requires versatility, extended capabilities, and customization not offered by standard packages. IDL is optimized for this role.**

- **Bridging gaps in standard packages**

    - **IDL is now being used to convert and analyze NRAO GBT data in ways not possible with AIPS++**

    - **Convenience of IDL interface now recognized in effort to develop Python-based "PYRAF" in order to make IRAF "more like IDL"**

- **Any moderate-scale computation requiring file manipulation or generation of numerical tables, graphics displays, or images**

    - **There might be dozens of such applications arising in a single project that would be more cumbersome to program in a compiled or scripting language, especially if graphics is required**

    - **Like a "super hand-calculator," IDL is instantly available for a wide range of such**

applications

- **Enhancing scientist efficiency**

    The main concern of working scientists in approaching software should be how much of <u>their own time</u> elapses before they get a given result. Speed of execution is secondary, whereas the speed of coding/configuring and testing software is primary.

    Although we tend to think of computers in the context of large-scale "pipeline" computations and applications which are CPU/memory-bounded, these are really specialties. Less than 10% of the overall computing effort in astronomy (measured in person-hours) involves such problems.

    Instead, the software effort of most astronomers is devoted to moderate-scale computations, interactive data inspection and evaluation, special cases not supported by large applications packages, production of graphics for publications, and so forth.

    This environment places a premium on software <u>convenience, transparency, modularity, portability, and versatility</u>---exactly where IDL excels.

    The intrinsic capabilities of IDL coupled with its interactive environment and extensive user code libraries greatly enhance scientist efficiency. A given result can be reached using IDL in a small fraction of the time it would take to do the equivalent programming in other high level languages.

    IDL supplants graphics-display software such as SuperMongo or PGPLOT. It duplicates much, though not all, of the mathematical functionality of MATLAB, Maple, and Mathematica. It can do much of what can be done with PERL. Finally, it duplicates all the functionality of Fortran or C and is to be preferred unless the speed of computation is <u>really</u> important.

- **As an educational tool**

VI. IDL DEMOS

- A **demo** of interactive computing and image processing will be shown in class
- A package of standard IDL demos is supplied by RSI. Start from the UNIX prompt and type `idldemo`.
- An **IDL Tutorial** designed for this class introduces IDL's basic features and its use in image processing. Other sites offering IDL tutorials are linked to the **Astronomy User's Library**.

VII. GENERAL TIPS FOR DEALING WITH COMPUTERS

- **Computers are tools, <u>not science</u>**
- **Despite appearances, computers have <u>not</u> increased the capacity of the human brain to absorb and process information**
- **Don't trust and <u>always verify</u>**
- **If it's important, read it from <u>paper</u>**

    [I have yet to meet anyone who can proof-read accurately from a computer screen. I am not sure why this is, but it is not a comforting observation.]

Reading and lab assignments for this lecture

- **[Guide to IDL for Astronomers](#)**

- **[Laboratory II: Interactive Computing & Image Processing](#)**

Web links:

- **[List of Local & Other IDL Resources](#)**

- **[ASTR 511 IDL Tutorial](#)**

```
; IDL Version 5.2 (sunos sparc)
; Journal File for rwo@gemini.astro.Virginia.EDU
; Working directory: /net/gemini.vela/rwo/idldocs/demos/2003
; Date: Wed Sep 17 13:58:26 2003


;;; CLASSROOM IDL DEMO---JOURNAL FILE

;;; [Some editing done to provide headers & remove blunders]

;;; Warning: some routines, like "vline", "show", "maxmin", "zoomer", "boxer"
;;;    "resetcon", "rainbow2" are my own and not part of the Users Library.
;;;    I can make these available to you if you wish.

;;; SCALARS

a=3.0e10
z=a^2
print,z
;    9.00000e+20
print,a^2
;    9.00000e+20
print,a^2.26
;    4.76754e+23
print,a^8
;            Inf
; % Program caused arithmetic error: Floating overflow
b=alog10(a) & print,b
;        10.4771
print,10.0^b
;    3.00000e+10

;; VECTORS

x=fltarr(5)
print,x
;      0.00000      0.00000      0.00000      0.00000      0.00000
x=fltarr(5,2)
print,x
;      0.00000      0.00000      0.00000      0.00000      0.00000
;      0.00000      0.00000      0.00000      0.00000      0.00000

z=fltarr(5)
print,z+1
;      1.00000      1.00000      1.00000      1.00000      1.00000
z=fltarr(5)+1
z=z*5 & print,z
;      5.00000      5.00000      5.00000      5.00000      5.00000
print,z^2
;      25.0000      25.0000      25.0000      25.0000      25.0000

x=findgen(5) & print,x
;      0.00000      1.00000      2.00000      3.00000      4.00000
chan,9
plot,x
plot,x,psym=5
plot,x,psym=1
plot,x,psym=1,symsize=2

x=findgen(200)*0.1
print,max(x)
;      19.9000
print,min(x)
;      0.00000
?sin
plot,x,sin(x)
plot,x,sin(x)+x
plot,x,2*sin(x)+x
```

```
plot,x,5*sin(x)+x
plot,x,x*sin(x)+x
y=x*sin(x)+x


;;; WHERE utility


find=where(y gt 20)
print,find

; 132 133 134 135 136 137 138 139 140 141 142 143 144 145 146 147 148 149 150 151 152
; 153 154 190 191 192 193 194 195 196 197 198 199


oplot,x(find),y(find),psym=5


print,5/2.
;      2.50000
print,5/2
;      2


print,x(find)   ;;; [NOTE! My editor truncated some of the following
                ;;;     output lines.]


; 13.2000 13.3000 13.4000 13.5000 13.6000 13.7000 13.8000 13.9000
14.0000 14.1000 14.2000 14.3000 14.4000 14.5000 14.6000 14.7000
14.8000 14.9000 15.0000 1
;5.1000 15.2000 15.3000 15.4000 19.0000 19.1000 19.2000 19.3000
19.4000 19.5000 19.6000 19.7000 19.8000 19.9000


print,y(find)

; 21.0154 22.2053 23.3210 24.3511 25.2846 26.1116 26.8230 27.4109
27.8685 28.1903 28.3720 28.4108 28.3055 28.0560 27.6639 27.1325
26.4661 25.6709 24.7543 2

;3.7251 22.5933 21.3701 20.0680 21.8477 23.8336 25.7917 27.7026
29.5475 31.3080 32.9665 34.5060 35.9108 37.1661


;;; USER-SUPPLIED ROUTINE/PLANCK FUNCTION


;;;     DISPLAY INFORMATION HEADER FOR THIS ROUTINE


man,'planck
;        PLANCK()
; PURPOSE:
;        To calculate the Planck function in units of ergs/cm2/s/A
; CALLING SEQUENCE:
;        bbflux = PLANCK( wave, temp)
; INPUT PARAMETERS:
;        WAVE   Scalar or vector giving the wavelength(s) in **Angstroms**
;                at which the Planck function is to be evaluated.
;        TEMP   Scalar giving the temperature of the planck function in degree K
; OUTPUT PARAMETERS:
;        BBFLUX - Scalar or vector giving the blackbody flux (i.e. !pi*Intensity)
;                in erg/cm^2/s/A in at the specified wavelength points.
; EXAMPLES:
;        To calculate the blackbody flux at 30,000 K every 100 Angstroms between
;        2000A and 2900 A
;        IDL> wave = 2000 + findgen(10)*100
;        IDL> bbflux = planck(wave,30000)
;        If a star with a blackbody spectrum has a radius R, and distance,d, then
;        the flux at Earth in erg/cm^2/s/A will be bbflux*R^2/d^2
; PROCEDURE:
;        The wavelength data are converted to cm, and the Planck function
;        is calculated for each wavelength point. See Allen (1973), Astrophysical
;        Quantities, section 44 for more information.
; NOTES:
;        See the procedure planck_radiance.pro in
;        ftp://origin.ssec.wisc.edu/pub/paulv/idl/Radiance/planck_radiance.pro
```

```
;        for computation of Planck radiance given wavenumber in cm-1 or
;        wavelength in microns
; MODIFICATION HISTORY:
;        Adapted from the IUE RDAF                 August, 1989
;        Converted to IDL V5.0   W. Landsman    September 1997
;        Improve precision of constants     W. Landsman  January 2002


lam=findgen(40000)+500.

chan,9
plot,lam,planck(lam,5000)
plot_io,lam,planck(lam,5000)
plot,lam,planck(lam,10000)
plot,lam,planck(lam,1000)


;;; Relevant to Problem Set 2:

plot,lam,planck(lam,6000),xrange=[4000,6000]
oplot,lam,planck(lam,5000)
oplot,lam,planck(lam,5200)
oplot,lam,planck(lam,5500)
vline,5500

!p.title='Planck Fcn for various t'
!x.title='Wavelength'
plot,lam,planck(lam,6000),xrange=[4000,6000]

;;;
;;;  2-D ARRAYS

im=fltarr(25,25)+20.
im(5,15)=10000.
im(10,23)=10000.

chan,0
ctvscl,im,min=0,max=100
show,im,5
;

;;; READ FITS FILE

sd,'data
;/net/gemini.vela/rwo/idldocs/demos/2003/data

fits_read,'m87i-ex.fits',m87i,hdm87i

help,m87i

maxmin,m87i
;      432.874     -666.000

;;; IMAGE HISTOGRAM

chan,9
plothist,m87i
plothist,m87i,xrange=[0,200]
plothist,m87i,xrange=[0,20]
find=where(m87i eq -666,count) & print,count
;          2
;
show,m87i,2,min=0,max=20

;;; SLICES THRU IMAGE
;
plot,m87i(*,150)
plot,m87i(*,250)
```

```
;;; ZOOM

chan,0
ctvscl,m87i
zoomer
;Left for zoom center, Middle for new zoom factor, Right to quit


;;; AVAILABLE COLOR TABLES

retall
cdel,18
resetcon

show,m87i,2,min=0,max=170
;
rainbow2,1

exit

;;; ================== END OF FIRST PART OF DEMO =================

; IDL Version 5.2 (sunos sparc)
; Journal File for rwo@gemini.astro.Virginia.EDU
; Working directory: /net/gemini.vela/rwo/idldocs/demos/2003
; Date: Mon Sep 22 13:55:28 2003


;;; Continue IDL Demo, 9/22/03

;;; USE OF "SD" COMMAND

sd
;/net/gemini.vela/rwo/idldocs/demos/2003
sd,'data
;/net/gemini.vela/rwo/idldocs/demos/2003/data

;;; LIST FITS ("Flexible Image Transport System") FILES

fitsdir
;FITS File Directory Mon Sep 22 14:10:21 2003
;/net/gemini.vela/rwo/idldocs/demos/2003/data/*.fits
;
; NAME              SIZE      DATE-OBS   TELESCOP OBJECT            EXPTIME
;
;m87-GC1-stisim-ex 0         2001-04-23 HST      NGC4486-GCFIELD-1
;m87b-ex           301 301   2001-07-24
;m87i-ex           301 301   2001-07-24

;;; READ & DISPLAY ANOTHER FITS FILE:

fits_read,'m87-GC1-stisim-ex.fits',im,hdim
help,im

chan,0
ctvscl,im
ctvscl,im,min=0,max=200
ctvscl,im,min=90,max=200
ctvscl,im,min=90,max=800


chan,9
plot,im(*,300)    ;;; Plots a slice


chan,0
zoomer
;Left for zoom center, Middle for new zoom factor, Right to quit

;;; UNSHARP MASKING
```

```
blur=median(im,11)
chan,1
ctvscl,blur,min=90,max=800

diff=im-blur

ctvscl,diff
ctvscl,diff,min=20,max=80
ctvscl,diff,min=20,max=60


;;; USE FIND ALGORITHM FROM DAOPHOT TO ID POINT SOURCES

chan,0

find,im,xc,yc
;Enter approximate FWHM:
;  6
;RELATIVE ERROR computed from FWHM      0.788343
;Enter minimum value above background for threshold detection:
;  250
;Enter low and high cutoffs, press [RETURN] for defaults:
;Image Sharpness Statistic (DEFAULT = 0.2,1.0):
;
;Image Roundness Statistic [DEFAULT = -1.0,1.0]:
;
;114 local maxima were located above threshold
; Do you want to continue at this HMIN? [YES]
;
;             STAR      X       Y      FLUX     SHARP      ROUND
;                0   531.3    58.8   1492.8     0.86       0.00
;                1   489.1    67.2    357.2     0.86       0.15
;                2   289.7    69.0    566.5     0.82      -0.04
;                3   413.0    72.7   3153.4     0.99       0.05
;                4   516.4    91.0    344.0     0.90      -0.02
;                5   283.2   111.6    840.0     0.86       0.06
;                6   330.1   126.9    524.9     0.97      -0.05
;                7   538.2   137.1   1757.8     0.91       0.04
;                8   318.8   138.3   1978.8     0.79      -0.02

;;; ...abbreviated listing here

;               37   923.9   506.2    990.1     0.93       0.01
;               38   225.8   508.2    544.5     0.94      -0.05
; No. of sources rejected by SHARPNESS criteria        75
; No. of sources rejected by ROUNDNESS criteria         0
; No. of sources rejected by CENTROID  criteria         0
; No. of sources ACCEPTED            39
; Threshold above background (HMIN) for this pass was    250.0
;Enter new threshold or [RETURN] to exit:
;


;;; MARK IDS ON ORIGINAL DIPLAYED IMAGE

chan,0
boxer,13,xc,yc


;;; CALL ATV, an IDL GUI image display/analysis package similar to XIMTOOL,
;;;    SAOImage, DS9

atv,im


;;; <<<<<<<<<<<<<<<<<<<<<<<<<<< END DEMO <<<<<<<<<<<<<<<<<<<<<<<<<<<<<<<<<
```

STATISTICS OF OBSERVATIONS & SAMPLING THEORY

References:

    Bevington "Data Reduction & Error Analysis for the Physical Sciences"

    LLM: Appendix B

    <u>Warning</u>: the introductory literature on statistics of measurement is remarkably uneven, and nomenclature is not consistent.

Is error analysis important? Yes! See next page.

Parent Distributions
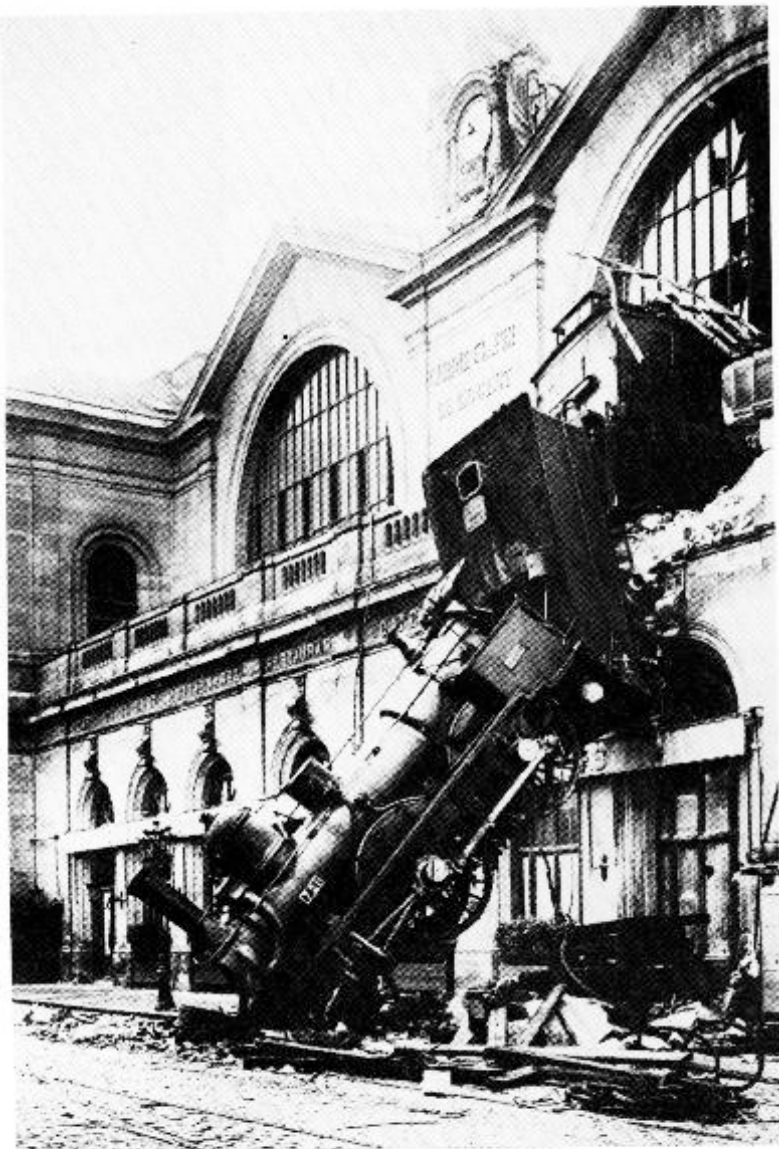
Measurement of any physical quantity is always affected by uncontrollable random ("stochastic") processes. These produce a statistical scatter in the values measured.

The <u>parent distribution</u> for a given measurement gives the probability of obtaining a particular result from a single measure. It is fully defined and represents the idealized outcome of an infinite number of measures, where the random effects on the measuring process are assumed to be always the same ("stationary").

An Introduction to Error Analysis
The Study of Uncertainties in Physical Measurements

John R. Taylor

Precision vs. Accuracy

- **The parent distribution only describes the stochastic scatter in the measuring process. It does <u>not</u> characterize how close the measurements are to the <u>true</u> value of the quantity of interest. Measures can be affected by <u>systematic errors</u> as well as by random errors.**

  In general, the effects of systematic errors are not manifested as stochastic variations during an experiment. In the lab, for instance, a voltmeter may be improperly calibrated, leading to a bias in all the measurements made. Examples of potential systematic effects in astronomical photometry include a wavelength mismatch in CCD flat-field calibrations, large differential refraction in Earth's atmosphere, or secular changes in thin clouds.

- **Distinction between <u>precision</u> and <u>accuracy</u>:**

  - **o A measurement with a large ratio of value to statistical uncertainty is said to be "precise."**

  - **o An "accurate" measurement is one which is close to the <u>true</u> value of the parameter being measured.**

  - **o Because of systematic errors precise measures may <u>not</u> be accurate.**

  - **o A famous example: the primary mirror for the Hubble Space Telescope was figured with high precision (i.e. had very small ripples), but it was inaccurate in that its shape was wrong.**

- **The statistical infrastructure we are discussing here does not permit an assessment of systematic errors. Those must be addressed by other means.**

Moments of Parent Distribution

The parent distribution is characterized by its <u>moments</u>:

- **Parent probability distribution:** $p(x)$

- **Mean: first moment.** $\mu \equiv \int x\, p(x)\, dx$

- **Variance: second moment.**

$$Var(x) \equiv \int (x - \mu)^2\, p(x)\, dx$$

- **"Sigma":** $\sigma \equiv \sqrt{Var(x)}$

- **Aliases:** σ **is the <u>standard deviation</u>, but is also known as the "dispersion" or "rms dispersion"**

- μ **measures the "center" and** σ **measures the "width" of the parent distribution.**

> **NB: the mean can be very different from the <u>median</u> (50th percentile) or the <u>mode</u> (most frequent value) of the parent distribution. These represent alternative measures of the distribution's "center." But the mean is the more widely used parameter.**

Poisson Probability Distribution

Applies to any <u>continuous counting process</u> where events are <u>independent</u> of one another and have a <u>uniform</u> probability of occurring in any time bin.

The Poisson distribution is derived as a limit of the "binomial distribution" based on the fact that time can be divided up into small intervals such that the probability of an event in any given interval is arbitrarily small.

If n is the number of counts observed in one δt bin, then

$$p_P(n) = \frac{\mu^n}{n!}\, e^{-\mu}$$

Properties:

$\sum\limits_{n=0}^{\infty} p_P(n) = 1$

Asymmetric about μ; mode $\leq \mu$

Mean value per bin: μ. μ need not be an integer.

Variance: μ
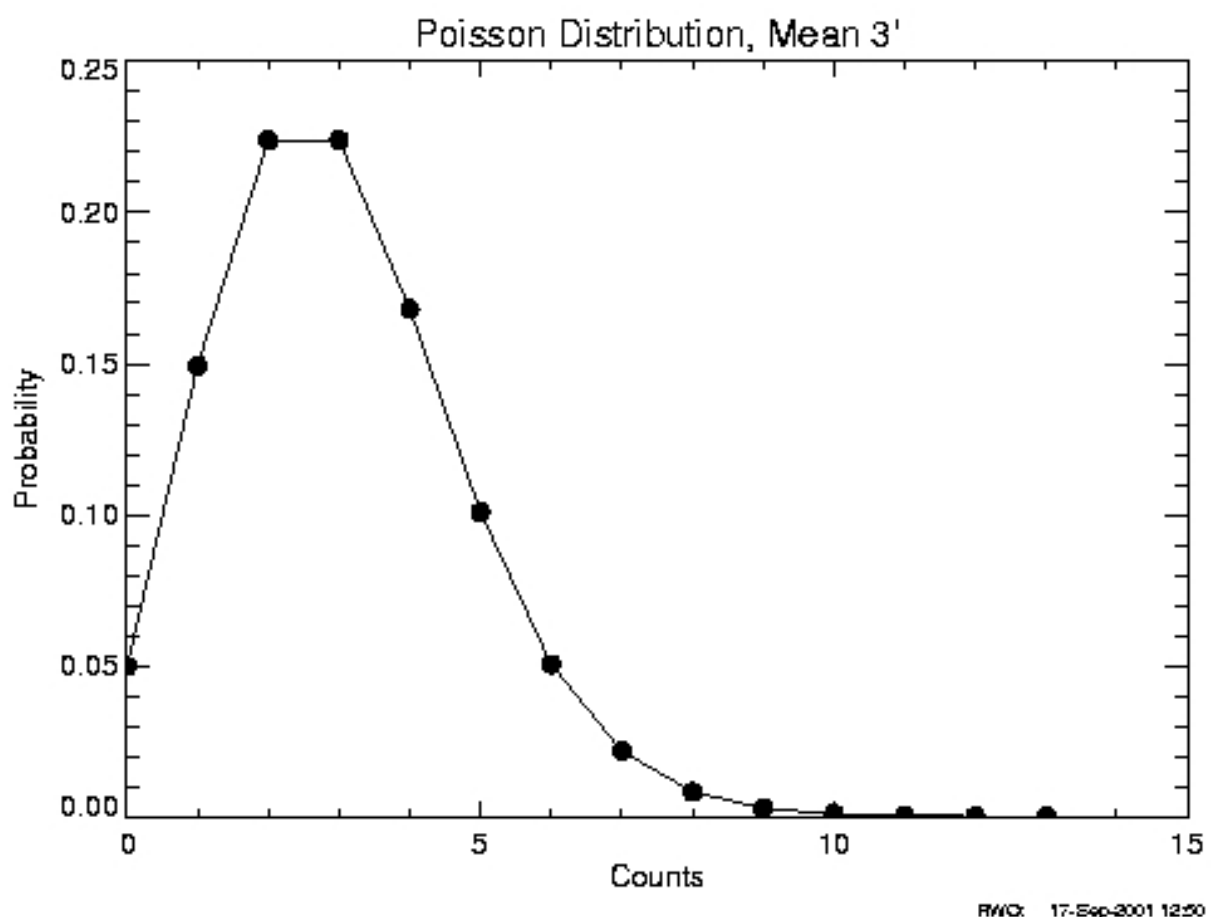
Standard deviation: $\sigma = \sqrt{\mu}$

Implies mean/width $= \mu/\sqrt{\mu} = \sqrt{\mu}$
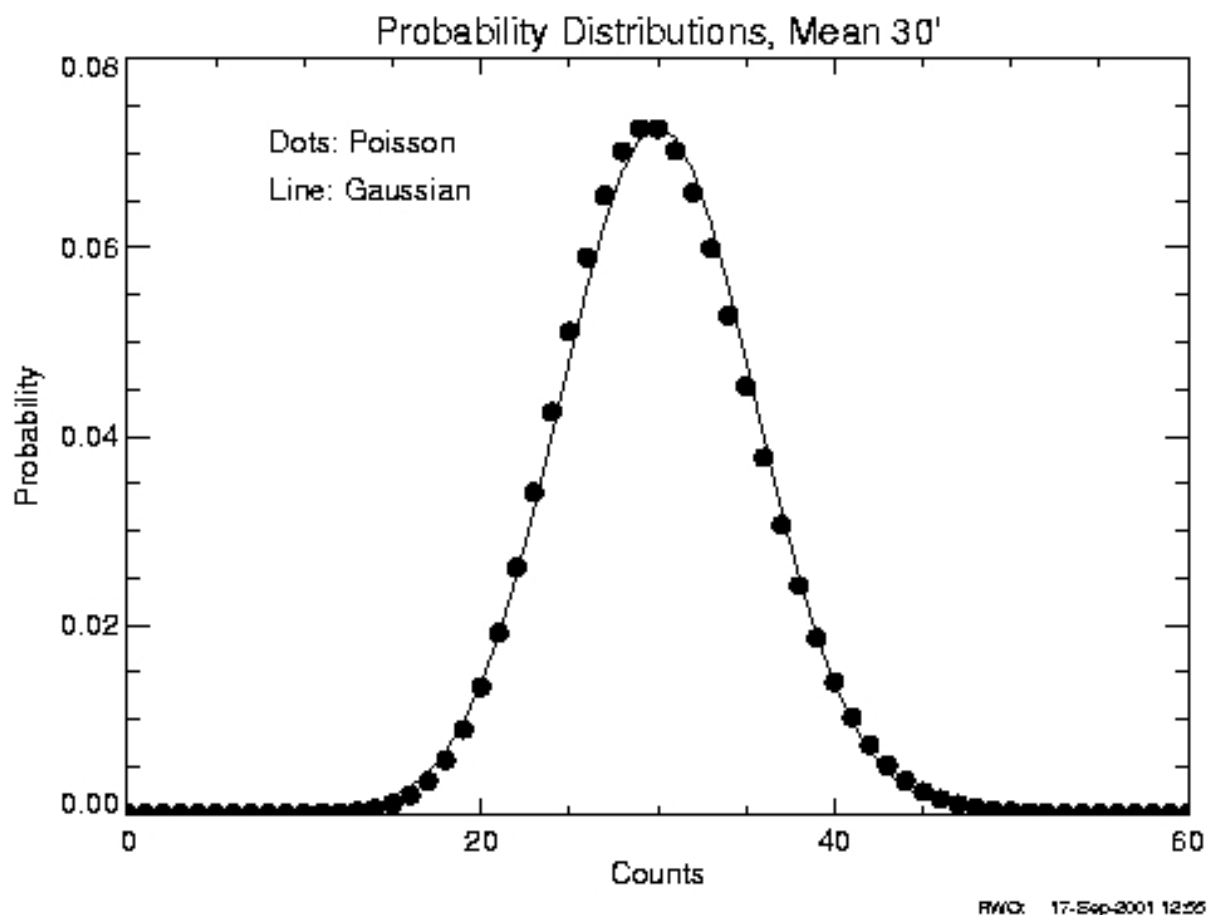
$\rightarrow$ "Square root of n statistics"

NB: the Poisson distribution is the proper description of a uniform counting process for small numbers of counts. For larger numbers ($n \gtrsim 30$), the Gaussian distribution is a good description and is easier to compute.

SAMPLE POISSON DISTRIBUTION

POISSON AND GAUSSIAN COMPARED

Probability Distributions, Mean 30'

Dots: Poisson
Line: Gaussian

RWO: 17-Sep-2001 12:55

Gaussian Probability Distribution

The Gaussian, or "normal," distribution is the limiting form of the Poisson distribution for large μ ($\gtrsim 30$)

Probability distribution:

$$p_G(x) = \frac{1}{\sigma\sqrt{2\pi}} \exp\left[-\tfrac{1}{2}\left(\tfrac{x-\mu}{\sigma}\right)^2\right]$$

Properties:

$$\int\limits_{-\infty}^{+\infty} p_G(x)\, dx = 1$$

"Bell-shaped" curve; symmetric about mode at μ

Mean value: μ (= median and mode)

Variance: σ^2
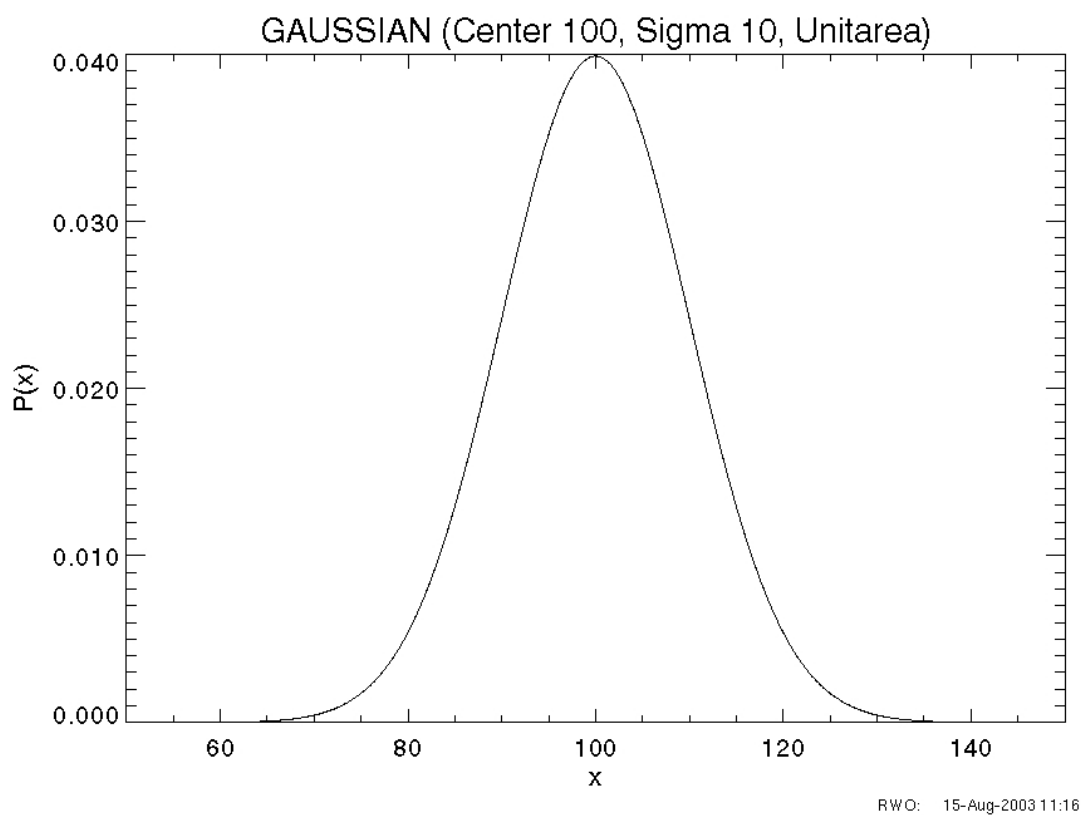
Full Width Half Maximum = $2.355\,\sigma$

If refers to a counting process ($x = n$ in bin), then $\sigma = \sqrt{\mu}$
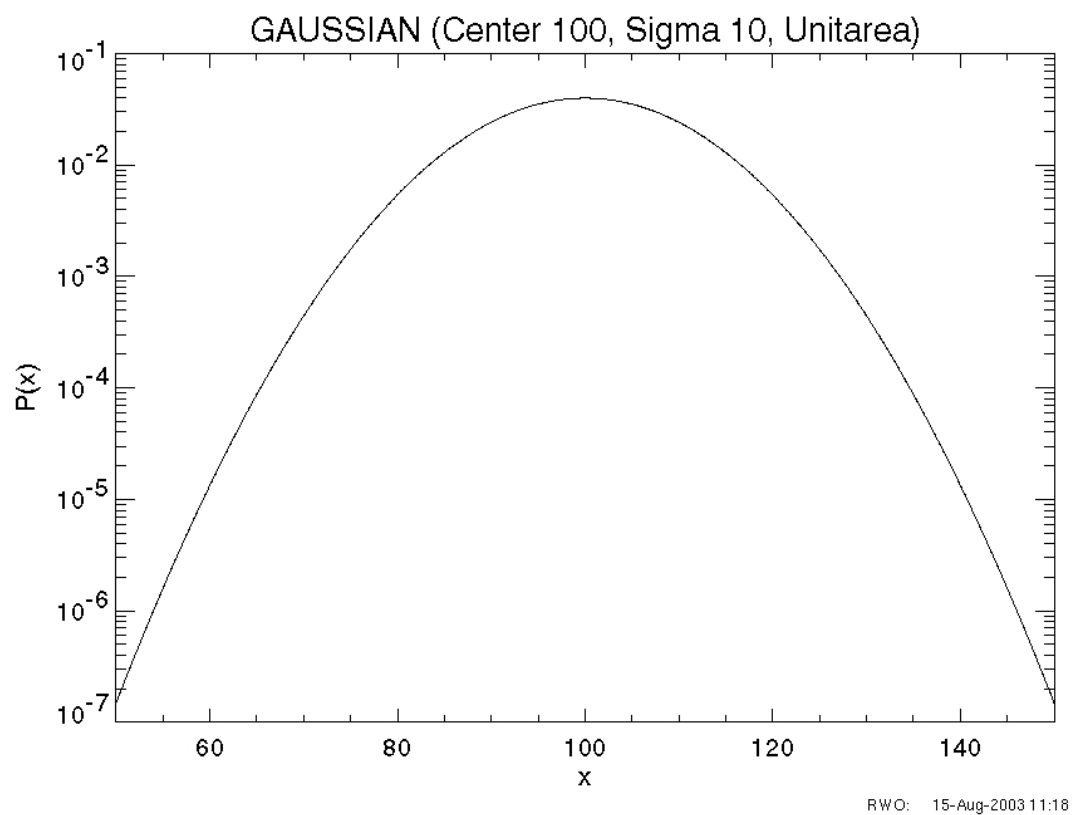
Importance:

> The "central limit theorem" of Gauss demonstrates that a Gaussian distribution applies to any situation where a large number of independent random processes contribute to the result. This means it is a valid statistical description of an enormous range of real-life situations. Much of the statistical analysis of data measurement is based on the assumption of Gaussian distributions.

SAMPLE GAUSSIAN DISTRIBUTION (Linear)

GAUSSIAN (Center 100, Sigma 10, Unitarea)

RWO: 15-Aug-2003 11:16

SAMPLE GAUSSIAN DISTRIBUTION (Log)

GAUSSIAN (Center 100, Sigma 10, Unitarea)

RWO: 15-Aug-2003 11:18

Chi-Square Probability Distribution

The Chi-Square (χ^2) function gives the probability distribution for any quantity which is the sum of the squares of independent, normally-distributed variables with unit variance. In the method of maximum likelihood it is important in testing the functional relationship between measured quantities.

Probability distribution:

$$p_\chi(\chi^2, \nu) = \frac{1}{2^{\nu/2}\,\Gamma(\nu/2)}\,(\chi^2)^{0.5(\nu-2)}\,\exp[-\chi^2/2]$$

...where the Gamma function is defined as follows:

$\Gamma(n+1) = n!$ if n is an integer

$\Gamma(1/2) = \sqrt{\pi}$ and $\Gamma(n+1) = n\Gamma(n)$ if n is half-integer

Properties:

Only one parameter, ν, the "number of degrees of freedom." $\nu =$ the number of independent quantities in the sum of squares.

Mean and mode: ν. Variance: 2ν

Asymmetric distribution

Sampling Theory

In practice, we usually do not know the parameters of the parent distribution because this requires a very large number of measures. Instead, we try to make <u>inferences</u> about the parent distribution from finite (& often small) <u>samples</u>. Sampling theory describes how to <u>estimate</u> the moments of $p(x)$.

The results here are based on applying the "method of maximum likelihood" to variables whose parent distribution is assumed to be <u>stationary and normally distributed</u>.

Suppose we obtain a sample consisting of M measurements of a given variable characterized by a normal distribution (with mean μ and standard deviation σ). Define the following two estimators:

- **Sample mean:** $\bar{x} \equiv \dfrac{1}{M} \displaystyle\sum_{i=1}^{M} x_i$

- **Sample variance:** $s^2 \equiv \dfrac{1}{M-1} \displaystyle\sum_{i=1}^{M} (x_i - \bar{x})^2$

These two estimators have the property that as $M \to \infty$,
$$\bar{x} \longrightarrow \mu \text{ and } s^2 \longrightarrow \sigma^2$$

SAMPLING THEORY (cont)

How well determined is $\bar{x}$?

> **The "uncertainty" in $\bar{x}$ is its variance. But this is <u>not</u> the same as the variance in x. $\bar{x}$ is a random variable, and its variance can be computed as follows:**

$$s_{\bar{x}}^2 \equiv Var(\bar{x}) = \frac{1}{M^2} \sum_{i=1}^{M} Var(x_i) = \frac{1}{M} Var(x)$$

$$s_{\bar{x}}^2 \sim \frac{1}{M} s^2$$

$$s_{\bar{x}}^2 \sim \frac{1}{M(M-1)} \sum_{i=1}^{M} (x_i - \bar{x})^2$$

> $s_{\bar{x}}$ **is known as the "standard error of the mean"**

> **Important! $s_{\bar{x}} << \sigma$ if M is large.**

> **The distinction between σ and $s_{\bar{x}}$ is often overlooked by students and can lead to flagrant overestimation of errors in mean values.**

> **The mean of a random variable can be determined very precisely regardless of its variance. This demonstrates the importance of repeated measurements...if feasible.**

SAMPLING THEORY (cont)

Probability Distribution of $\bar{x}$:

By the central limit theorem, if we repeat a set of M measures from a given parent distribution a large number of times, the resulting distribution of $\bar{x}_M$ will be a normal distribution regardless of the form of the parent distribution $p(x)$. It will have a standard deviation of $\sigma/\sqrt{M}$.

Inhomogeneous samples:

A sample is inhomogeneous if σ of the parent distribution is different for different measurements. This could happen with a long series of photometric determinations of a source's brightness, for instance.

Here, the values entering the estimates of the sample mean and variance must be weighted in inverse proportion to their uncertainties. The following expressions assume that the variance of each measurement can be estimated in some independent way:

Sample mean:
$$\bar{x} = \sum_{i=1}^{M} w_i x_i \, / \sum_{i=1}^{M} w_i$$

Variance of the mean:
$$s_{\bar{x}}^2 = 1 / \sum_{i=1}^{M} w_i$$

... where $w_i = \dfrac{1}{\sigma_i^2}$

The "Signal-to-Noise Ratio" (SNR) for Flux Measurements

We adopt the <u>sample mean</u> $\bar{x}$ as the best estimate of the flux and $s_{\bar{x}}$, the <u>standard error of the mean</u> (not the standard deviation of the parent distribution), as the best estimate of the uncertainty in the mean flux.

Our working definition of signal-to-noise ratio is then:

$$SNR \equiv \bar{x}/s_{\bar{x}}$$

$s_{\bar{x}}$ here must include <u>all</u> effects which contribute to random error in the quantity x.

This is a basic "figure of merit" that should be considered in both planning observations (based on expected performance of equipment) and in evaluating them after they are made.

Propagation of Variance to Functions of Measured Variables

If $u = f(x, y)$ is a function of two random variables, x and y, then we can propagate the uncertainty in x and y to u as follows:

$$\sigma_u^2 = \sigma_x^2 \left(\frac{\partial u}{\partial x}\right)^2 + \sigma_y^2 \left(\frac{\partial u}{\partial y}\right)^2 + 2\sigma_{xy}^2 \left(\frac{\partial u}{\partial x}\right) \left(\frac{\partial u}{\partial y}\right)$$

where the "covariance" of x and y is defined as

$$\sigma_{xy} \equiv \lim_{M \to \infty} \frac{1}{M} \sum_i [(x_i - \bar{x})(y_i - \bar{y})]$$

For <u>independent</u> random variables, $\sigma_{xy} = 0$.

So, we obtain for the following simple functions:

$$Var(kx) = k^2 \, Var(x) \text{ if } k \text{ is a constant}$$
$$Var(x + y) = Var(x) + Var(y) + 2\sigma_{xy}^2$$
$$Var(xy) = y^2 \, Var(x) + x^2 \, Var(y) + 2xy\sigma_{xy}^2$$

Confidence Intervals

A "confidence interval" is a range of values which can be
expected to contain a given parameter (e.g. the mean) of the
parent distribution with a **specified probability**. The smaller the
confidence interval, the higher the precision of the measure.

(A) In the ideal case of a single measurement drawn from a
normally-distributed parent distribution of **known** mean and
variance, confidence intervals for the mean in units of σ are
easy to compute in the following form:

$$P(\pm k\sigma) = \int_{\mu - k\sigma}^{\mu + k\sigma} p_G(x, \mu, \sigma)dx$$

where p_G is the Gaussian distribution. Results from this
calculation are as follows:

k	$P(\pm k\sigma)$
0.675	0.500
1.0	0.683
2.0	0.954
3.0	0.997

Intepretation: A single measure drawn from this distribution
will fall within $1.0\,\sigma$ of the mean value in 68% of the
samples. Only 0.3% of the samples would fall more than
$3.0\,\sigma$ from the mean.

CONFIDENCE INTERVALS (cont)

(B) In the real world, we have only <u>estimates</u> of the properties of the parent distribution based on a finite sample. The larger the sample, the better the estimates, and the smaller the confidence interval.

To place confidence intervals on the estimate of the parent mean (μ) based on a finite sample of M measures, we use the probability distribution of the <u>"Student" t variable</u>:

$$t = (\bar{x} - \mu)\sqrt{M}/s$$

where s^2 is the sample variance. The probability distribution of t depends on the number of degrees of freedom, which in this case is $M - 1$. The probability that the true mean of the parent distribution lies within $\pm t\, s_{\bar{x}}$ of the sample mean is estimated by integrating the Student t-distribution from $-t$ to $+t$.

$$P(\mu \in \bar{x} \pm t\, s_{\bar{x}})$$

t	$M = 2$	$M = 10$	$M = \infty$
0.5	0.295	0.371	0.383
0.6745	0.377	0.483	0.500
1.0	0.500	0.657	0.683
2.0	0.705	0.923	0.954
3.0	0.795	0.985	0.997

CONFIDENCE INTERVALS (cont)

Interpretation & comments on the t-distribution results:

- **Entries for $M = \infty$ correspond to those for the Gaussian parent distribution quoted earlier, as expected.**

- **Values for small M can be very different than for $M = \infty$. The number of observations is an <u>important</u> determinant of the quality of the measurement.**

- **The entry for 0.6745 is included because the formal definition of the <u>"probable error"</u> is $0.6745\, s_{\bar{x}}$. For a large number of measures, the probable error defines a 50% confidence interval. But for small samples, it is a <u>very weak</u> constraint.**

- **A better measure of uncertainty is the <u>standard error of the mean</u>, $s_{\bar{x}}$, which provides at least a 50% confidence interval for all M.**

- **Careful authors often quote "$3\,\sigma$" confidence intervals. This corresponds to $t = 3$ and provides 80% confidence for two measures and 99.7% for many measures. It is a strong contraint on results of a measurement.**

- **NB; the integrals in the preceding table were derived from an IDL built-in routine. The table contains output from the IDL statement: `P = 2*T_PDF(t,M-1)-1`.**

GOODNESS OF FIT (χ^2 TEST)

Widely used standard for comparing an observed distribution with a <u>hypothetical functional relationship</u> for two or more related random variables. Determines the likelihood that the observed deviations between the observations and the expected relationship occur by chance. Assumes that the measuring process is governed by <u>Gaussian</u> statistics.

Two random variables x and y. Let y be a function of x and a number k of additional parameters, α_j: $y = f(x; \alpha_1...\alpha_k)$.

1. **Make M observations of x and y.**

2. **For each observation, estimate the total variance in the y_i value, σ_i^2**

3. **We require $f(x; \alpha_1...\alpha_k)$. Either this must be known a priori, or it must be estimated from the data (e.g. by least squares fitting).**

4. **Then define**

$$\chi_0^2 = \sum_i^M \left(\frac{y_i - f(x_i)}{\sigma_i} \right)^2$$

5. **The probability distribution for χ^2 was given earlier. It depends on the number of degrees of freedom ν. If the k parameters were estimated from the data, then $\nu = M - k$.**

6. **The predicted mean value of χ^2 is ν.**

7. The integral $P_0 = \int\limits_{\chi_0^2}^{\infty} p(\chi^2, \nu) d\chi^2$ then determines the probability that this or a higher value of χ_0^2 would occur by chance.

8. The larger is P_0, the more likely it is that f is correct. Values over 50% are regarded as consistent with the hypothesis that $y = f$.

9. Sample values of χ^2 yielding a given P_0:

P_0	$\nu = 1$	$\nu = 10$	$\nu = 200$
0.05	3.841	1.831	1.170
0.10	2.706	1.599	1.130
0.50	0.455	0.934	0.997
0.90	0.016	0.487	0.874
0.95	0.004	0.394	0.841

10. Generally, one uses $1 - P_0$ as a criterion for <u>rejection</u> of the validity of f:

   E.g. if $P_0 = 5\%$, then with 95% confidence one can reject the hypothesis that f is the correct description of y.

11. Important caveat: the χ^2 test is <u>ambiguous</u> because it makes 2 assumptions: that f is the correct description of $y(x)$ <u>and</u> that a Gaussian process with the adopted σ's properly described the measurements. It will reject the hypothesis if <u>either</u> condition fails.

```
; IDL Version 5.2 (sunos sparc)
; Journal File for rwo@gemini.astro.Virginia.EDU
; Working directory: /net/gemini.vela/rwo/511/jnl
; Date: Wed Sep 24 14:06:01 2003

 ;;; Generate a 200x200 array filled with random noise characterized
 ;;;  by a Poisson distribution with mean 10/pixel

noise=randomn(seed,200,200,poisson=10)
show,noise,3
;

zoomer
;Left for zoom center, Middle for new zoom factor, Right to quit

chan,9

 ;;; Plot row slices through array. Does it "look" random?

plot,noise(*,100)
plot,noise(*,101)
plot,noise(*,102)
plot,noise(*,108)

 ;;; Plot histogram for individual pixels in full array

plothist,noise
meanarray,noise
;
;      Mean         RMS      SE(Mean)        Max          Min
;      9.998       3.159      0.016      2.6000e+01   0.0000e+00


 ;;; Generate  20 pixel samples and find means; repeat a total
 ;;;    of 200 times:

samp20=fltarr(200)

for i=0,199 do samp20(i)=mean(noise(0:19,i))

 ;;; Compare parent histogram to histogram of 20-pixel means

plothist,samp20,xs,ys,bin=0.2,/noplot
chan,9
plothist,noise
oplot,xs,ys*200,psym=10

 ;;; The width of the sample mean distribution should be
 ;;;  smaller by factor sqrt(20).
```
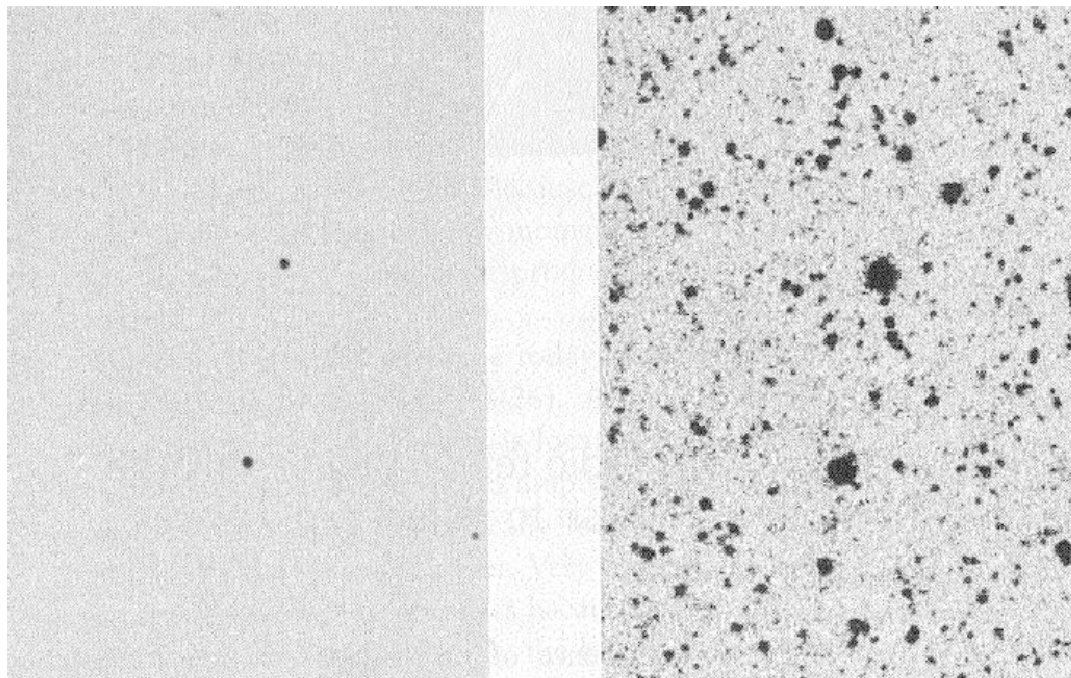
UVOIR FLUX MEASUREMENTS AND SIGNAL-TO-NOISE RATIOS

Comparison of photographic and CCD exposures of same field with 4-m;
Left: 45 min photographic plate; Right: 2 hr CCD (stacked)

Hale's Lament

"Starlight is falling on every square mile of the Earth's surface, and the best we can do is gather up and concentrate the rays that strike an area 100 inches in diameter." [G. E. Hale, 1928]

I. Introduction

In 75 years, we have progressed to 400-inch diameters for optical telescopes, but we still collect a pitifully small fraction of the photons incident from cosmic sources.

This lecture discusses the important considerations in making optimal use of the photons we do have at our disposal.

References:

> **LLM: Chapter 6 on EM signals (though treatment differs from that here)**
>
> **LLM: Chapter 2 on effects of Earth's atmosphere**

II. The Observer's Problem

The Problem: How to maximize the reliable astrophysical content of observations?

Translates to: How to make <u>accurate</u> flux measurements with a <u>precision or SNR</u> appropriate to the scientific goals given the practical constraints?

Key factors affecting SNR:

- **<u>Source</u>: Luminosity and distance**

    Brightness is usually a strong function of wavelength

- **<u>Destruction</u> or deflection of source photons on way to detection**

- **<u>Noise</u> in process of measuring source photons**

    Telescope <u>size</u>

    <u>Background</u> photons

    <u>Bandwidth</u> (should be maximum consistent with desired information content)

    <u>Instrument</u> throughput, detector sensitivity, noise characteristics

    "Detective quantum efficiency" $= DQE = \left[\frac{SNR_{\text{out}}}{SNR_{\text{in}}} \right]^2$

    Extent to which equipment can be <u>calibrated</u> to characterize random and systematic errors.

    Real-world <u>time constraints</u> on access to equipment & therefore exposure times

III. Mechanisms for Photon Destruction/Deflection

(Or: Requiem for Photon Demise in Mixed Media)

These effects are mostly not stochastic in character. They must be calibrated for good accuracy in the results and produce <u>systematic</u> errors if this is not done properly.

Almost all are more important <u>at shorter wavelengths</u>

(1) Interstellar extinction (see Lec 15)

   Depends on dust grain column density in direction of source

(2) Atmospheric extinction (see Lec 14)

   Depends on total atmospheric path length ($\propto sec\, Z$, where Z is the angular distance to the zenith)

(3) Atmospheric refraction

   Prismatic effect of differential refraction for $Z > 0$ causes elongation/chromatic separation of point sources

(4) Atmospheric turbulence ("seeing") (see Lec 21)

   Causes blurring and jitter of images

(5) Absorption/scattering by optical surfaces

   Reflecting and refracting surfaces and transmitting media destroy a large fraction of photons incident on the telescope aperture

IV. Statistical Models of Flux Measurements

Every EM flux measurement is affected by the stochastic processes described in the "Statistics of Observations" pages (Lec 6).

> Every time you try to determine the SNR of a measurement, you are applying an <u>implicit statistical model</u> for the parent distribution.
>
> The appropriate model will differ with the instrument, detector, and waveband. In principle, each system should be analyzed <u>separately</u>. Rules of thumb for one do not necessarily apply to others.
>
> The discussion here is aimed at UVOIR observations made with CCD detectors.

Gaussian Distributions?: We can assume that most stochastic components entering astronomical flux measurements are governed by a Gaussian parent distribution.

> <u>Photon noise</u>, the fundamental source of EM noise, is governed by Poisson/Gaussian statistics in practice.
>
> However, other aspects of photon detection (e.g. amplifier gain variations, seeing variations, dark current, atmospheric transparency changes, etc.) may <u>not</u> be Gaussian. For instance, airglow emission lines usually vary non-randomly. Other elements of a detection system might be governed by Lorentzian or log-normal distributions. For accurate work, it is important to empirically confirm the nature of the statistics governing your measurements.

Multiple Measures: The BEST approach to error estimation is always to make <u>many repeated measures of a value</u>, say $N > 10$. But in practice this may be difficult.

V. Sources of Noise in UVOIR Flux Measures

In the following pages we discuss the major contributors to noise in UVOIR flux measurements. These are

>   **(A) Photon noise**
>
>   **(B) Background noise**
>
>   **(C) Measuring process noise**
>
>   **(D) Other sources of noise**

(A) Photon Noise

Fundamental statistical fluctuations in photon arrival times imply that the photon count rate is a random variable (even if the source is strictly constant in luminosity).

- o **Photon arrivals** from most astronomical sources are an independent counting process and are described by **Poisson** statistics (for small mean counts per unit time) or **Gaussian** statistics (for larger means).

- o **Photon statistics apply both to source photons and background photons.**

- o **Implications of photon statistics:**

   If we consider only noise from photon counting statistics from the source of interest, then

   $SNR = N/\sigma(N) = N/\sqrt{N} = \sqrt{N}$, **where** N **is the total number of source photons counted.**

   Known as "square root of N statistics":

N	SNR
100	10
1000	32
10000	100

   Because of the contribution of other sources of noise in real measurements, these values are upper limits to the combined SNR.

Caveat on Photon Statistics:

Photons are Bose-Einstein particles, which means that a given quantum state can contain many photons. This gives rise to photon "bunching".

In a photon stream originating in TEQ, the variance in photon arrivals is larger than for a Poisson process:

$$Var(n) = n(1 + \delta), \text{ where } \delta = \frac{1}{(e^{h\nu/kT} - 1)}$$

The correction term δ is important if $\lambda \gtrsim 2/T$ cm—i.e. in the infrared for normal stellar temperatures.

However, because typical detection systems (optics, detectors) are inefficient, the probability that more than one bunched photon will be detected is <u>small</u>, and the bunching effect can usually be ignored in practice. Photon bunching could be more important in non-thermal sources.

Hanbury-Brown and Twiss (1958) built a special optical "intensity interferometer" which took advantage of the bunching effect to measure the diameters of a small number of hot, bright stars.

(B) Background Noise (Unwanted Signals)

Background light sources are affected by photon statistics but in some cases (e.g. Earth's atmosphere) also by <u>intrinsic variations</u> in flux.

(1) Diffuse Sky Photon Background:

o **Earth's atmosphere: scattered city lights, airglow, aurorae, thermal continuum (IR). Both continuum & emission lines. Emission lines (e.g. [O I] and OH) can be <u>highly variable</u>. Atmosphere is not an issue for space observatories at optical/IR wavelengths. However, skyglow emission lines (Lyα, O I) from residual atmosphere above 500 km are important in far-UV.**

o **Moonlight: drastic ($\gtrsim 3$ mag arcsec^{-2}) effect on brightness of optical sky background, depending on phase. Scattered moonlight is blue, so red/IR observations preferred when Moon is bright.**

> **"Bright time": Full Moon ± 5 days**
> **"Dark time": New Moon ± 5 days; reserved for faint target astronomy at most observatories.**

o **Zodiacal light (sunlight scattered by IP grains); strong direction dependence, but not time dependence; has Solar spectrum. Thermal emission in IR.**

o **Galactic background light. In UVOIR, is primarily starlight scattered by IS grains at lower galactic latitudes; has hot-star spectrum but is faint.**

> **Mid, Far-IR ($\lambda > 20\mu$) emission from warm dust: "IR cirrus"**

SKY BACKGROUND
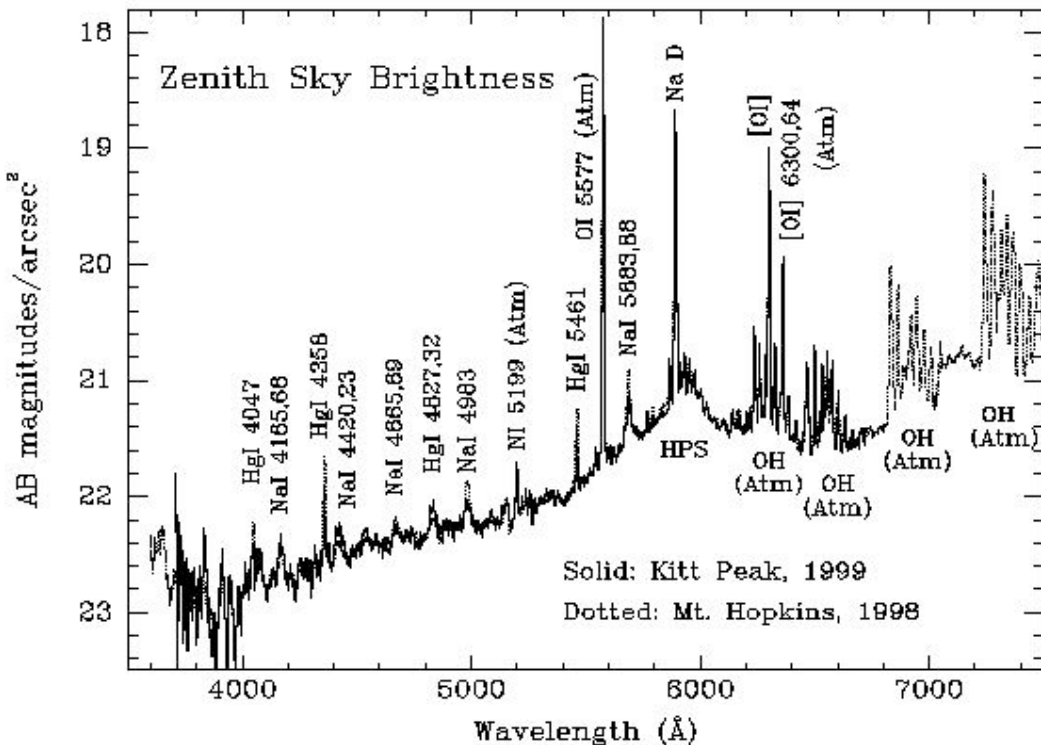
Table 2-1. Broadband sky brightness for Mauna Kea

Band	Central λ (μm)	Brightness (mag arcsec^{-2})	(AB mag arcsec^{-2})	(μJy arcsec^{-2})	Flux (photon cm^{-2}s^{-1}μm^{-1}arcsec^{-2})
U	0.36	21.6	22.5	3.3	1.74×10^{-2}
B	0.44	22.3	22.2	4.8	1.76×10^{-2}
V	0.55	21.1	21.1	13.2	3.62×10^{-2}
R	0.64	20.3	20.6	20.9	5.50×10^{-2}
I	0.79	19.2	19.7	47.9	1.02×10^{-1}
J	1.23	14.8	15.6	2089.3	2.49
H	1.66	13.4	14.7	4786.3	4.20
K	2.22	13.5	15.4	2511.9	1.74

Broad-band (continuum & line emission) sky background levels (no Moon) at Mauna Kea

Note dramatically increased brightness for JHK bands.
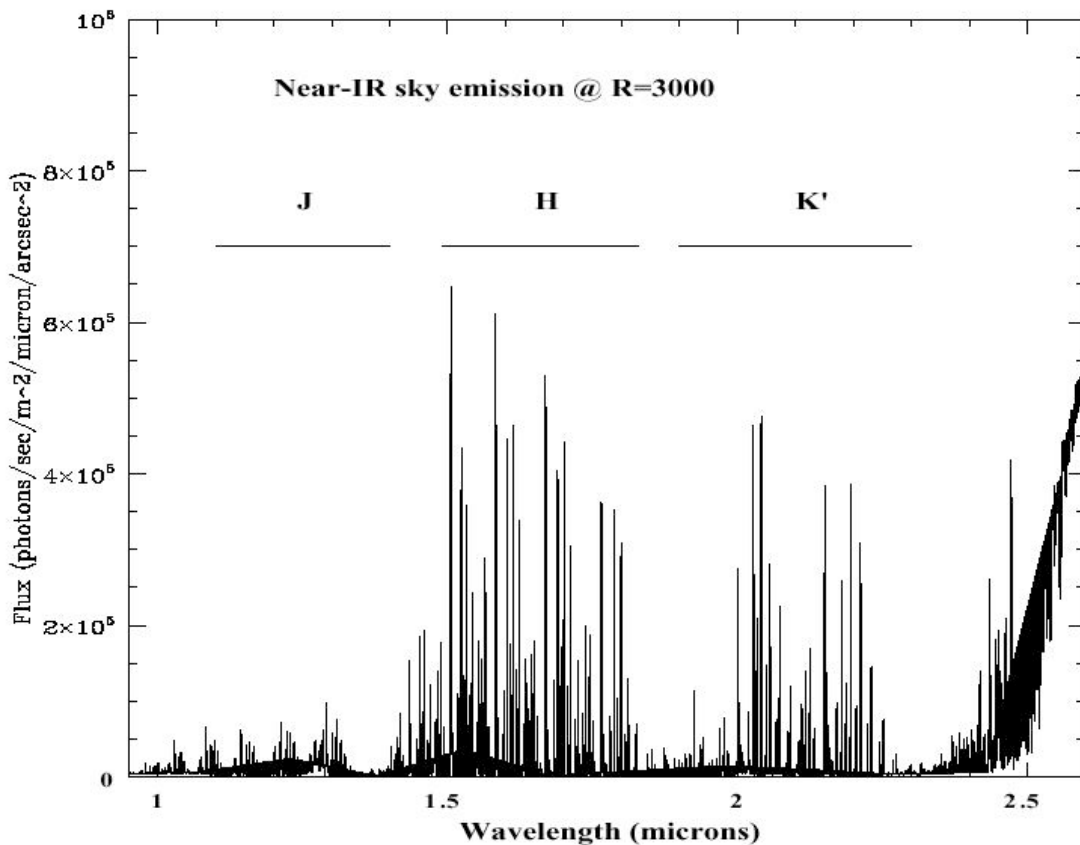
SKY BACKGROUND

Night sky spectrum from KPNO

Shows red continuum, Hg, and Na emission lines from scattered city lights. (HPS = "high pressure sodium" lamps). Strong [O I] lines are auroral. Region redward of 6200 Å shows start of forest of upper-atmospheric OH lines, which continues through near-IR.

SKY BACKGROUND

Near-IR sky emission @ R=3000

Night sky emission lines (mainly OH), near-IR

Shows continuation of atmospheric OH spectrum from preceding KPNO plot. OH forms at 75 km altitude, so affects all ground-based sites. Impact of lines is devastating for certain kinds of observations. Natural extra-atmospheric background at these wavelengths is up to 1000 times fainter.

SKY BACKGROUND

Changes in Sky Brightness for Dark Astronomical Sites

Growth of city light contamination (A. Walker)

**No sites are free of serious & increasing light pollution except McDonald
Observatory (in west Texas, where apparently nobody wants to live). Of
special interest for us at UVa are Mount Graham and Sacramento Peak.**

SKY BACKGROUND
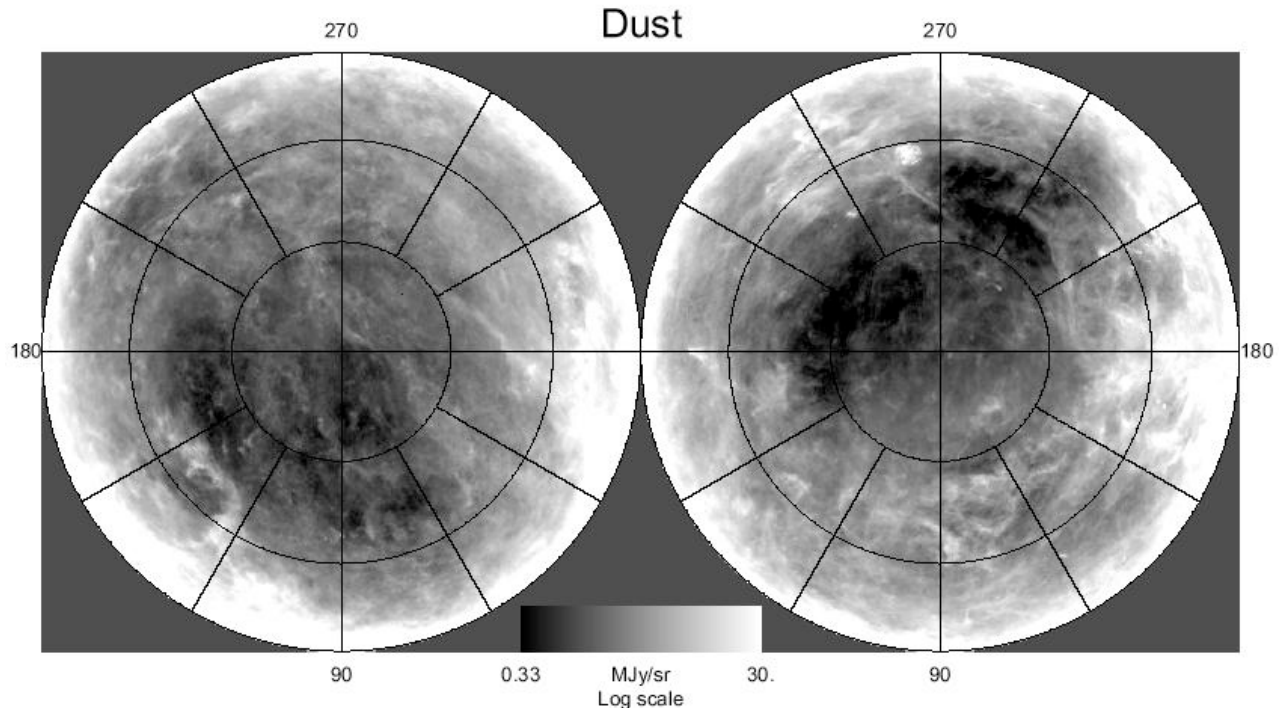
FIG. 8.—Full-sky dust map for the NGP (*top*) and SGP (*bottom*)

Hemispheric images of far-infrared "cirrus" (COBE/DIRBE)

"Cirrus" emission is produced by warm interstellar dust grains at typical distances of 100-3000 pc within the Galaxy. Far-IR (50–200 μ) observations can be importantly affected by this strongly non-uniform background. Must make good determination of local 2D cirrus structure in order to remove its effects.

BACKGROUND NOISE (cont)

(2) Discrete Cosmic Sources

o **Field stars (e.g. scattered light from bright stars; produce an "exclusion zone" around stars)**

Star light scattered, refracted, or diffracted by the atmosphere and by telescope optics and structures can produce effects at large distances from a star. King (1971) showed that the profile of a star image has a Gaussian core, but then an exponential shoulder and a power law at $r > 30$ arcsec.

o **Extended envelopes from nearby galaxies**

o **Faint distant galaxies (serious problem at faint levels since are thousands per square degree)**

o **"Confusion" caused by source blending within spatial resolution cell. More serious in radio astronomy, but a major UVOIR problem in some cases, e.g. star clusters**

(3) Detector Noise

o **Chemical fog (photographic emulsions)**

o **"Dark current": thermal emission in absence of signal; major problem; requires detector cooling**

For a semiconductor such as a CCD array, the dark current behaves as: $\dot{n}_{dark} = AT^{3/2}e^{-E_g/2kT}$, where E_g is the band gap energy and T is the temperature. (See Lec 11 for discussion of semiconductors.)

Is a more serious problem for IR detectors because of smaller band gaps.

o **Cerenkov photons**

o **CCD's: variations in electronic "bias"**

BACKGROUND NOISE (cont)

(4) Telescope Backgrounds

o IR: emission ($T \sim 280$ K) of optics and other structures visible to detector ($\lambda \gtrsim 1.5\mu$)

o Diffraction & scattering (e.g. from dust on optics) contributes to background at all λ's

Note the <u>ADVANTAGE</u> of 2D digital array detectors for background determination:

Ordinarily 2D devices provide a <u>large number</u> <u>of background samples</u> surrounding a source of interest.

The samples are also usually obtained (in imaging, for instance) <u>simultaneously</u> with the source observations, which is very important in the case of large & variable backgrounds. As long as the background contains only low spatial frequencies, it can be well modeled and removed, greatly improving the detection of faint sources.

The 2-D advantage is especially important in the near-IR, where the sky, telescope, and detector backgrounds can be fierce.

NOISE IN UVOIR MEASUREMENTS (cont)

(C) Measuring Process Noise

(1) Amplifier noise

  o E.g.: CCD "readout noise" (RON) produced by gain variations in on-chip amplifiers

  Usually quoted as "equivalent electrons" (n_{RON}) of rms noise per pixel

  Implies additional variance of n^2_{RON} per pixel

  Adds as much variance to signal as $n_d = n^2_{\mathrm{RON}}$ detected photons

  Is <u>independent</u> of integration time whereas ratio of photon and dark current noise to signal is reduced for longer integration times

  If RON is important, want to minimize # of readouts

(2) Gain variations in electron multipliers (e.g. PMTs, image tubes, microchannel plates) and electronic readout devices (e.g. delay line anode grids)

(3) Microdensitometer readout gain variations (Pg plate digitization)

(D) Other Sources of Noise

(1) Sensitivity variations across 2-D detectors

  o Grain noise in Pg plates (grain size $\sim 25\mu$)

  o "Flat field" effects (pixel-to-pixel sensitivity variations) in CCDs and other semiconductor devices. For CCDs, typically of order $\sim$5% with a strong wavelength dependence.

    o **Extreme "hot" or "cold" pixels in array detectors; cosmetic defects, e.g. bad columns. Worse in IR detectors. Can be induced by cosmic ray damage.**

    o **Intra-pixel variations; can be important if point spread function is undersampled by pixels (as in high-resolution space telescopes), but is technically difficult to measure.**

(2) CCD's: charge transfer inefficiencies (worsened by cosmic ray damage)

(3) Variations in atmospheric turbulence/seeing

(4) Strong and/or variable absorption in atmosphere (general extinction; clouds; bands of H_2O, O_2, O_3)

(5) Cosmic rays: tracks easily detected in CCD, other devices; produce serious, though localized, effects; incidence is governed by Poisson stats.

(6) Interference (light leaks, TV, radio, radar, cell phones, etc)

(7) Radioactive decay glow in filters/windows

(8) Guiding errors

(9) Mechanical flexure in telescope or instrument; focus shifts

NOISE IN UVOIR MEASUREMENTS (cont)

NOTE on the <u>Near-Infrared "Quadruple Whammy"</u>:

If you were paying attention to the earlier material, you will realize that this spectral region (0.8–3 μ) is affected by multiple difficulties, including:

(i) Bright sky and telescope background continuum emission; (ii) bright atmospheric emission lines; (iii) strong atmospheric absorption lines (mainly H_2O); and (iv) high detector dark currents.

In the past, the problem was compounded by low sensitivity detectors and the absence of large format 2D detectors. Older, single-element IR detectors required that telescopes be capable of rapid "chopping" (spatial offsets) between target and nearby sky.

The advent of high QE, 2D detectors for the NIR has meant a terrific improvement in performance, among other things usually eliminating a requirement for telescope chopping.

However, the presence of bright & variable OH emission lines, as well as widespread H_2O absorption, still greatly complicates spectroscopy of faint targets in the NIR.

VI. Example: Effects of Background on SNR
In Fixed Aperture Photometry

- **Application: photometry with a photomultiplier tube (one detection element) or from a 2-D image array using a virtual aperture of <u>fixed size</u>. Consider <u>only photon statistics</u>.**

- **Measure a compact source ($<$ aperture size) and background nearby with the <u>same-sized</u> aperture**

- **Yields two measurements: "on source" and "background" with total detected photon counts T & B, respectively. What is SNR?**

  o **Net signal: source count $S = T - B$**

  o **Variance?**

  $$Var(S) = Var(T) + Var(B) = T + B = S + 2B$$

  o **Then $SNR \equiv S / s_{\bar{S}} = \dfrac{S}{\sqrt{S+2B}}$**

  > NB: the background term enters twice because both
  > measurements include the background

  o **Re-write as a function of S, B/S:**
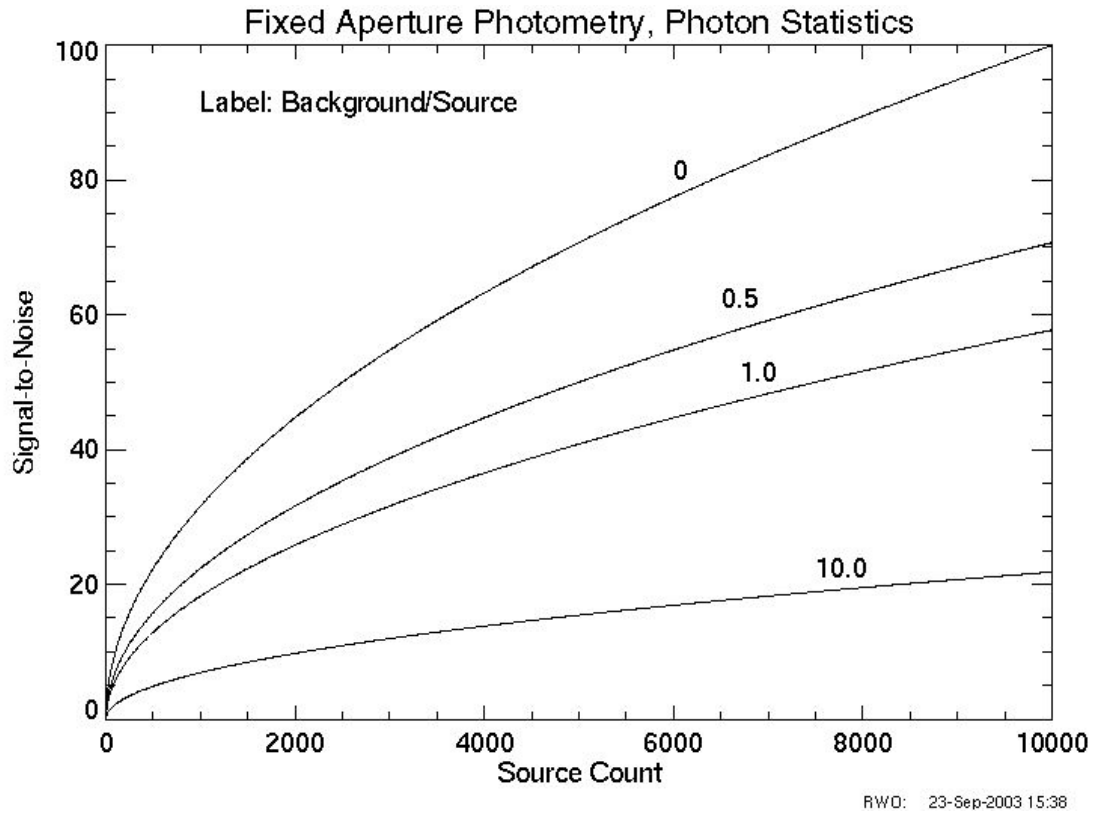
  $$SNR = \frac{\sqrt{S}}{\sqrt{1 + 2\frac{B}{S}}}$$

  o **Plot result (see next page)**

  o **Limiting behavior:**
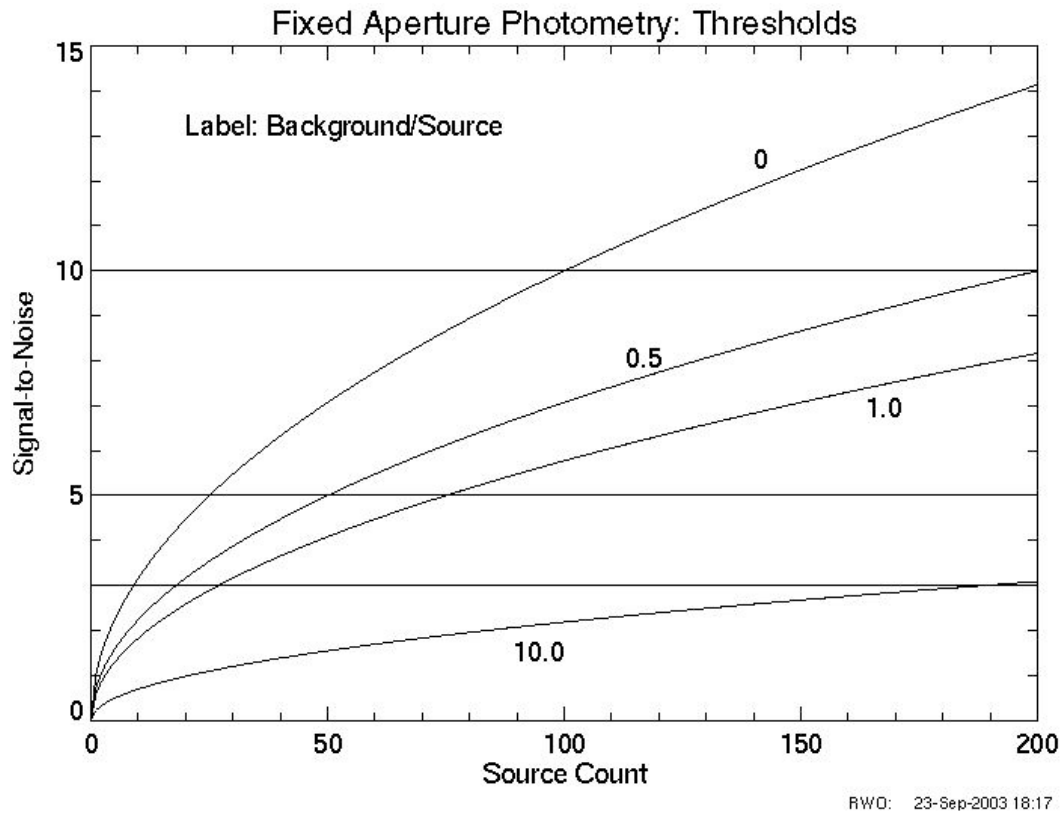
  > **"Source limited": $S >> B \implies SNR = \sqrt{S}$**
  > **"Background limited": $B >> S \implies SNR = \dfrac{S}{\sqrt{2B}}$**

Signal to noise ratio as function of source count and background ratio in fixed aperture photometry

In near-IR applications, can easily find situations where $B/S > 100$.

Fixed Aperture Photometry: Thresholds

"Threshold detections" in Fixed Aperture Case

Follow line for chosen $SNR_{\min}$ to obtain the minimum number of source counts required for different background ratios. X-ray astronomers would consider SNR = 3 to be a threshold detection, but UVOIR astronomers tend to be more discriminating (SNR of 5 to 10).

VII. Example: SNR in Photometry With Large Background Sample

- **Assume two <u>different</u> aperture sizes: one (N pixels) containing all the light of a compact source and one (M pixels) containing only the background. M can be very large.**

    E.g. DAOPHOT uses a small circular aperture for the source and a large circular annular aperture for the background, though the shape is not relevant to this derivation.

- **Let $\bar{b}$ be the mean background count <u>per pixel</u>. If B is the total background count in the large background aperture, then we can estimate $\bar{b}$ and its variance as follows:**

$$\bar{b} = B/M \text{ and } Var(\bar{b}) = \frac{1}{M^2}(B = M\bar{b}) = \frac{\bar{b}}{M}$$

- **We estimate the source count as $S = T - N\bar{b}$. Then:**

$$Var(S) = Var(T) + Var(N\bar{b})$$

$$Var(S) = T + N^2 Var(\bar{b}) = T + \frac{N}{M}N\bar{b}$$

$$Var(S) = S + N\bar{b}\left(1 + \frac{N}{M}\right)$$

$$\implies \quad SNR = \frac{S}{\sqrt{S + N\bar{b}\left(1 + \frac{N}{M}\right)}}$$

- **Get same result as (VI) if $M = N$ but can reduce coefficient of background term from 2 to 1 if $M >> N$.**

VIII. Effect of Exposure Time and Readout Noise on SNR

In preceding examples, the quantities entering the SNR calculation are proportional to the exposure time. I.e. in the fixed aperture case:

$$S = \dot{S}t \quad \text{and} \quad B = \dot{B}t$$

where t is the total exposure time of the observation, and $\dot{S}$ and $\dot{B}$ are the <u>rates</u> at which source photons and background photons, respectively, are detected. This implies:

$$SNR = \frac{S}{\sqrt{S + 2B}} = \frac{\dot{S}\sqrt{t}}{\sqrt{\dot{S} + 2\dot{B}}}$$

Interpretation: Although the noise and the signal both increase as t increases, the signal increases faster, hence SNR improves...but <u>not</u> in direct proportion to t.

Improvement of SNR in proportion to $\sqrt{t}$ is a consequence of photon statistics and applies generally to any situation where they dominate measurement uncertainty. (Also applies to sources of detector noise—e.g. <u>dark current</u>—which are characterized by Poisson statistics.)

> From a practical perspective, this can be viewed as a <u>slow</u> improvement of SNR for a given investment of time. When observing time is at a premium, there will be a fairly obvious point of diminishing returns.

However, this does not apply to a large class of detector noise which is <u>independent</u> of integration time. Detectors with this behavior are sometimes called "Class II" detectors. Photographic emulsions, bolometers, infrared array detectors, and CCDs are all in this category.

In CCDs <u>readout noise</u> is independent of integration time and in some cases is an important constraint on the SNR.

To illustrate the effect of readout noise, rewrite the result for the fixed aperture case as follows:
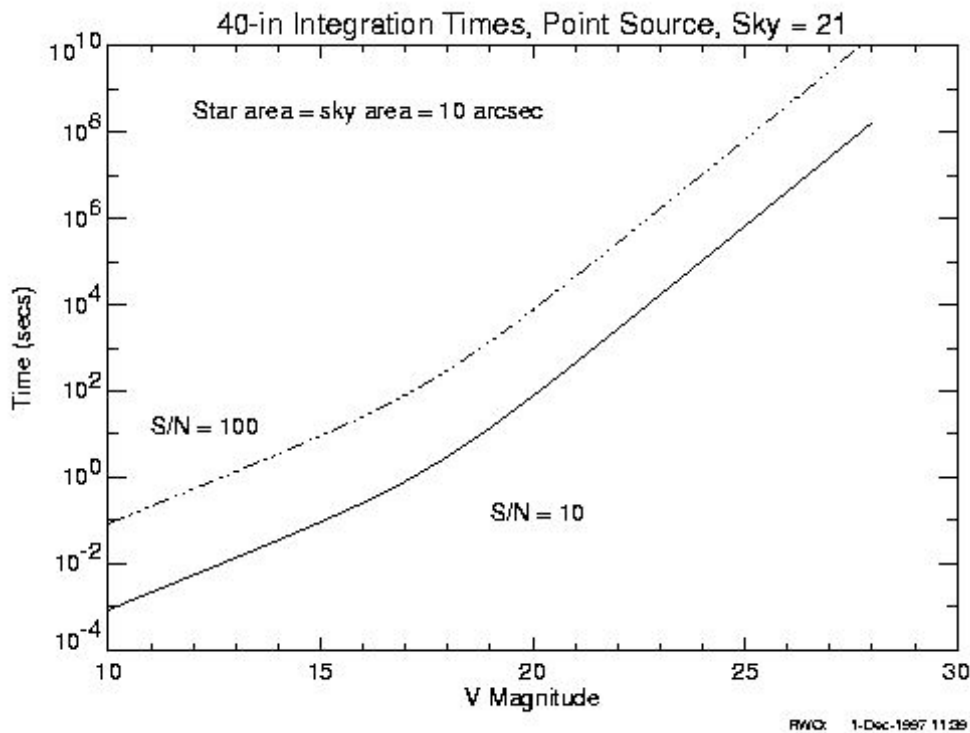
$$Var(S) = \dot{S}\,t + 2N(\dot{b}\,t + \dot{d}\,t + n_{\mathrm{RON}}^2)$$

where N is the number of pixels in the measuring aperture, $\dot{b}$ and $\dot{d}$ are, respectively, the detected background photon rate and the dark count rate per pixel, and n_{RON} is the readout noise per pixel (quoted in numbers of equivalent electrons of noise). A single readout after exposure time t is assumed.

The resulting signal-to-noise is then:
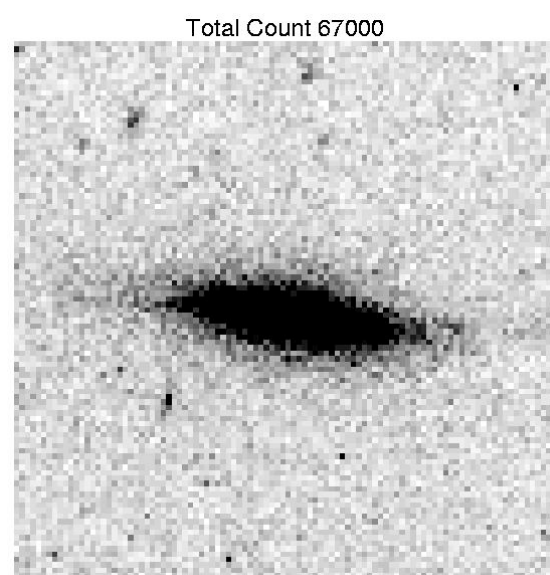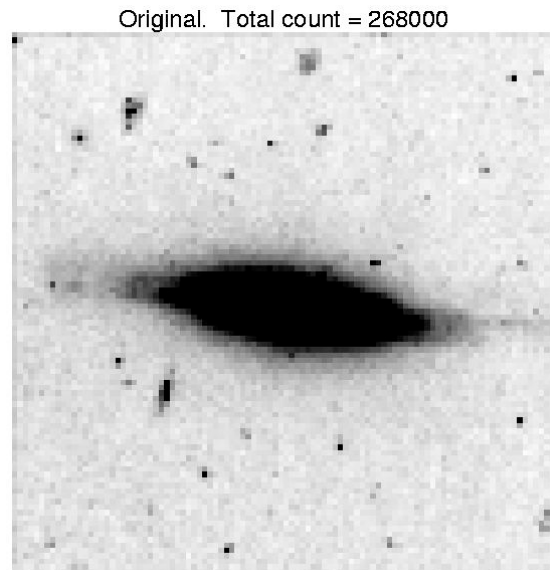
$$SNR = \frac{\dot{S}\sqrt{t}}{\sqrt{\dot{S} + 2N\left(\dot{b} + \dot{d} + \frac{n_{\mathrm{RON}}^2}{t}\right)}}$$

When RON is important, one wants to <u>minimize the number of readouts</u> for a given total exposure time and also to minimize the <u>number of pixels</u>, N, covering the region of interest.

40-in Integration Times, Point Source, Sky = 21

Star area = sky area = 10 arcsec

S/N = 100

S/N = 10

Time (secs)

V Magnitude

RWO: 1-Dec-1997 11:39

Example estimate of integration times for the Fan 40-in CCD imaging system including the effects of source noise, sky background, and readout noise.

Note change of slope at $V \sim 18$, which is the transition between background noise dominance (for fainter sources) and source photon noise dominance (brighter). Diagrams like this allow you to optimize your observing program by making trades-off between SNR, source brightness, and integration time.

Original. Total count = 268000

Total Count 67000
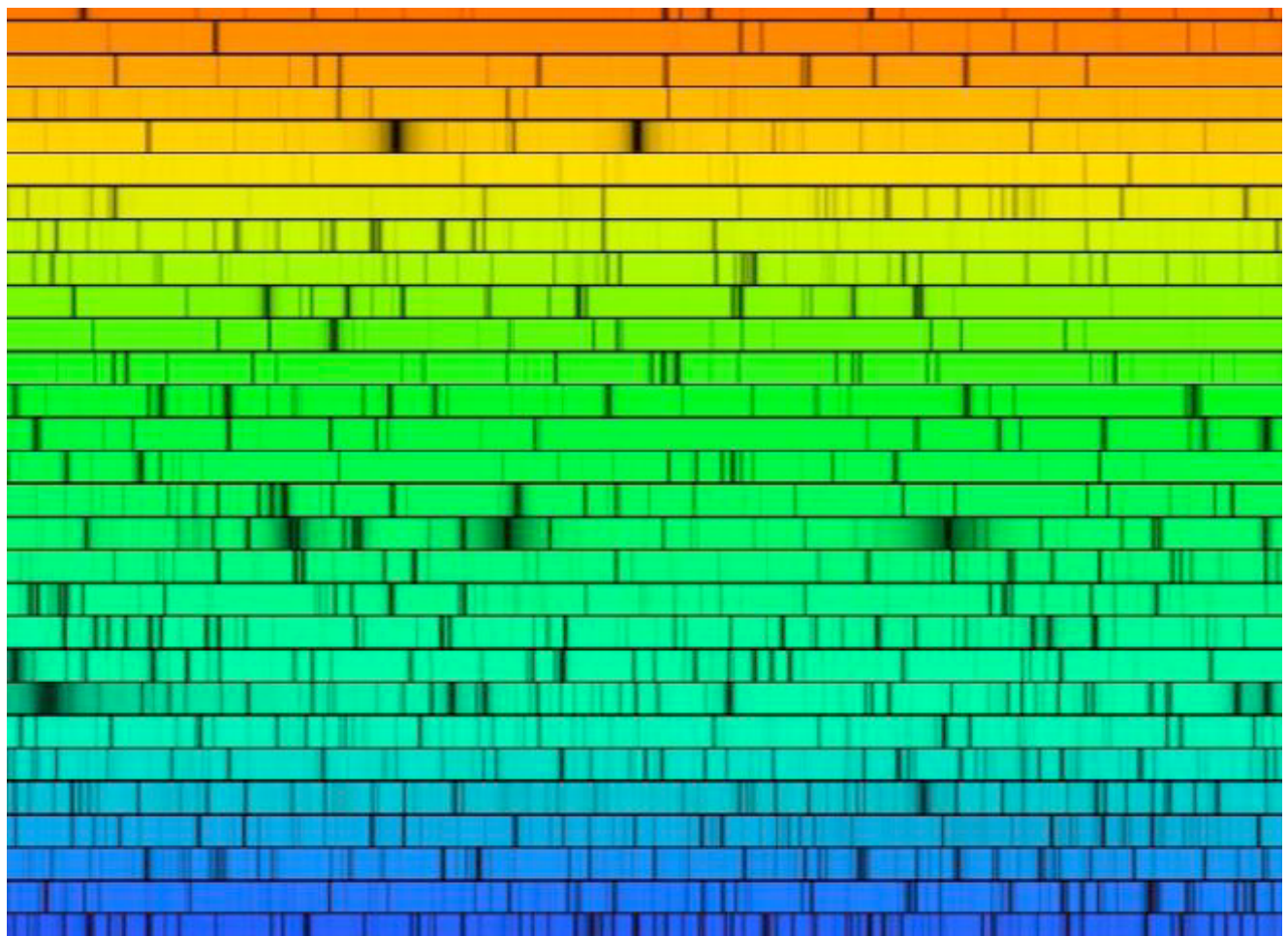
Effect of SNR on appearance of a digital image

Upper image has SNR 2.3X that of lower image.
The lower image is a Poissonian sample using the upper image as a parent distribution.

UVOIR SPECTROSCOPY

High resolution, optical band solar spectrum

SPECTROSCOPY: INTRODUCTION

Spectral analysis is the source of most of our astrophysical knowledge. See Lectures 2 and 3 for discussion of the interpretation of spectral energy distributions.

<u>Spectral resolution</u> is usually quoted as $\Re \equiv \frac{\lambda}{\delta\lambda}$, where λ is the observing wavelength and $\delta\lambda$ is the smallest wavelength interval that can be isolated from its neighbors.

UVOIR <u>Detectors</u>: intrinsically very <u>poor</u> spectral resolution; broad-band.

> **Exception: $\sim$sharp threshold determined by internal energy levels which impose a cutoff $h\nu_{\min} = E_q$, where E_q is an activation energy.**

Spectral resolution must therefore be provided by <u>additional optical elements</u>.

We discuss three types of elements providing UVOIR spectral resolution: filters, prisms, and diffraction gratings.

> **Filters have many uses and can provide high $\Re$ but, with a few exceptions, offer isolation of only one waveband at a time.**

> **Prisms and gratings <u>disperse</u> light such that a wide range of wavelengths can be simultaneously observed. They are the basic elements used in <u>spectrographs</u>.**

References:

> **Kitchin: Chapter 4 (Spectroscopy)**
>
> **LLM: Chapter 5 (Spectral Analysis)**
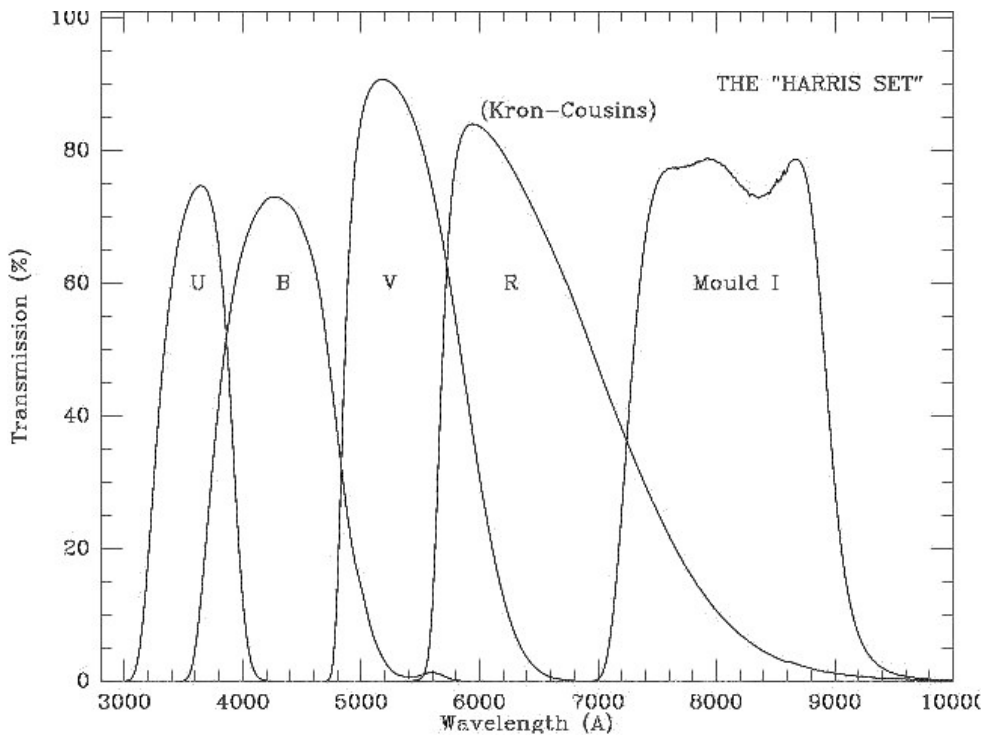
I. FILTERS

A. Glass Filters

Transmissive/absorptive properties of glasses depend on their solid state band structure. Tunable by selecting materials or dyes.

Apart from their short-wavelength cutoff (caused by absorption for $\nu > E_q/h$), colored glasses have broad ($\gtrsim 500\,\text{Å}$), slowly changing transmission curves. Rarely exceed $\Re \sim 10$.

Dozens of types of glass filters are used in astronomy, the best known being the broad-band UBVRIJHK system.

B. Interference Filters

Thin film layers (thickness $\sim 100\,\text{Å}$) of metals and dieletrics deposited on glass substrates in vacuo produce constructive interference effects through multiple internal reflections. This can yield narrow, sharply defined transmission bands.

Fabry-Perot etalon: classic two-layer interference filter

The throughput of the etalon is given by:

$$I\,/I_0 = \frac{1}{1 + \frac{4\,R\,\sin^2(\delta/2)}{(1-R)^2}}$$

where $\delta = \frac{2\pi}{\lambda}\,2d\,\cos\theta$, R is the reflection coefficient of the coating, d is the spacing between the layers, and θ is the angle of incidence with respect to the normal to the layers. (Assumes no absorption by etalon.)
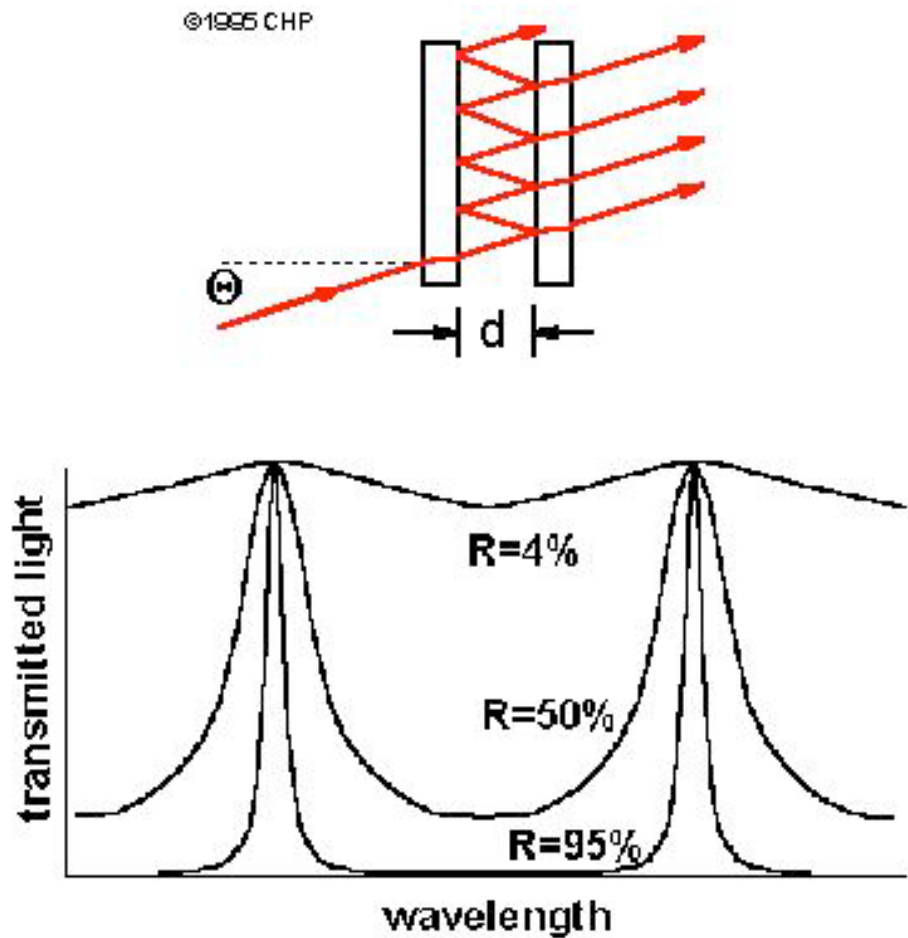
Yields multiple maxima ("orders") in the throughput since $\delta = m\,2\pi \rightarrow I = I_0$, where m is any integer.

Note that such maxima exist even if $R \sim 1$!

The spectral resolution of the etalon (defined by half-power points on the response curve) is

$$\Re = \frac{2\pi\,d\,\sqrt{R}}{\lambda\,(1-R)}$$

and is tunable by changing either d or R.
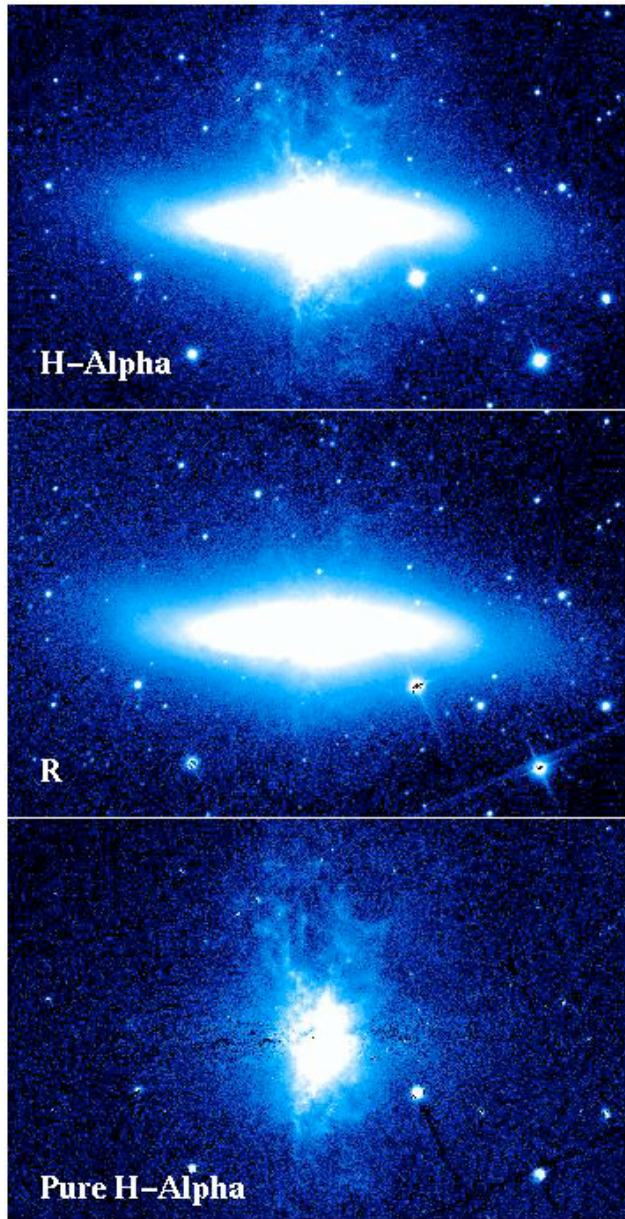
Structure and throughput of a Fabry-Perot etalon; note how increased reflectivity sharpens the response function

Modern IF filter technology:

o **Multiple layering techniques; highly versatile.**

o **For fixed-band interference filter, colored glass (or additional layering) used to suppress unwanted orders in the throughput.**

o **Typical bandwidths for astronomy are in the 10–500 Å range, with $\Re \sim$ 10–500.**

o **Narrower bandwidths typically produce poorer peak throughput because of requirement for out-of-band order suppression.**

o **Widely-used IF filters include designs for:**

> **Emission line isolation: e.g. Hα, [S II], or [O III]**

> **Prominent stellar absorption features: e.g. Mg I "b", Ca II "k", CN**

> **Intermediate-band diagnostics of stellar abundance, gravity: e.g. the Strömgren filters;**

> **Trimming response of wide-band filters: e.g. the Sloan Digital Sky Survey filters**

o **Large complements of IF filters are being used in the COMBO-17 project and in WFC-3 on HST.**

o **<u>Variable-spacing</u> IF filters have wedge-shaped layers so that their central wavelength varies continuously with position. They come in both circular and linear types. VS IF filters are carried by both WFPC-2 and ACS on HST.**

o **Classic two-layer etalon is also used in astronomy as a "Fabry-Perot Interferometer," where gas pressure or pizeo-electric positioners are used to adjust d in order to create a tunable, high resolution 2D imaging filter. Most applications are to emission-line sources. (E.g. "HIFI" system, Bland & Tully 1989, AJ, 98, 723.)**

INTERFERENCE FILTERS

Example of use of interference filter to map emission line gas in the edge-on starburst galaxy M82. The "Hα" image (IF filter, 89 Å FWHM) contains both emission lines and stellar continuum but is dominated by the former. The "R" image (standard broad-band filter, 1500 Å FWHM) contains both line emission and continuum but is dominated by the latter. The "Pure" image results from subtracting the R image from the Hα image after scaling to yield zero net flux in regions without line emission.

II. PRISMS

Wavefronts entering a flat glass surface at other than normal incidence are tilted by virtue of the change in the <u>index of refraction</u>, n, between air and glass. Since n is a function of wavelength (higher at smaller λ), the wavefronts are <u>dispersed</u> in direction according to λ (bluer light deflecting more).

A standard triangular prism has the cross section of an isosceles triangle. Light entering on one long side as shown below emerges through the opposite side and is dispersed further.

The spectral resolution of this type of prism is $\Re = B \frac{dn}{d\lambda}$, where B is the length of the prism base.

WHITE

Dispersion Angle

Glass [n=1.5]
Air [n=1.0]

RED
ORANGE
YELLOW
GREEN
BLUE
INDIGO
VIOLET
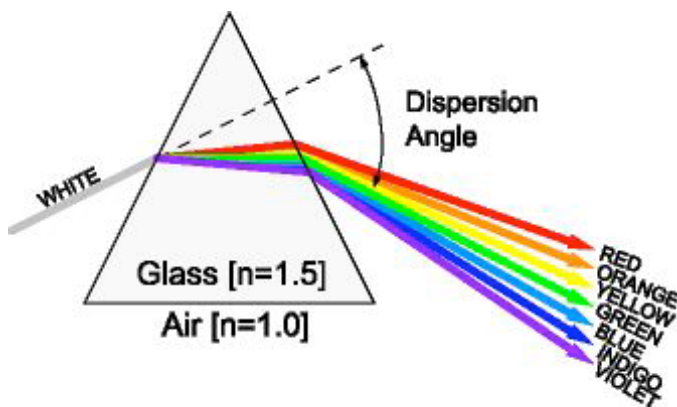
Fig. 4.8 Refraction through a prism.
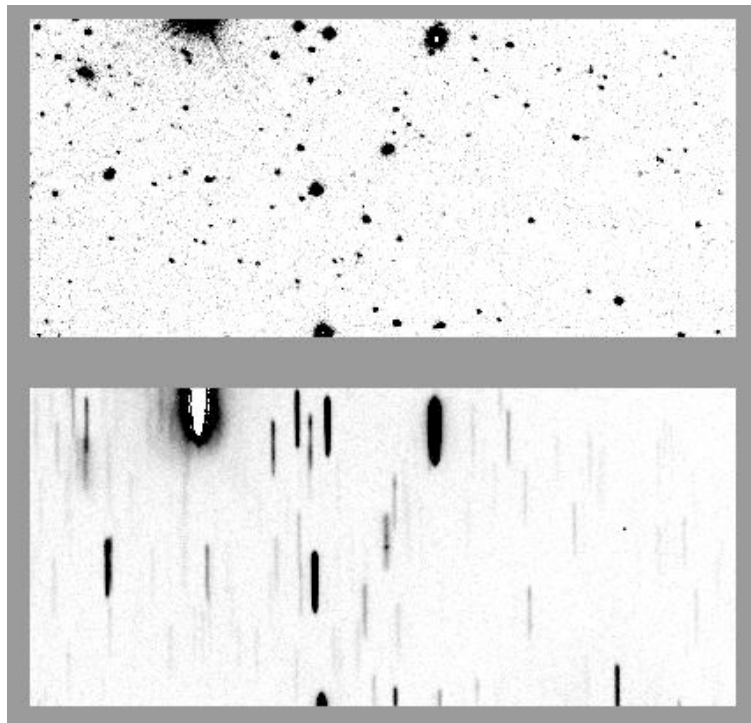
Advantages of prism spectrographs:

  o **High throughput; useful for faint-object spectroscopy (e.g. Hubble Mt. Wilson nebular spectrograph)**

  o **Wide field possible for multiobject samples**

  o **Cheap, simple; predominant in early astronomical spectroscopy**

Disadvantages of prism spectrographs:

- o $\Re$ can be a strong function of wavelength, yielded crowding at long wavelength end of response

- o Wide band coverage difficult

- o Internal absorption limits use in UV

- o More complex data reduction because of variable dispersion

"Objective" prism imagers: place prism over telescope primary $\rightarrow$ simultaneous low dispersion spectra over wide field. E.g.: Henry Draper and Vyssotsky (UVa) surveys of stellar spectra. Schmidt telescope surveys for QSO's/emission line galaxies (e.g. Markarian, KISS).

Direct and spectroscopic images of a field from the KISS objective prism survey. An emission line source is detected in the center of the dispersed image. (J. Salzer)

III. DIFFRACTION GRATINGS

A diffraction grating is a set of multiple, identical slits (transmitting or reflecting) separated by a distance comparable to the wavelength of light. Plane or concave surface.

Fraunhofer (ca. 1820) pioneered the study of such gratings. Henry Rowland (JHU, ca. 1880) produced the first of the modern grating ruling "engines" capable of making large, precision gratings useful in astronomical spectrographs. These use diamond tools to cut uniformly spaced grooves (up to 10,000/mm) on metal or glass subtrates. Less expensive "replica" gratings, transferred from a cut master to a resin layer, are in widespread use.

The theory of Fraunhofer diffraction from a plane grating predicts that the diffracted light is distributed as:

$$I(\theta) = I_0 \, f_1 \, f_2,$$

where I is the output intensity leaving the grating in direction θ with respect to the normal, I_0 is the input intensity at the grating, f_1 is the diffraction pattern for a single grating slit, and f_2 is the pattern for a set of N identical apertures. The two patterns are given by:
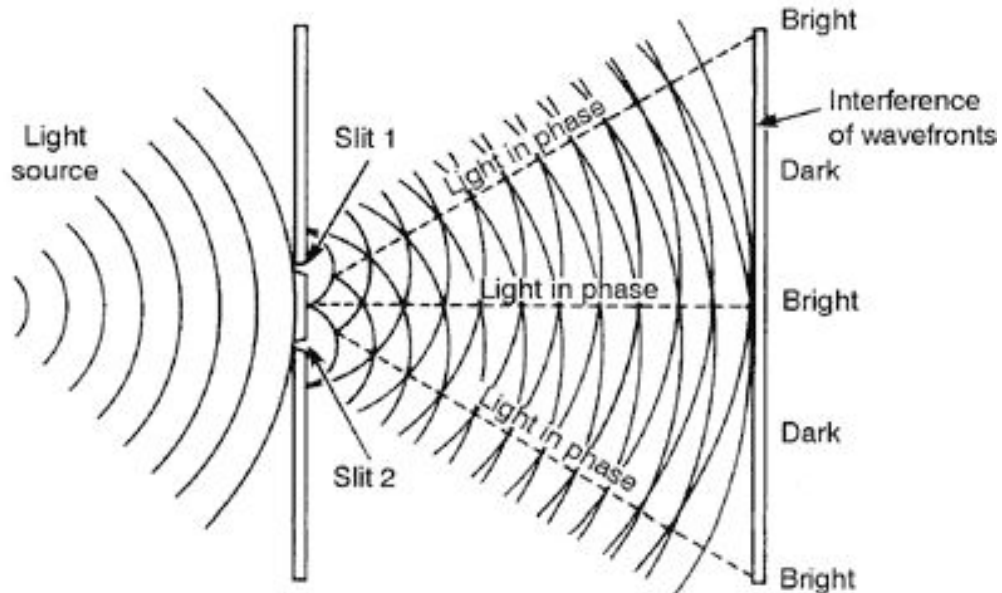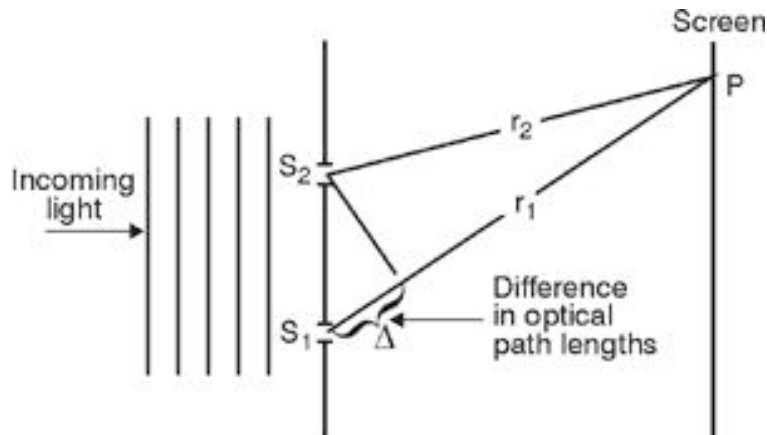
$$f_1 = \frac{\sin^2(\pi\alpha)}{(\pi\alpha)^2}, \quad \alpha = \frac{a \sin\theta}{\lambda}$$

$$f_2 = \frac{\sin^2(N\pi\delta)}{\sin^2(\pi\delta)}, \quad \delta = \frac{d \sin\theta}{\lambda}.$$

where a is the linear width of the (assumed rectangular) apertures and d is the linear separation between them. We assume normal incidence of the incoming light here. For non-normal incidence ($\theta_1 \neq 0$), replace the $\sin\theta$ term with $\sin\theta_1 + \sin\theta_2$.

DIFFRACTION GRATINGS (cont)
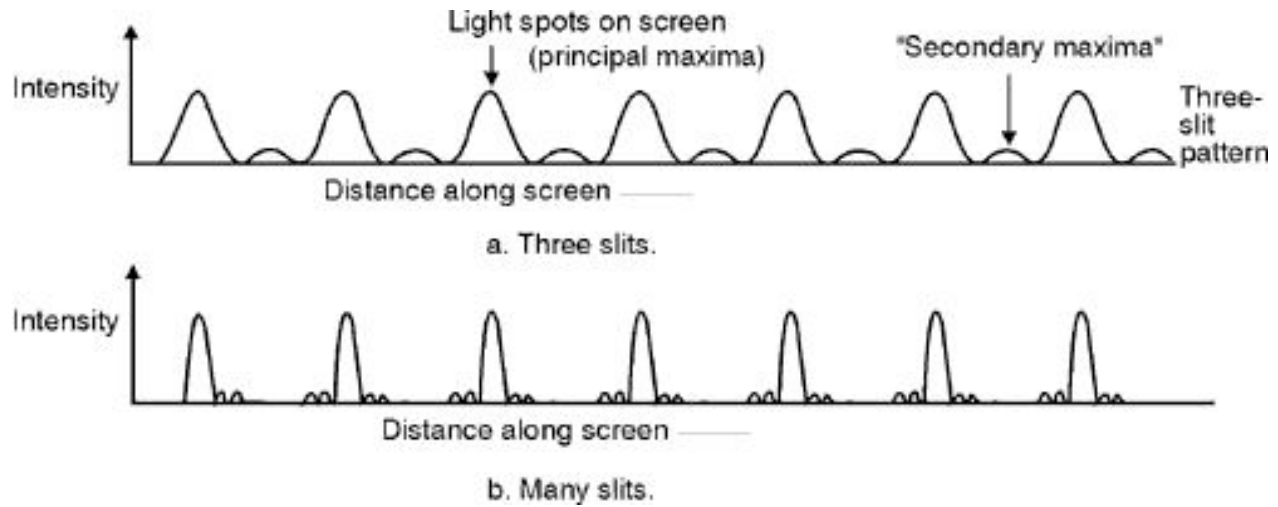
Interpretation: Consider monochromatic light. Maxima ("orders") in the multislit pattern occur for $\delta = n$, where n is any integer. This implies the path difference between adjacent slits (Δ in the first diagram below) will be n wavelengths, which produces constructive interference as shown in the second diagram. Maxima in the output intensity occur at a sequence of angles $\sin\theta_n = n\,\lambda/d$.
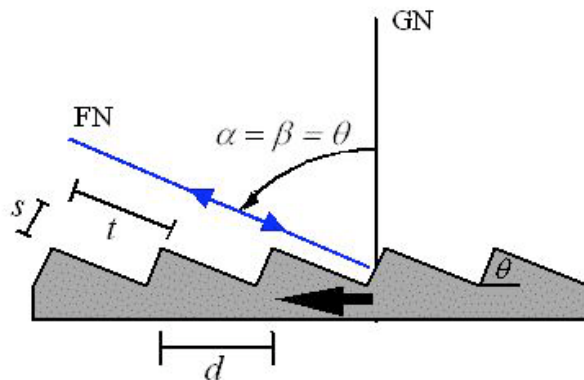
DIFFRACTION GRATINGS (cont)

The monochromatic multi-slit pattern for 3 slits and a large number of slits is shown below. Each peak corresponds to a particular order. The addition of slits increases the sharpness and brightness of the peaks but leaves the locations of the orders unchanged.

For a real grating, the single-aperture diffraction pattern would be superposed on the multi-slit pattern (here centered on $\theta = 0$).

a. Three slits.

b. Many slits.

"Echelle" gratings: Achieve very high resolutions by operating at large $n \sim 50 - 100$ and angle of incidence $\theta_1 \sim 90°$. Yield $\Re \gtrsim 10^5$.

DIFFRACTION GRATINGS (cont)

Resolution

Consider output of grating in polychromatic light. In a given order, redder light is diffracted to larger angles than blue light. The maxima for adjacent wavelengths in a given order are offset slightly.

Spectral resolution for order n is determined by the wavelength shift needed to place the diffraction pattern maximum for $\lambda + \delta\lambda$ on the first minimum in the pattern for λ. The resolution is

$$\mathfrak{R} = \frac{\lambda}{\delta\lambda} = nN$$

so it depends both on the order and on the total number of slits illuminated on the grating.

"Angular dispersion" in order n is given by

$$\frac{d\theta}{d\lambda} = \frac{n}{d\cos\theta}$$

"Higher" dispersion corresponds to larger values of this quantity. Echelles take advantage of both n and θ dependence to maximize dispersion.

NB: Astronomers often use the word "dispersion" to refer to $\frac{d\lambda}{dx}$ in the spectrograph focal plane, usually quoted in Å per mm. This is more properly called the "linear reciprocal dispersion" (K). It is inversely related to the angular dispersion, so <u>lower</u> values correspond to higher wavelength dispersion.

   In K units, "low" dispersion corresponds to $\gtrsim 200\,\text{Å/mm}$ and "high" to $\lesssim 10\,\text{Å/mm}$

DIFFRACTION GRATINGS (cont)

Grating Advantages

o **Dispersion same for all wavelengths in given order**

o **Large dispersions/resolutions possible (large n)**

o **Transmission or reflection gratings available; plane or curved**

o **High UV throughputs possible (depending on reflection coating)**

o **Grating technology highly developed, extensive customization possible**

Grating Disadvantages

o <u>**Size limited**</u> **by capacity of ruling engine. Use of mosaic gratings with large beam telescopes possible but performance compromised.**

o <u>**Order superposition**</u>**: red light of a given order is spatially coincident with blue light from a higher order. Wavelength λ_m in order m is superposed on light from wavelength λ_n in order n if**

$$\lambda_m = \frac{n\lambda_n}{m}$$

For instance, $\lambda_1 = 10000$Å, $\lambda_2 = 5000$Å, and $\lambda_3 = 3330$Å are coincident.
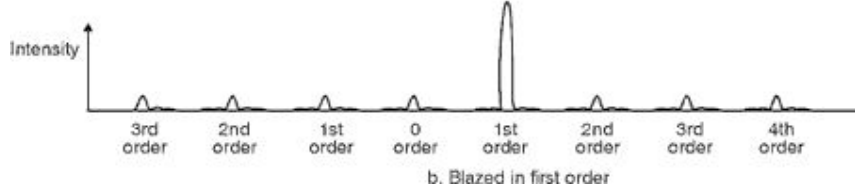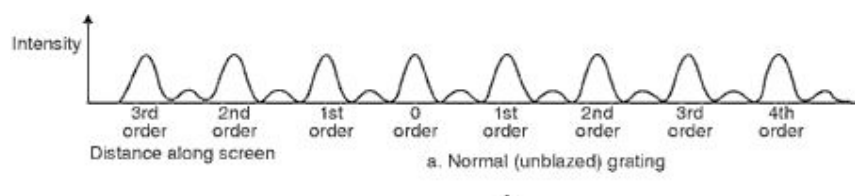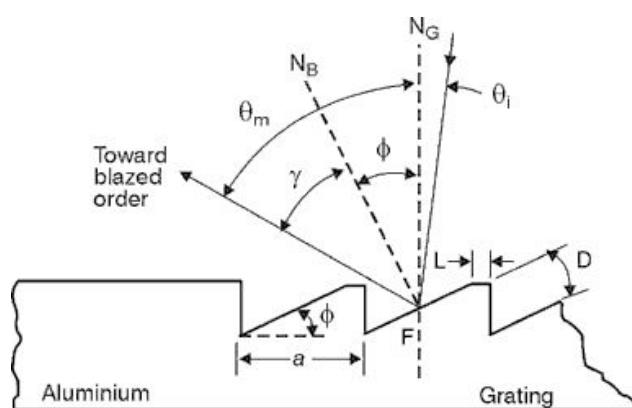
Solution: Use <u>"order separating" filters</u> to block out the unwanted orders (through this becomes difficult for large n). In case of high order echelle spectrographs, use a <u>second</u> grating as a "cross-disperser".

DIFFRACTION GRATINGS (cont)

o <u>Low efficiency</u>: **Gratings distribute light across a large number of orders (including the zeroth order, which has no dispersion). Flux decreases rapidly with order, $\sim n^{-2}$ for $n \geq 1$.**
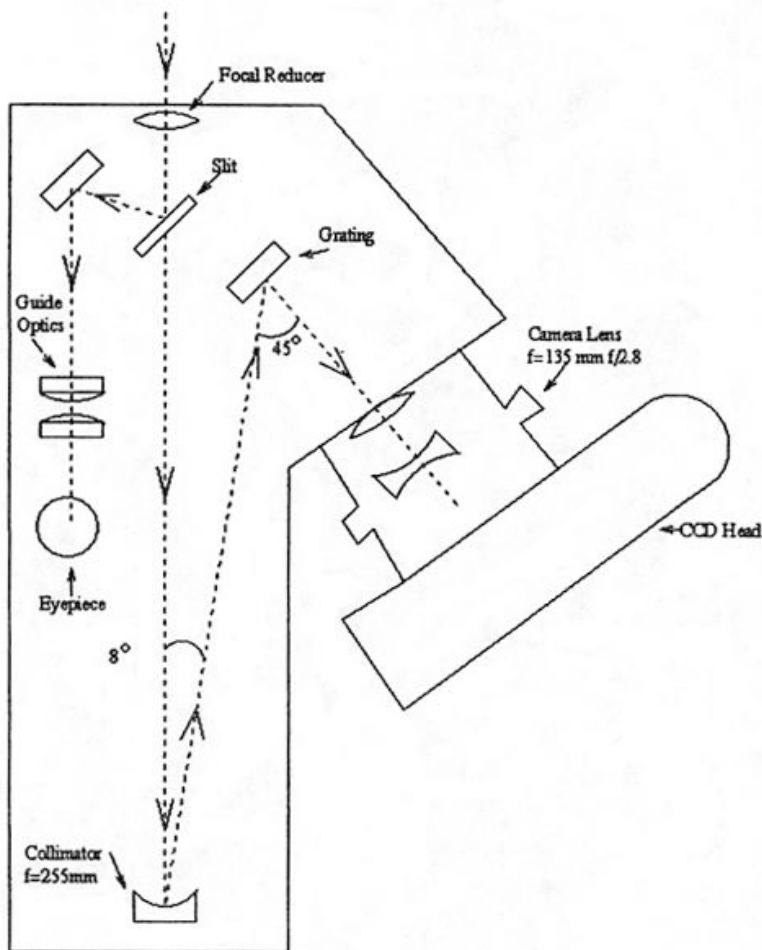
Solution: <u>"Blazed" reflection gratings</u>, in which the facets of the slits are cut at an angle that places the maximum of the single-aperture pattern at a chosen wavelength and order. For the grating in the diagram below, the "wavelength of the blaze" is $\lambda_{BL} = \frac{d}{n} \sin 2\phi$.

Achievable efficiencies for blazed gratings are in the 60-90% range, but throughput in a given order now depends on λ, which is not true of an unblazed grating. The effect of a blaze on the diffraction pattern in monochromatic light is shown in the second figure

a. Normal (unblazed) grating

b. Blazed in first order

SPECTROGRAPH DESIGN

Diagram below shows a typical medium-dispersion spectrograph

McCormick Observatory Opto-Mechanics Model 10C Spectrograph

Main elements:

o **<u>Entrance apertures</u> at focal plane of telescope**

> **None ("slitless"): resolution determined by size of sources as projected on spectrograph focal plane; large sky background superposed on spectra of all sources**

Adjustable slit: most common; intended for single point source or 1-D slice through extended source. Slit usually smaller than size of point source $\rightarrow$ improves resolution $\sim 2 - 10\times$. Greatly reduces background contamination compared to slitless design. Slit plate is usually aluminized on side facing telescope so can view target and field in reflected light.

Aperture plate: multi-object; cut small apertures to match each field of interest; computer-controlled measuring and cutting process; requires large format detector. Up to several 100 targets/field. Must avoid overlapping spectra in cutting plate. Special designs use lenslets or configurable microarrays.

Fiber-fed: use fiber bundles to transfer light of selected targets in focal-plane field to spectrograph input. Fiber positioning usually done by computer control. Alternative: plug fibers into pre-drilled aperture plate. Output end of fibers usually a linear array. Requires large format detector. Up to several 100 targets/field. Details: Jeff Crane guest lecture.

o <u>Collimator</u>: mirror or lens to convert diverging beam from telescope into parallel beam for input to disperser

o <u>Disperser</u>: grating or prism, usually on rotating stage so can adjust central wavelength.

o <u>Camera</u>: to re-focus parallel output beam from disperser onto focal plane of detector.

o <u>Order separating devices</u>: filters, cross-dispersing gratings

o <u>Comparison sources</u>: lab lamps/arcs to calibrate wavelength scale using known spectrum of selected gases (e.g. He, Ne, Ar, Hg, Fe). Arrange to inject such that light path parallels that of astronomical targets.

o <u>Slit-viewer optics</u>: microscopes/cameras to view entrance aperture (from front or rear) to verify target acquisition/tracking.

SPECTROGRAPH DESIGN

In order to provide an optimal match in the standard design shown above (no loss of light, best resolution), the component optics of the spectrograph must satisfy the following conditions:

$$\left(\frac{F}{D}\right)_{\text{coll}} = \left(\frac{F}{D}\right)_{\text{tel}}$$

where **F** is the focal length and **D** is the diameter, and

$$D_{\text{coll}} = D_{\text{grat}} = D_{\text{cam}}$$

The linear reciprocal dispersion in the camera focal plane is then given by

$$K = \frac{d\cos\theta}{nF_{\text{cam}}}$$

where F_{cam} is the focal length of the camera, d is the grating slit spacing, and n is the order.

The "speed" of the spectrograph is proportional to the photon flux at the detector. For a slit spectrograph the speed will be proportional to:

$$\frac{s}{\beta^2}\left(\frac{D}{F}\right)_{\text{tel}}^2$$

where s is the linear width of the slit and β is the diameter of the seeing disk of the star (radians). This assumes that the slit is smaller than the star image (i.e. $s < \beta F_{\text{tel}}$).

SPECTROGRAPH DESIGN

The minimum resolution element in the spectrum is determined by the width of the image of the slit as projected on the detector and is

$$\delta\lambda_{\mathrm{min}} = \frac{s\,K}{R}$$

where R is the "slit-to-plate reduction factor" $R = F_{\mathrm{coll}}/F_{\mathrm{cam}}$.

According to the Nyquist criterion, optimum sampling of such an element requires <u>two</u> detector elements across it, so the physical size of a detector pixel should be

$$\Delta x_{\mathrm{pix}} = \frac{\delta\lambda_{\mathrm{min}}}{2\,K} = \frac{s}{2\,R}$$

EXAMPLE SPECTROGRAPH DESIGNS
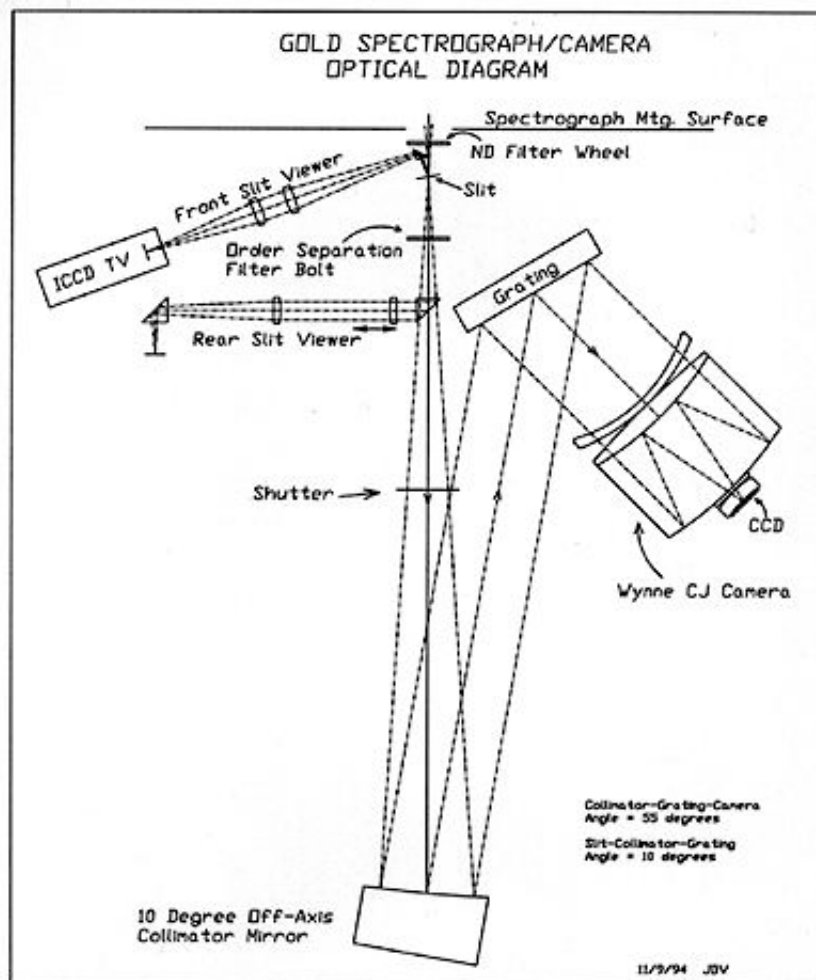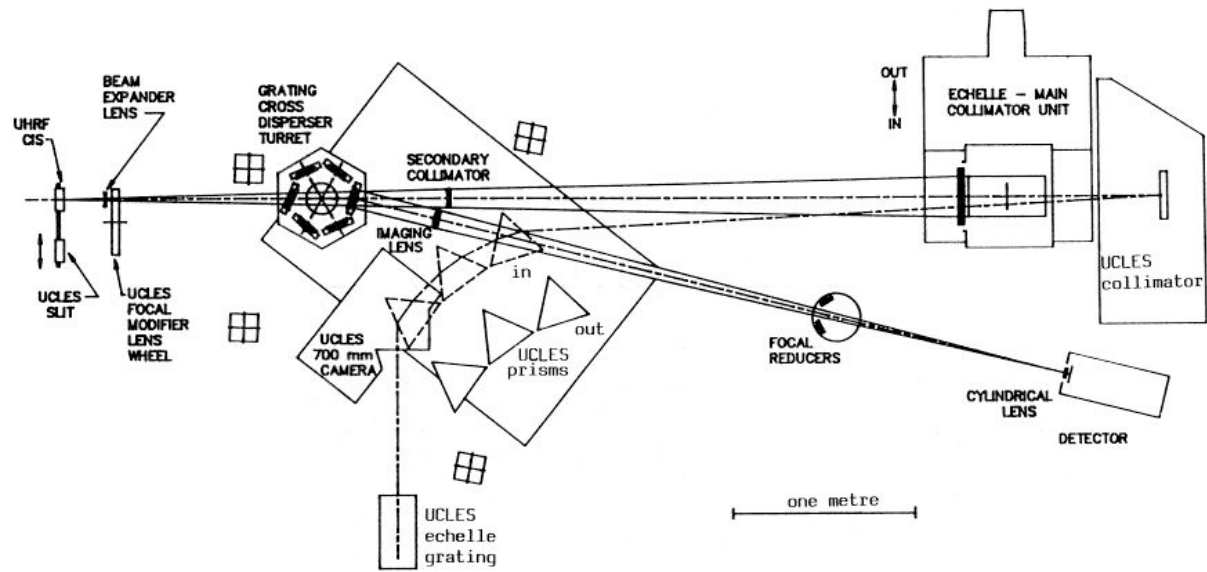
Figure 1: GCAM Spectrograph Optical Diagram
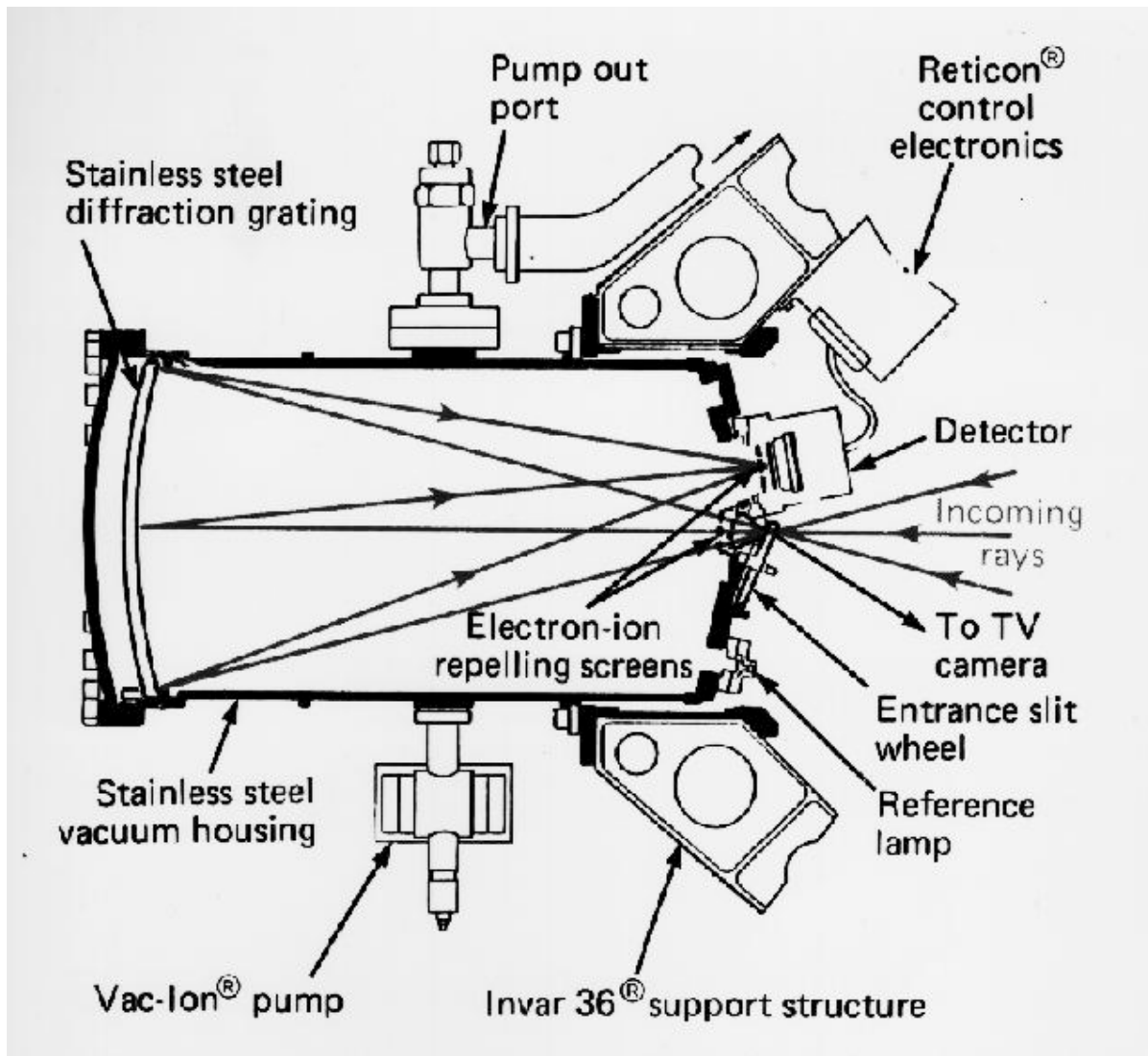
KPNO "Gold" Spectrograph: medium dispersion grating spectrograph with fast camera

EXAMPLE SPECTROGRAPH DESIGNS
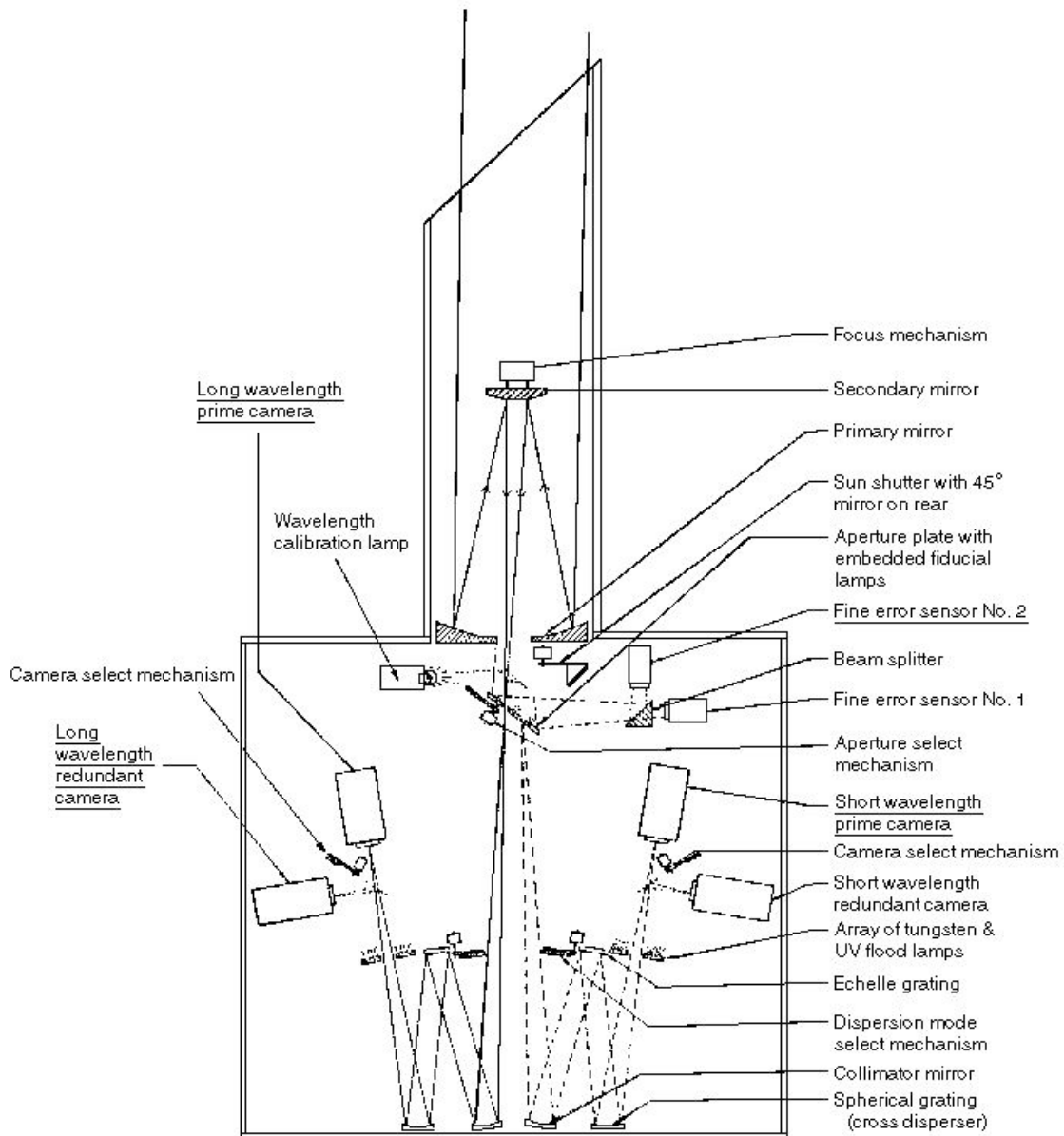
Ultra High Resolution Facility (AAO): echelle spectrograph, with selectable grating cross-dispersers; $\Re: \ 300,000 - 940,000$.

EXAMPLE SPECTROGRAPH DESIGNS

Hopkins Ultraviolet Telescope Far-UV spectrograph. Rowland circle design, 600 line/mm concave grating with SiC coating. Operated from Space Shuttle.

EXAMPLE SPECTROGRAPH DESIGNS

International Ultraviolet Explorer Satellite: optical path, showing telescope, and two-sided (Far-UV, Near-UV) echelle spectrographs

Optical Spectroscopy and Spectrographs

ASTR 511

6 October 2003

Topics:

• Brief (very) overview of spectroscopy

• Mechanics of slit spectrographs

• Fiber-fed systems

• The Fan Mountain spectrograph
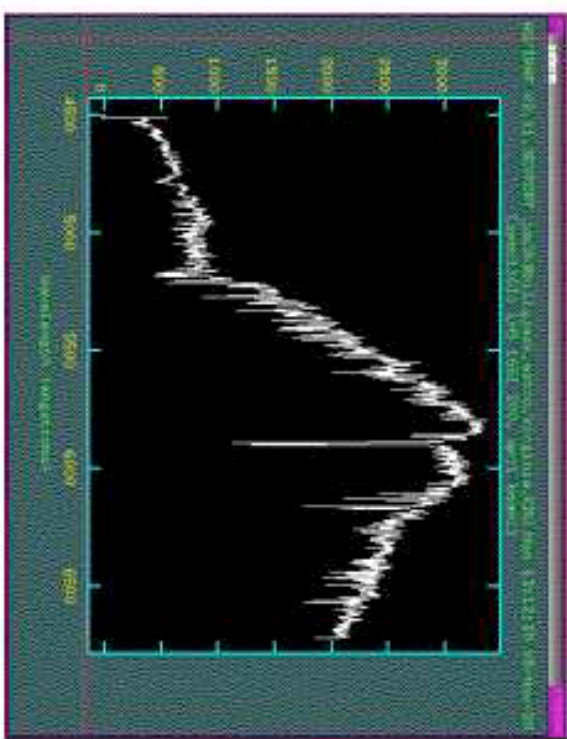
Spectroscopy in General

What useful information is gathered?

Stars:

- Spectral class
- Radial velocity
- Metallicity
- Gravity (luminosity class)
- Effective temperature
- Other derivative information such as multiplicity, distance, mass
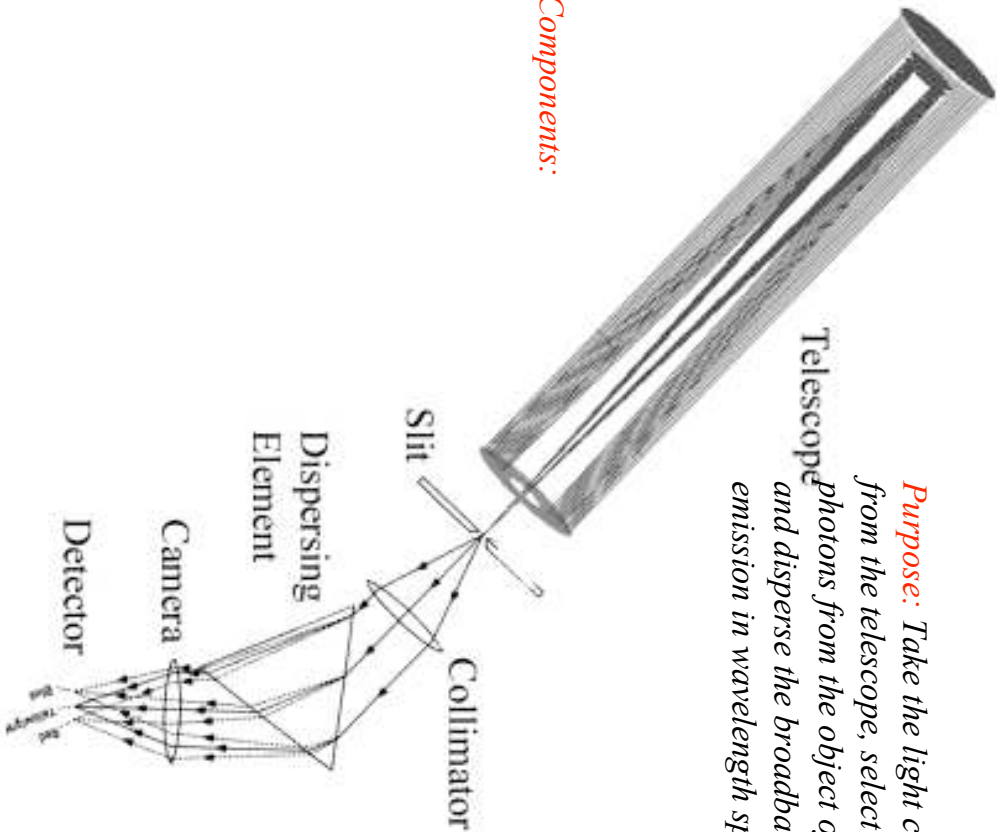
Galaxies:

- Velocity dispersion
- Rotation curves
- Distance (redshift)
- Other stuff

Spectrograph Mechanics
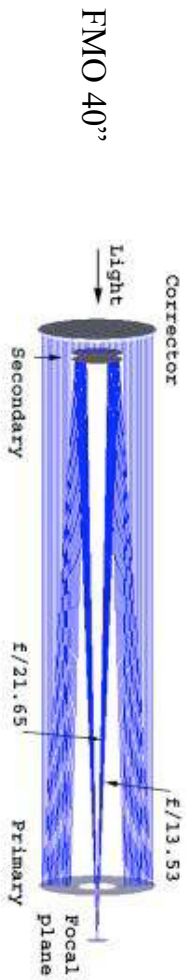
Purpose: Take the light collected from the telescope, select only photons from the object of interest, and disperse the broadband emission in wavelength space.

Basic Components:

Telescope

Slit

Dispersing Element

Camera

Detector

Collimator

The Telescope

- Serves as a "Light Bucket" – Collects light over a broad range of wavelengths and over a large Field of View.

- Takes parallel light and converges it over a range of f/ratios

  (f/ratio is [f/D]$_{optic}$)

FMO 40"

The Entrance slit

• Selects light from a particular object in the telescope's focal plane.

• Helps to give good "shape" and resolution to the spectrum produced by the instrument.

Telescope FOV

...masked by a short slit (focus on a star)
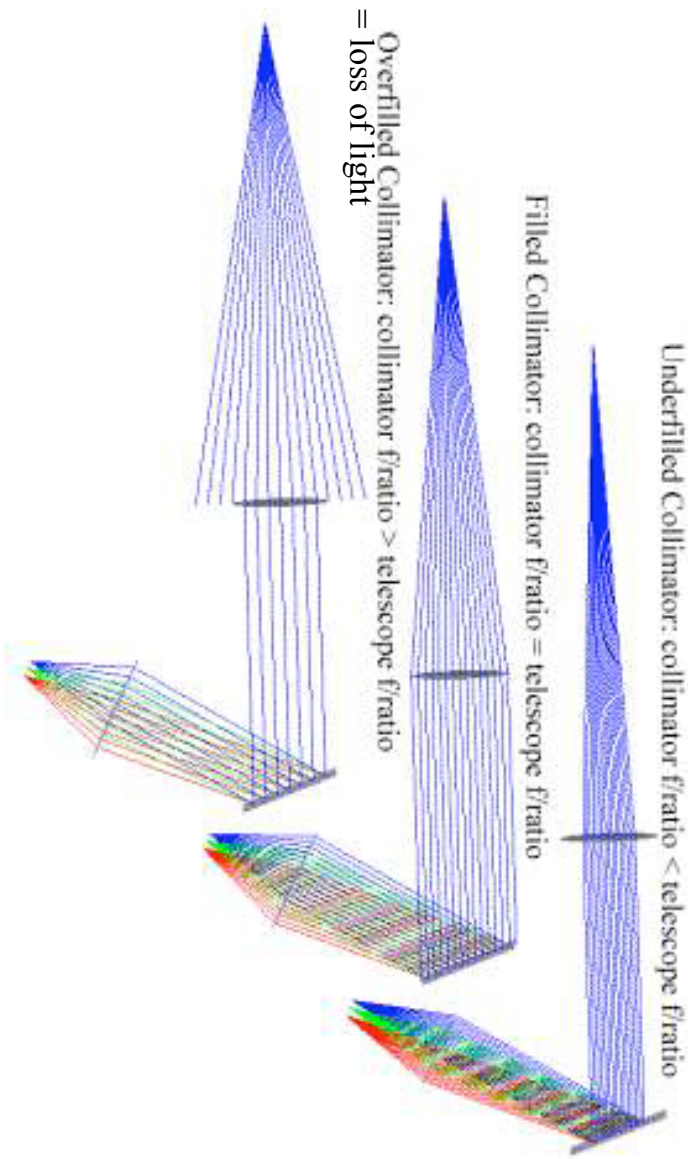
...masked by a long slit (focus on galaxy)
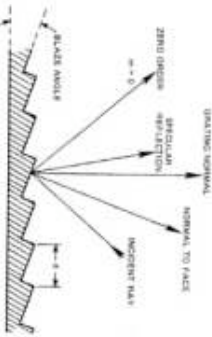
The Collimator

- Takes the diverging (post-telescope focus) rays and collimates them

- Can either be refractive (lens) or reflective (mirror) optics

- f/ratio should match that of the incoming telescope-focused light

- Underfilled collimator = loss of resolution

- Overfilled collimator = loss of light

Overfilled Collimator: collimator f/ratio > telescope f/ratio

Filled Collimator: collimator f/ratio = telescope f/ratio

Underfilled Collimator: collimator f/ratio < telescope f/ratio

http://www.astro.virginia.edu/class/oconnell/astr511/f03-crane-speclec/ASTR511-100603...
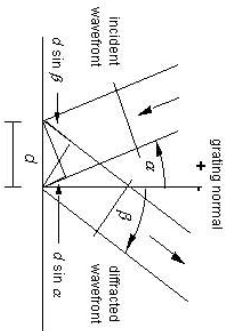
Dispersing Element

• Can be a prism, etalon, grating, or grism

    (we will focus on the reflection grating)

• Reflection grating is basically a large number of long, but very very thin, parallel mirrors

• The grating as a whole acts as a mirror, but convoluted with the diffracting effect of all of the parallel reflecting lines.

• For a given grating line density, diffraction order, and angle a of collimated input, each wavelength has a unique diffraction angle b

$$ml = d(\sin a + \sin b)$$

Camera (focusing) Optics
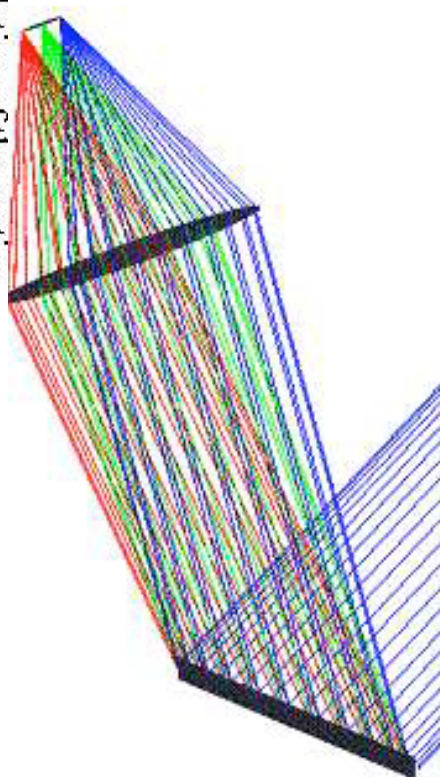
• The diffracted light is just a continuum of monochromatic, collimated beams; optics are required to focus this light onto a detector.

• Can be either refractive or reflective

• Typically has to be quite *fast* (small f/ratio) compared to the collimator.   Why?

... because the spectral resolution is a convolution of the grating function and the width of the *image* of the entrance slit.

$$(De)magnification of slit \sim f_{camera}/f_{collimator}$$

The camera/collimator system is an *imaging* system, which produces an image of the entrance slit on the detector. This usually determines the width of spectral features.

Fiber-fed spectrographs

The spectrograph can be separated from the telescope, fed light by optical fibers aligned on objects in the telescope's focal plane.

Some possible uses/benefits:

- *Work requiring great stability* –
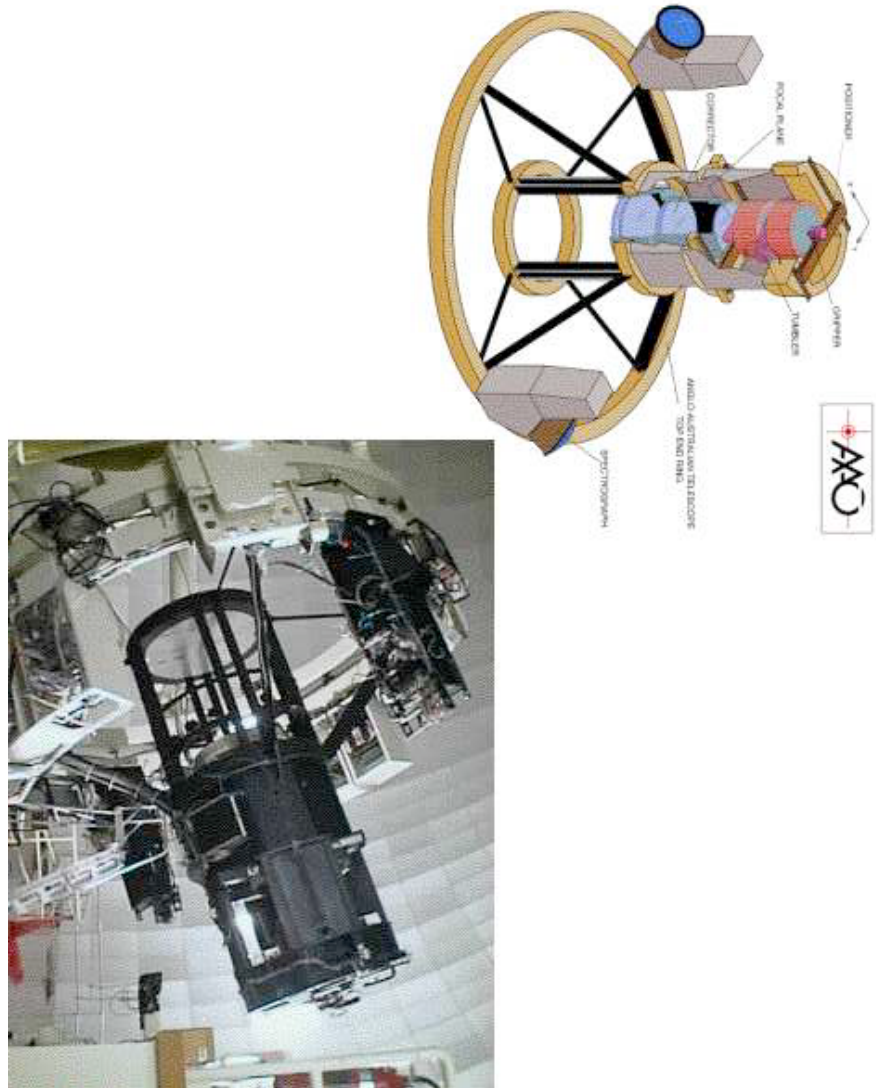
By disconnecting the spectrograph from the telescope, flexure effects are removed and spectra become more homogeneous.

Example: FMO spectrograph

- *Multi-object spectroscopy* –

Collect spectra from many objects at one time by positioning many fibers.

Example: 2dF at AAO

1999/5/22

http://www.astro.virginia.edu/class/oconnell/astr511/f03-crane-speclec/ASTR511-100603...
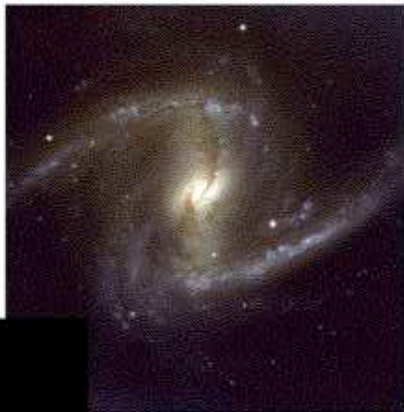
Integral Field Spectroscopy –

Collect spectra from many parts of an extended object simultaneously

Telescope FOV

...masked by an
array of optical
fibers

Difficulties with fiber-fed systems

• Added complexity

• Lower efficiency (throughput) for an individual spectrum, although this can be made up for by collecting lots of spectra simultaneously

• Problems associated with Focal Ratio Degradation (FRD)

- *microbending* in optical fibers leads to a net lowering of the f/ratio of light transmitted to the spectrograph

- uncertainty of spectrograph input f/ratio can make choice of collimator difficult

- since the collimator ends up being *faster*, the camera in turn has to be equivalently faster. Ugh.
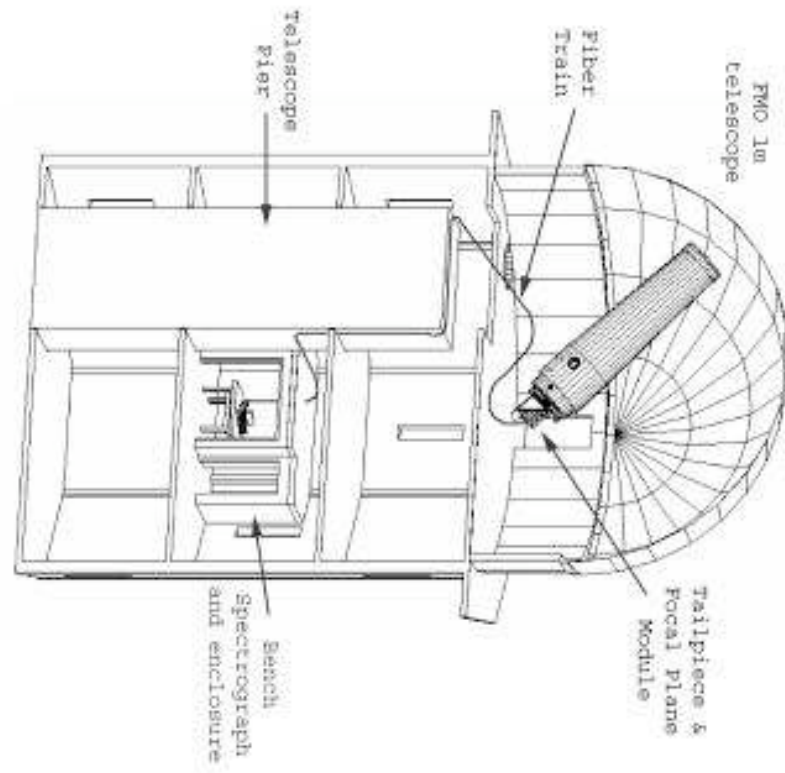
Fan Mountain Observatory
Bench Spectrograph

Project Overview:

- Single object, fiber-fed, bench-mounted spectrograph

- Low to medium spectral resolution

- Primary wavelength coverage: $470 < \lambda < 670$ nm

  (although full visual coverage eventually)

- Target velocity resolution: 7-10 km/s

Instrument components:
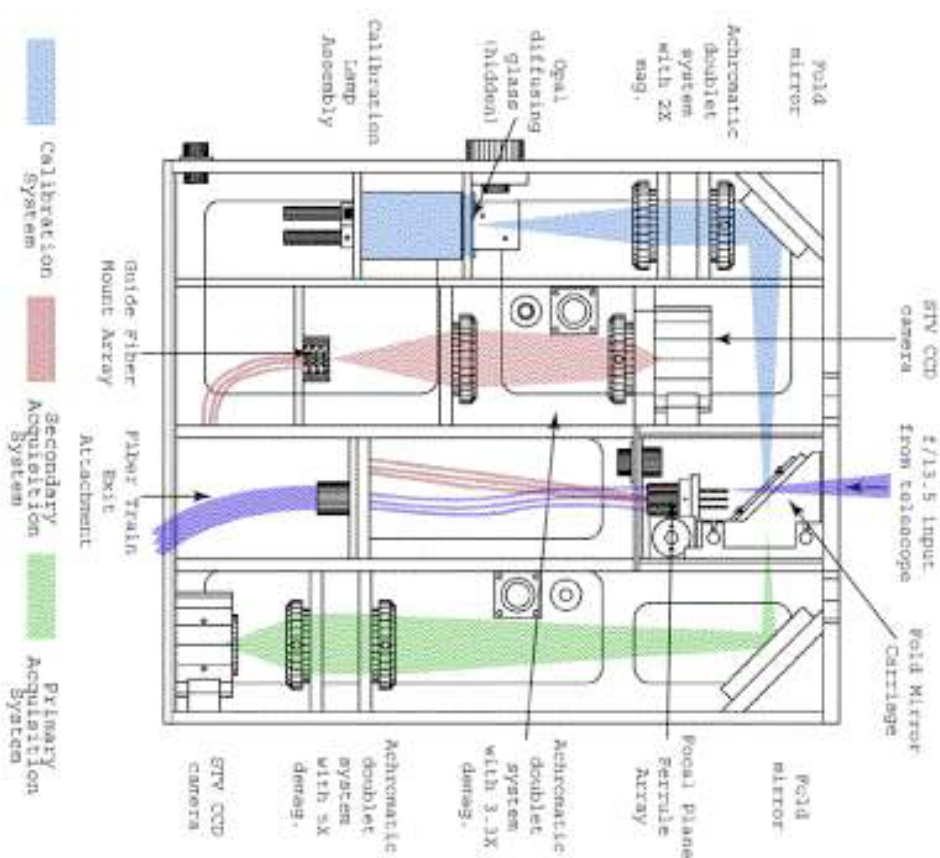
- Focal plane module

- Fiber train

- Bench spectrograph

FMO 1m
telescope

Fiber
Train

Telescope
Pier

Tailpiece &
Focal Plane
Module

Bench
Spectrograph
and enclosure

Focal Plane Module

Functions:

• Fiber alignment, coarse

• Fiber alignment, fine

• Calibration light injection

Fiber Train

Functions:

• Transmit stellar light to spectrograph

• Transmit guide fiber light to acquisition camera

Science Fiber

Guide Fibers

Stainless Steel Capillary Tube

Teflon Tubing Attachment
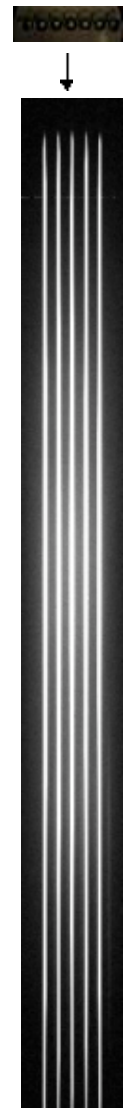
Bench Spectrograph

Design Overview:
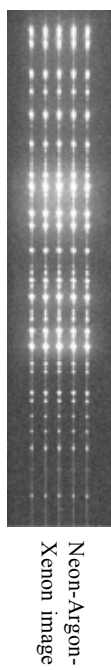
- Linear array of 7 science fibers, f/4-f/5 output
- f/5 Achromatic Doublet collimator
- 1200 line/mm reflection grating
- f/2 SLR lens for camera
- SITe 2048x2048 CCD

Science Fiber Mount
~f/5 output expected
for 200 μm fiber cores

Achromatic Double
Collimator Mount
effectively f/5 with
iris diaphragm

Rotatable
Grating Mount

115mm f/2 SLR
camera lens

Dewar Mount + dewar
for SITe 2048 X 2048
24 μm pixel CCD

Data

Quartz lamp image
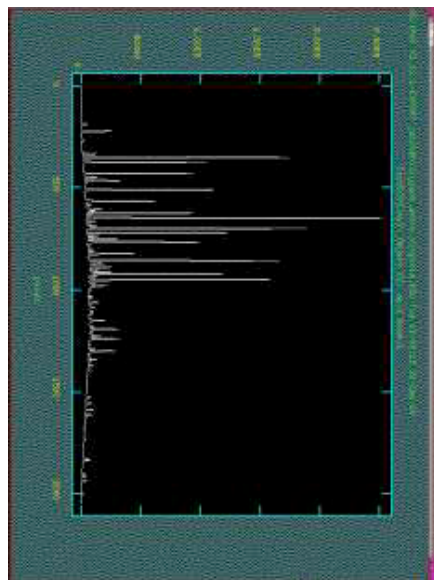
Neon-Argon-
Xenon image

Neon-Argon-
Xenon spectrum
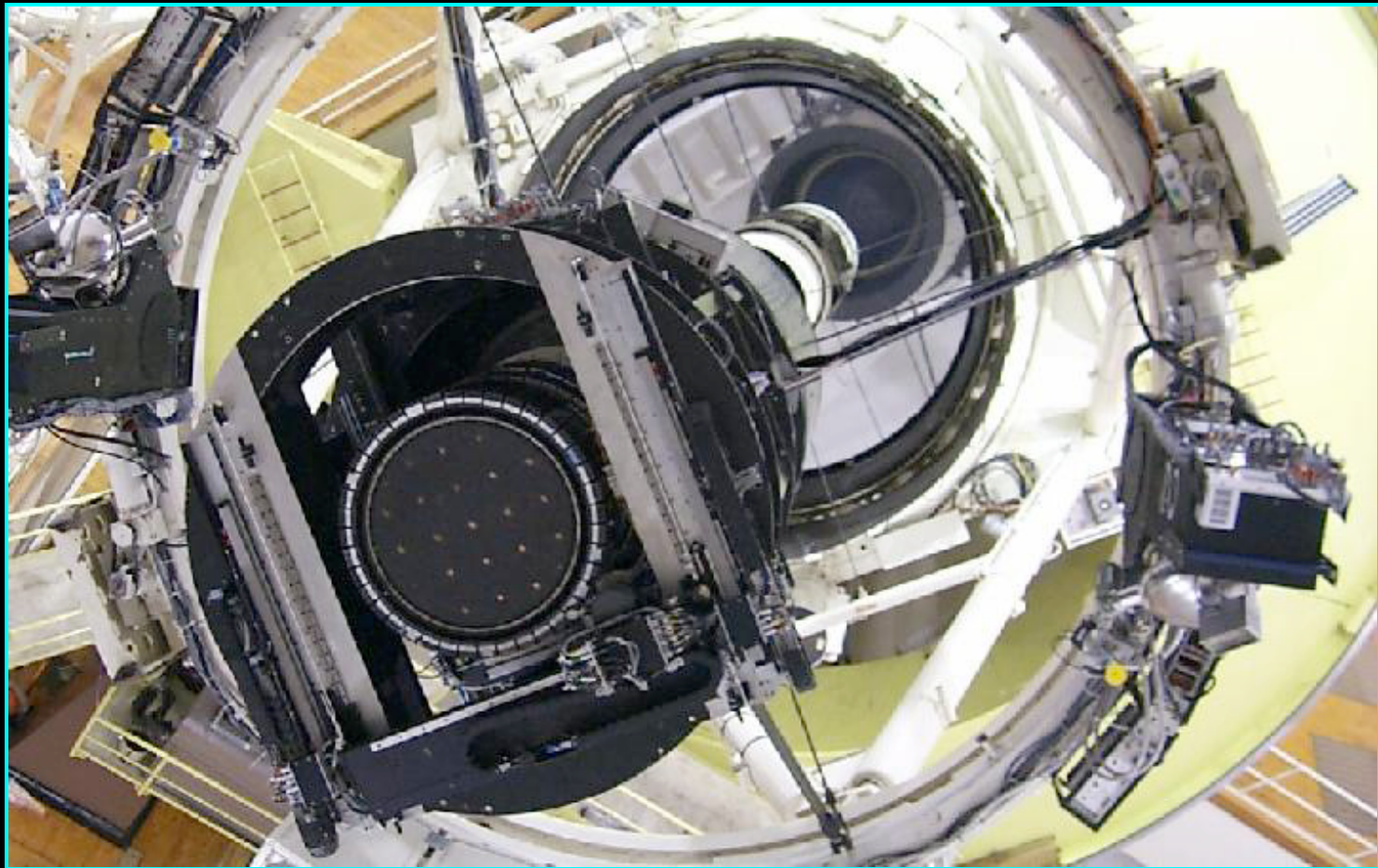
In addition to target spectra, you need…

• Quartz lamp spectra to determine how to trace the fainter spectra

• Arc lamp spectra for wavelength calibration

• Flat fields to remove pixel-level variations

• Bias frames

• Standard stars, depending on your science

ASTR 511 (O'Connell) Lecture Notes

STATE OF THE ART SPECTROSCOPY

Two Degree Field Fiber Spectrograph on AAT (J. Pogson)

Multi-beam spectrographs are among the most sophisticated and expensive instrumentation used by astronomers today, costing upwards of $5M on a large telescope. Here are some state-of-the-art examples. The primary application of these systems has been to large samples of faint galaxies.

FIBER-FED MULTI-OBJECT INSTRUMENTS

Fiber-optic transfer devices typically offer small (2-4 arcsec) entrance apertures for each target. Fibers must be repositioned with high precision for each new field. This is usually done by mechanical robots. In most designs, individual fiber apertures are clamped magnetically on a flat focal-plane plate. Output of fiber unit is usually a linear (slit-like) array at spectrograph input.

- 2dF (AAT 4-m)

    Prime focus instrument; 2 spectrographs (R ~ 1000)

    2 degree FOV

    400 fibers per field; magnetically attached to field plate; positioned by robot; 200 to each spectrograph

    Two fiber focal plane units (one positioning while other observes; flip to replace)

- **SDSS spectrograph (2.5-m)**

    Cassegrain mounting

    Two dual spectrographs (R ~ 2000). Red/blue light split in each by diagonal dichroic mirror [red light transmitted, blue reflected]

    640 fibers (320 each spectrograph) manually plugged into precision drilled aperture plate covering 3 degree FOV

- Hectospec (MMT 6.5-m)

    300 fibers feeding bench spectrograph (R ~ 1000)

    Two robot fiber positioners; placement time: 5 min

    1 degree FOV

- HYDRA (NOAO/WIYN, 3.5-m)

    100 fibers feeding bench spectrograph

    1 degree FOV

- VIRMOS (VLT, 8.2-m)

APERTURE PLATE MULTI-OBJECT INSTRUMENTS

Aperture-plate spectrographs use small apertures in a focal-plane mask at the spectrograph entrance to transmit light from selected targets. Usually, computer-controlled devices (mechanical cutters, lasers) used to cut slits in a thin, shaped, metallic mask. Early designs used photographic masks. The slits can be of arbitrary shape and length within overall constraints set by the spectrograph focal plane.

Main operational problem is to avoid overlap of spectra and to maximize use of the detector area in a given field; this requires special optimizing software. In principle, aperture plate designs should have better throughput, better sky background subtraction, and better flux calibration than fiber designs. Fiber designs can accommodate more targets, however (because the output format on the detector is independent of the spatial distribution of targets).

- IMACS (Magellan, 6.5-m)

    Laser-cut slit masks covering 27 arcmin FOV

    Selectable gratings/grisms

    8000x8000 CCD detector

    First spectrum (240 slits)

- DEIMOS (Keck 10-m)

    Slitmasks: 85 slitlets x 2 barrels; field size 16 arcmin

    2000x4000x8 CCD detectors

INTEGRAL FIELD UNITS

An integral field unit (IFU) produces distinct spectra for many contiguous elements in a given field. Powerful for the study of extended objects like globular clusters or nearby galaxies. Aperture positions and sizes are fixed and generally cover a square/retangular area. IFU's have been designed using fiber bundles, lenslet arrays, and configurable microaperture or micromirror arrays.

- SAURON

    Design

Telescope image is focussed on array of microlenses which break up 40x33 arcsec field into 1 arcsec images.

Grism disperser

Slight rotation of dispersion direction wrt lenslet array achieves cross-dispersion so spectra (if short) don't overlap; limit spectral length using IF filter

Example SAURON science: kinematics and absorption line maps in early-type galaxies

- JSWT NIRSpec

  The Near Infrared Spectrograph on the James Webb Space Telescope, now under construction, employs an integral field unit based on a microshutter array. The array contains over 62,000 cells (about 100x200 microns each) that can be opened or closed by a magnetic controller to admit light to the detector.

  More information on JWST microshutters (S.H. Moseley)

HIGH PRECISION DOPPLER SHIFT SPECTROSCOPY (Planet Detection)

The most conspicuous use of high precision spectroscopy has been in the detection of extra-solar planets through stellar reflex Doppler shifts, where velocity differences of order 5 m/s must be measured. Requires both high spectral resolution and great mechanical/optical stability in spectrograph. Suitable designs employing digital detectors have been around for > 20 years, but were not energetically exploited until the surprising detection of a Jupiter mass planet in a sub-AU orbit made in 1995 by Mayor & Queloz at Haute-Provence Observatory.

- Marcy-Butler Technique

  Cross-dispersed echelle spectrometer, R ~ 60000

  Use a gaseous iodine cell at entrance slit to impress a calibration absorption spectrum on each stellar spectrum taken. Dense molecular spectrum yields ~10 wavelength standard lines per Å

  Wavelength standard passes through optics in exactly same way as stellar light and simultaneously with it

  Perform cross-correlation analysis on large number of spectral segments of star+iodine spectrum covering ~ 800 Å to determine wavelength shift of star

  SNR ~ 200 in flux yields velocity precision ~ 3 m/s. Since world-class athletes can achieve ~ 10 m/s, we can now detect stars moving at a human pace.

NB: 3 m/s precision corresponds to effective Doppler shift resolution of ~ c/(3 m/s) = 10^8!

- All exoplanets to date have been detected by the reflex Doppler technique, but it is anticipated that many more will be found by transit eclipses in the future

    - Sample velocity curve (51 Peg) (first exoplanet to be detected)

    - Summary/results of planet searches

OTHER ILLUSTRATIONS

    - Keck Hi-Res Spectrograph Schematic

    - Keck Hi-Res Spectrum
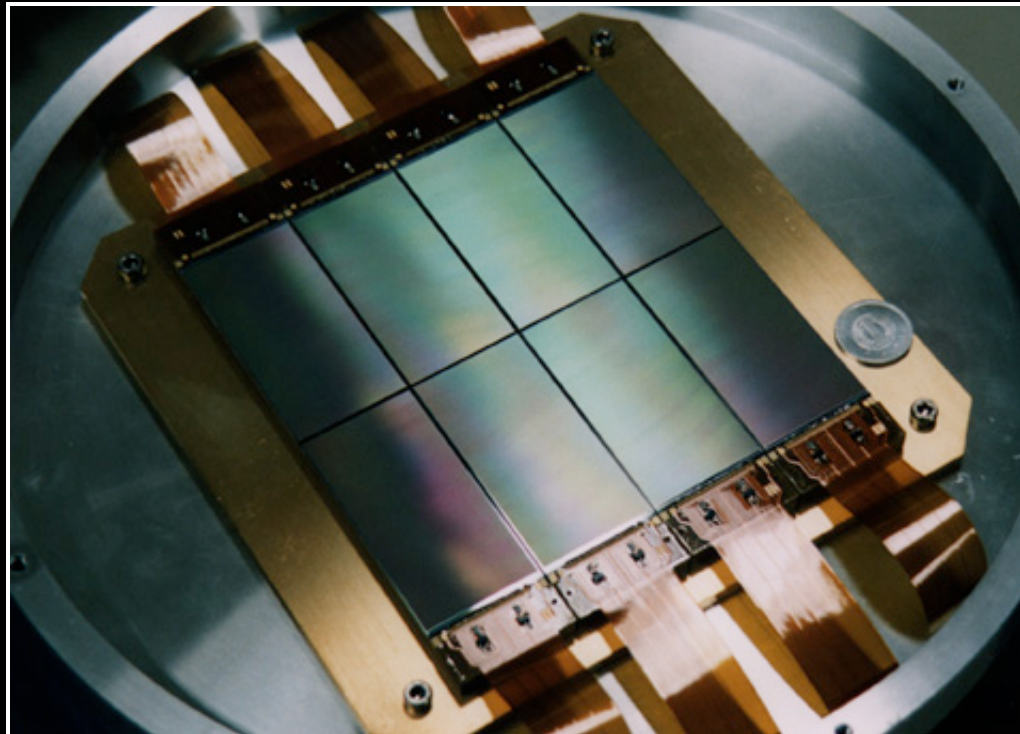
Last Lecture   **Lecture Index**   **Next Lecture**

*Last modified **June 2007** by rwo*

Text copyright © 2001-2007 Robert W. O'Connell. All rights reserved. These notes are intended for the private, noncommercial use of students enrolled in Astronomy 511 at the University of Virginia.

ASTR 511 (O'Connell) Lecture Notes

CCD'S IN ASTRONOMY

Subaru CCD Mosaic 8 x (2k x 4k)

Charged coupled devices (CCD's) have been used in astronomy since the late 1970's. They are now nearly ubiquitous in observations made at wavelengths between the near-IR (~1 μ) and the X-ray. They have transformed the way astronomy is done.

I. REFERENCES FOR CCD'S

<u>General</u>

- Buil, *CCD Astronomy*
- Howell, *Handbook of CCD Astronomy*

- Kitchin, *Astrophysical Techniques*
- LLM Sec. 7.3.3.
- MacKay, Ann Rev Astr Ap, 24, 255, 1986
- Rieke, *Detection of Light* : general introduction to detector physics
- Timothy, PASP, 95, 810, 1983: discussion of many detector types
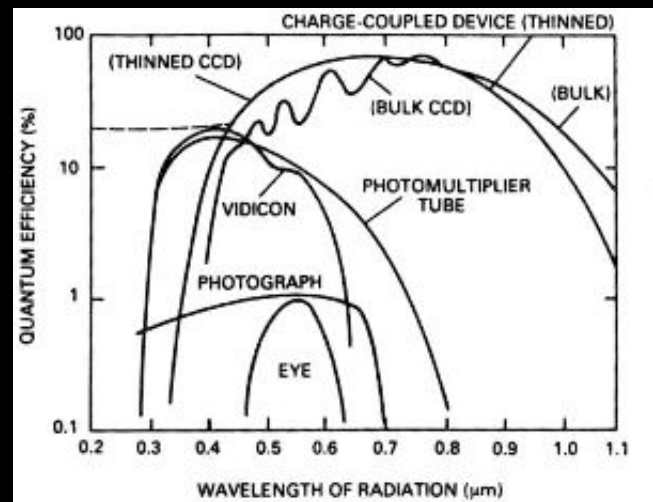
CCD Data Reduction and Applications

- Abbott, "In Situ CCD Testing"
- Franx et al. AJ, 98, 538, 1989: sample application to surface photometry
- Fruchter, "Imaging Dithering and CR Rejection in Undersampled HST Data"
- Massey, A User's Guide to CCD Reductions with IRAF (1997)
- Stetson: many papers on CCD applications to point source photometry, especially of star clusters
- Tyson, JOSAA, 3, 2131, 1986: high precision technique

II. GENERAL DETECTOR CHARACTERIZATION

- **QUANTUM EFFICIENCY**

  - QE = percentage of photons incident on detector which produce measurable signals

  - Strong wavelength dependence (e.g. threshold activation cutoffs set by workfunction/band gap)

  - Typical peak values:

    - Eye: 1-2%
    - Photographic plate: 1-2%
    - Photomultiplier tube: 20-30%
    - CCD: 70-90%
    - IR array (HgCdTe): 30-50%

Schematic QE curves for various classes of detector

  - "Detective quantum efficiency" is defined as $[(SNR_{out})/(SNR_{in})]^2$, where "in" and "out" refer to the input and output signals to/from the detector, respectively. DQE combines basic QE with the noise introduced by the detector. This quantity is really what matters in comparing detectors, but it is so dependent on specific details of operations/applications that it is rarely used.

- **SPECTRAL RANGE**

- ○ **Wavelength region over which QE is sufficient for operation**

- **DYNAMIC RANGE**

  - ○ **Definition: ratio of maximum to minimum measurable signal**

    - ■ **E.g. maximum number of events in a CCD pixel is determined by photoelectron "full well" capacity or digitization maximum (typically 2 bytes); minimum is determined by dark current/readout noise**

  - ○ **Applies to a *single exposure*; effective dynamic range can be increased with multiple exposures**

  - ○ **Typical values: 100 (Pg); 10^4 (CCD); 10^5 (PMT)**

  - ○ **Related concepts:**

    - ■ <u>**Linear Range**</u>**: range of signals for which [Output] = k x [Input], where k is a constant. Generally smaller than *calibrateable* range**

    - ■ <u>**Threshold**</u>**: minimum measurable signal. Influenced by detector noise or other intrinsic characteristics (e.g. fog on Pg plates)**

    - ■ <u>**Saturation point**</u>**: level where detector response ceases to change with signal**

- **NOISE CHARACTERISTICS**

  See discussion of various types of detector noise in <u>Lecture 7 notes</u>

- **RESOLUTION**

  - ○ <u>**Temporal**</u>

    - ■ **PMT: ~0.0001 ms**
    - ■ **CCD: ~10 ms per pixel**

  - ○ <u>**Spatial**</u> **(array detectors)**

    - ■ **Pixel = minimum measureable area of detector surface. Typically 10-50 μ on Pg or semiconductor types. Pixels are not necessarily independent of one another.**

    - ■ **Resolution cell: according to the *Nyquist criterion*, the resolution cell is 2x the size of the minimum *independent* measurable area. For proper sampling of image, need at least 2 pixels per resolution cell. A lower pixel density implies "undersampled" imaging. A significantly higher pixel density does not provide more information and is a waste of pixels.**

For an imaging application, the Nyquist criterion implies that 1 pixel should span ~ (FWHM)/2, where FWHM is the full width half maximum of the point spread function.

- ○ <u>Spectral</u>

    - Most UVOIR detectors are broad-band; inherently poor spectral resolution. Must use external elements (filters, gratings) to provide spectral resolution

    - Exception: superconducting "3D" detectors, which measure photon energy as well as position; current spectral resolution is R ~ 100

III. BRIEF HISTORY OF ASTRONOMICAL DETECTORS

PHOTOGRAPHIC ASTRONOMY:

Photographic emulsions work by storing in AgBr crystals the photoelectrons ejected following absorption of photons during exposure to light. Chemical reactions during development cause the crystals to precipitate grains of silver, which form a permanent image.

Film was the detector of choice for almost all applications in astronomy from around 1900 to 1960 and for imaging until about 1980. It is impossible to exaggerate its importance to the development of modern astronomy. Even with relatively low QE, photographic plates offered <u>decisive advantages</u> over visual observations:

1. Very long exposure times (up to a week in early applications), meaning limiting fluxes thousands of times fainter
2. A permanent, objective record of astronomical images and spectra
3. Geometric stability, important for astrometry and morphology
4. Large formats for wide field surveys
5. Extension of observations to EM bands beyond the "visual" band (the classic "photographic" band is centered around 4500 Å)

However, the photographic emulsion had serious limitations with which astronomers had long struggled:

1. It is relatively insensitive, with QE ~ 1%.
2. Pg materials have non-negligible thresholds (a minimum of ~4 electrons per grain), a strongly non-linear response function, and limited dynamic range. These properties plus the use of hard-to-control chemical processes for emulsion deposition & development makes them very difficult to calibrate quantitatively.
3. Each individual plate (or at the best, each co-processed "batch" of plates) has different characteristics.
4. Conversion of data to quantitative form (e.g. with microdensitometers) is
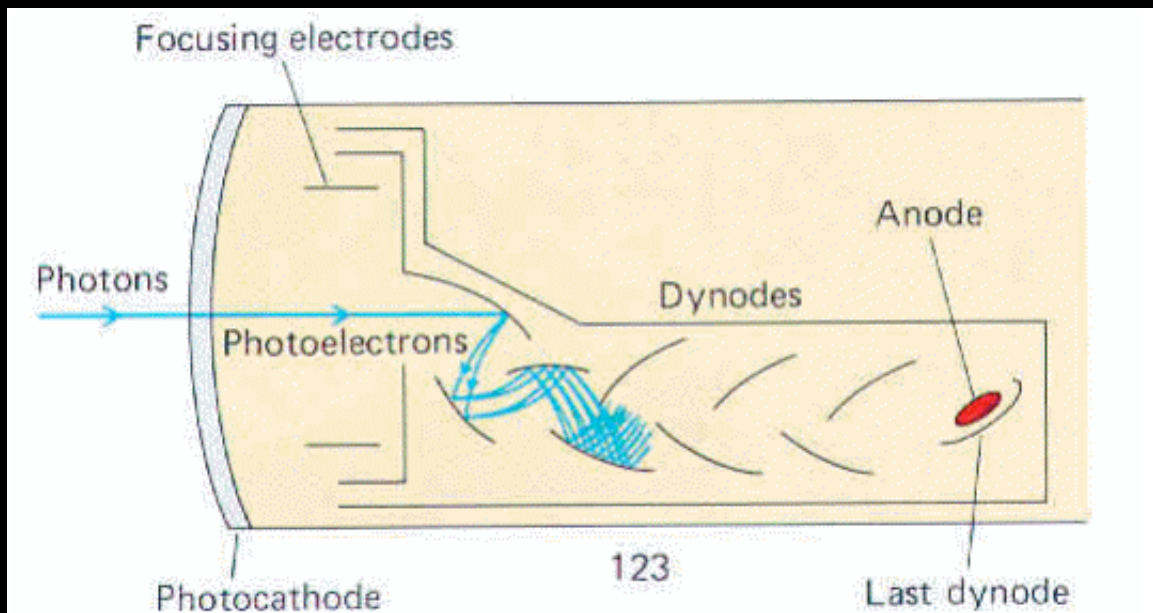
slow and cumbersome.

For details on photography at low light levels, see Smith & Hoag 1979, ARAA, 17, 43.

PHOTOELECTRIC ASTRONOMY TO 1980:

In 1907, Joel Stebbins (UIll, UWisc) began testing various types of photoelectronic detectors. These, such as selenium phototubes, were largely experimental and tempermental, but use of PE devices spread after the 1920's. World War II greatly accelerated these technologies, with mass production of high quality vacuum tubes and sensitive electronics for detection of faint signals.

The key design for astronomy was the photomultiplier tube (PMT), the first widely used example of which was the RCA 1P21. The initial detector in a PMT is a *photo-emissive* cathode surface, made from alkali metal compounds, which ejects a single electron in response to a photon absorption. A series of other "secondary electron emissive" surfaces (the "dynode chain") amplifies this into a burst of ~10^{6-7} electrons. (See illustration below.)

PMT's require cooling to suppress dark current and were typically operated at dry-ice temperatures (-78C). The photocathode QE's of PMT's in the optical region reached 20-40% by the 1960's, with very wide acceptance bands.

PMT's became the workhorses of multicolor photometry and spectrophotometry (e.g. the Johnson & Morgan broad-band UBV system) after 1950. They featured excellent linearity and stability, which implied an unprecedented capacity for accurate calibration of photometric measurements. PMT photometry routinely reached the 1% level for flux calibration. In turn, this was responsible for an explosion in quantitative astrophysics.

Although PMT's were initially operated in a "direct current" mode, the pulse-like

character of PMT output led to the adoption in astronomy of the same kinds of high speed <u>digital electronics</u> that had been developed earlier for accelerator and nuclear physics. This kind of "pulse-counting" operation permitted the detection of <u>individual photons</u> from cosmic sources.

PMT's offered much higher sensitivity and linearity than film and broader wavelength response, but they were <u>single element devices</u>. They were not easily adaptable to 1-D, let alone 2-D, applications (such as imaging), despite heroic attempts such as the <u>Palomar Multichannel Photoelectric Spectrometer (Oke, 1969)</u>.

For more details on PMT's and PMT-based photometers, see the articles by Lallemand and Johnson in *Astronomical Techniques*, ed. W. A. Hiltner (Stars & Stellar Systems Vol II).
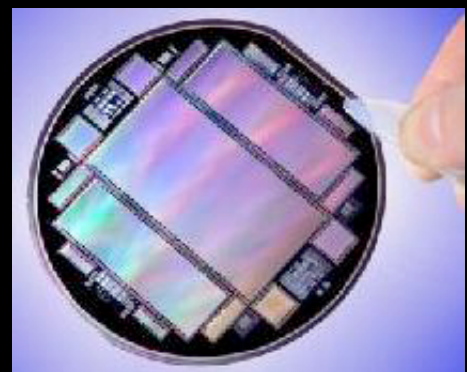
Around 1960, a plethora of efforts began to develop robust **1-D and 2-D electronic devices** suitable for astronomy. A dozen or so of these produced practical systems (e.g. the Secondary Electron Conduction Vidicon, the Intensified Dissector Scanner, the Intensified Reticon Scanner, the Image Photon Counting System, and the Multi-Anode Microchannel Array detector).

> Most of these employ some type of <u>image intensifier</u> vacuum tube as a key element. This technology was developed for military night vision systems. Intensifiers produce easily detectable light pulses in a 2-D image field from individual incident photons by accelerating the photo-electrons to high energies and/or producing a cascade of electrons, then focussing these on a luminescent output screen. Disadvantages include the frequent use of high voltages (e.g. 25 kV) and serious image blur which, however, can be reduced by the use of <u>pulse centroiding</u> electronics. Fiber optic input/output plates were commonly used with intensifiers after 1970. <u>Microchannel plate</u> (MCP) intensifiers have often been used in space astronomy missions (including HST, GALEX, and FUSE).

SOLID STATE ARRAY DETECTORS:

> But by far the most successful 2-D devices for astronomy emerging in the last 30 years have been <u>solid state, semiconductor arrays</u>. These are based on *photo-conductive* materials fabricated with embedded microelectronic integrated circuits on thin wafers by <u>photolithography</u>. Although lower quality devices can be mass-produced by microchip "foundries," professional grade detectors still need to be custom-processed.

Wafer containing a number of co-fabricated CCDs and other

> Solid state arrays are now employed as astronomical detectors from the X-ray to the far-infrared. The most widely used is the *Charge-Coupled Device* (CCD), which operates at wavelengths from the X-ray to ~1 μ. The basic CCD architecture was invented at Bell Labs in the late 1960's. By the mid-70's, CCDs were being tested as

1900's. By the mid-70's, CCDs were being tested as
astronomical detectors. They did not come into
widespread use until ca. 1980, following extensive
development efforts associated with the Wide Field &
Planetary Camera on the Hubble Space Telescope.

devices.

IV. SEMICONDUCTORS

Semiconductors are crystalline materials which are not normally good conductors of
electricity but which can be made to conduct under certain circumstances. The central
useful property of semiconductors employed in astronomy is that their electrical properties
change significantly after absorption of photons.
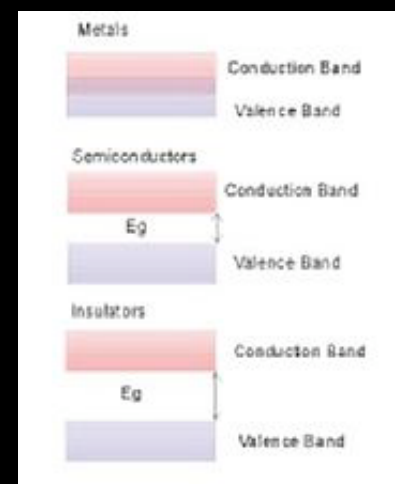
BAND GAPS: The properties of semiconductors are
manipulated by changing the structure of their internal energy
levels, which are spread out into "bands" by the proximity of
the component atoms of the solid. The "valence" band,
corresponding to the outermost electrons in a normal,
unexcited atom, is the lowest energy band where electrons are
able to move between ions. However, no net conduction occurs
as long as the band is full. Above this lie the "conduction"
bands, which are not filled, and where electrons will move
freely in response to external EM fields. The separation
between the valence and first conduction band is called the
"band gap energy", E_g.

Different materials have a wide range of band gaps.
"Conductors" have a zero gap, meaning that electrons are
always available to transfer charge. "Insulators" have very large
gaps, implying zero conduction except under extreme
circumstances. "Semiconductors" have intermediate gaps.

Absorption of a photon can push a valence electron into the conduction band and produce
a potential electrical signal. The photon energy must exceed E_g, which implies that there is
a maximum wavelength for excitation given by:

$$\text{Lam}_{max} = 12{,}400 \text{ Å}/E_g(\text{eV})$$

Obviously, materials with band gaps in the few eV range are of interest as potential UVOIR
detectors. Band gaps and max wavelengths for some important materials are given in the
following table:
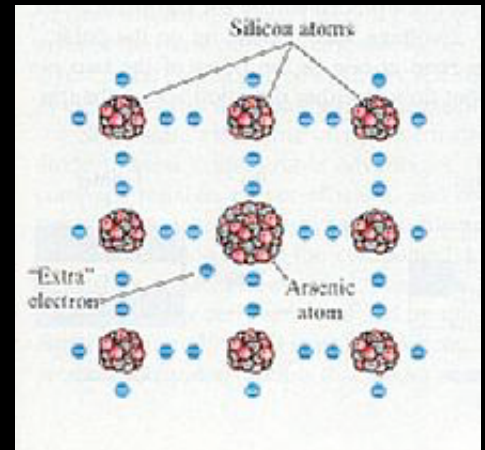
Material	E_g(eV)	Lam_{max} (Å)
Pure Si	1.1	11,300

GaAs	1.43	8,670
InSb	0.36	34,400
$Hg_{1-x}Cd_xTe$	1.55x	8,000/x

DOPING: The "elemental" semiconductors are those elements in group IVa of the **Periodic Table** (including Si and Ge). These have four electrons in their valence shells, half the maximum allowed. These are shared among the ions in "co-valent bonds." There are many other types of "compound" semiconductors, however, composed for instance of atoms from group IIIa and Va of the Table; two of these are listed in the table above.
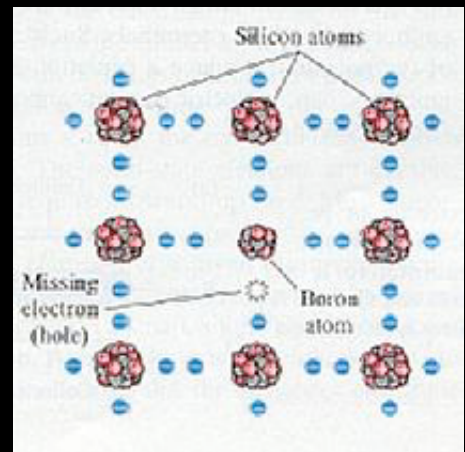
The electrical properties of pure semiconductors can be dramatically altered by adding ("doping with") small amounts (~1 part in 10^6) of an impurity. The result is called an "extrinsic" semiconductor.

n-type doping
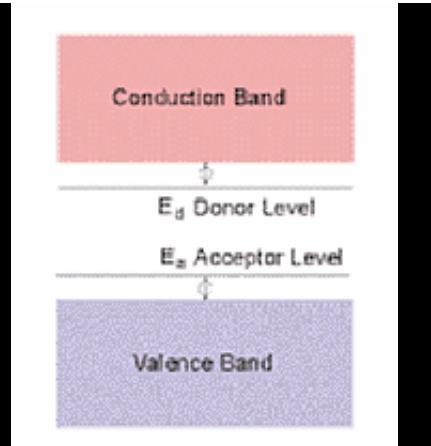
- **n-type**: a material with more than 4 valence electrons is added (As, from group Va, in the illustration). The extra electrons cannot be accommodated in the valence band and so occupy the conduction band. They represent a persistent set of negative carriers

- **p-type**: a material with fewer than 4 valence electrons is added (e.g. B, from group IIIa). This has one fewer electron than normal and creates a small "vacuum" in the electron sea of the valence band. This is called a "hole." As valence electrons shift to fill it, the hole propagates like a positive charge in the opposite direction. The holes represent a persistent set of positive carriers.

p-type doping

In pure semiconductors, conduction electrons and holes can also exist, if electrons are excited by thermal effects, for instance. But they always occur in pairs. Electrons and holes in n- and p-type materials, respectively, have no counterparts. Extrinsic material is electrically neutral but is more responsive than pure materials to a difference in electrical potential.

By adjusting the amount of doping, the band gap of the semiconductor (donor/acceptor levels in diagram at right) can be customized. By layering n/p regions, the response to applied potentials can be adjusted to create a large variety of electronic devices.

Doping affects energy levels

Photons are primarily absorbed by electrons in the valence band. For photon energies above E_g, the electron is boosted to the conduction band, leaving a hole behind. If a positive voltage is applied at one side of the semiconductor, the electron will be attracted toward it while the hole will be repelled.

V. BASIC CCD DESIGN

Apart from <u>sensitivity</u>, the key design issues for solid state arrays are to <u>localize</u> photon-produced charges on their surfaces and then arrange to <u>amplify and read them out</u> without distorting the image or introducing unacceptable amounts of noise.

A CCD is a <u>charge-transfer device</u>. Its storage, transfer, and amplification electronics are all fabricated on a single piece of silicon (unlike most IR arrays). During an exposure, it traps released photoelectrons in small voltage wells. After the exposure, the electrons are shifted in a series of "charge-coupled" steps across the CCD surface, amplified, read out of the CCD, and stored in a computer memory. This is <u>"destructive readout"</u>---i.e. one cannot read the same signal again (unlike other array architectures, where each pixel is coupled to a separate amplifier).

BASIC STRUCTURAL ELEMENT: The basic element in a CCD design is a "Metal-Oxide-Semiconductor" capacitor. See the illustration above. This serves both to store photoelectrons and to shift them wholesale. The bulk material is p-silicon on which an insulating later of silicon-oxide has been grown. P-silicon can be made to have very small numbers of free electrons ("high resistivity") before exposure to light; this is important for best performance. A set of thin conducting electrodes of semitransparent "polysilicon" are applied.

Before exposure, the central electrode is set to a positive bias while the two flanking electrodes are set negative. This creates a "depletion" region under the central electrode containing no holes but a deep potential well to trap electrons. The region shown is about 10µ thick.

OPERATION SEQUENCE: During exposure (controlled by a separate shutter), light enters through the "front-side" electrodes. Photoelectrons generated under the central electrode will be attracted toward the electrode and held below it. The corresponding holes will be swept away into the bulk silicon. Good performance requires little diffusion of electrons away from the potential well.

The surface of the CCD is covered with MOS capacitors in a pattern like that at right. In this particular design, there are three electrodes per pixel. A single pixel is shown shaded in the diagram. Typical pixel sizes are 10-40 µ. The "parallel shift" registers are shown as rows

running across the whole face of the CCD. These are separated by insulating "channel stops."

At one end is a column of **"serial shift"** electronics and an output amplifier. Note that there is only one amplifier in this design. Contemporary large chip designs involve several amplifiers (but always many fewer than the number of pixels!).

At the end of the exposure, readout of the collected electrons is accomplished by cycling ("clocking") the voltages on the electrodes such that the charge is <u>shifted bodily</u> to the right along the rows. The figure at the right shows how this is done. Good performance depends on <u>near-100% transfer</u> of the electrons to/from each electrode with no smearing or generation of spurious electrons.

Each parallel transfer places the contents of one pixel in each row into the serial register column. This column is then shifted out vertically through the output amplifier and into computer memory before the next parallel transfer occurs.

Figure 2b The basic layout of a three-phase two-dimensional CCD. The sequence 1, 2, 3 on each set of electrodes indicates the normal direction of charge transfer in the parallel and serial registers.
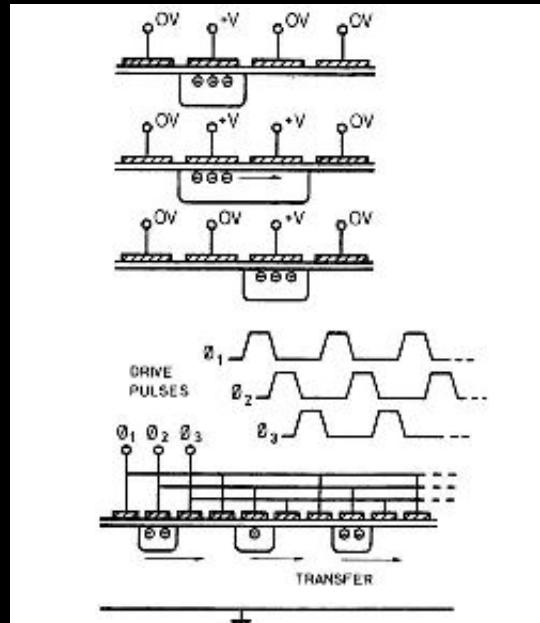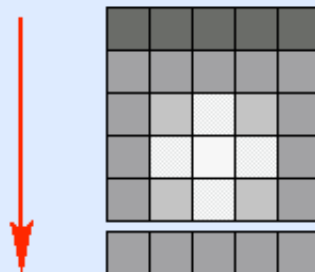
Figure 2a The charge-transfer mechanism employed in three-phase CCDs.

BUCKET BRIGADE: The resulting transfer and readout process is illustrated in the animation below:

Clocking Parallel Register

ADU CONVERSION: For storage in memory, the electrical signal generated by the amplifier must be digitized. This is done by an **"analog-to-digital converter"**. This is normally adjusted such that one digital unit corresponds to <u>more</u> than one photo-electron. Typical values of this conversion are 2 to 8 electrons per stored digital unit.

The stored values are called "ADU's", for analog-to-digital-unit. The corresponding constant of transformation, normally quoted in units of "electrons per ADU", is often called the "Gain" (although this is confusing nomenclature because a larger Gain results in reduced ADU values).

Note that the use of such a conversion importantly affects the <u>statistical properties</u> of the recorded signal. If **x** is the recorded signal in ADU's, **y** is the original signal in photo-electrons, and G is the gain, then from <u>Lecture 8</u> we see that:

$$Var(x) = Var(y)/G^2$$

VI. CCD DESIGN ISSUES

CCDs have undergone a long optimization process since 1980. Contemporary designs have excellent performance but still require careful calibration in order to overcome inherent limitations. There are also only a handful of reliable manufacturers of professional-grade chips.

Here are some of the issues affecting electronic design and manufacture of CCDs:
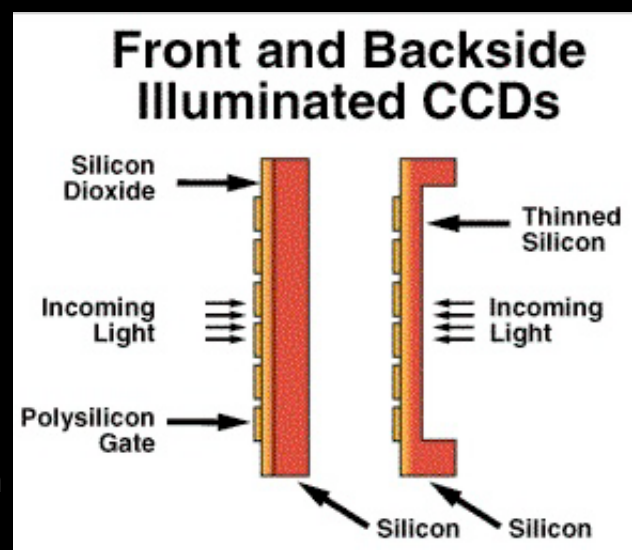
- **INTRINSICALLY LOW BLUE RESPONSE (< 4500 Å):**

  Caused by absorption in bulk Si and by electrode structures in <u>"Frontside-Illuminated" chips</u>.

  Mitigation:

  - Use special thin, polysilicon material for electrodes. But cannot be completely transparent.

  - <u>Special Coatings</u>: "Anti-reflection" coatings trap photons, causing multiple reflections as in Fabry-Perot etalons, and therefore enhance absorption. "Downconverter" coatings are phosphors which absorb blue photons but emit green photons at wavelengths where the CCD QE is higher (e.g. "mouse milk," coronene, lumogen).

  - <u>"Thinned, Backside-Illuminated" chips</u>:

Front and Backside Illuminated CCDs

shave off silicon subtrate, leaving only ~10μ deep unit; illuminate from backside; greatly improves blue response. For techniques, see **Mike Lesser's UofA website**.

Difficulties with thinned chips:

- **Fragile**
- **Non-uniform thinning**
- **Surface trapping by SiO_2 layer of photo-electrons produced nearby (shorter wavelengths)**
- **Interference effects if wavelength ~ chip thickness (i.e. in IR). Strong spatial modulation of response = "Fringing". Especially serious for night sky emission lines. Can be well calibrated for narrow-band filters or for broad-band filters. Hard for intermediate band filters.**
- **Thinning reduces red response. For good response 5000--10000 Å, prefer thick (~500μ) front-illuminated chips.**

- **CHARGE TRANSFER EFFICIENCY (CTE)**

  - **CTE can be better than 99.999% per transfer, but has to be, since throughput of chip with 2048 required shifts = CTE^{2048}.**

  - **Radiation damage to CCD's in space seriously decreases CTE over several years' time.**

  - **Mitigation:**

    Operational: add (electronically or with diffuse light source) a pedestal background signal (a "fat zero") over whole chip to increase mean electron density per pixel. However, adds additional noise and not suitable for very faint source applications.

    Technical design: change number phases, clocking cycles; add "minichannels."
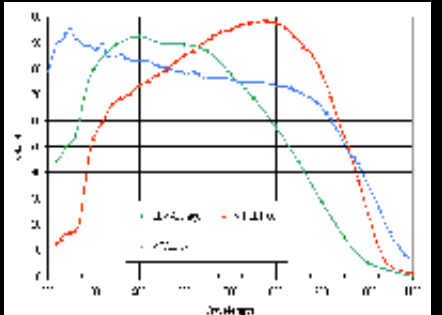
VII. ADVANTAGES OF CCD DETECTORS

- **HIGH QUANTUM EFFICIENCY: To 80-90% at peak in optical. Much effort was expended to reach these high levels.**

  - **This had tremendous impact on astronomical**

imaging & spectroscopy. It meant the detection threshold with any instrument was extended <u>4-5 magnitudes</u> and that therefore a 1-m telescope could now pursue the kind of science previously possible only with 4-m class telescopes.

Sample CCD QE curves (ESO)

- A key corollary: since we are already near 100% QE, at least in the optical region, achieving significantly lower threshold fluxes requires <u>larger telescopes</u> rather than better detectors.

  NB: "Quantum yield" can be over 100% for far-UV and X-ray photons (i.e. more than one photoelectron can be generated but fewer than 100% of photons produce responses).

- **LINEAR RESPONSE: Until approach full-well capacity (typically 200,000 e/pixel). This implied much improved flux calibrations and much higher precision for flux measurements at all levels.**

- **EXCELLENT DYNAMIC RANGE: Typically 10^4.**

- **WIDE WAVELENGTH RESPONSE : Intrinsically sensitive from X-ray to ~1μ. Other materials (e.g. InSb$_2$, HgCdTe) with similar architectures usable in IR.**

- **GEOMETRICALLY STABLE: good for astrometry**

- **ONLY LOW VOLTAGES REQUIRED (~5-15 v)**

- **RELATIVELY CHEAP, AVAILABLE, SIMPLE: Compared to other digital 2-D systems. Standard chips cost ~$2-200 K.**

- **RELATIVELY LOW NOISE : Compared to many other classes of astronomical detectors, e.g. Pg plates, Reticons, SEC vidicons, etc. But noise is not negligible. Typical read noise now 2-10 e/pixel, and dark current is largely suppressed by cooling.**

- **SMALL PIXELS : Typically 10-30 μ. Usually an advantage, but want to match pixel size to 1/2 of smallest resolvable picture element in optical system.**

- **SPECIAL FORMAT/READOUT DESIGNS: By changing electrode structure and clocking cycles, can arrange for many different integrate/readout modes.**

  <u>Rapid clocking/video</u>: inherent in CCDs intended for TV application. For bright sources, readout rates of 100 MHz possible.

  <u>Drift scanning</u> for large area surveys or to reduce flat-field effects (see below)

"Nod/Shuffle" technique" take advantage of capability to shift image wholesale on CCD without reading out to obtain much better sky subtraction (e.g. in near-IR where atmospheric OH emission is very bright and variable).

On-chip binning: change clocking to combine electrons from several pixels together before reading out through amplifier. E.g. combine a 2x2 pixel region on the chip into a single output pixel. This reduces the effect of amplifier readout noise on each pixel in the final data. Also reduces memory and storage requirements. Adds considerable practical flexibility to CCD systems. Obviously, however, reduces the spatial resolution of the output. Is useful for applications such as imagery of very faint, extended sources (e.g. galaxy halos), low spatial resolution spectroscopy, photometry of point sources under poor seeing conditions, etc.
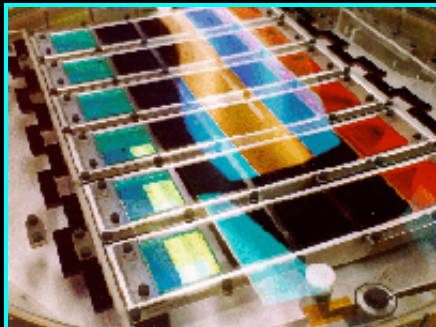
- **UBIQUITOUS** : Now almost universally used in astronomy (amateur & pro). Photographic materials and older electronic detectors being phased out.

- **IMMEDIATE DIGITAL CONVERSION OF DATA:** The other advantages of array detectors notwithstanding, it is the immediate conversion of astronomical signals into a form capable of computer storage/computation which has so <u>dramatically transformed</u> UVOIR astronomy since 1980. The practice, pace, & scope of UVOIR astronomy are entirely different now than in the "photographic" era that preceded widespread use of CCDs and other array devices. Digital conversion of images and spectra has enabled quantitative analysis of observations on a scale not possible before.

   Among other things, rapid digital processing allows much improved use of observing time---notably in surveys (e.g. for variable sources in MACHO and supernova searches; moving targets such as asteroids/Kuiper Belt objects; or combined imaging/spectroscopic surveys such as SDSS, 2dF).
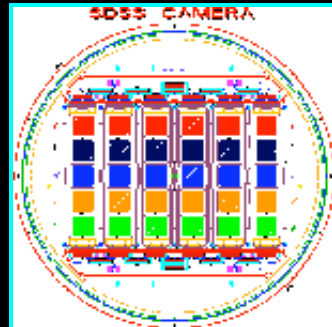
VIII. LIMITATIONS/DISADVANTAGES OF CCD'S

- **SMALL SIZE** : Individual chips typically less than 7 cm square. Cover only ~20% of high quality imaging field on typical modern telescope. Size limited by small fabrication yield of large, defect-free chips. Largest routinely available chips are 4096x2048.

   - However, MOSAICKING technology now well developed. Typical mosaic now uses 4096x2048 chips.

   - Examples: (click on images below for enlargements):

      - Sloan Digital Sky Survey: 54 chip mosaic for drift scanning in 5 bands simultaneously

      - Canada-France-Hawaii-Telescope MegaPrime mosaic: 40 4096x2048 chips

covering 1 degree FOV

Sloan DSS Camera   Sloan DSS Camera   CFHT MegaPrime Mosaic

- **CRYOGENIC COOLING REQUIRED: To reduce dark noise, cooling to below -100 C necessary. Thermoelectric coolers usually not adequate, so cryogens (e.g. liquid N_2) required. Introduces many practical complications. Optimal low-T chips differ from commercial types used at room temperature in digital cameras, etc.**

- **READOUT NOISE: Produced by variations in amplifier gain. Much effort to reduce. Now typically 2-10 e/pix.**

  What matters is not the noise per pixel but rather the total noise per <u>image area</u>, which can extend over many pixels, depending on the application.
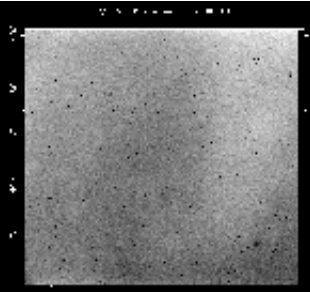
  Even at these very low levels, RON can compromise some types of observations (spectroscopy, surface photometry), see <u>Lecture 7</u>.

  Can reduce RON effects in some applications using on-chip binning (see above). In some cases, it may be more advantageous to use "pulse counting" detectors, which can unambiguously detect individual photons, than CCD's.
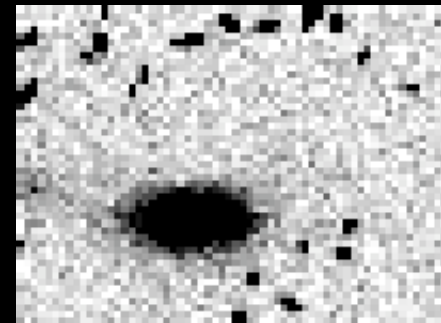
- **FULL WELL CONSTRAINTS: Bright sources which over-fill pixels can produce "blooming" or "bleeding" along columns, making parts of the chip other than the immediate vicinity of the source useless. Best solution is operational.**

- **RESPONSE NONUNIFORMITIES ("FLAT FIELD" EFFECTS): Caused by small variations in masks used to manufacture chips, deposition irregularities, thinning variations, etc. Typically 5% pixel-to-pixel. Color dependent. Requires extensive calibration, with color-matching to targets. Use "dome flats" or "twilight flats." Special observing procedures to reduce flat field effects include:**

  - **<u>Drift Scanning</u>: Clock chip slowly along columns**

while moving telescope to keep star image centered on electron cloud. Continuously read out chip to produce a strip-image of the sky. Integration time is limited to drift time across chip. Is now a standard method for wide-field CCD sky surveys (e.g. the Sloan Digital Sky Survey).

CCD Flatfield Frame (AAO)

Simplest approach is to align columns east-west, keep telescope fixed on sky, and clock chip westward at sidereal rate. A sample application of drift scanning is described <u>here</u>.

- o <u>Multiple Offset</u>: Break exposure into 4-5 parts, offset ~50 pixels between exposures. Combine exposures during data reduction. "Dithering" is a related technique involving smaller offsets to achieve sub-pixel spatial resolution. These methods result in reduced field of view because not all parts of original field will have uniform exposures.

- **SENSITIVITY TO COSMIC RAYS:** Especially thick chips. Must remove effects during processing. CR's are a <u>major problem</u> for spacecraft detectors (e.g. HST/WFPC2). Requires that exposures be broken into multiple parts (called "CRSPLITs" on HST) so that CR events can be detected. CR hits can be removed from data frames, but this always leaves "holes" which have less exposure than other parts of the image.

CR's on HST/WFPC2 2400 sec image (extract)

- **SENSITIVITY TO X-RAYS:** An advantage for X-ray astronomy, but some materials in vicinity of CCD's, e.g. special glasses used for windows, can produce a diffuse background of X-rays which add noise to observations.

- **CHARGE TRANSFER EFFICIENCY:** Good CTE is often possible only for signal levels above threshold ~10-50 e/pix. For low light levels, require adding <u>"fat zero"</u> (typ. 1000 e/pix) electronically or by preflash. Creates added noise (10-30 e/pix).

- **AVAILABILITY HOSTAGE TO COMMERCIAL MARKET:** CCD availability has always been driven more by commercial and military applications than science. Scientific CCD manufacture represents only about 10% of the overall $1B CCD market. A serious near-term issue, since industry is moving to "active pixel sensors," a different technology with amplifiers incorporated in each pixel. Requirements for good performance at low (astronomical) light levels are considerably different than for room-temperature, short-exposure, mass-produced equipment.

- **DATA GLUT!** CCDs typically produce 2 x N_{pix} bytes of data per readout, where N_{pix} is

the number of pixels. For a 8096x8096 mosaic, this is 130 MB. Data storage/manipulation was a serious problem when CCD's were first introduced, and this influenced the style of data processing systems such as IRAF. Disk and tape storage now much improved, but long-term stability of massive amounts of data now being produced is a non-trivial issue. [All that data is really important and worth saving...isn't it?]

IX. EXAMPLE CCD SYSTEMS

- **HST: WIDE FIELD PLANETARY CAMERA 2 (1992)**

  - **4 CCD's, optically mosaicked with beam-splitter**
  - **Loral 800x800, 15μ pixel chips**
  - **Front-illuminated, lumogen phosphor coating for UV response**
  - **RON 5 e/px; QE (6000 Å) 35%**

- **HST: WIDE FIELD CAMERA 3 (2001)**

  - **2 CCD's, physically mosaicked, contiguous**
  - **Marconi 4096x2048, 15μ pixel chips**
  - **Thinned, back-illuminated; anti-reflection coating for enhanced blue/UV response**
  - **Minichannel for improved CTE**
  - **RON 3 e/px; QE (6000 Å) 70%**

- **SLOAN DIGITAL SKY SURVEY (1997)**

  - **Drift scanning mosaic (not contiguous) containing 54 chips**
  - **Tektronix/SITe 2048x2048, 24μ pixel chips in 5x6 array; for simultaneous broad-band photometry. Both frontside and thinned backside with AR coating. QE (6000 Å) ~60%; RON < 5 e/px**
  - **Tektronix/SITe 2048x400, 24μ pixel chips; for astrometry & focus check. Frontside illuminated, RON < 15 e/px.**

- **FAN MOUNTAIN CCD SYSTEM (Gen II)**

X. CCD HIGH PRECISION CALIBRATION PROCEDURE

A. DATA REQUIRED

- **Bias frames**
- **Dark frames (optional)**
- **Flat field frames**

- **Sky flat/fringe frames (optional)**
- **Flux calibrator fields**
- **Target frames**

B. REDUCTION PROCEDURE

- **SUBTRACT BIAS FRAME : Bias frames (zero exposure time) taken with chip unexposed to light from telescope. These measure electronic pedestal of chip. For high precision, average many bias frames, before and after observations. Check for bias drift during night. With some chips, can determine electronic bias level from overscan region on chip. For optical "fat zero" subtract average of many frames.**

  - **Optional: SUBTRACT DARK FRAME: Median filter many long (~30 min) dark exposures; note possible LED activity of CCD electrodes. Scale result to integration time of each data frame before subtracting.**

- **DIVIDE BY TWILIGHT OR DOME FLAT FIELD: To remove residual pixel-to-pixel variations (typical 5%). Make exposures of twilight sky (good diffuse source, but tricky to get exposure level right; only 2 chances per night). Or make many exposures of diffusely illuminated screen in dome (disadvantage: often not uniformly illuminated). Must be done for each filter used (color sensitive effects).**

  [Note: photon statistics must yield S/N significantly in excess of final desired S/N---i.e. if desire S/N = 100, require over 10,000 photons per pixel in net flat field image.]

  - **Optional: SUBTRACT SKY FLAT/FRINGE frame: Remove night sky emission line fringing effects (worse in near-IR) by observing uncrowded field in night sky. Take several exposures, moving telescope by, say, 25 arc-sec between them. Use "adaptive modal filter" technique to zap star images and create mean sky frame. Scale to target frames and subtract. Resulting flat field as good as 0.1% can result. Require a sky flat determined this way for each filter.**

- **USE MULTIPLE OFFSETS, DITHERING OR DRIFT SCANNING FOR TARGET FRAMES: For faintest possible photometry, use multiple-offset exposure technique---e.g. 500 sec exposures shifted by about 20 arc-sec each--- to reduce flat field errors. Always want more than one exposure anyway for "reality check," empirical determination of photometric errors, cosmic ray removal, etc.**

- **INTERPOLATE OVER OR MASK OUT BAD PIXELS/REMOVE COSMIC RAY EVENTS**

- **REGISTER AND COMBINE TARGET FRAMES: Re-register offset frames to sub-pixel accuracy (e.g. "Drizzle" softare). Median filter. Trim off "lost" parts of image.**

- **CALIBRATE FLUX SCALE: Observe "standard stars" in recommended CCD calibrator fields (e.g. star clusters) to determine nightly atmospheric extinction and telescope throughput. No need to take on non-photometric nights (variable clouds), but no flux calibration either. Important that calibrator stars overlap targets of interest in color.**
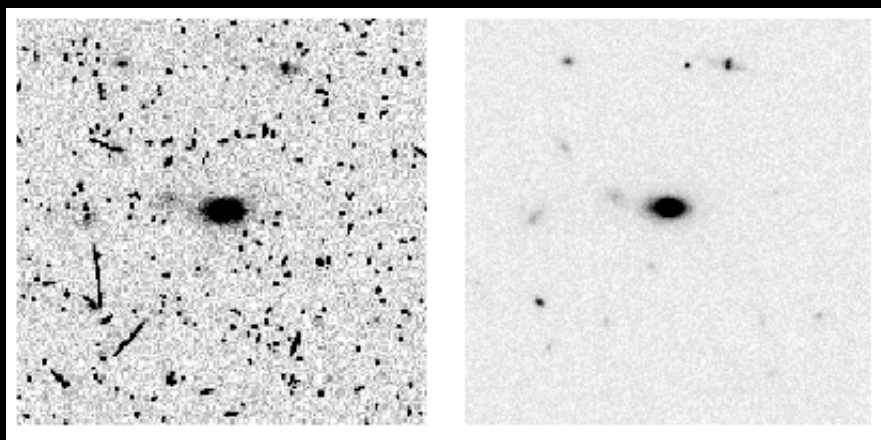
These frames are reduced exactly like target frames, apparent fluxes extracted, and correction factors to determine true fluxes of targets are obtained.

- **APPLY GOOD PHOTOMETRIC REDUCTION SOFTWARE: for source IDs, flux measurements (point or extended source).**
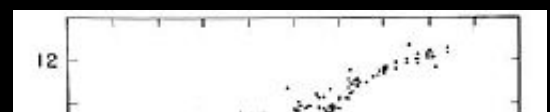
    =====> RESULT : PHOTOMETRIC CALIBRATION GOOD TO 0.005 MAG
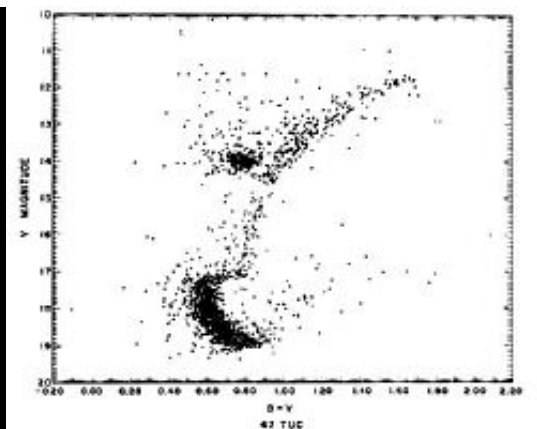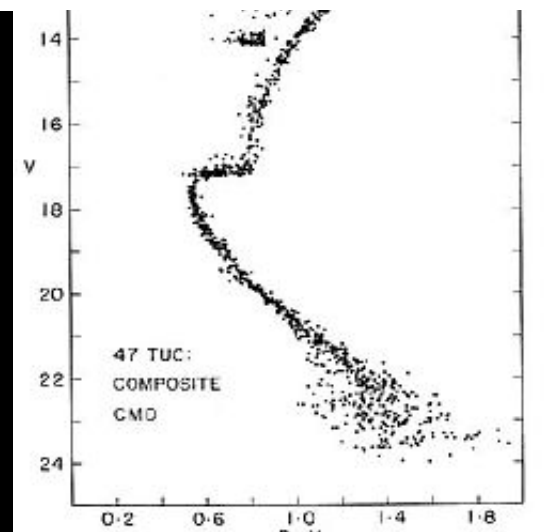
C. EXAMPLE SCIENTIFIC APPLICATIONS

- **<u>Subpixel registration</u> of dithered HST imaging by A. Fruchter's "drizzling" technique. On left is one original frame (I-band, 2400 sec exposure). On right is result of drizzled processing of 12 such frames. Combined image has limiting magnitude of I ~ 28. It would be impossible to reach such levels with photographic detectors.**

- **Example of improvement in <u>color-magnitude diagram</u> for star cluster 47 Tuc. On left is 1977 state-of-the-art CMD based on widefield photographic images with photoelectric calibrations (Hesser & Hartwick, 1977). On right is a 1987 CMD derived from CCD photometry (Hesser et al. 1987). The greatly improved photometric precision reveals new features of astrophysical interest: e.g. the thinness of the main sequence near turnoff, which places strong limits on the range of ages present in the cluster.**

Photographic CMD

CCD CMD

XI. NON-UVOIR USE OF CCD & RELATED DEVICES

A. X-RAY: CHANDRA/ACIS DETECTOR

ACIS is a 10-CCD (1024x1024 chips) focal plane array used on Chandra for both imaging and spectroscopy. It uses both back-illuminated and front-illuminated versions.

It is operated in a pulse-detection mode, unlike the standard procedure at UVOIR wavelengths.

Each X-ray photon releases more than one electron in the CCD, in fact, the mean number released is ~ E_{XR}/3.7 eV. Since Chandra operates at ~ 5 keV, the average electron cloud corresponding to one photon has ~ 1000 electrons.

The standard operation sequence is to expose for 3.2 seconds, then rapidly read out the array in 40 ms. The resulting image is analyzed by on-board software to catalogue the x,y position and the pulse amplitude of each valid photon pulse.

Because the pulse amplitude is proportional to the photon energy, ACIS achieves a spectral resolution of R ~ 10-50.

A difficulty with the ACIS design is that if more than one photon strikes the same pixel during the exposure time, the counting analysis becomes distorted, and the photon flux is underestimated. This is called "pileup." Fortunately, most X-ray sources are faint enough that this is not a problem.

B. INFRARED ARRAYS

The table in Sec. IV above shows that pure silicon photoconductor arrays will not work at IR wavelengths, but there are a number of other materials that will.

There are many varieties of IR detectors in use today. Some of these are monolithic, i.e. fabricated on single subtrates like CCD's, and some are **hybrids** in which the readout electronics are fabricated separately from the photon-detection devices.

Hybrids typically use silicon wafers for the readout electronics. Some actually use CCD-type architecture. The readout is connected to the photon-sensing material using conducting "bump-bonded" indium studs. If the wafers ultimately produce readout though a small number of output amplifiers, they are called "multiplexers" or "MUX's".

Here is a cross-section of the HST/NICMOS infrared detector, which uses a HgCdTe ("mercad-telluride") photon detector.

IR arrays will be discussed further in the guest lecture by Mike Skrutskie and in ASTR 512 (Spring 2004).

Additional Web links:

CCD-World (forum for discussions about CCDs and their use)

Basics:

> **Digital Imaging/CCD Tutorial at Molecular Expressions**
>   (thorough, elaborate illustrations, but aimed at microscopy)
> **Britney's Guide to Semiconductor Physics** (decorative tutorial)
> **Semiconductor physics at HyperPhysics** (succinct, with many illustrations)
> **Simon Tulloch CCD Primer (PPT)** (aimed at advanced amateurs)

Example Systems & Development Efforts:

> **Sloan Digital Sky Survey CCD Camera (54 chips!)**
> **NOAO CCD Mosaic Camera Manual**
> **CTIO CCD Mosaic Camera Manual**
> **ESO Optical Detector Homepage**
> **AAO Instrumentation Page.**
>   Good, detailed descriptions of performance characteristics of individual CCDs.
> **Lawrence Berkeley CCD Development Program (Progress report, PDF)**
> **JPL CCD ``Delta-Doping'' Project**

Last modified July 2005 by

EXPOSURE TIME ESTIMATION

An essential part of planning any observation is to estimate the total exposure time needed to satisfy your scientific goal. General considerations are described in Lecture 7. A number of on-line "Exposure Time Calculators" (e.g. at STScI) provide examples of sophisticated estimators. Here, we discuss the basics of this process.

From Lecture 7.F, we can re-write a general expression for the signal-to-noise ratio for digital array photometry as follows:

$$SNR = \frac{N\dot{s}\,t}{\sqrt{N\dot{s}\,t + N(1 + \frac{N}{M})\left(\dot{b}t + \dot{d}t + n_{\mathrm{RON}}^2\right)}} \qquad (1)$$

Here, $\dot{s}$ and $\dot{b}$ are the <u>mean rates</u> at which source photons and sky background photons, respectively, are detected <u>per pixel</u>. t is the total integration time. $\dot{d}$ is the dark count rate per pixel, and n_{RON} is the readout noise per pixel (quoted in numbers of equivalent electrons of noise). We assume the source was measured with a virtual aperture containing **N** pixels and the background with an aperture of **M** pixels, where $M \geq N$.

This expression is usable for either a compact (e.g. point-like) source or an extended source. In the case of a compact source which is completely contained within the **N** pixel source aperture, $\dot{s} = \dot{S}/N$, where $\dot{S}$ is the total source photon detection rate.

The next question is how to estimate the photon rates appearing in this expression, starting from an estimate of the flux of the source at the top of Earth's atmosphere. It is straightforward to do this.

The flux of detected photons (counts per second per cm^2) at the detector for a given source will be:

$$\Phi_i = \frac{\frac{\pi}{4}D_e^2}{\frac{\pi}{4}(\beta L)^2} \int e^{-k(\lambda)\,\sec Z}\, T_i(\lambda)\, \frac{F_\lambda(\lambda)}{h\nu}\, d\lambda \qquad (2)$$

Here:

D_e **is the <u>effective</u> diameter of the telescope after correction for central obscuration. (The correction can be significant, depending on the optical design.)**

β **is the angular diameter of the source (radians).** $\beta = 4.85 \times 10^{-6}\,\beta_s$, **where** β_s **is the angular diameter in arcseconds.**

L **is the effective focal length of the optical system feeding the detector.**

k **is the "extinction coefficient" for absorption in Earth's atmosphere. (This is small, $\lesssim 0.2$ except in the near-UV and can usually be ignored for ET estimates.)** k **is smaller for higher altitude observatories. An extinction curve for Mauna Kea is shown in Lecture 4.**

$\sec Z$ **is the secant of the "zenith distance" angle. This quantity is also known as the "air mass," since it gives the total atmospheric path length toward the source in terms of the vertical thickness of the atmosphere.**

T_i **is the net system optical efficiency. This includes the fractional transmission of the optical system, including the telescope and all other optical elements preceding the detector, and the detector quantum efficiency.**

$F_\lambda(\lambda)$ **is the spectral flux density of the source, in energy units per unit wavelength, at the top of Earth's atmosphere. For an <u>extended</u> source, enter $F'_\lambda(\lambda)$, the mean spectral flux density per square arcsecond, and set $\beta_s = 1$.**

Estimating $F_\lambda(\lambda)$:

If you can estimate m_λ, the monochromatic magnitude of the source, then:

$$F_\lambda(\lambda) = 3.63 \times 10^{-9} \, 10.0^{-0.4 \, m_\lambda(\lambda)} \text{ erg s}^{-1} \text{ cm}^{-2} \text{ Å}^{-1}$$

for any wavelength.

More commonly, you have an estimate of the source brightness in a particular band of a broad-band magnitude system. If the magnitude in band i is m_i, then

$$< F_\lambda(\lambda) >= F_{0,i} \, 10.0^{-0.4 \, m_i} \text{ erg s}^{-1} \text{ cm}^{-2} \text{ Å}^{-1}$$

where $F_{0,i}$ is the flux zeropoint for band i. The best compilation of such zeropoints is by Bessell et al. (A&A, 333, 231, 1998; Table A2). See Lecture 13 for more details. The estimate here is, of course, for the mean flux within the band.

For an extended source, you would substitute $\mu_\lambda(\lambda)$, in standard units per square arcsecond, for m in the expressions above. See Lecture 2 for the definition of μ.

Estimating $T(\lambda)$:

Accurate determinations of the total optical efficiency of a system can only be made after observing calibrator sources. However, the following rules of thumb serve adequately in the absence of more detailed information.

$T(\lambda)$ is the product of the transmissions of each optical element in the system and the detector quantum efficiency.

$$T(\lambda) \approx r_m^{n_m}(\lambda)\ r_l^{2\,n_l}(\lambda)\ R_f(\lambda)\ Q(\lambda)$$

Here:

r_m is the reflectivity of a mirror and n_m is the number of mirrors in the optical path. For fresh aluminum coatings on mirrors $r_m \sim 0.88$ in the optical bands. Silver has better IR reflectivity but poorer blue reflectivity. In the UV, special coatings such as MgF or LiF are used.
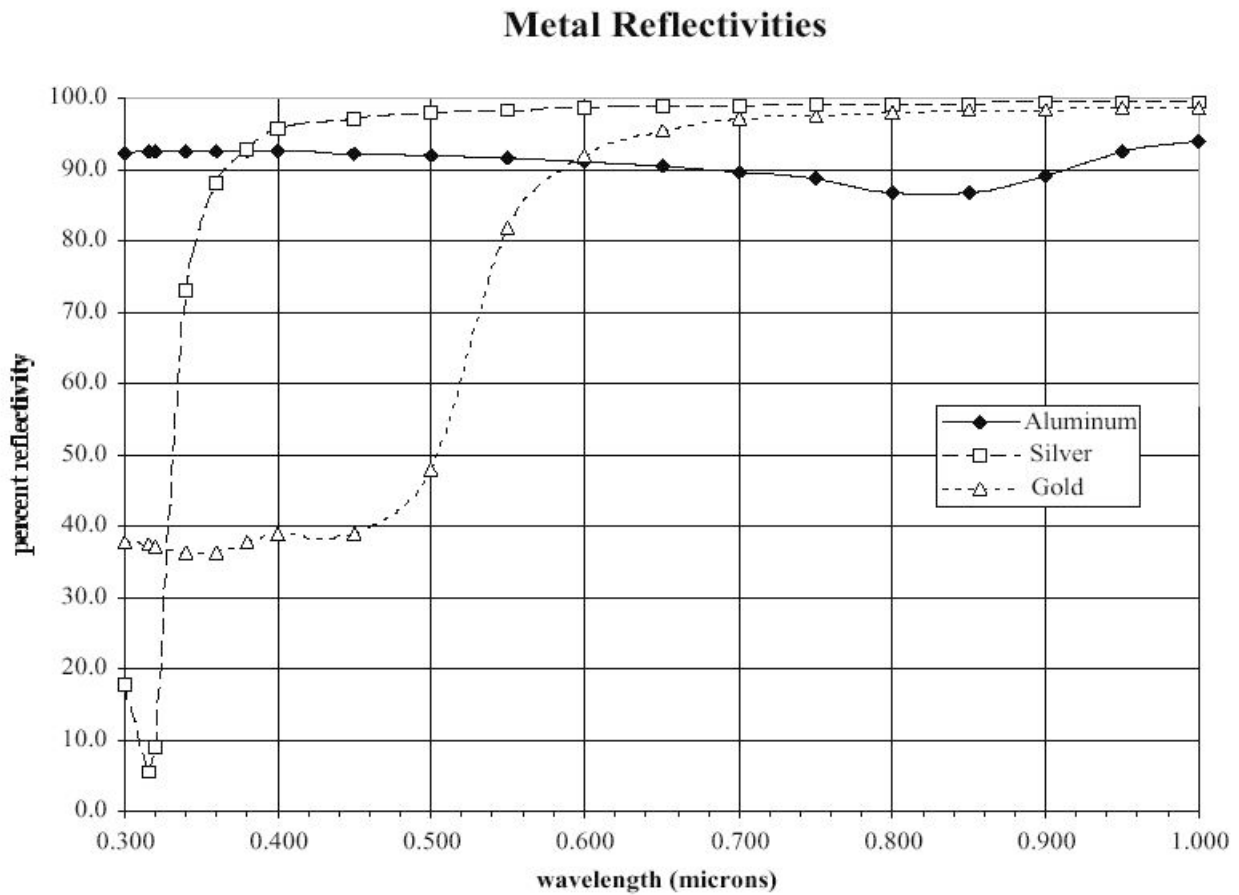
r_l is the transmissivity of a single glass-air interface and n_l is the number of refractive elements in the optical path. For normal glasses in the optical band, $r_l \sim 0.95$. Should include dewar windows, etc., in this factor.

$R_f(\lambda)$ is the filter (or grating, prism) transmission curve. Typical glass filters have $< R > \sim 0.40 - 0.90$ (including the effects of the glass/air interface). Inteference filters have generally lower values. Since it is usually easy to look up filter properties, and filter responses vary dramatically, this is one term that you should try to estimate accurately.

$Q(\lambda)$ is the quantum efficiency of the detector. Again, this can usually be looked up.

This expression assumes no other light losses (e.g. due to vignetting of the light beam).

Note that this long string of factors will normally result is only <u>modest</u> overall throughput. For instance, in a standard Cassegrain telescope with 2 mirrors, 2 refractive elements, a filter with 75% transmission, and a CCD with 50% QE, the net throughput is only 0.24. 75% of the photons incident on the primary mirror have been lost!

Metal Reflectivities

Reflectivities of common large mirror coatings

Approximating the Flux Integral (equation 2):

If we substitute mean values in (2) above, we get:
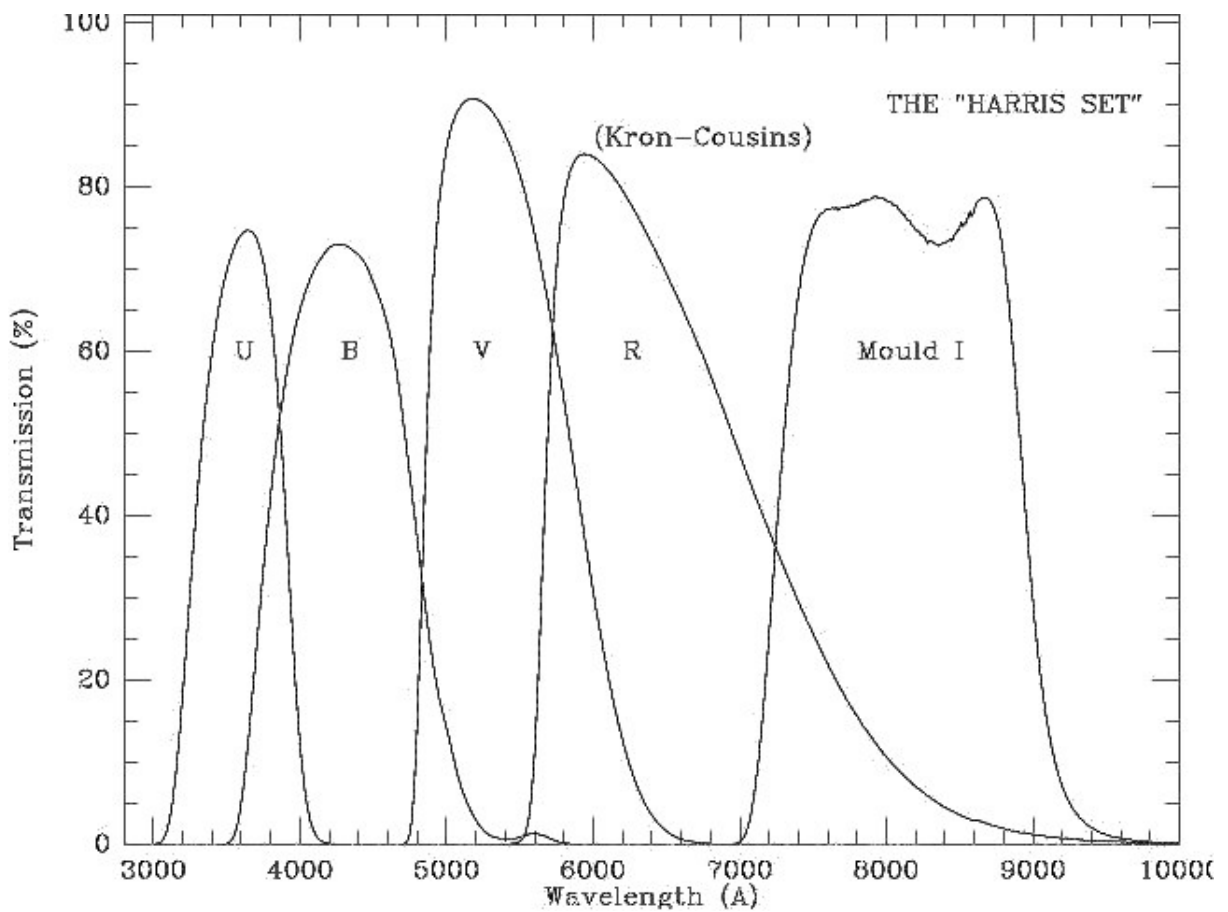
$$\Phi_i \approx \frac{D_e^2}{(\beta L)^2} \ < T_i > \ \frac{< F_{\lambda,i} >}{h\nu} \Delta\lambda$$

where $\Delta\lambda$ is the bandwidth of the filter. This is obviously a critical term and should be carefully determined. A standard approach is to compute $\Delta\lambda = \int \frac{R_f(\lambda)}{R_0} d\lambda$, where R_0 is the peak response of the filter.

Values for the standard UBV filters are given below, and plots of the UBVRI responses are given on the next page.

Band	$< \lambda >$ (Å)	$\Delta\lambda$ (Å)
U	3600	560
B	4400	990
V	5500	880

If the bandwidth is particularly large, the source energy distribution changes significantly across the band, or $T(\lambda)$ is not well represented by a top-hat function, then good results may require that the actual integral be evaluated.

Standard UBVRI broad-band filter response curves (KPNO)

Predicting Signal-to-Noise:

To complete evaluation of equation (1):

Evaluate $\Phi_{s,i}$ for the source by entering $< F_{\lambda,i} >$ for a compact source and the appropriate β_s; or entering $< F'_{\lambda,i} >$ for an extended source with $\beta_s = 1$. For a point source, β_s is the FWHM of the point spread function of the telescope+atmosphere in arcseconds.

Then the term $\dot{s}$ in equation (1) is

$$\dot{s} = \Phi_{s,i}\, y_p^2$$

where y_p is the size of one pixel in cm (assuming square pixels).

This expression applies for those pixels which are within the projected image of the source. If the source is compact, such that its light is completely contained within the source measuring aperture of N pixels, then

$$N\dot{s} = \Phi_{s,i}\, \frac{\pi}{4}(\beta L)^2$$

If the source is not contained within the N pixels but is also not well approximated by a uniform surface brightness, then you must estimate the total flux in the source aperture using an assumed spatial profile.

Then evaluate $\Phi_{b,i}$ for the sky background by entering the $< F'_{\lambda,b,i} >$ which is appropriate for the sky surface brightness, $\mu_{b,i}$ (typical values for dark sites are given in Lecture 7). Use $\beta_s = 1$. Then:

$$\dot{b} = \Phi_{b,i}\, y_p^2$$
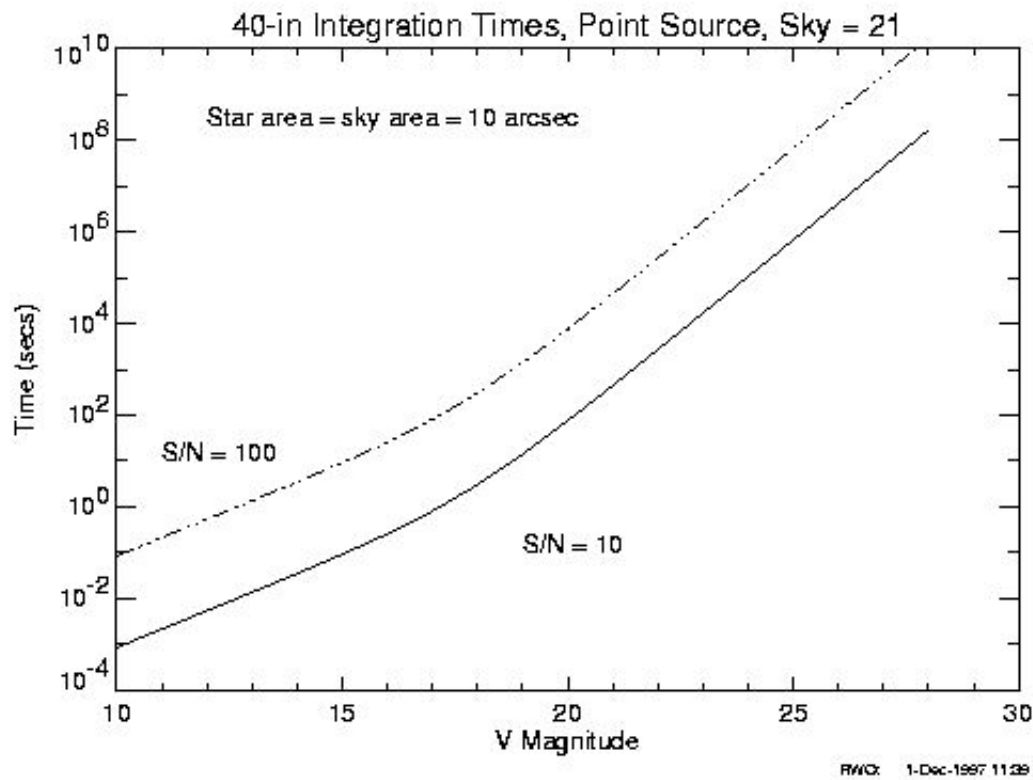
Obtain values for $\dot{d}$ and n_{RON} from published specifications for the detector you are using.

Substitute all of the above into equation (1).

It is easiest to solve equation (1) numerically for various sets of assumptions. The most common approaches are: (i) to solve for SNR given source/background brightnesses and exposure time t; (ii) to solve for t given source/background brightnesses and SNR; and (iii) to solve for the source brightness given SNR, t, and the background.

Remember that a <u>threshold</u> detection requires $SNR \sim 5 - 10$.

For a plot of a type (ii) evaluation for the 40-in CCD system in the V-band, see the next page.

Example estimate of integration times for the 40-in CCD imaging system including the effects of source noise, sky background, and readout noise.

Note the change of slope at $V \sim 18$, which is the transition between sky background noise dominance (for fainter sources) and source photon noise dominance (for brighter sources). Because this is a log-log diagram, such small changes in slope have large impacts in practice.

Limiting Cases (Point Sources):

The dependence of the results on the parameters of the telescope plus instrument system are best illustrated in limiting cases.

(1) Source limited: $\dot{s} >> \dot{b}$

$$SNR \sim D_e \sqrt{F_\lambda\, T\, \Delta\lambda\, t}$$

(2) Sky background limited: $\dot{b} >> \dot{s}$ **(assuming** $M >> N$**)**

$$SNR \sim D_e\, F_\lambda\, \sqrt{\frac{T\, \Delta\lambda\, t}{N F'_{\lambda,b,i}}}$$

Note that in both cases,

$$t \sim \frac{(SNR)^2}{D_e^2\, T\, \Delta\lambda}$$

This implies, as noted in Lecture 7, that it is expensive in observing time to increase SNR. There is also an important advantage for larger telescopes. However, the dependence on $F_{\lambda,i}$ is very different in the two cases. In the sky limited case, $t \sim F_\lambda^{-2}$, meaning that faint sources become very difficult to detect.

(3) A final interesting case is the sky background limit for a point source with a <u>diffraction limited</u> telescope, for which $\beta \sim 2.4\,\lambda/D_e$**. Here, we assume the source measuring aperture is decreased in proportion to** β**. Then**

$$t \sim \frac{\lambda^2}{D_e^4}\, (SNR)^2$$

Here, there is an enormous advantage for larger telescopes. This case applies in practice to optical-IR space telescopes (HST, JWST) or to large ground-based telescopes operating in the IR region using "adaptive optics" to eliminate the image smearing from the Earth's atmosphere.

One caveat, among others: the IR sky background from the Earth's atmosphere is strongly variable and is not well approximated by Poissonian statistics.

Final Remarks:
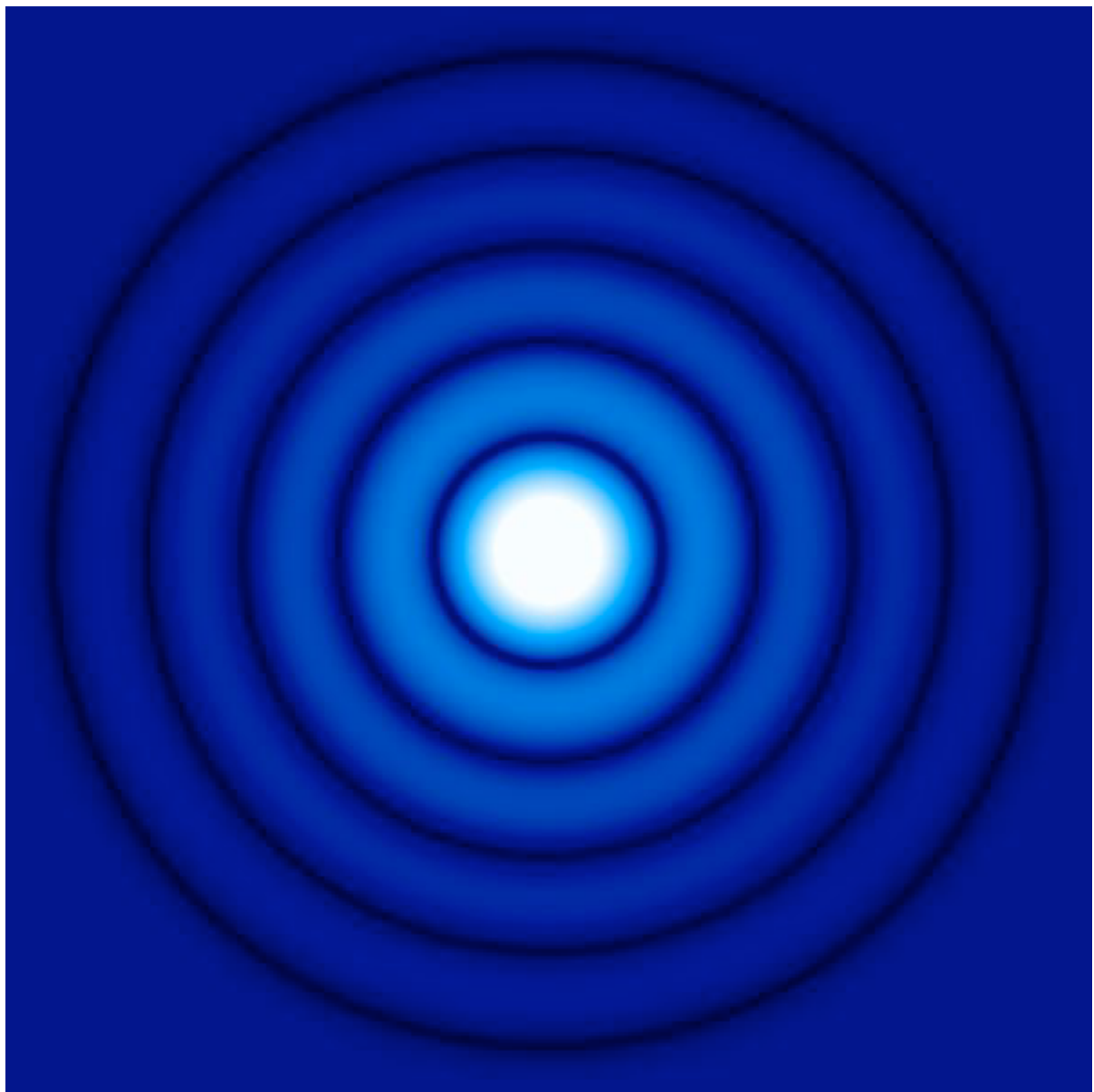
On-line Exposure Time Calculators are for specific instruments. They include all the relevant information on T, R_f, Q, and so forth, and produce real integrals across the bandwidth. They generally accept a number of different ways of specifying or estimating source brightness. They usually include a high-resolution version of the background sky spectrum, so the effects of strong sky emission lines are properly estimated.

Finally, remember that equation (1) is a <u>prediction</u> of SNR for a specific set of assumptions about the measuring process.

The best way to judge the <u>true SNR</u> of an observation is to analyze the <u>scatter in repeated measures</u>.

Therefore, you should always break an observation up into <u>multiple parts</u> (assuming it is not dark or readout-noise limited) in order to assess statistical scatter as well as to reduce the effects of cosmic rays, flat field uncertainties, etc.

POINT SPREAD FUNCTIONS

"Point Spread Functions" describe the two-dimensional distribution of light in the telescope focal plane for astronomical point sources. Modern optical designers put a great deal of effort into reducing the size of the PSF for large telescopes.

Good PSF evaluation is especially critical for telescopes which are intended to have near-diffraction limited performance. That obviously includes space telescopes. But it also includes large ground-based telescopes which are equipped with "active" or "adaptive" optics sytems, which can greatly reduce the effects of atmospheric seeing on the PSF.

The PSF for a perfect optical system, based on circular elements, would be an "Airy Pattern," which is derived from Fraunhofer diffraction theory (scalar approximation applied to plane waves).

The Airy pattern is given by the following expression:

$$I(u) = \frac{1}{(1-\epsilon^2)^2} \left[\frac{2\,J_1(u)}{u} - \epsilon^2 \frac{2J_1(\epsilon u)}{\epsilon u} \right]^2$$
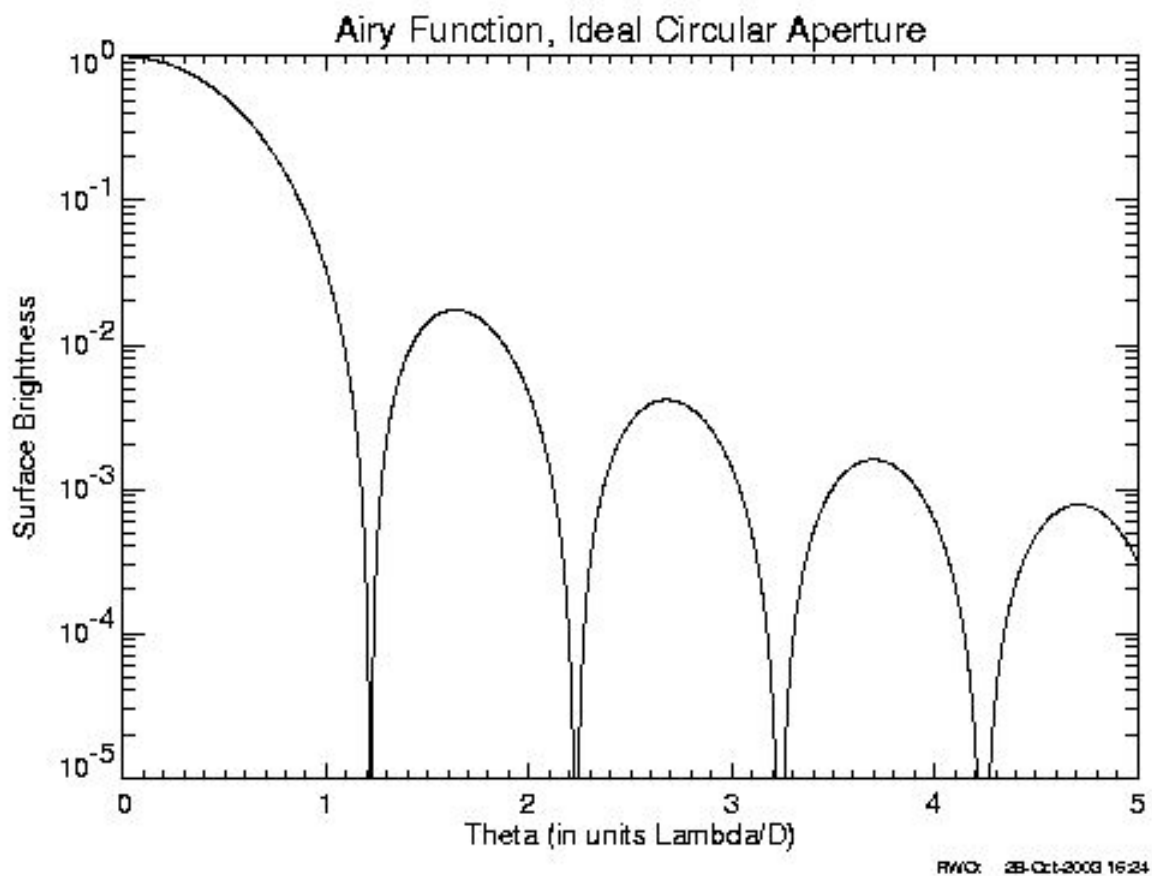
$I(u)$ is the surface brightness in the focal plane, normalized to its maximum at $u = 0$

u is a dimensionless distance from the optical axis in the focal plane and is related to the angular radius θ (as measured from the primary aperture) and the diameter D of the primary aperture as follows:
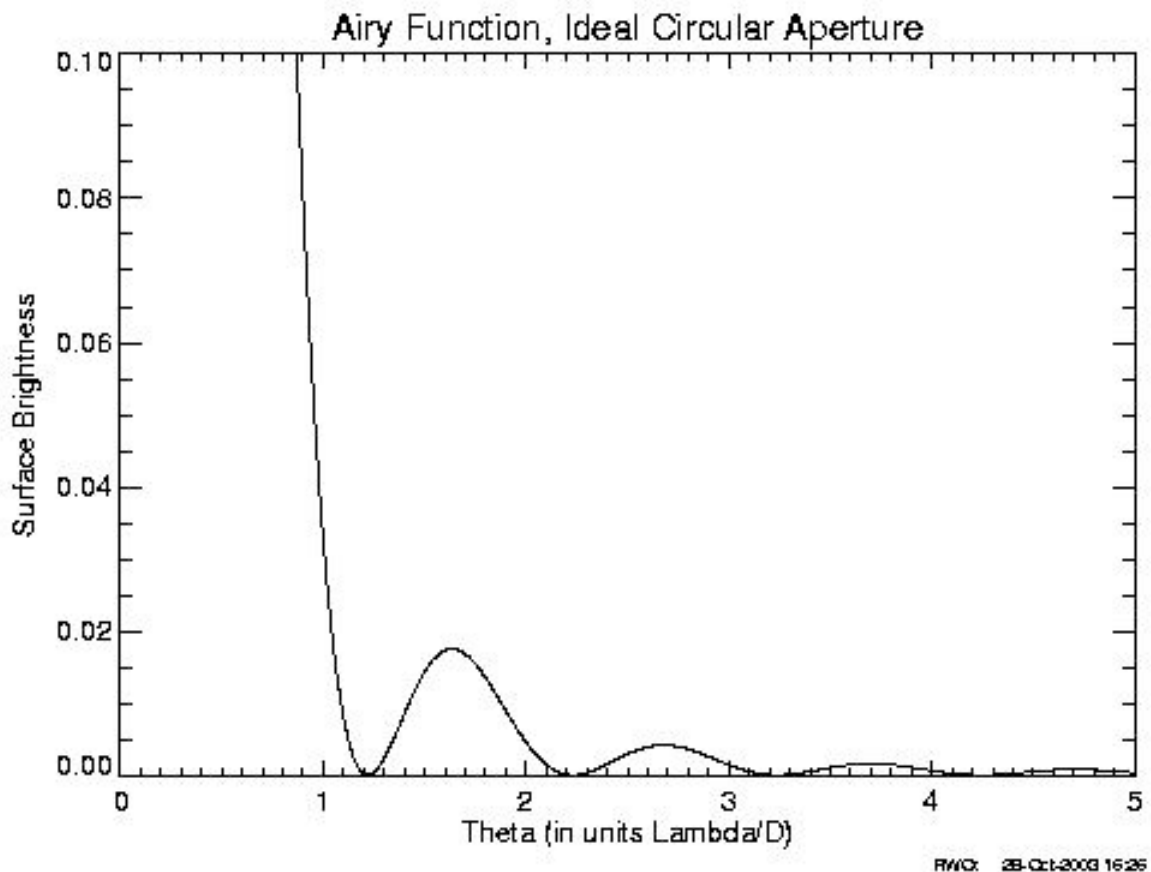
$$u = \frac{\pi}{\lambda} D\,\theta$$

ϵ is the fractional radius of the central obscuration of the primary aperture (assumed circular). Can be 0.

J_1 is the order 1 Bessel function of the first kind.

Airy Pattern (zero obscuration) in log intensity space showing the structure of the ring pattern.

Airy Pattern (zero obscuration) in linear intensity space (enlarged y axis)

THE AIRY PATTERN

The Airy pattern is shown as an image on the first page and is plotted on the two preceding pages.

It consists of a series of sharp dark rings alternating with broader bright rings.

The pattern drops to 50% power at a radius of 0.514 λ/D, so its $FWHM = 1.028\lambda/D$.

The core of the Airy Pattern, inside the first minimum is often called the "Airy Disk." It contains some 86% of the total light in the image.

The first three dark rings occur at radii of 1.22, 2.23, and 3.24 λ/D, respectively.

ENCIRCLED ENERGY
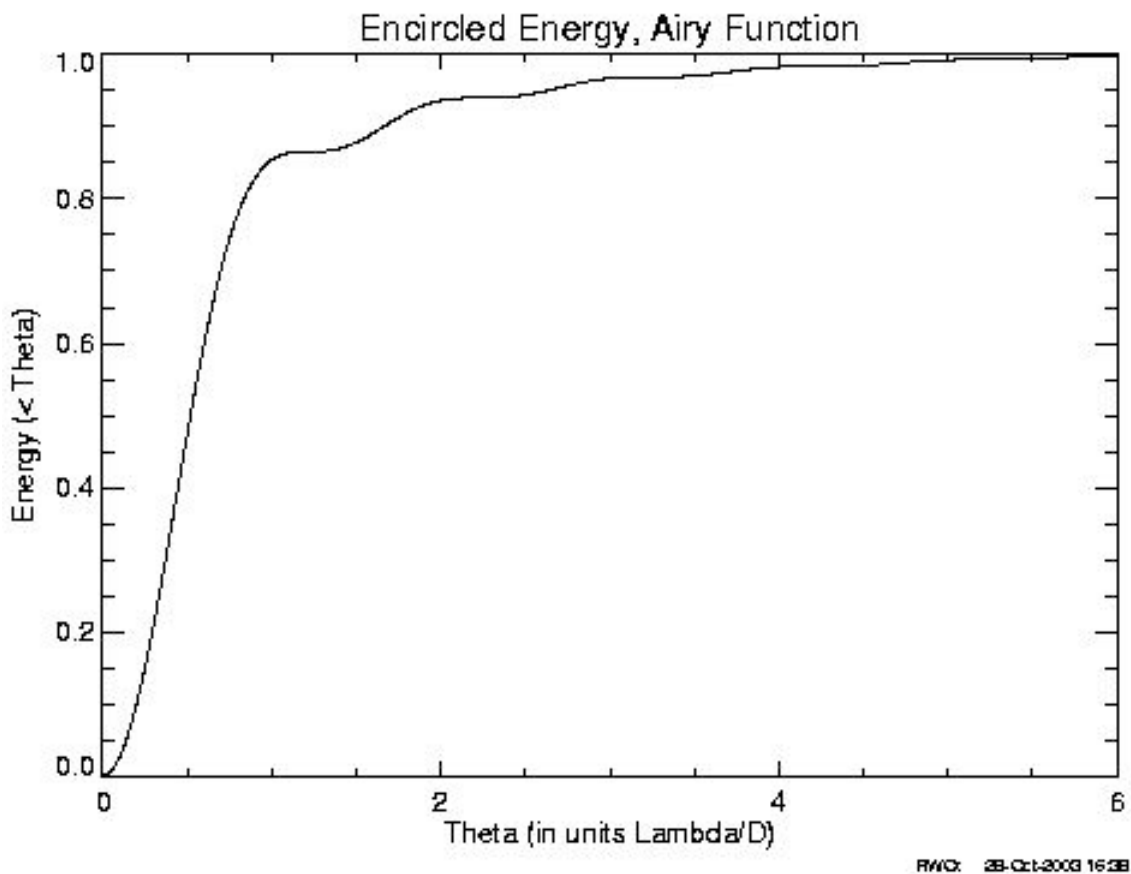
The size of the pattern is important for purposes of resolving sources, but for photometric measurements, we are more interested in the <u>encircled energy</u> distribution of the pattern. The encircled energy is the fraction of the total integrated flux in the image contained within a given radius r.

That is, $EE(R) = \int\limits_{0}^{R} 2\,\pi\,I(r)\,r\,dr / E_0$,
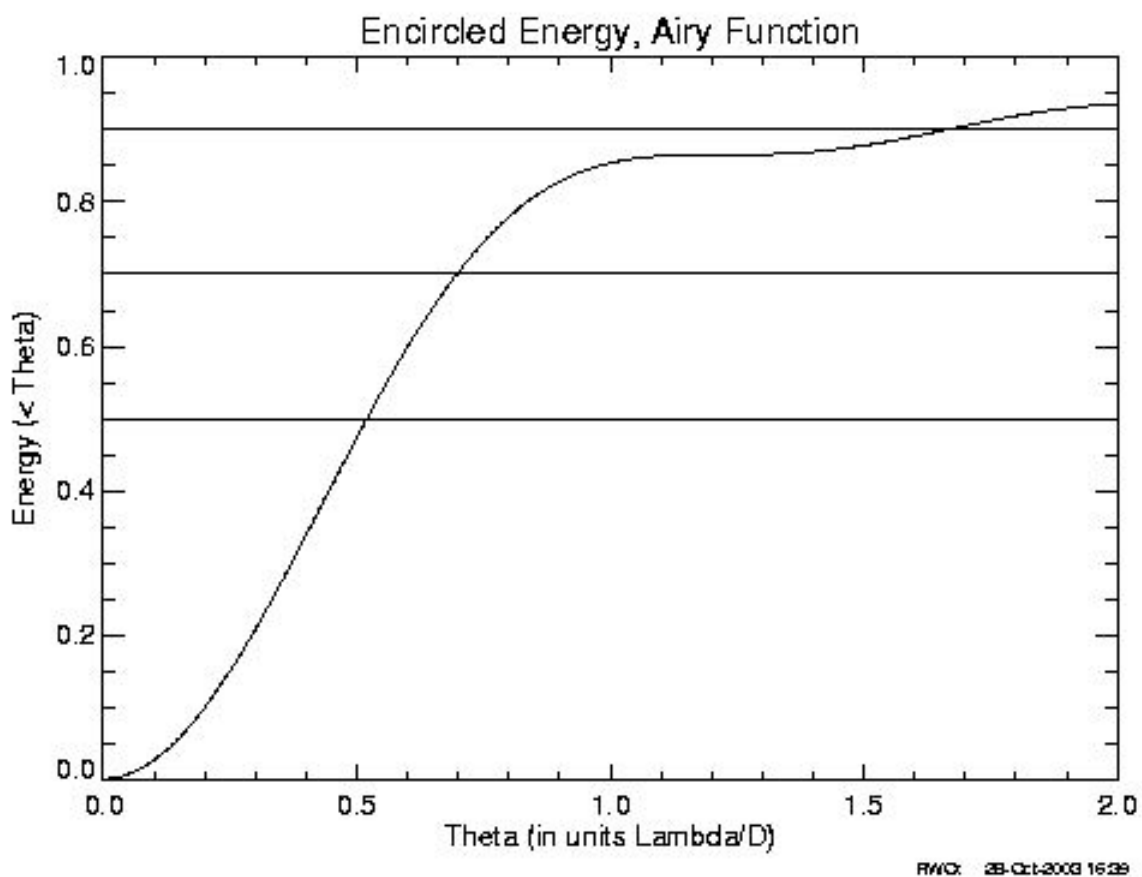
where $E_0 = \int\limits_{0}^{\infty} 2\,\pi\,I(r)\,r\,dr$
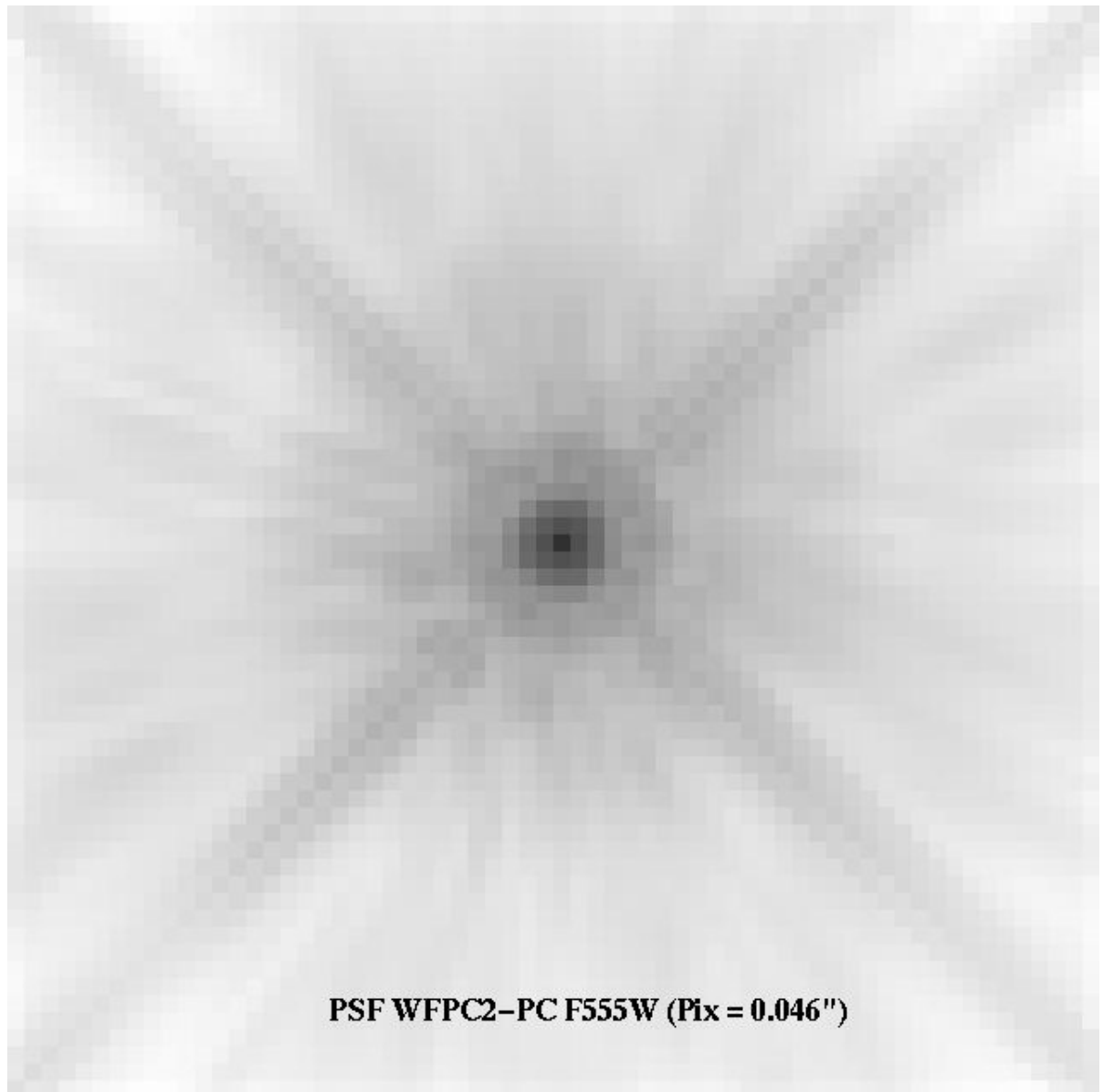
Real PSF's often have very extended wings, so for the purpose of characterizing photometric performance we often use the 70% encircled energy diameter, EED_70.

The plots on the next pages show the EE function for the Airy pattern.

Encircled Energy, Airy Function
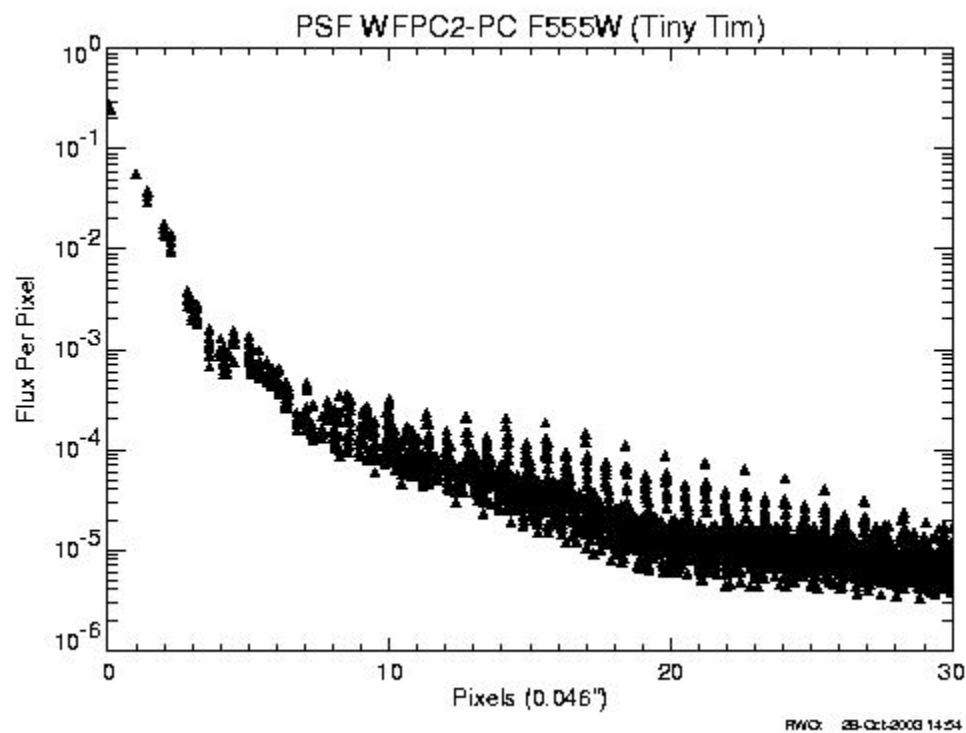
θ (λ/D units)	$EE(\theta)$
0.52	0.50
0.70	0.70
1.22	0.86
1.66	0.90

Encircled Energy, Airy Function

PSF WFPC2–PC F555W (Pix = 0.046")
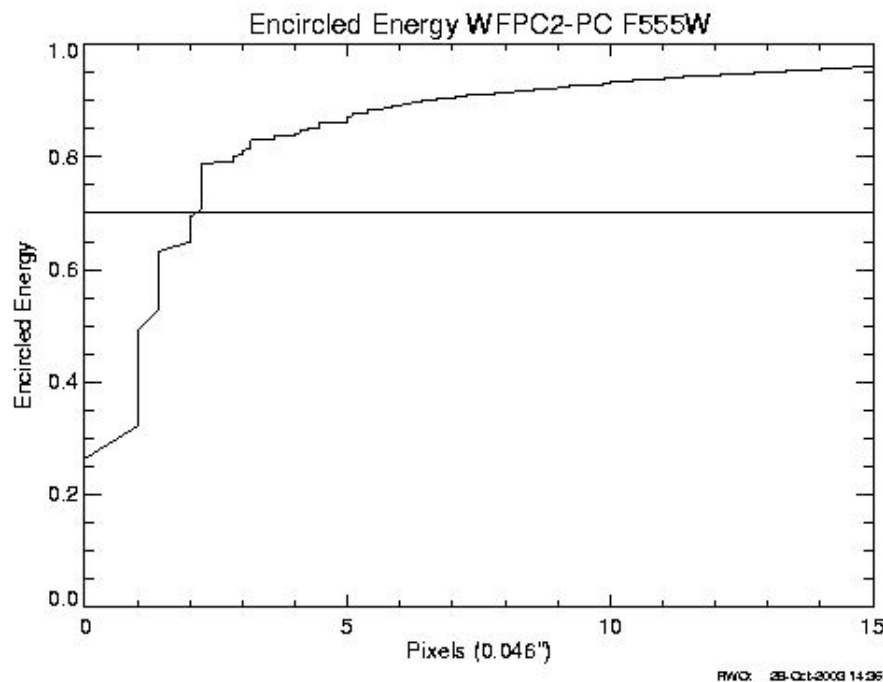
Point spread function image for the HST/WFPC-2 PC chip (Tiny Tim simulation)

Azimuthally averaged profile of WFPC2-PC PSF

Encircled energy for the WFPC2-PC PSF. The 70% EE radius
is 2 pixels or 0.092″

MAGNITUDE AND COLOR SYSTEMS

INTRODUCTION

"Magnitudes" are an ancient and arcane, but by now unchangeable, way of characterizing the brightnesses of astronomical sources. They were introduced by the Greek astronomer Hipparchus ca. 130 BC. He arranged the visible stars in order of apparent (naked eye) brightness on a scale that ran from 1 to 6, with stars ranked "1" being the brightest. The ranks were called *magnitudes*. The faintest stars visible to the eye under excellent sky conditions were ranked as sixth magnitude.

Much later it became clear that because of the way the human eye responds to a stimulus, magnitudes were proportional to the <u>logarithm</u> of the EM power entering the eye from the source.

The modern magnitude system has been quantified as follows:

$$ m = -2.5 \log_{10} \frac{f(i)}{Q(i)} $$

where f is the mean <u>spectral flux density</u> (see Lec. 2) from a source at the top of the Earth's atmosphere averaged over a defined band and Q is a normalizing constant for that band.

Although this definition looks peculiar, it offers two important practical conveniences: (1) Cosmic sources have an enormous range of brightness, and the magnitude system provides a quick shorthand for expressing these without referring to exponents. (2) The change of magnitude caused by a given (small) fractional change in the flux density of a source is numerically equal to the fractional change. E.g., a 5% error in flux density produces a 0.05 mag change.

Nonetheless, magnitudes are the source of considerable confusion among professional astronomers because there is not one magnitude system but instead several. For historical reasons within subfields, the definitions differ in two ways: **(1)** The spectral flux density can be expressed <u>either</u> as $f_\nu(\nu)$ or $f_\lambda(\lambda)$. **(2)** The normalizing constant $Q(i)$ differs among the systems; and even within a given system, it can differ with <u>waveband</u>.

The most widely used magnitude system through the year 2000 was based on a set of normalizing constants derived from the spectrum of the bright star Vega. We are now slowly moving to "absolute" systems based on calibrations in terms of physical flux units.

I. MONOCHROMATIC MAGNITUDE SYSTEMS

In Lecture 2 we introduced a "monochromatic" magnitude system, which is defined as:

$$m_\lambda(\lambda) \equiv -2.5 \log_{10} F_\lambda(\lambda) - 21.1$$

where $F_\lambda(\lambda)$ is the spectral flux density <u>per unit wavelength</u> of a source at the top of the Earth's atmosphere in units of $\mathrm{erg\ s^{-1}\ cm^{-2}\ \mathring{A}^{-1}}$. This is also known as the "STMAG" system because it is standard for the Hubble Space Telescope. For more details, see the *Synphot User's Guide* at **STScI**.

The corresponding system based on flux per unit <u>frequency</u> is

$$m_\nu(\lambda) \equiv -2.5 \log_{10} F_\nu(\lambda) - 48.6$$

where $F_\nu(\lambda)$ is in units of $\mathrm{erg\ s^{-1}\ cm^{-2}\ Hz^{-1}}$. This is also known as the "AB" or "AB$_\nu$" system. This system has been adopted by the Sloan Digital Sky Survey and **GALEX**. (The resulting magnitudes are therefore very different from the **STMAG** system in the UV, for example.)

These are the most intuitively obvious of the various magnitude scales used by astronomers since the normalizing constants are the same at all

wavelengths, and magnitudes are easily convertible to physical flux units regardless of the wavelength observed.

The zero points are defined to coincide with the zero point of the widely used "visual" or standard "broad-band" **V** magnitude system: i.e.

$$m_\lambda(5500\,\text{Å}) = m_\nu(5500\,\text{Å}) = V$$

However, the infinitesimal wavelength range inherent in the f_λ or f_ν definitions cannot actually be measured in practice. The monochromatic magnitudes are estimates based on observations made in wider bands, and the conversion to flux can only be as good as broader-band observations can be calibrated. In fact, these systems are the stepchildren of more basic broad-band systems in use by astronomers for over 100 years—but which are more awkward in definition and usage.

II. FILTER PHOTOMETRY SYSTEMS

Broad-band magnitude systems were introduced into astronomy by photography, which offered multi-wavelength response not confined to the acceptance band of the human eye (the "visual" band). As photoelectric detectors were implemented, systems defined using <u>filters</u> of varying widths proliferated. (Consult the bibliography for details.)

It is extremely difficult to calibrate astronomical photometric equipment the way one would calibrate laboratory equipment. Observations are made under field conditions, and there are no easily deployable laboratory flux standards. Each piece of photometric equipment, wavelength isolator, and telescope has different properties, and the throughput of the Earth's atmosphere changes nightly.

Thus, astronomical magnitude systems are defined in terms of the brightness of sources in specific wavebands <u>relative</u> to a <u>set of "standard stars"</u> selected by agreement. These relative brightnesses are <u>better determined</u> than any "absolute fluxes" which might derived from them. (Therefore, much astrophysical analysis is of the magnitudes rather than the fluxes.)

Apart from the difficulty of flux calibration, broad-band systems suffer from the fact that they are indeed <u>broad</u>, with typical optical bandwidths in the
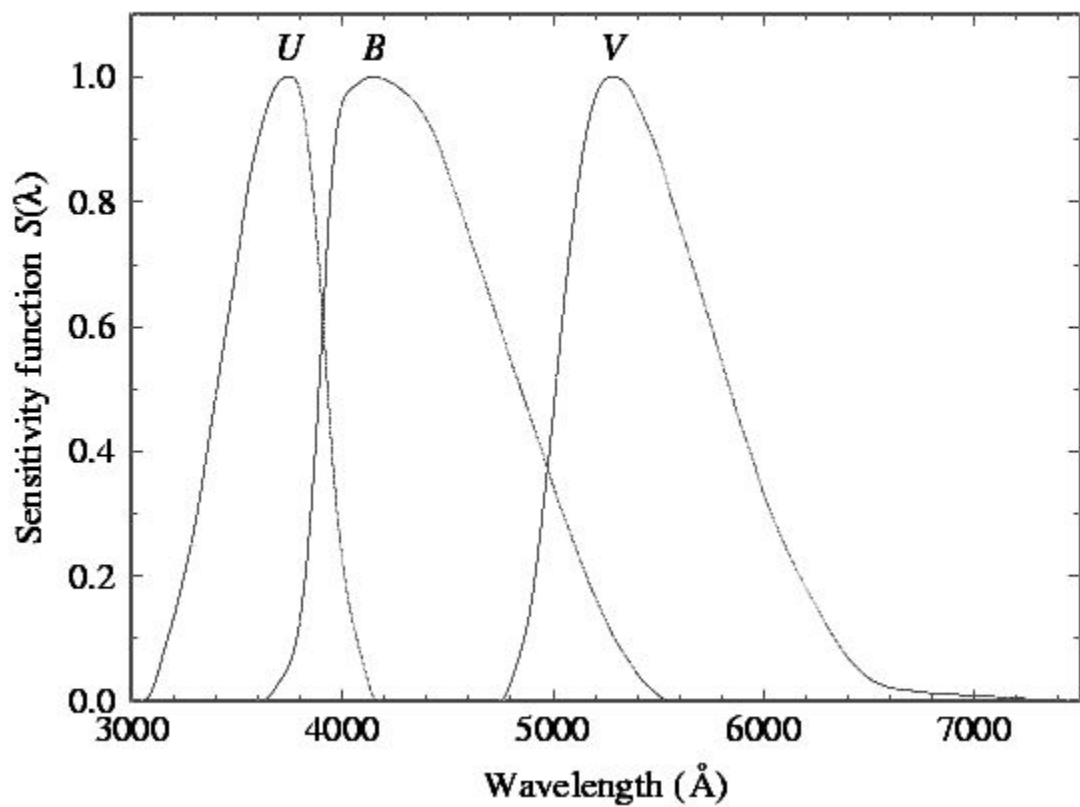
range ∼500–2000 Å. The reason for this is, of course, to enable study of faint astronomical sources. But wide bands introduce a host of difficulties arising from the fact that cosmic SED's and instrumental responses can change significantly <u>within</u> the bands.

A brief history:

- The original visual system was, of course, based on the response of the human eye. In the 19th century, various clever designs emerged which allowed simultaneous comparative "photometry" of the brightnesses of two stars or of a star and a calibration source. But visual measures were never very precise.

- The photographic plate gave rise to the "photovisual" system (Pv), using filters which approximated the eye's response, and the "photographic" system (Pg), which used a bluer filter to take advantage of the enhanced photographic response there. Aperture photometers and densitometers allowed quantitative extraction of information stored on a plate (subject, though, to significant uncertainties owing to the nonlinear and nonuniform responses of emulsions).

- The first photoelectric filter photometry system to be used for large numbers of measures of stars and galaxies was the "6-color" system of Stebbins and Whitford (1935-1960).

- The 1P21 photomultiplier tube (1945), with dramatically improved performance in both sensitivity and noise rejection (especially if operated in <u>pulse-counting</u> mode), ushered in a new era in photoelectric photometry. It had a CsSb ("S-4") photocathode, with excellent blue (4000 Å) sensitivity but a red cutoff at about 6300 Å. A number of later PMT designs (e.g. S-1, S-20) extended sensitivity to 8000-10000 Å.

- The prototype broad-band system for those in wide use today was the "UBV" system of Johnson & Morgan (ApJ, 117, 486, 1953). This was carefully defined in terms of specific choices of filter glass matched to the 1P21 PMT <u>and</u> the energy distributions of stars (see plot below). It was normalized to the SED of Vega.

- The UBV system was so successful in applications to stellar evolution, stellar populations, interstellar dust, and extragalactic astronomy that it was energetically extended to the red and infrared (R,I,J,H,K). Unfortunately, this work was undertaken by numerous workers using different filters and detectors, resulting in a confusing and incompatible

set of definitions (especially in R and I). Only in the last 20 years have these systems been consolidated (see bibliographic entries for Bessell).
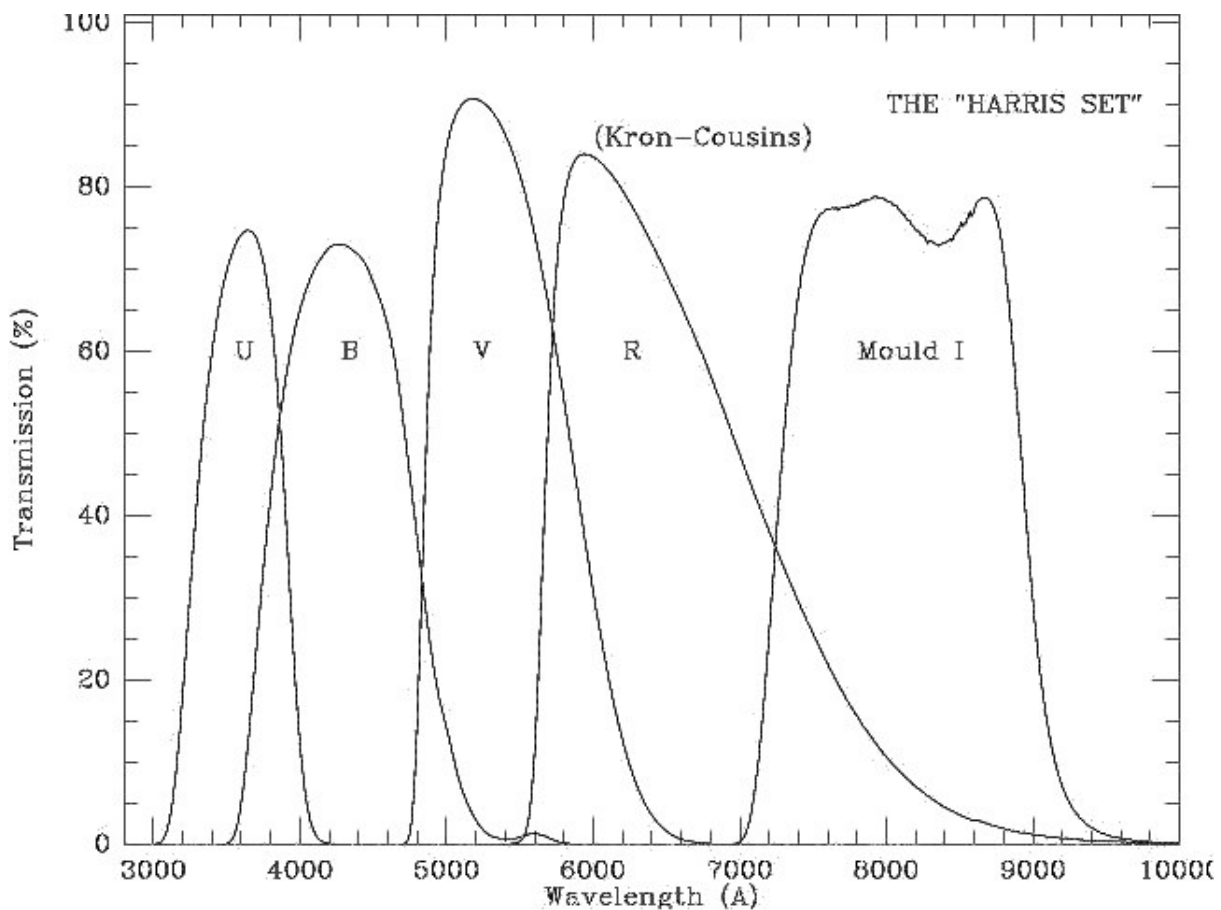
- The basic broad-band system in use today covers the optical range (3300-10000 Å) with UBVRI, the near-infrared (1.0-2.4μ) with JHK, and part of the mid-infrared (3.0-10μ) with LMN. In the future, the most widely used bands in the LMN region will be the four defined by the IRAC camera on the Spitzer Space Telescope.

- The Strömgren system was the first intermediate-band system to be widely used. Its filters (180-300 Å width) were tailored to measure abundance, temperature, and surface gravity effects in AF stars. Various other systems (e.g. DDO) extend this approach to later type stars and galaxies.

- Other useful broad-band systems include the Washington system (intended for faint GK stars) and the Thuan-Gunn system. The latter is like UBVRI but with filters optimized for faint galaxies by rejecting night sky lines; it is used for the Sloan Digital Sky Survey.

- You can find transmission data for all the widely used filter systems at: http://voservices.net/filter/.
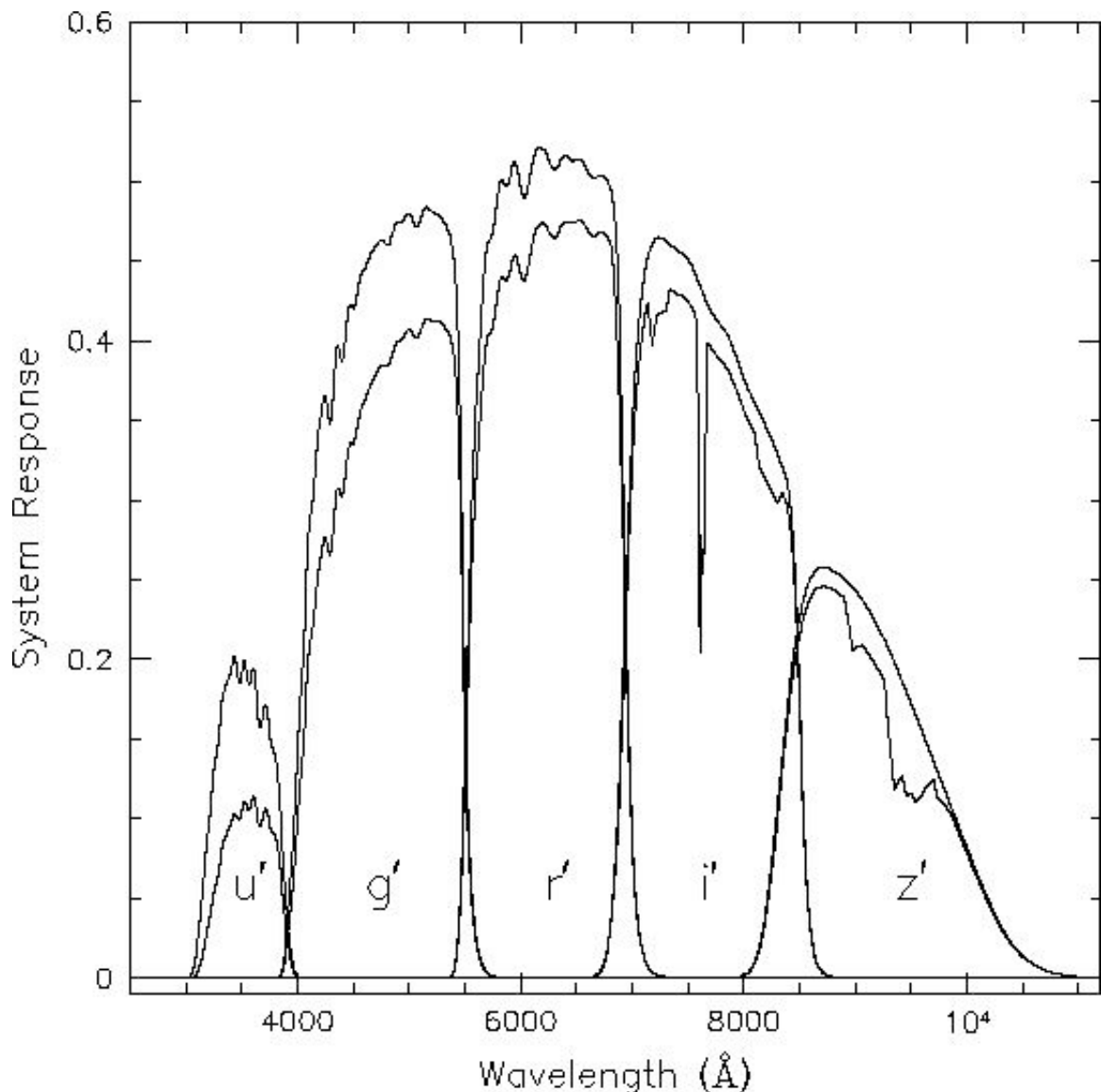
The Johnson-Morgan UBV filter system.

Approximate central wavelengths and bandwidths are:

Band	$< \lambda >$ (Å)	$\Delta\lambda$ (Å)
U	3600	560
B	4400	990
V	5500	880

Standard UBVRI broad-band filter response curves (KPNO).

Sloan Digital Sky Survey broad-band filter responses. Filters are on the Thuan-Gunn system. Compared to standard UBVRI, these have more sharply defined band limits and avoid stronger night sky emission lines. The g' band takes the place of standard B and V and z' extends the system to the red limit of standard CCD response. Curves here include net throughput of telescope and detectors. Lower curves show effects of atmospheric absorption at 1.2 airmasses.

III. THE VEGA MAGNITUDE SYSTEM

Following Johnson & Morgan, the set of calibrator stars for most filter photometry systems is defined by one "primary standard," the bright star <u>Vega</u> (α Lyrae), which in turn has been coupled through an elaborate bootstrap technique to a large set of "secondary" standards. The bootstrap involved extensive observational filter photometry and spectrophotometry as well as theoretical modeling of stellar atmospheres.

Ideally, the Vega magnitude system (or "vegamag") is defined as follows:
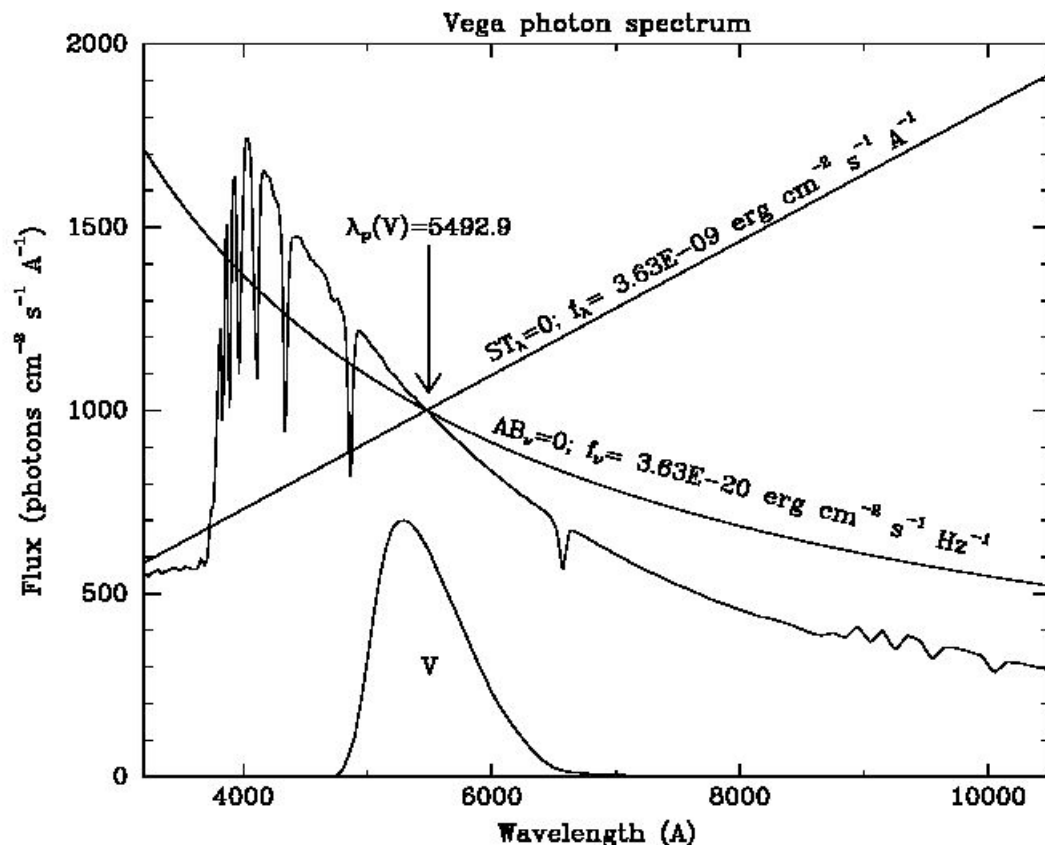
- **o Let $R_i(\lambda)$ be a transmission function for a given band i. R is usually determined primarily by a filter.**

- **o Then for a source whose spectral flux density at the top of the Earth's atmosphere is $F_\lambda(\lambda)$, the broad-band magnitude m_i is**

$$m_i = -2.5 \, \log_{10} \frac{\int R_i(\lambda)\lambda F_\lambda(\lambda)d\lambda}{\int R_i(\lambda)\lambda F_\lambda^{\mathrm{VEGA}}(\lambda)d\lambda} + 0.03$$

  where 0.03 is the V magnitude of Vega. The system is based on spectral flux density per unit wavelength.

- **o Here we have assumed a photon-counting detector, so that the system response is proportional to the <u>photon rate</u>. This is the origin of the additional λ term in the expression above (the photon rate is $[\lambda/hc]F_\lambda$).**

- **o Vega was chosen as the primary standard because it is easily observable in the northern hemisphere for more than 6 months of the year and because it has a relatively smooth spectral energy distribution compared to later type stars. Bright stars with the same spectral type are relatively common.**

- **o The SED of Vega is shown on the next page, and an IDL save file containing a digital version (theoretical) of the SED is linked to the Lectures web page.**

- **o Vital statistics for Vega (from Kurucz): Spectral type A0 V. Effective temperature $T_e = 9550$ K. Surface gravity $\log g = 3.95$. Metal abundance $\log Z/Z_\odot = -0.5$.**

Figure 2.1: Standard photometric systems generally use the spectrum of Vega to define magnitude zero. The spectrophotometric magnitudes AB_ν and ST_λ refer instead to spectra of constant f_ν and f_λ respectively. Magnitude zero in both systems is defined to be the mean flux density of Vega in the Johnson *V* passband. Thus all three of the spectra shown here produce the same count rate in the Johnson *V* passband. The pivot wavelength of Johnson *V* is defined to be the crossing point of the $AB_\nu = 0$ and $ST_\lambda = 0$ spectra.

**Plot of zeropoint spectra in three different magnitude systems.
(Note: ordinate is <u>photon</u> flux, not energy flux.)**

Although Vega has a reasonably smooth energy distribution, as compared, for example, to an M star, there are obviously large changes in the vegamag normalizing constants with wavelength.

Implications of this definition:

o **In each band, the system <u>weights</u> the photon SED of a source by the defined response function $R_i(\lambda)$. This is usually <u>not</u> a "top-hat" function with a flat top and vertical sides.**

   The R_i's for the basic bands are described. for example, in the articles by Bessell in the bibliography.

   Even under the best circumstances, any particular equipment will differ slightly in R_i from the standard system. This means that <u>transformations</u> to the standard system must be part of any photometric reduction.

   Calibration is more difficult the broader is the band. This is because of changes in the source SED and the weighting function within the band. Cf. equation (2) of Lecture 12.

o **For Vega, or any other A0 V type star,**

$$m_i = m_j = V \text{ for all } i, j$$

o **The zero point of the system is defined by the SED of an A0 V star, which means that the <u>zero point differs from band to band.</u>**

   Even if $m_i = m_j$, the corresponding mean fluxes, $< F_\lambda >_i$ and $< F_\lambda >_j$ are generally <u>not</u> equal. From the plot of Vega's SED, one can see that the flux zero point at 1μ, for instance, is significantly lower than at 5500 Å.

   This is a major departure from the monochromatic systems, for which equal magnitudes imply equal flux densities.

o **With modern highly sensitive detectors, Vega is too bright to observe directly for calibration. Instead, one must observe (every night) a selection of secondary or tertiary standards.**

o **The actual zero points of the system are defined by the <u>full set</u> of secondary standard stars. Small residual "closure" errors mean that the measured values in practice will depend on the particular set of standards observed on a given night.**

IV. FLUX CALIBRATION OF THE VEGA SYSTEM

The zero point of the Vega system is based on high quality data from PMT-based spectrophotometers obtained by Oke, Schild, Hayes, and Latham ca. 1967-1975 (see bibliography). These spectra were calibrated by direct observations of nearby laboratory light sources (e.g. platinum furnaces), though this introduced many complications (e.g. horizontal extinction across the mountain tops).

These data sets have been melded with increasingly high fidelity synthetic stellar spectra (theoretical) to extend and consolidate the system across the various bands. The best current calibration for the UBVRIJHK system is by Bessell, Castelli, & Plez (1998, see bibliography and next page). You were already introduced to the zero point of the V-band system in Lecture 2:

Fluxes for a $V = 0$ star of spectral type A0 V at 5450Å:

$$f_\lambda^0 = 3.63 \times 10^{-9} \text{ erg s}^{-1} \text{ cm}^{-2} \text{ Å}^{-1}, \text{ or}$$

$$f_\nu^0 = 3.63 \times 10^{-20} \text{ erg s}^{-1} \text{ cm}^{-2} \text{ Hz}^{-1}, \text{ or}$$

$$\phi_\lambda^0 = f_\lambda^0/h\nu = 1005 \text{ photons cm}^{-2} \text{ s}^{-1} \text{ Å}^{-1}$$

Note that the effective wavelength of the filter shifts with the SED of the source and is closer to 5500 Å for G-K stars.

The flux zero point in filters other than V is then defined by the spectral energy distribution of an A0 V star. The relationship between the magnitude in a given filter and the mean flux in that filter is then given by:

$$m_i = -2.5 \log_{10} \left(\frac{< F_\lambda >_i}{F_{0,i}} \right)$$

where $F_{0,i}$ is the zero point for band i as given in the Bessell listing (units: $\text{erg s}^{-1} \text{ cm}^{-2} \text{ Å}^{-1}$).

BROAD BAND SYSTEM ZEROPOINTS (BESSELL ET AL. 1998)

	U	B	V	R	I	J	H	K	Kp	L	L*
λ_{eff}	0.366	0.438	0.545	0.641	0.798	1.22	1.63	2.19	2.12	3.45	3.80
f_ν	1.790	4.063	3.636	3.064	2.416	1.589	1.021	0.640	0.676	0.285	0.238
f_λ	417.5	632	363.1	217.7	112.6	31.47	11.38	3.961	4.479	0.708	0.489
$zp(f_\lambda)$	0.770	-0.120	0.000	0.186	0.444	0.899	1.379	1.886	1.826	2.765	2.961
$zp(f_\nu)$	-0.152	-0.602	0.000	0.555	1.271	2.655	3.760	4.906	4.780	6.775	7.177

$f_\nu \ (10^{-20} \ \mathrm{ergs \ cm^{-2} \ sec^{-1} \ hz^{-1}})$
$f_\lambda \ (10^{-11} \ \mathrm{ergs \ cm^{-2} \ sec^{-1} \ \AA^{-1}})$
$mag_\lambda = -2.5 \log (f_\lambda) - 21.100 - zp(f_\lambda)$
$mag_\nu = -2.5 \log (f_\nu) - 48.598 - zp(f_\nu)$

Bessell's 1998 values for the effective wavelength of each filter (for an A0 V spectral type) and the corresponding flux zeropoints are given above. These, together with mean colors for various spectral types on the Johnson system (which differs from Bessell), will also be handed out.

Note two important typos in the published table: the fourth row of the table should be labeled zp(f_ν) and the fifth row should be labeled zp(f_λ).

V. COLORS

A "color" is simply a difference between magnitudes for a given source in two different bands:

$$C_{ij} \equiv m_i - m_j = -2.5 \, \log_{10} \left(\frac{< F_\lambda >_i}{< F_\lambda >_j} \right) + const_{ij}$$

where the constant is a function of the zeropoints of the two bands.

Colors measure the <u>slope</u> of the spectral energy distribution between bands i and j.

Note that the definition is such that a more positive color implies a larger flux in the <u>second</u> (j) band.

It is usual, though not universal, that the two bands are entered in order of increasing wavelength.

Colors are used in all of the magnitude systems defined above. However, the historical precedent of the classic Johnson-Morgan system is such that labels such as **UBVRIJK** are understood to refer to the Vega system unless otherwise explicitly stated.

The **V** band is often a convenient reference, so colors like B-V, V-I, V-K are widely used. The standard "UBV" system employs U-B and B-V. Cool sources which emit little light below 8000 Å are often characterized by I-K, J-K, H-K, etc.

VI. ATMOSPHERIC EXTINCTION

The effect of atmospheric extinction on photometry (cf. Lec 4) is usually expressed as:

$$m_{obs} = m_{true} + k(\lambda) \sec Z$$

Here, m_{true} is the magnitude of the source outside the Earth's atmosphere, and m_{obs} is the magnitude observed.

> The "air mass," $\sec Z$, where Z is the angular zenith distance, is given by the following expression (for plane-parallel geometry):
>
> $$\sec Z = [\sin \phi \, \sin \delta + \cos \phi \, \cos \delta \, \cos h]^{-1}$$
>
> where ϕ is the latitude of the observatory, h is the hour angle of the source, and δ is the declination of the source.
>
> $\sec Z$ is the total atmospheric pathlength toward the source in units of the vertical pathlength. For best photometry, keep $\sec Z \lesssim 2$.

$k(\lambda)$ is the "extinction coefficient."

Several different physical effects contribute to continuous extinction. These include Rayleigh scattering ($\sim \lambda^{-4}$), ozone or H_2O molecular absorption, and aerosol scattering. Each of these is characterized by a different effective scale height, so that their mixture will <u>change</u> with altitude.

Extinction coefficients have been carefully measured for a number of observatories. A table for Palomar (Hayes & Latham 1975) is included on the next page.

Ignoring its multi-component nature, approximate values of extinction for a given site can be obtained from those for another (assuming a hydrostatic, isothermal atmosphere) as follows:

$$k(X_1) = k(X_0) \exp \left(- \left[\frac{(X_1 - X_0)}{H_0} \right] \right)$$

where X_1 and X_0 are the altitudes of the two observatories and H_0 is the scale height of the atmosphere (7950 meters for STP).
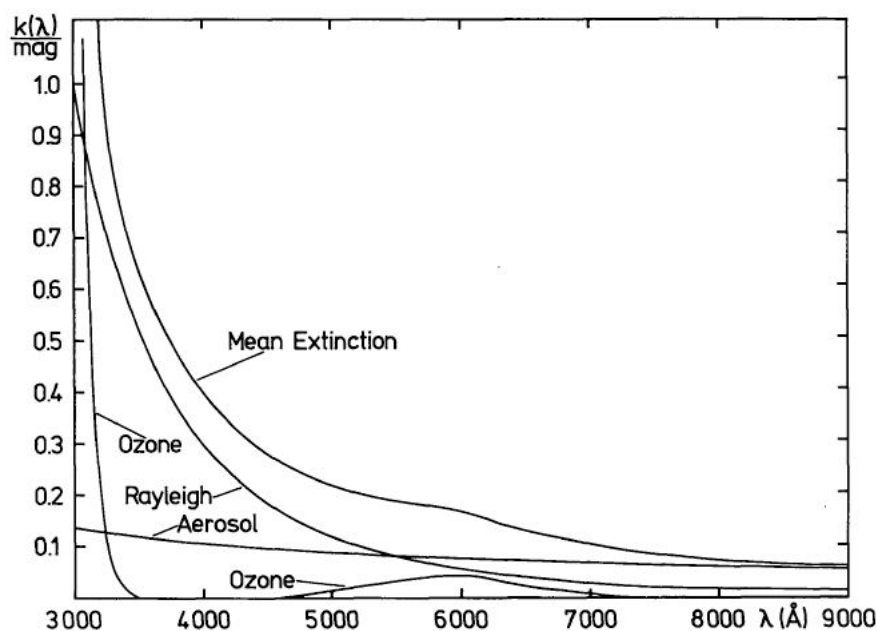
Fig. 1. Mean vertical extinction at Flagstaff, Arizona, in May-June 1976. The assumed ozone and Rayleigh contributions are shown separately

TABLE 5

MEAN EXTINCTION COEFFICIENTS FOR PALOMAR MOUNTAIN
FABRICATED WITH OUR PROCEDURE

Wave-length (Å)	$A(\lambda)$ [mag (air mass)$^{-1}$]	Wave-length (Å)	$A(\lambda)$ [mag (air mass)$^{-1}$]
3200......	1.058	5263......	0.164
3250......	0.911	5556......	0.151
3300......	0.826	5840......	0.140
3350......	0.757	6055......	0.133
3390......	0.719	6435......	0.104
3448......	0.663	6790......	0.084
3509......	0.617	7100......	0.071
3571......	0.575	7550......	0.061
3636......	0.537	7780......	0.055
3704......	0.500	8090......	0.051
3862......	0.428	8370......	0.048
4036......	0.364	8708......	0.044
4167......	0.325	9832......	0.036
4255......	0.302	10255......	0.034
4464......	0.256	10610......	0.032
4566......	0.238	10795......	0.032
4785......	0.206	10870......	0.031
5000......	0.183		

ATMOSPHERIC EXTINCTION (cont)

Apart from the continuous absorption just described, molecules in the Earth's atmosphere produce <u>discrete absorption features</u> that can be very troublesome in certain wavelength ranges. The features can be quite strong and/or variable.

Here are some of the most important absorption features in the optical range:
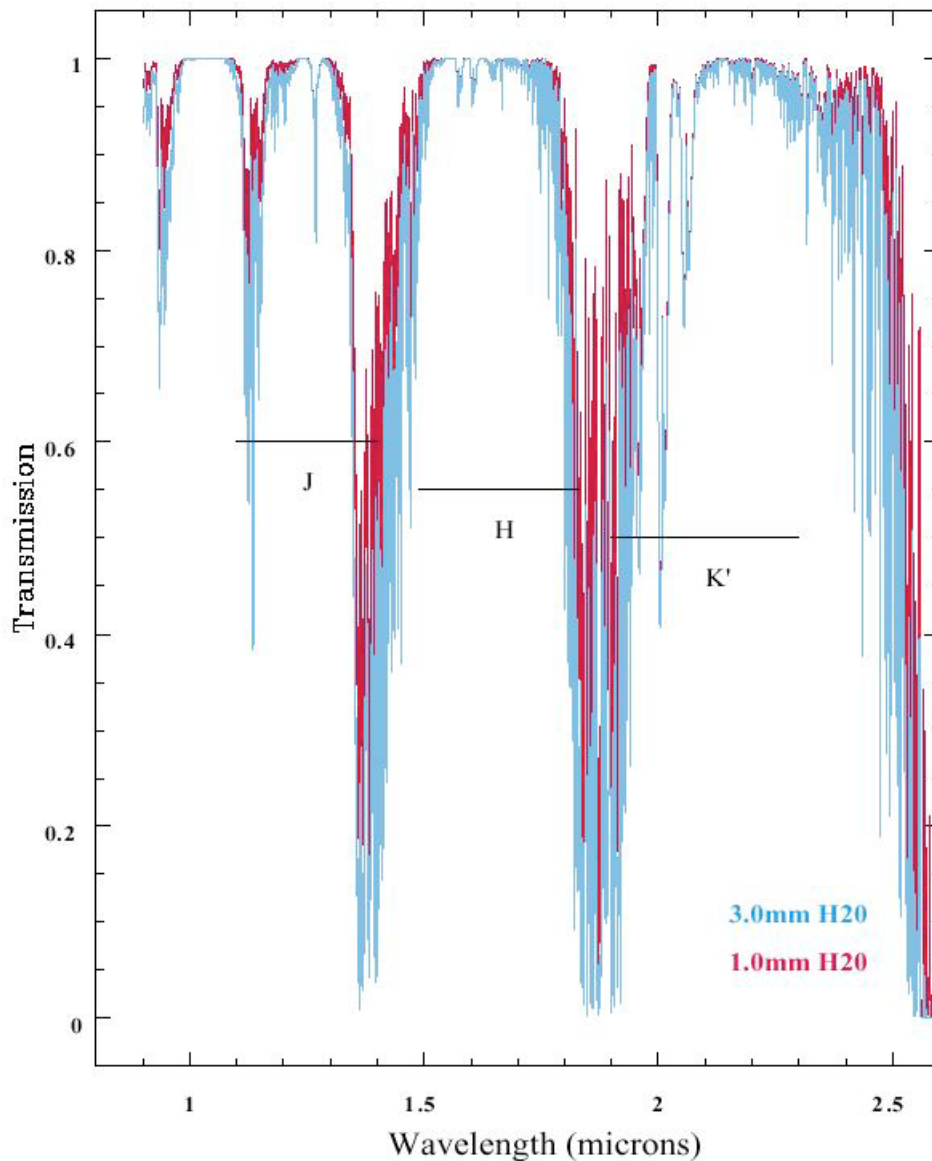
Wavelength	Species
6275-6300 Å	O_2
6860-6950 Å	O_2 "B" band
6900-7100 Å	H_2O
7580-7700 Å	O_2 "A" band
8050-8350 Å	H_2O
9000-9800 Å	H_2O

The very strong H_2O absorption in the 1-3 μ range is shown on the next page.

Because of the large number of transitions within a given molecular band and the potentially rapid change of optical depth with transition, extinction by the bands often does not have the simple $\sec Z$ dependence described above. Some transitions saturate faster than others.

It is best to avoid these regions. Standard broad-band filter systems are designed to avoid the stronger absorption features (e.g. J,H,K', as shown on the next page). However, it is not always possible to do this in narrow-band photometry and spectroscopy. The best way to deal with the features is to find hot reference stars (i.e. with smooth SEDs) near each target and observe them at the same zenith distances.

LINE ABSORPTION IN THE NEAR-IR

Transmission of the Earth's atmosphere in the near-infrared. Absorption is dominated by H_2O. Horizontal lines show the definitions of the J, H, and K' photometric bands, which lie in relatively clean regions.

VII. PHOTOMETRIC CALIBRATION & REDUCTION

Calibration of photometric observations and reduction to the standard
broad-band system require observation of standard stars. These are used to
determine the effects of atmospheric extinction and the "transformation"
between the response of your equipment and that of the standard system.

(i) Atmospheric transmission varies from night to night. You must make
sufficient standard observations each night to calibrate that
independently of other nights of your run.

(ii) However, you can use combined data from several nights to determine
the photometric transformations between your filter set and the
standard set.

(iii) Calibration can have strong <u>color-dependent</u> terms. This means that
your standards must span the color range of your "unknowns." The
larger is that range, the larger is the standard set you need to observe.

(iv) Standards must be in the range of brightness appropriate for your
equipment.

Recalling equation (2) of Lecture 12, the count rate $\dot{s}$ (detected photons
per second in filter i) for a given source is

$$ \dot{s}_i \propto \frac{\pi}{4} D_e^2 \int e^{-k(\lambda)\,\sec Z}\, T_i(\lambda)\, \frac{F_\lambda(\lambda)}{h\nu}\, d\lambda $$

A. Narrow-Band Observations

If the bandwidth of the filter is so narrow that all of the terms in the
above expression are well approximated by mean values, then it is
straightforward to calibrate your data. The basic relation is:

$$ m_{ij} = -2.5 \log_{10} \dot{s}_{ijk} - K_i \sec Z_k - a_i $$

Here m_{ij} is the broad-band magnitude in filter i for standard star j;
$\dot{s}_{ijk}$ is the count rate for the kth observation of this star at zenith
distance Z_k.

K_i is the atmospheric extinction coefficient for band i and a_i is the transformation term between the local and standard photometric systems.

The problem is to determine K_i and a_i. More than two standard star observations overdetermine the problem, but a large set of calibration observations gives valuable information on the scatter from random and systematic errors (e.g. secular variation in atmospheric transparency).

B. Broad-Band Observations

The complexity here arises from the fact that the various terms in the proportion above are not constant across a broad-band filter. The effect of this will depend on the distribution of light of the source within the band, i.e. on the spectral slope of the source. This means there will be <u>color terms</u> in both the effective atmospheric extinction and in the transformation.

The normal approach to this problem is to first define "instrumental colors," based on the relative count rates of two adjacent filters. For example:

$$C_i \equiv -2.5 \log_{10} \left(\frac{\dot{s}_{i+1}}{\dot{s}_i} \right)$$

Then, rewrite the calibration equation above to include color terms in both the extinction and transformation as follows:

$$m_{ij} = -2.5 \log_{10} \dot{s}_{ijk} - [K_{0,i} + K_{1,i} C_i] \sec Z_k - a_{0,i} - a_{1,i} C_i$$

The problem now includes 4 unknowns, and solution depends on having a large range of color in the standard star observations. Many more standard observations are needed than in the narrow-band case.

To provide a more robust solution, one normally starts with an estimate of the K terms (based on average atmospheric conditions) and iterates on those.

For more details on extinction corrections and reduction, see the bibliography (the Young articles are very thorough).

BIBLIOGRAPHY FOR STELLAR PHOTOMETRY AND SPECTROSCOPY

October 2003

RELEVANT IAU PUBLICATIONS

IAU Symposium No. 189, *Fundamental Stellar Properties*, 1997

IAU Symposium No. 111, *Calibration of Fundamental Stellar Quantities*, 1985.

IAU Colloquium No. 64, *Automated Data Retrieval in Astronomy*, 1982.

IAU Symposium No. 96, *Infrared Astronomy*, 1980.

IAU Symposium No. 54, *Problems of Absolute Magnitudes and Temperatures of Stars*, 1975.

IAU Symposium No. 50, *Spectral Classification and Multicolor Photometry*, 1973.

SPECTRA & SPECTRAL CLASSIFICATION

Corbally, Gray, & Garrison, *The MK Process at 50 Years*, 1994.

Buscombe, *MK Spectral Classification, 10th Catalog*, 1992.

Kaler, J.B. *The Stars and Their Spectra*, (Cambridge University Press), 1989.

Jaschek and Jaschek, *The Classification of Stars* (Cambridge University Press) 1987.

Margon, *A Display Atlas of Stellar Spectra*, (University of Washington), 1986. [Enlarged plots of data from Jacoby et al. 1984, *Ap.J. Suppl.*, **56**, 257.] QB881.M37 1986z.

Turnshek, Turnshek, Craine, & Boeshaar, *An Atlas of Digital Spectra of Cool Stars*, 1985.

Morgan, Abt and Tapscott, *Revised MK Spectral Atlas for Stars Earlier than the Sun*, 1978.

Meinel, Aveni, Stockton: *Catalog of Emission Lines in Astrophysical Objects*, 1969.

Keenan, "Spectral Classification," in *Basic Astronomical Data*, ed. K. Strand.

Morgan, Keenan, and Kellman, *An Atlas of Stellar Spectra*, (the "MKK" Atlas).

FILTER PHOTOMETRY TECHNIQUES

Straizys & Davis Philip, *Conference on Photometric Systems and Standard Stars*, 1996

Sterken and Manfroid, *Astronomical Photometry, A Guide* (Kluwer), 1992.

C.R. Kitchin, *Astrophysical Techniques* (Adam Hilger Ltd.) Chapter 3, 1998.

Henden and Kaitchuk, *Astronomical Photometry* (Van Nostrand) 1982. Undergrad. level; practical aspects stressed.

A. Young, in *Methods of Experimental Physics*, Vol. **12**, Part A, pp. 1-192, 1974. Comprehensive discussion; the basic reference for all the details.

Photon counting: Morton, *Applied Optics*, **7**, 1, 1968. Keyes and Kingston, *Physics Today*, March 1972.

Handbooks and manuals at major observatories (e.g. NOAO, STScI, AAO, ESO, etc.)

Journals: *Applied Optics; Advances in Electronics and Electron Optics.*

DEFINITIONS AND DATA FOR STANDARD PHOTOMETRY SYSTEMS: BASIC REFERENCES

Most important catalogs are available in digital form, either on CDROM's or over the Internet. However, the original articles in digital or printed versions are often very useful to have as well, especially for details of calibration and technique, and some are identified next.

A. Broad Band Filter Photometry

UBVRI passbands: Bessell, *PASP*, **102**, 1181, 1990.

UBV definition, standards: Johnson and Morgan, *Ap.J.*, **117**, 486, 1953.

JHKLM standard systems: Bessell & Brett *PASP*, **100**, 1134, 1988.

HST-WFPC2 UBVRI System: Holtzman et al. *PASP*, **107**, 1065, 1995.

Thuan-Gunn broad band system (modifed UBVR for faint galaxies): Thuan & Gunn, *AJ*, **88**, 543, 1976; the Sloan Digital Sky Survey (SDSS) system is a wider-band version of the TG system (Fukugita et al., *A.J.*, **111**, 1748, 1996).

Consolidated data sets (stars): UBV, *US Naval Obs. Publ.*, Ser. II, **21**, 1968; Nicolet, *Astr. Ap. Suppl.*, **34**, 1, 1978; UBVRI, Lanz, *Astr. Ap. Suppl.*, 1986.

UBVRIJKL, values for common stellar types: Johnson, *Ann. Rev. Astr. Ap.*, **4**, 193, 1966. [Handy, but beware later changes in definitions of bands longward of V.]

UBV, consolidated galaxy data set, Longo & de Vaucouleurs, *Univ. Texas Monographs* 3A (1983), supplement 1985. 0.5-1.0μ photometry: Monograph 5, 1988.

Washington broad-band system (intended for faint GK stars): Canterna, *AJ*, **81**, 228, 1976.

Infrared, consolidated: Gezari, Schmitz and Mead, *Catalog of Infrared Observations*, 3rd ed., 1993 (NASA Reference Publication 1294); and later supplements.

IR Sky Surveys: The Infrared Processing and Analysis Center (IPAC) maintains the IRAS (mid-far IR) data archives and has released several IRAS catalogs including the Point Source Catalog and the Faint Source Survey. The *Explanatory Supplement* to the Faint Source Survey (Moshir *et al*. 1992) gives an overview of IRAS data analysis and products. IPAC also now maintains the 2MASS ground-based JHK all-sky survey (most documentation digital).

B. Intermediate Band Filter Photometry

Stromgren photometry: Definition, "Spectral Classification Through Narrow Band Photometry", *Ann. Rev. Astr. Ap.*, **4**, 1966.

Stromgren, consolidated: Lindemann and Hauck, *Astr. Ap. Suppl.*, **11**, 119, 1973; Hauck and Mermilliod, *Astr. Ap. Suppl.*, **40**, 1, 1980; Standard stars: *A.J.*, **75**, 978 and *A.J.*, **71**, 114.

DDO System: Definition, McClure and van den Bergh, *A.J.*, **73**, 313, 1968. Data: McClure and Forrester, *Publ. Dom. Astrophys. Obs.*, **15**, 439, 1981.

"European Late-Type Star System", Dickow et al. *Astr. Ap. Suppl.*, **2**, 1, 1970.

DDO + Wood System, Galaxies: Definition and data, Faber *Ap.J.*, **179**, 731, 1973.

C. <u>Flux Calibration</u>

UBVRIJHK zero points, temperature calibrations, bolometric corrections, for model atmospheres: Bessell, Castelli, & Plez, *Astr. Ap.*, **333**, 231, 1998. [Supersedes Bessell, *PASP*, **91**, 589, 1979.]

UBV zero points: Buser & Kurucz, *Astr. Ap.*, **70**, 555, 1978; Kurucz, *Ap.J. Supp.*, **40**, 1, 1979.

V-band zero point; spectrophotometry of Vega: Hayes & Latham, *Ap.J.*, **197**, 593, 1975. Oke & Schild, *Ap.J.*, **161**, 1015, 1970.

DDO zero points: Tripicco & Bell *A.J.*, **102**, 744, 1991.

Sloan Digital Sky Survey revised AB_ν system: Fukugita et al., *A.J.*, **111**, 1748, 1996.

D. <u>Spectrophotometry</u>

Optical SED's for common types of stars: Jacoby, Hunter and Christian *Ap.J. Suppl.*, **56**, 257, 1984; Gunn and Stryker, *Ap.J. Suppl.*, **52**, 121, 1983; Pickles, *PASP*, **110**, 863, 1998; *STELIB: a Library of Stellar Spectra at* $R \sim 2000$ Le Borgne et al. *A&A*, **402**, 433L, 2003.

IUE UV spectra, all types of stars: Wu et al., *IUE Ultraviolet Spectral Atlas (IUE Newsletter No. 22; No. 43)*, NASA Goddard, 1983, 1991; Heck, IUE Low-Dispersion Spectra Flux Catalogue 1984, *A&AS*, **57**, 213; Fanelli, O'Connell, Burstein, and Wu 1991, *Ap.J. Suppl.*, **82**, 197, 1992.

Empirical and theoretical data relevant to stellar populations & galaxies: *A Data Base for Galaxy Evolution Modeling*, Leitherer et al., *PASP*, **108**, 996, 1017, 1996. CDROM published in the AAS-CDROM Series.

SYNPHOT Manual (HST software to convert spectrophotometry to filter photometry on various systems): `http://stsdas.stsci.edu/Files/SynphotManual.pdf`.

DIGITAL CATALOGS

Nearly all standard catalogs of data on cosmic sources are now available over the Internet or on CDROM. Here are some recommended starting points:

ASTR 511 Recommended Web Links: see 511 home page.

Local IDL Databases: available databases are listed by typing *dbhelp* during an IDL session. More databases in IDL format are available from GSFC.

Local CDROMs: see listing on departmental Computer Home Page, under "Hardware": Astronomical CDROM Library.

Astronomical Internet Resources: *http://www.stsci.edu/astroweb/astronomy.html*. See "Data Resources": Data and Archive Centers; Astronomical Information Systems.

Among the better listings:

CDS/SIMBAD: Sets of Identifications, Measurements, and Bibliography for Astronomical Data. Master depository of all types of data for over 800,000 individual stars and 200,000 nonstellar sources. Best place to start looking for data, references on individual stars. *http://cdsweb.u-strasbg.fr/CDS.html*

GCPD: General Catalogue of Photometric Data (Mermilliod et al.): Collection of stellar photometric data, 80 systems. `http://obswww.unige.ch/gcpd/gcpd.html`

NED: NASA/IPAC Extragalactic Database. Like SIMBAD, but for galaxies only. Best place to start looking for data, references on individual galaxies. `http://nedwww.ipac.caltech.edu/`

SKYVIEW: depository of images from a number of important sky surveys (full EM spectrum) with nice retrieval interface. Easiest source of digital finding charts and multiband overlays. `http://skyview.gsfc.nasa.gov/cgi-bin/titlepage.pl`

MAST: the Space Telescope Science Institute Multimission Archive at Space Telescope, including the HST master data archive and the Guide Star Catalog. `http://archive.stsci.edu/`

HEASARC: NASA/GSFC High Energy Astrophysics Science Archive Research Center. Complete set of high energy (extreme UV, X-ray, Gamma-ray) databases with useful links to other data sets. Nice retrieval interface. `http://heasarc.gsfc.nasa.gov/`
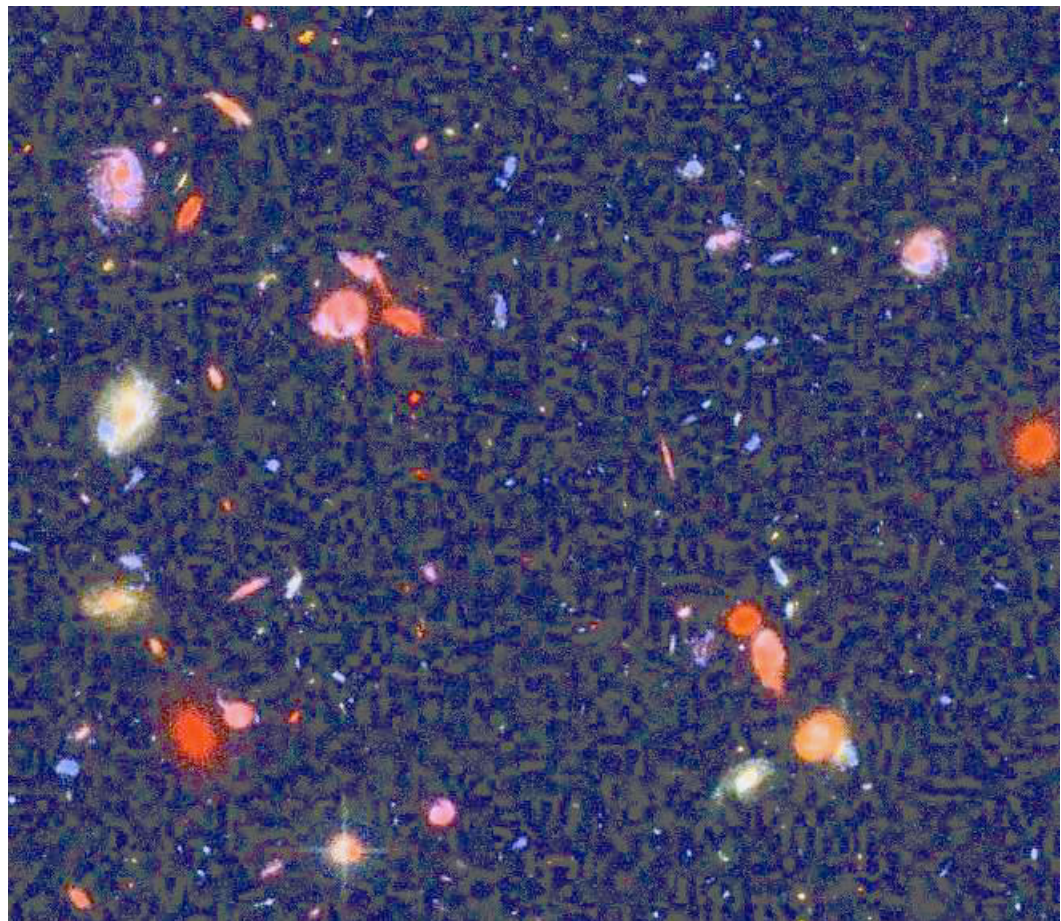
Astrophysics Data System (ADS): NASA-sponsored depository of about 190 catalogs as well as the indispensable database of Astrophysics Abstracts. `http://adswww.harvard.edu/`

Sloan Digital Sky Survey: digital catalogue of 100 million stars & galaxies in π steradians of the northern sky. Multiband photometry and spectroscopy. `http://www.sdss.org/`

2MASS: Two Micron All Sky Survey, JHK bands, containing fluxes for 473 million sources (including 1.6 million galaxies). `http://www.ipac.caltech.edu/2mass/`

Astronomical Data Center (ADC): NASA/GSFC depository of catalogs and other data. Formerly very handy, but shut down by NASA, apparently for budgetary reasons. Many web site still link to this defunct service.

MULTICOLOR ANALYSIS OF
STARS & GALAXIES

Hubble Ultra Deep Field (Luptonized)

MULTICOLOR ANALYSIS: INTRODUCTION

Probably the most influential application of multicolor analysis of stars has been in the form of <u>color-magnitude diagrams</u> (CMD's). Photoelectric photometry allows high precision CMD comparisons between theory and observation which in the last 50 years have provided a <u>nearly complete understanding of stellar evolution</u> from the main sequence through giant phases. But we can't discuss that vast(!) undertaking here. See ASTR 551 (Majewski) and ASTR 543 (Li) for examples. Instead, we focus here on what can be learned from color-color diagrams and other forms of multicolor analysis, which have many applications beyond stellar evolution.

I. THE UBV TWO-COLOR DIAGRAM: Stellar Temperatures, Gravities, Abundances

The Johnson & Morgan UBV system was defined (see filter specifications in Lec. 14) such that:

   (U-B) measures the "Balmer Jump" (hot stars) or the "4000 Å break" (cooler stars) between 3600 Å and 4400 Å.

   (B-V) measures the slope of the "Paschen continuum" between 4400 Å and 5500 Å; sensitive to stellar <u>temperature</u>

   The U band is sensitive to stellar <u>surface gravity</u> (g) and <u>metal abundance</u> (Z) as well as temperature.

   The UBV system demonstrates that simple observations can be powerful astrophysical discriminants

The standard "two-color diagram" plots (B-V) vs. (U-B)

   Sense of plot is such that hottest objects (bluer) are in upper left of diagram, coolest in lower right (redder)

   Stars are confined to a relatively small domain of 2-color space. (Why?)

   Temperature is the dominant parameter, but g and Z are also important

   Most conspicuous feature: "dwarf" (Class V) line: a locus of varying temperature/spectral type.

UBV TWO-COLOR DIAGRAM (continued)

The S-curve is introduced by the Balmer Jump (i.e. continuum absorption for $\lambda < 3650$ Å by neutral hydrogen in $n = 2$ level), which reaches a maximum near $T = 10000$ K (early A stars).

Surface gravity affects the ionization of absorbers in an atmosphere through gas pressure. For a given T, lower gravity implies lower gas pressure and therefore higher ionization. For instance, near $T = 10000$ K, there will be more neutral hydrogen in the atmosphere of a dwarf (high gravity) than a supergiant.
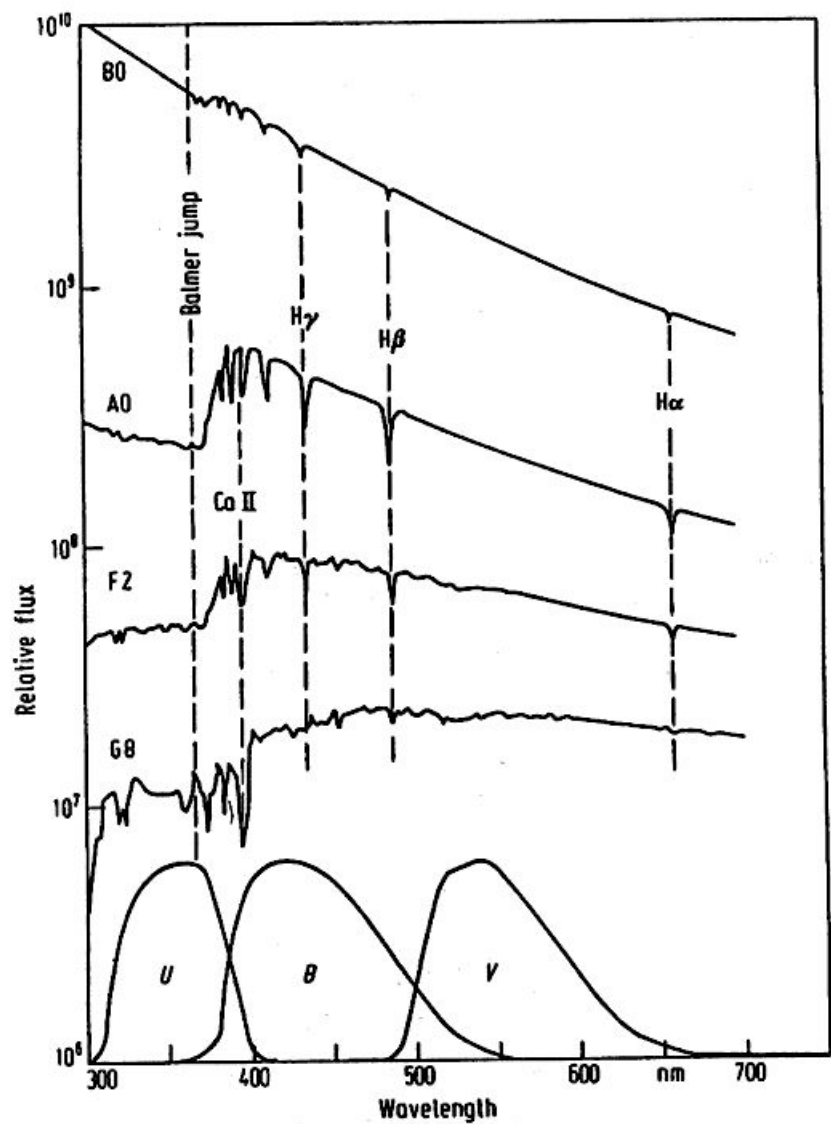
For FG stars, (U-B) is very sensitive to "line blanketing" by metals and therefore to Z. Lower Z stars have a "UV excess" (more short wavelength light for a given long wavelength spectral slope).

The ability of the UBV diagram to separate out stars by temperature and abundance has made it a major tool in study of stellar populations in our own & other galaxies.
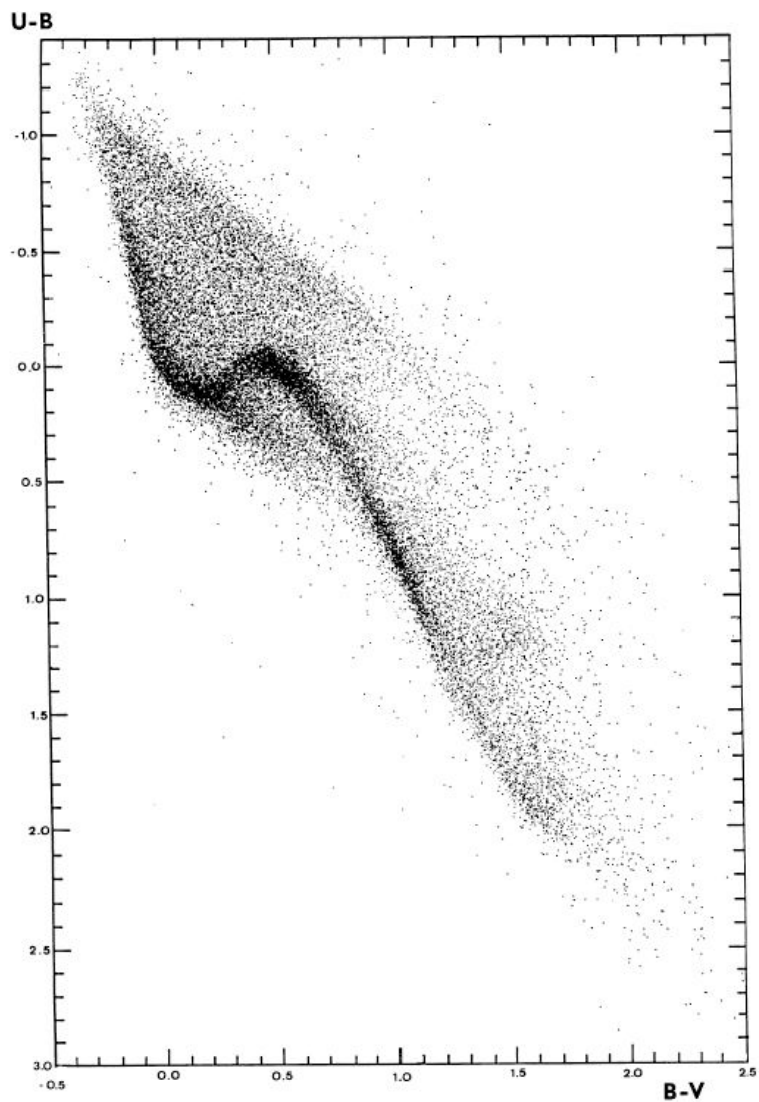
The UBV diagram also allows identification of special types of sources (e.g. QSO's, brown dwarfs, white dwarfs) by colors alone.

Fiducial (U-B), (B-V) values:

Object	(U-B)	(B-V)
Hottest Stars	-1.1	-0.32
A0 V	0.0	0.0
Sun (G2 V)	0.17	0.68
M5	1.20	1.60
Carbon Star	8.0	5.0

Location of the UBV Filters (Johnson & Morgan 1953)

Composite 2-Color Diagram (Nicolet 1980)
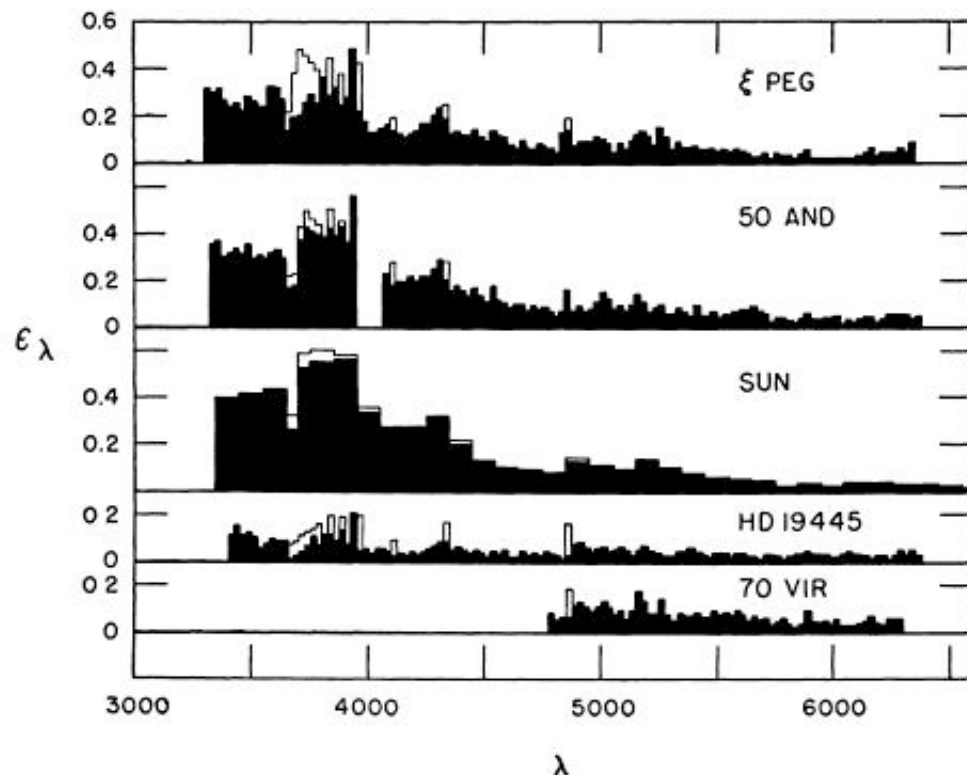
FIG. 1.—The fractional blocking coefficients, $\epsilon(\lambda)$, for the program stars. The data for the sun are from Michard (1950). The non-filled areas of the histograms represent absorption by the hydrogen lines.

Line Blanketing in Stars (Wildey et al. 1962)

The plot shows the amount of energy removed by absorption features as a function of wavelength.
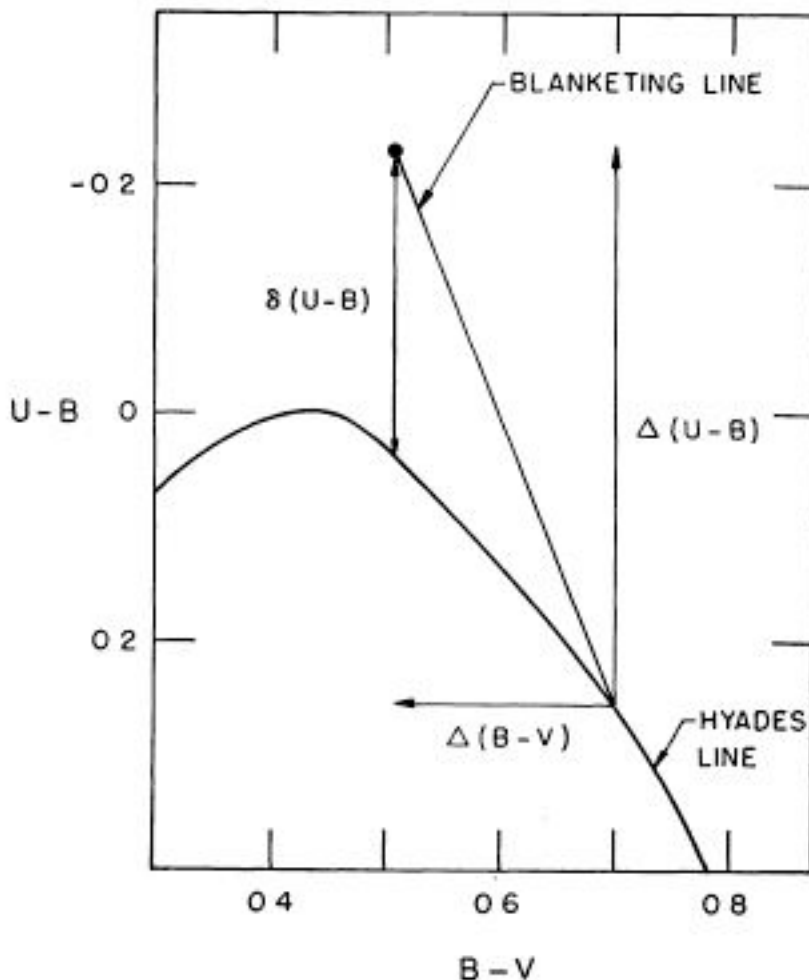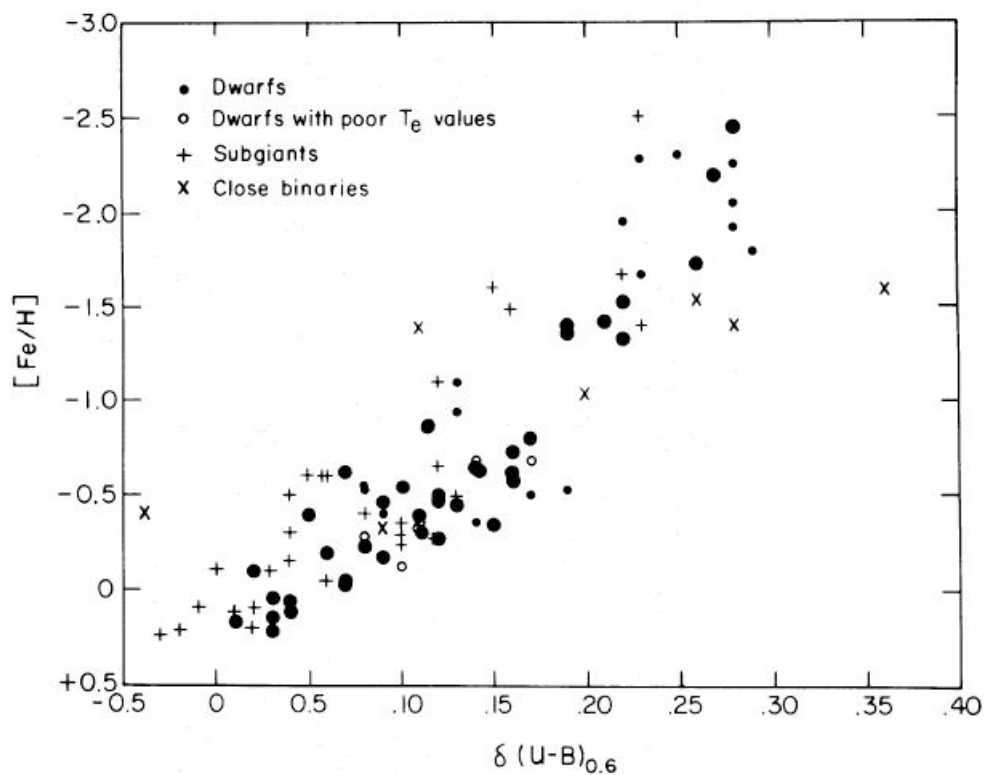
FIG. 5.—The definitions of $\Delta(B - V)$, $\Delta(U - B)$, and the ultraviolet excess, $\delta(U - B)$

Definition of the "UV Excess" for Cool Subdwarfs

The diagonal line shows how a star of a given T_e, g will move if its metal abundance is reduced from solar (on the "Hyades line") to Pop II values (about 1/100 solar). The resulting (U-B) color excess allows such objects to be easily identified in large field samples. But stars with abundances significantly lower than 1/100 solar are not distinguishable in broad band measures because metallic line absorption is so small. Search techniques for these are based instead on narrow band photometry of the Ca II "K" band, for instance.

UV Excess vs. Metallicity (Carney 1979)

II. COLORS OF COMPOSITE STELLAR POPULATIONS

The composite, integrated light of unresolved stellar systems, such as galaxies and distant star clusters, is usually analyzed with the help of "spectral synthesis" models, which combine the light of individual stellar types in the appropriate mixtures.

The composite spectral energy distribution (SED) is given by

$$F(\lambda) = \sum n_j s_j(\lambda)$$

where s_j is the SED for stars of type j and n_j is the number of such stars in the population. The luminosity zero point is often unimportant, so it is usually best to normalize the SED's to a standard wavelength such as the V band. In flux-ratio form, this expression becomes:

$$G(\lambda) = \sum p_j f_j(\lambda)$$

where p_j is the fractional contribution of type j to the total light at V, $G = F(\lambda)/F(V)$, $f = s_j(\lambda)/s_j(V)$, and $\sum p_j = 1.0$.

Such computations are usually done for high to moderate spectral resolution ($\sim$ 1-30 Å), based on "libraries" of observed spectra for nearby stars or of theoretical synthetic spectra from model atmospheres.

Broad-band colors can be obtained for composites either by integrating the filter responses over a high spectral resolution sythetic model or by directly combining the flux ratios corresponding to the colors of the component stars (e.g. $f(B) = 10.0^{-0.4(B-V)}$).

One property of such composites in the standard 2-color UBV diagram is that they will always lie above and to the right of the locus for individual stars.

There are many grids of synthetic spectra for composite populations available on the web, with varying degrees of sophistication and fidelity. A series of SED's for a single-burst population with a 1 Gyr duration viewed at different ages is shown in a later figure. The SED for any possible star formation history can be synthesized by a combination from a sufficiently fine-grained grid of single-generation models.

COMPOSITE POPS (continued)

The goal of spectral synthesis analysis is to extract information on the chemical abundance structure and star formation history (SFH) of distant stellar populations. Abundances and SFH must be simultaneously determined, since they are strongly linked. Wavelength "leverage" is very important in this process. A long wavelength baseline allows you to "dissect" the population, since stars of different types dominate different wavelengths.

A subsequent plot illustrates "dissection" for an old (> 5 Gyr) population.

> In the V-band ($\sim$ 5500 Å) the red giant branch and main sequence turnoff make comparable contributions. Derived population parameters (age, abundances) depend on good modeling of evolutionary rates and surface gravity effects.

> In the mid-UV ($\sim$ 2200-3200 Å), the turnoff stars dominate. This is the most sensitive region to age.

> In the near-IR (> 8000 Å), the red giant branch and aysymptotic giant branch stars (K and M types) dominate (not shown). In general, these are more sensitive to abundance than age.

> Except in hotter populations, there are almost no "pure" absorption features, and feature blending must be properly modeled. Blending is, in general, less serious at longer wavelengths.

> In the far-UV (< 2000 Å), the minority populations of low mass stars on the hot and "extreme" horizontal branch dominate in old populations. These are sensitive to age and metal abundance and also to helium abundance.

> Note that lower main sequence ($\lesssim 0.7 M_\odot$) stars are <u>never</u> very important at any wavelength. Yet the LMS usually contains most of the <u>mass</u> of the population. Determining the mass of a population from its SED therefore requires extrapolation of the stellar mass function and is highly model-dependent. The ratio of mass-to-light (M/L) is least subject to evolutionary effects in the K-band (2.2μ).

In younger populations ($<$ 1 Gyr):

> **Massive main sequence stars become more important at all wavelengths. The Balmer lines and Jump are among the best age indicators.**
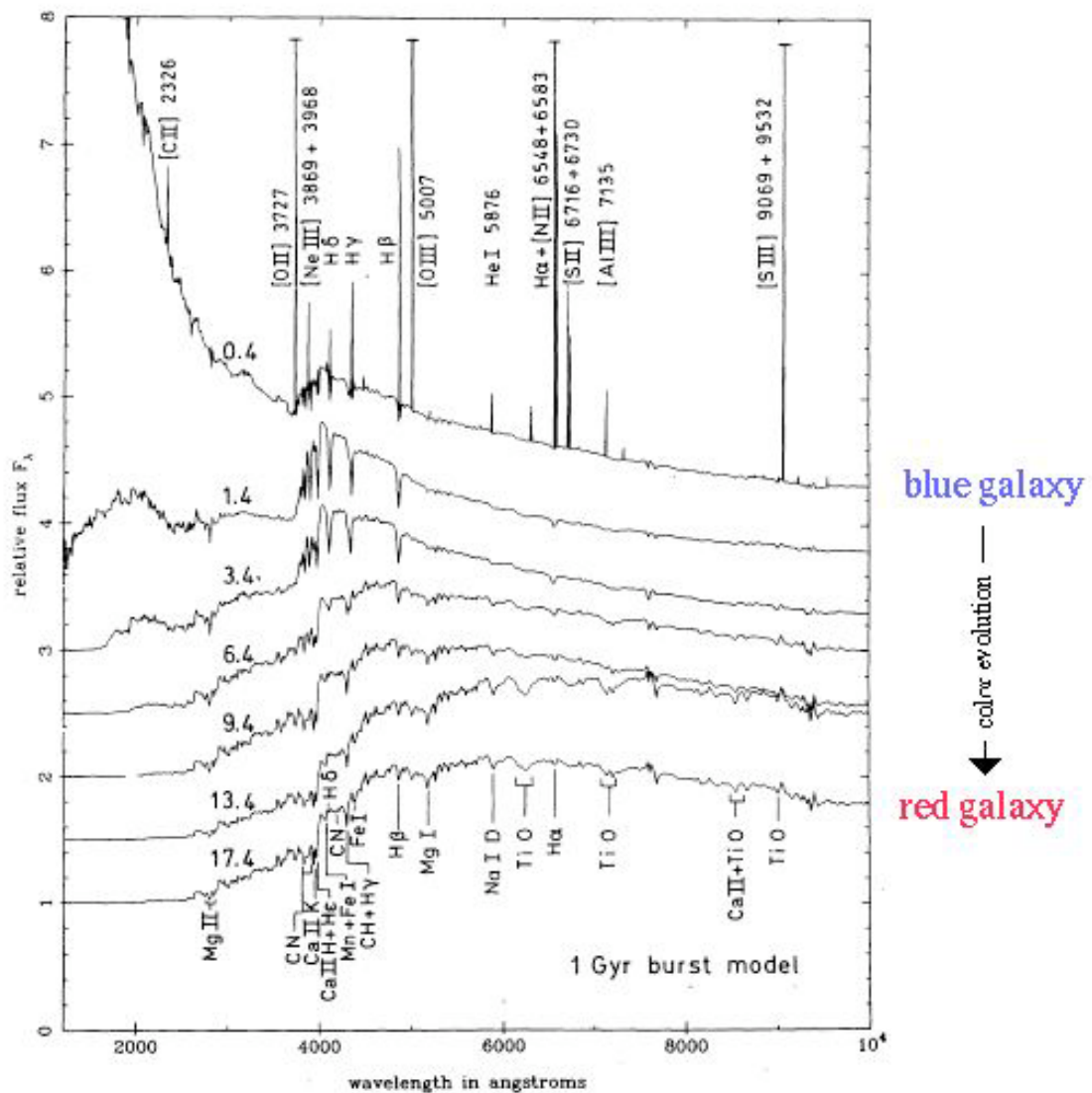
> **M supergiants are very important in the near-IR for a small range of ages $\sim$10-25 Myr. They are a strong marker for this age range.**

> **In very young populations ($\lesssim$ 8 Myr), containing stars $\gtrsim$ 5 M$_\odot$ capable of strong ionization, emission lines become important. These can be used to estimate the total far-UY ionizing luminosity and hence the star formation rate.**
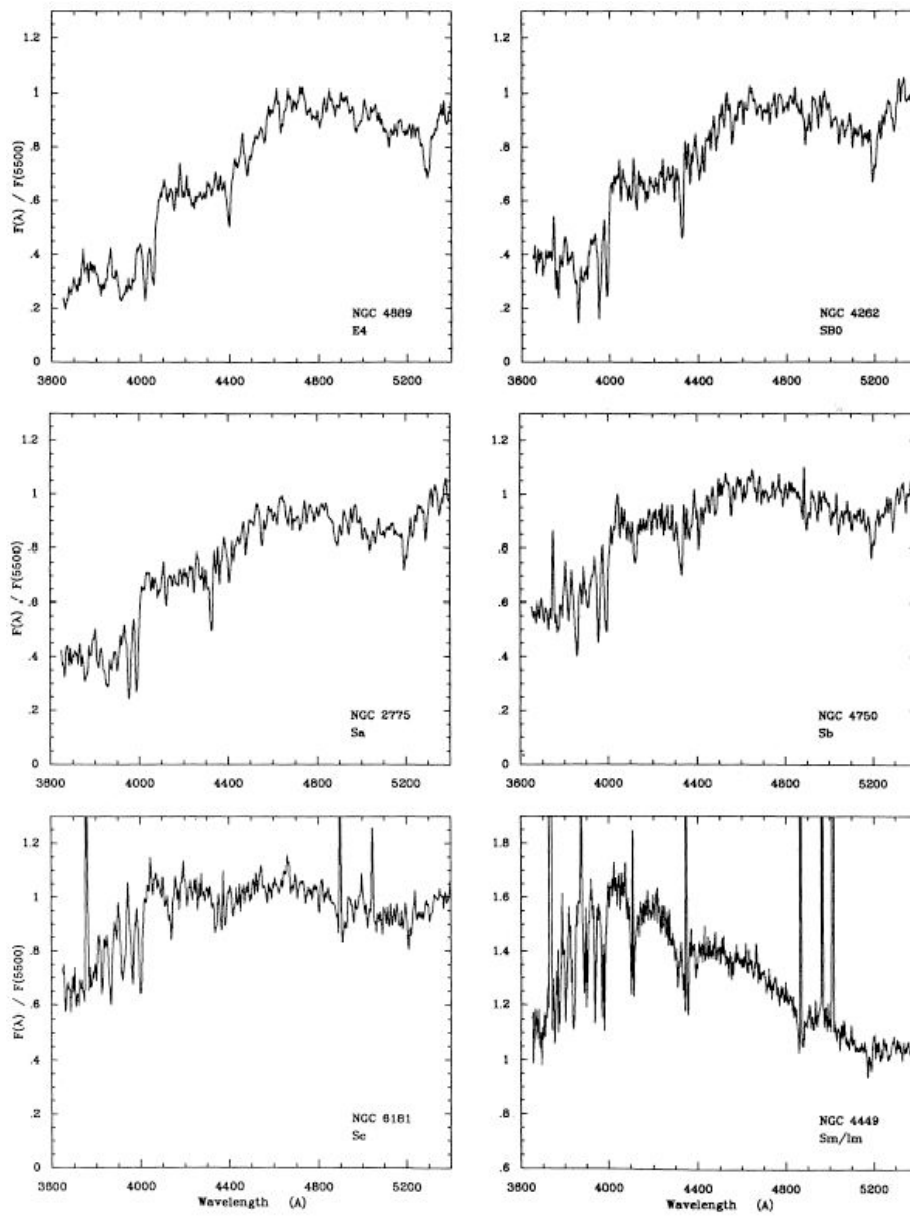
> **Younger populations are, unfortunately, often involved in dust, so correction for extinction effects (as well as emission line contamination) is important to determining stellar properties.**

> **SED changes for a single generation are roughly proportional to the <u>logarithm</u> of age. It is most appropriate to think of analyzing the SFH of a population in terms of bins which are equally spaced in log(t).**
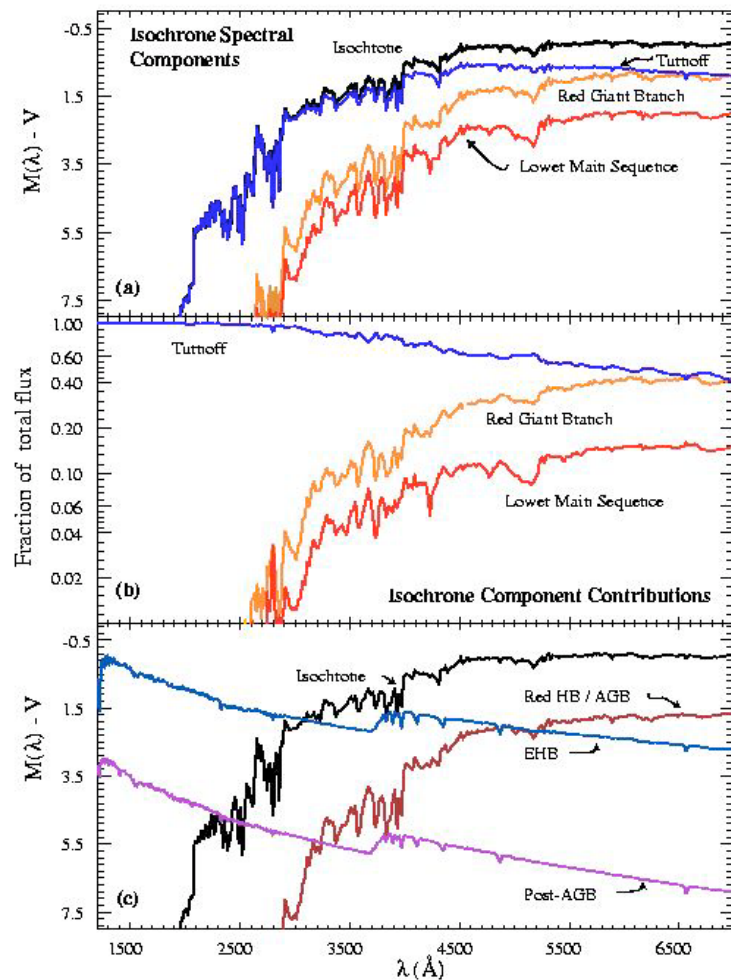
The subsequent pages show applications of synthesis models to the problem of both young, star-forming galaxies and old, quiescent galaxies.
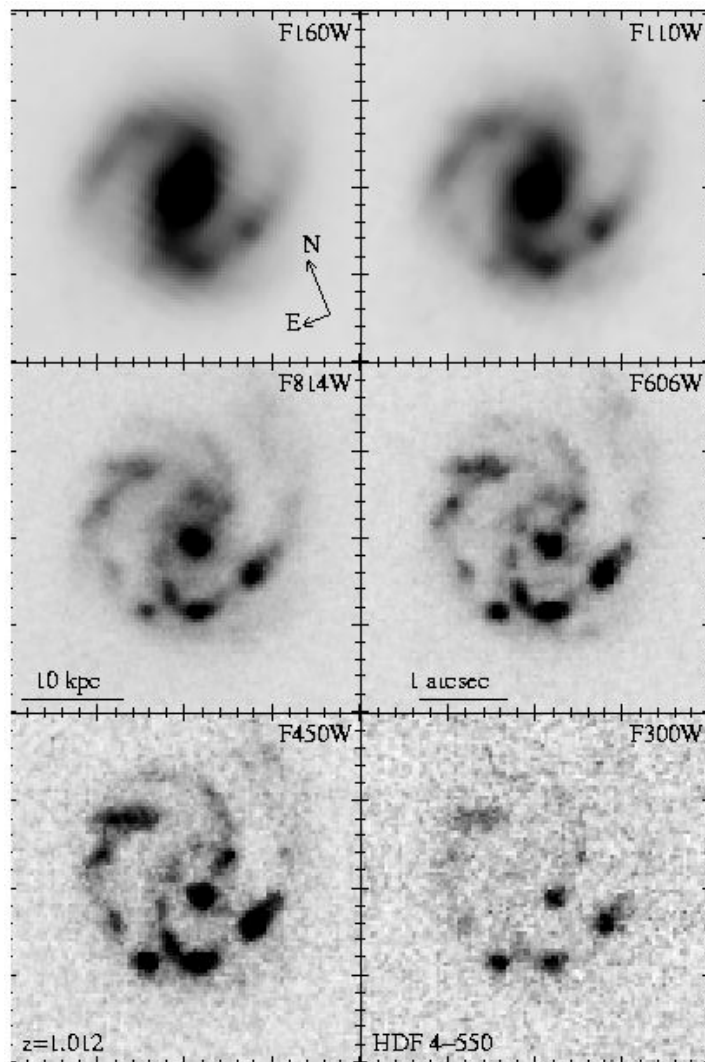
Synthetic spectra predicted for a burst population (1 Gyr duration) viewed at different ages (listed in Gyr at the left hand side).

Integrated spectra of selected bright galaxies (Kennicutt 92)

**Wavelength "Dissection" of Population Components
in the Integrated Light of Old Population**

**Multiband Population Dissection in Image
of Redshift ∼1 Galaxy (Bunker 1999)**

**HST images from the Hubble Deep Field. Lab-frame filter wavelengths
listed: in four lower panels in nm units; in two upper panels, in 10 nm units.
Rest-frame wavelengths are half the lab-frame values.**

**Dramatic morphological changes occur from the rest-frame near-IR (top) to
the UV (bottom).**
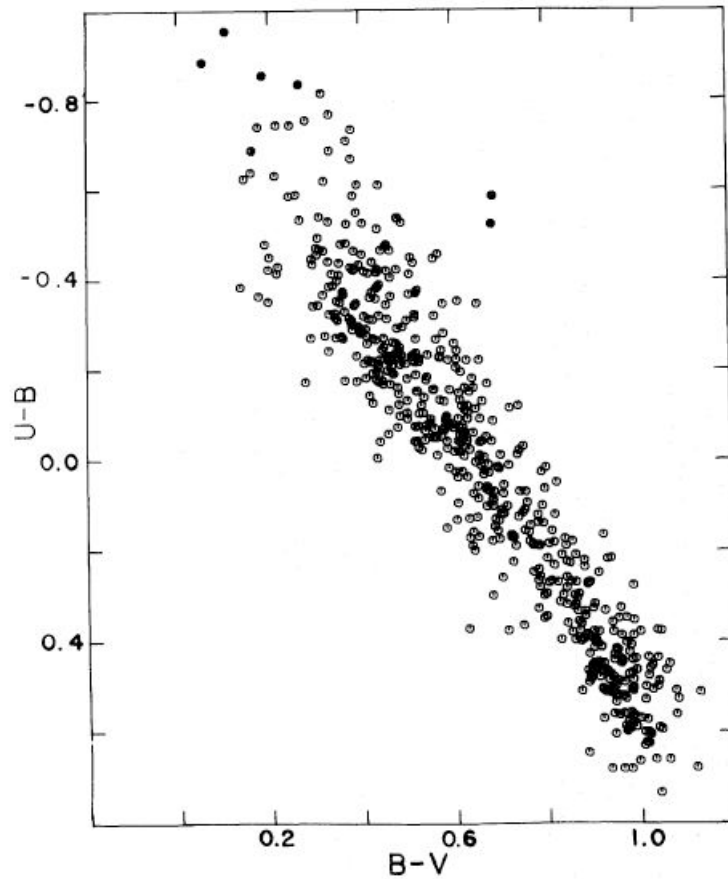
FIG. 1.—The two-color distribution of galaxies. The data include measurements of field galaxies from de Vaucouleurs (1961) and de Vaucouleurs and de Vaucouleurs (1972), Markarian galaxies from Huchra (1977*a*), Zwicky galaxies from Sargent (1970), and Haro galaxies from Du Puy (1968, 1970). The filled circles near the top of the diagram represent observations of parts of galaxies—H II regions—by Huchra (1977*a*, *b*) and Sandage and Tammann (1974*b*).

Observed colors of blue galaxies, dominated by younger populations, in the two-color diagram (Huchra 1977)
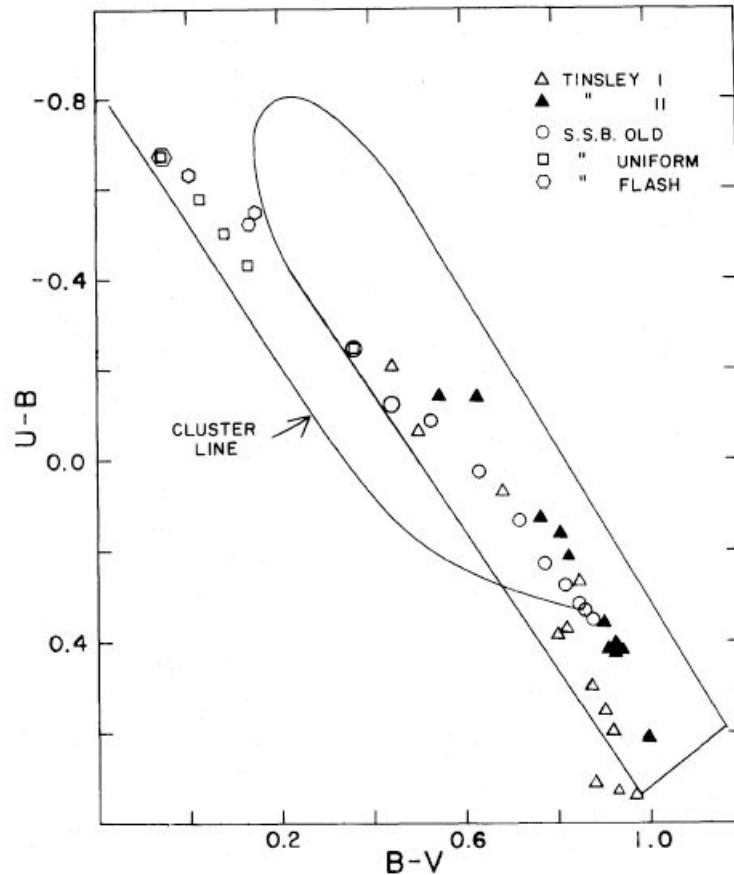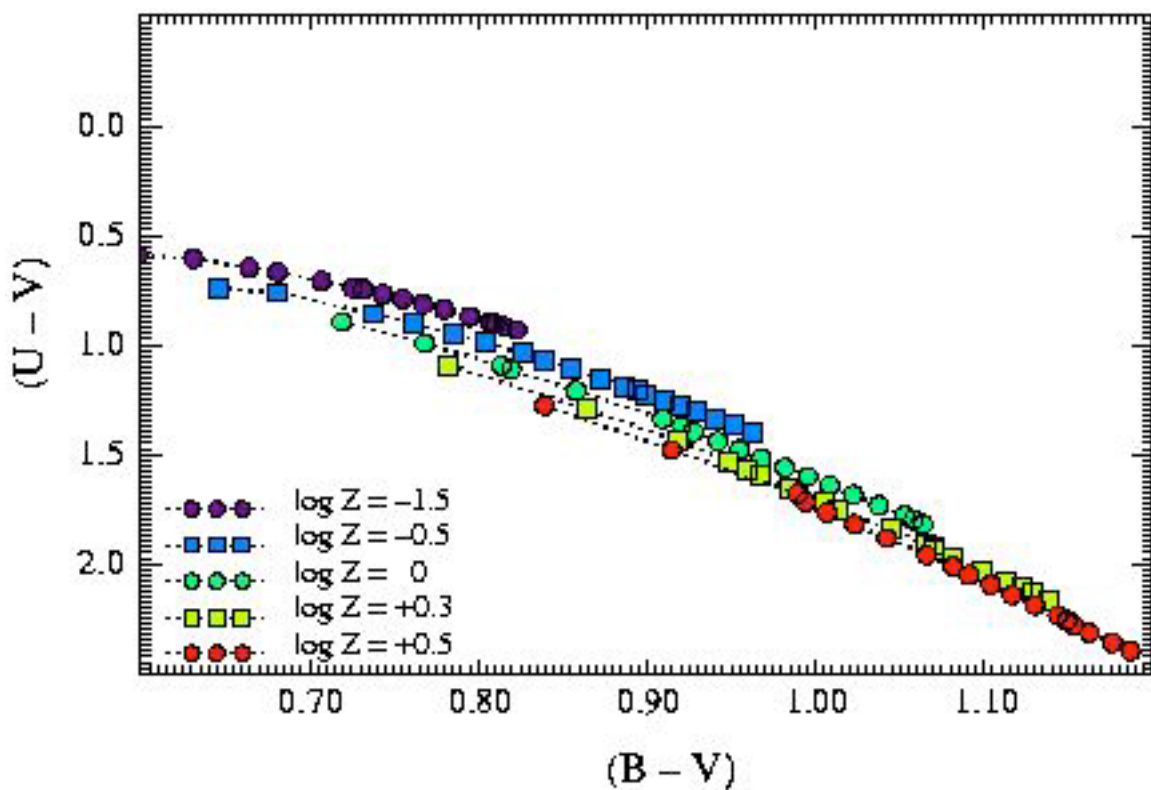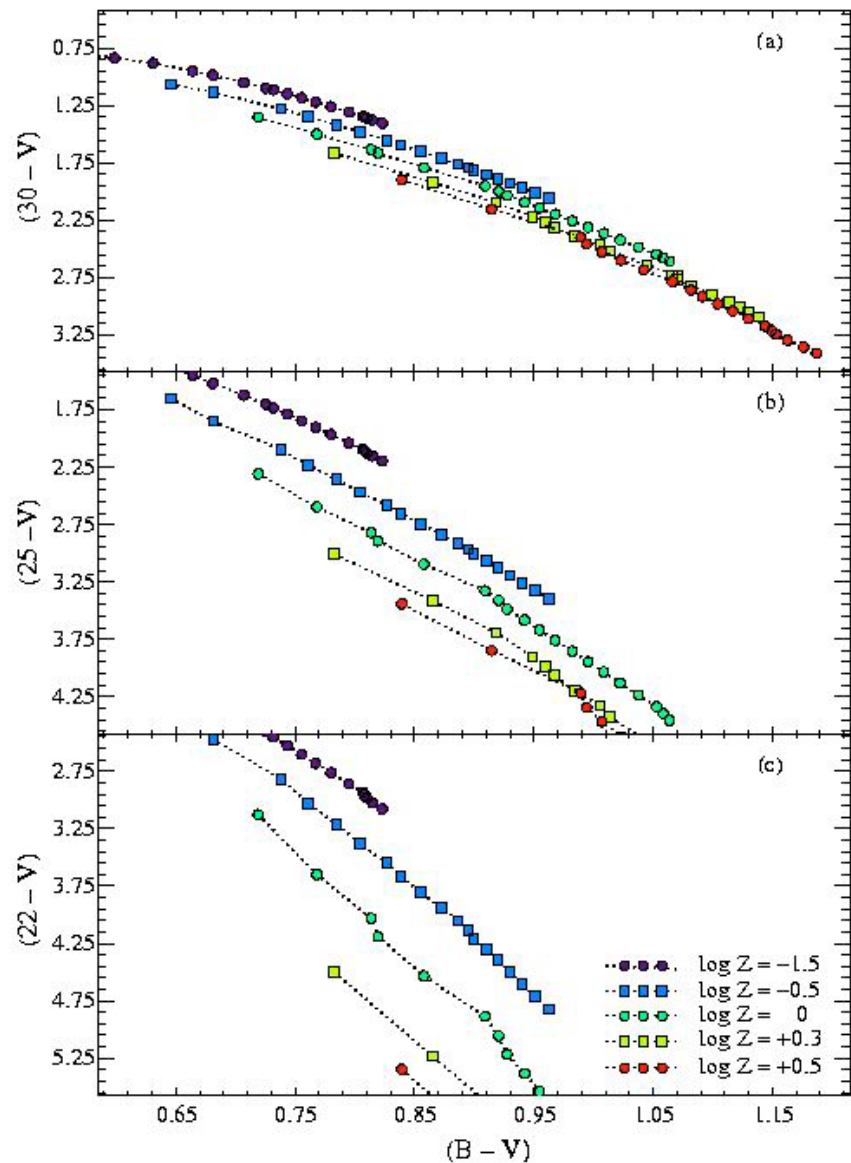
FIG. 2.—Colors for existing models of galaxies superposed on the observed envelope of galaxy colors from Fig. 1. The open and filled triangles are for models from Tinsley (1968, 1972); open circles, squares, and hexagons are from old, uniform, and "flashing" galaxy models by Searle *et al.* (1973). Also shown is the evolutionary track for star clusters with an initial delta function star-formation rate (Searle *et al.* 1973).

Synthetic models for young pops in the two-color diagram (Huchra 1977).
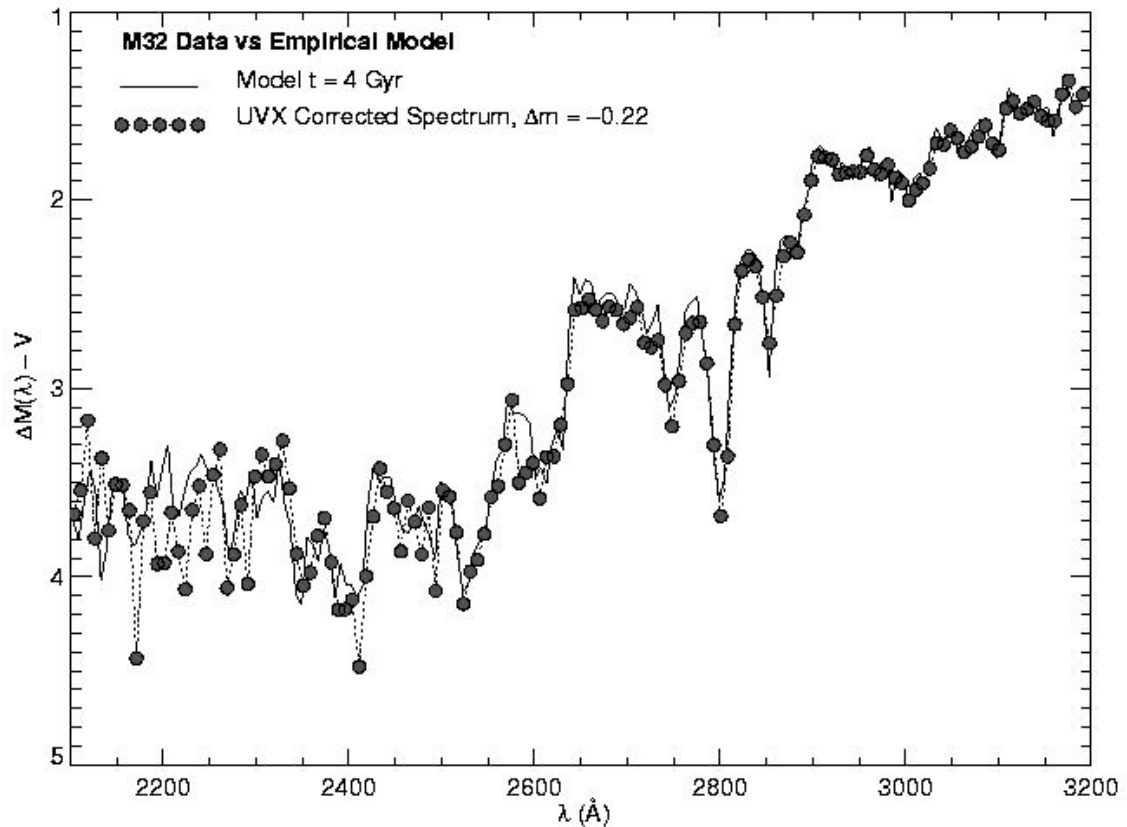
The outline shows the empirical color envelope from the preceding plot. The models do not overlap the blue tip of the envelope. Only models involving strong, short-lived <u>bursts</u> of star formation in old populations fit there. This was among the first evidence that the star formation history of galaxies can be strongly discontinuous.

Old population colors in standard UBV (DOR 03), showing a small degree of age/abundance separation

Old population colors in the Mid-UV (DOR 03), showing much better age/abundance separation

Fit of 4 Gyr old, solar abundance synthetic model to the mid-UV spectrum of elliptical galaxy M32 (DOR 03).

This is evidence (now widespread) for "intermediate-age" star formation in early type galaxies, possibly induced by mergers or tidal captures involving gas-rich neighbors.

III. INTERSTELLAR EXTINCTION

Interstellar extinction is caused by dust grains. Typical grain properties were described in Lecture 4. Grain opacities are generally higher at shorter wavelengths, so the net effect of extinction is to "redden" spectral energy distributions by removing excess blue light.

The optical depth of grains in a given direction can be written
$\tau(\lambda) = n_g\, L\, \kappa(\lambda)$

...where n_g is the number density of grains per unit volume in the ISM, κ is the effective radiative cross-section per grain (cgs units cm^2), and L is the pathlength

According to the equation of transfer for a "foreground screen" of dust in front of a source with intrinsic intensity I_o (and assuming no significant thermal radiation or scattering from grains at the wavelengths involved), the emergent specific intensity is decreased as follows: $I = I_o\, e^{-\tau(\lambda)}$, or converting to magnitudes:

$$m(\lambda) = m_o(\lambda) + 1.086\, n_g\, L\, \kappa(\lambda)$$

Typical extinction in the V-band is about 1 mag per 2×10^{21} gas atoms cm^{-2} in our Galaxy.

The wavelength dependence of the grain opacity is called the "extinction law" or "reddening curve"

Detailed dependence of the law has been determined by photoelectric filter photometry or spectrophotometry of pairs of stars with same spectral types but different colors [e.g. Whitford 1958].

It is traditional to normalize the extinction law to its difference between the B and V band wavelengths, as follows. (Notation here is non-standard.)

$$\zeta(\lambda) \equiv \frac{\kappa(\lambda)}{\kappa(B) - \kappa(V)}$$

and then rewrite the magnitude increase from extinction as:

$$A(\lambda) \equiv m(\lambda) - m_o(\lambda) = E(B - V)\, \zeta(\lambda)$$

where $E(B - V)$ is known as the "(B-V) color excess" and characterizes the amount of extinction toward a given source.

EXTINCTION (continued)

ζ will be the <u>same</u> for all sources as long as the character of the dust grains is the same.

$\zeta(V)$ is also known as "R", the "ratio of total to selective extinction."

For the kind of dust prevalent in the diffuse interstellar medium of our Galaxy, $R \sim 3.1$ and

$$\zeta(\lambda) \sim -0.98 + \frac{2.24}{\lambda_\mu}$$

where λ_μ is the wavelength in microns. This relation is a fair approximation for the range 4000–10250 Å. Outside of this region, the extinction law shows significant curvature.

The dust extinction law has been found to <u>vary</u> from place to place in our Galaxy and to differ between galaxies. It is especially subject to variations at ultraviolet wavelengths and in young star-forming regions.

For a complete description of ζ see Savage & Mathis (ARAA, 17, 73, 1979) and Cardelli, Clayton & Mathis (ApJ, 345, 245, 1989). The latter paper gives careful fitting formulae which can be used to estimate the extinction law for any R. The IDL Astronomy Users Library program `ccm_unred` is the easiest way to access the CCM formulae.

Reddening effect on sources in the UBV two-color diagram:

Reddening effects on broad bands are usually estimated as though all the light is emitted at the mean wavelength of the bands.

The <u>slope</u> of the reddening trajectory in UBV is

$$\frac{\Delta\,(U - B)}{\Delta\,(B - V)} = 0.72$$

Since OB stars often suffer significant extinction, this creates a diffuse envelope of sources running downward from the intrinsic hot star locus. Reddening trajectories are <u>straight lines</u> in this diagram.

As long as the reddening and temperature vectors are at a significant <u>angle</u> to one another, one can obtain a unique solution for a hot star's color by backtracking along the reddening vector. Note that the method gives ambiguous results for redder objects.

EXTINCTION (continued)

Other geometries:

Since 1980 it has become apparent that the preceding simple description of extinction by a foreground screen does not adequately capture the behavior of complex sources, such as star-forming regions observed in external galaxies. This is often encountered in UV observations, since the grain opacity is highest there.

Different dust/star geometries and photon scattering must be considered, and these can produce very different effects than the foreground screen case.
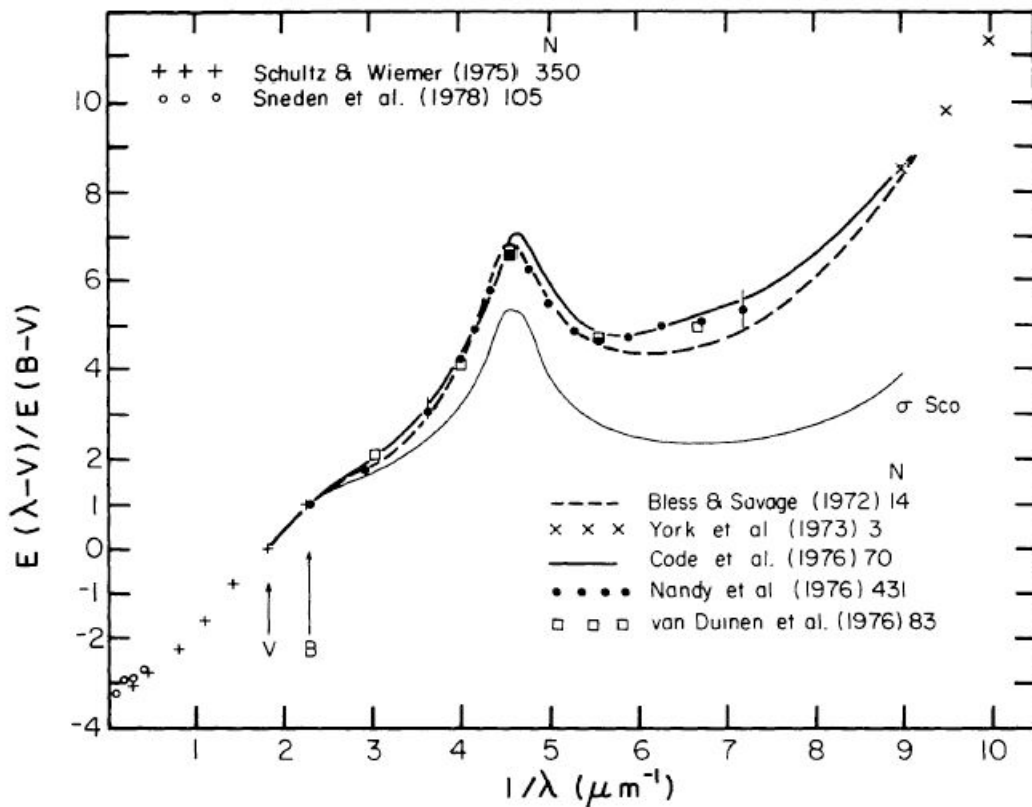
For example, if the dust and stars are <u>uniformly mixed</u> together (e.g. in a compact, young star cluster), then referring to Lecture 4 we find that:

$$I(\lambda) = I_o(\lambda) \frac{1 - e^{-\tau(\lambda)}}{\tau(\lambda)}$$

Here, I_o is the intensity from the source that would be observed in the absence of internal dust and τ is the total optical depth in dust.

In this situation we see light from approximately one optical depth into the source, and the visible volume will increase with wavelength because the opacity decreases with wavelength.

The reddening trajectory for this geometry is very different than for the foreground screen. For a discussion of such effects and their influence on observations, see the Calzetti (2001) review and Witt, Thronson, & Capuano (1992).

Mean Extinction Law (Savage & Mathis 1979)

Note the large range in extinction over the IR-to-UV bands. The UV "2175 Å bump" is characteristic of extinction laws in our Galaxy and the LMC. But it is absent along some sightlines and in the SMC and is frequently absent in other galaxies. It probably originates in small, carbonaceous grains which are sensitive to the surrounding environment.

Table 2 An average interstellar extinction curve

	$\lambda(\mu m)$	$\lambda^{-1}(\mu m^{-1})$	$E(\lambda-V)/E(B-V)$	$A_\lambda/E(B-V)$
	∞	0	-3.10	0.00
L	3.4	0.29	-2.94	0.16
K	2.2	0.45	-2.72	0.38
J	1.25	0.80	-2.23	0.87
I	0.90	1.11	-1.60	1.50
R	0.70	1.43	-0.78	2.32
V	0.55	1.82	0	3.10
B	0.44	2.27	1.00	4.10
	0.40	2.50	1.30	4.40
	0.344	2.91	1.80	4.90
	0.274	3.65	3.10	6.20
	0.250	4.00	4.19	7.29
	0.240	4.17	4.90	8.00
	0.230	4.35	5.77	8.87
	0.219	4.57	6.57	9.67
	0.210	4.76	6.23	9.33
	0.200	5.00	5.52	8.62
	0.190	5.26	4.90	8.00
	0.180	5.56	4.65	7.75
	0.170	5.88	4.77	7.87
	0.160	6.25	5.02	8.12
	0.149	6.71	5.05	8.15
	0.139	7.18	5.39	8.49
	0.125	8.00	6.55	9.65
	0.118	8.50	7.45	10.55
	0.111	9.00	8.45	11.55
	0.105	9.50	9.80	12.90
	0.100	10.00	11.30	14.40

Tabulated Mean Extinction Law (Savage & Mathis 1979)
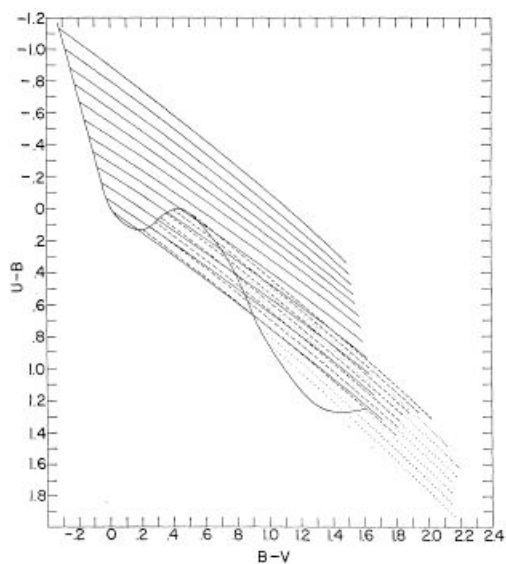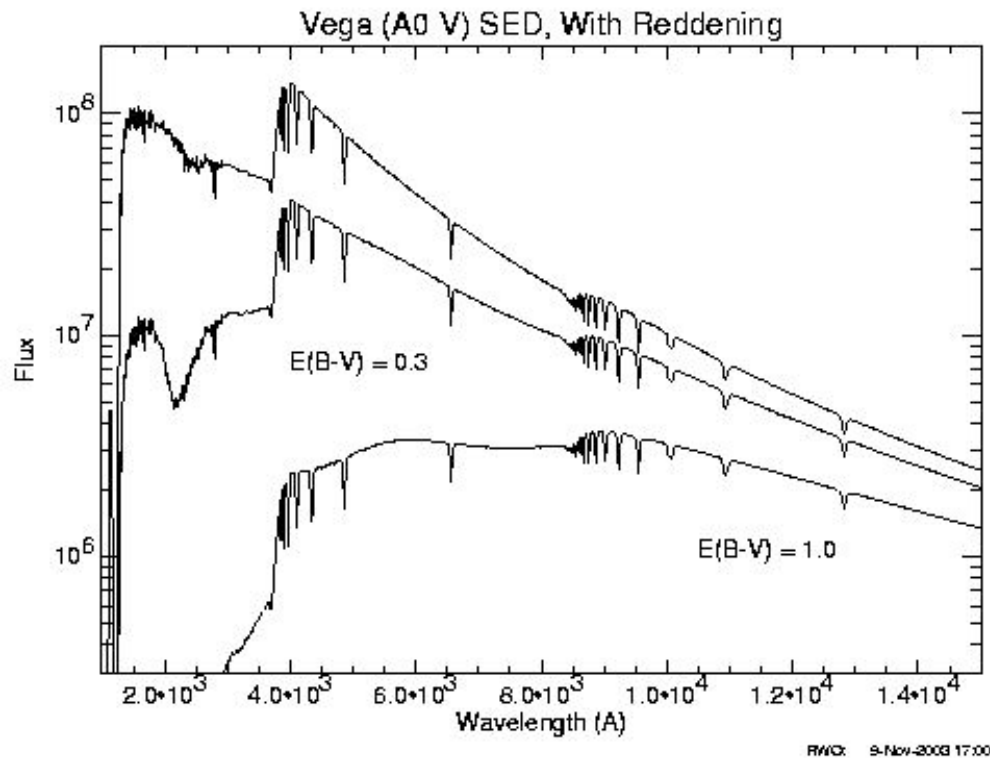
FIG. 4. Reddening trajectories in the color–color diagram terminated on the intrinsic relationship for luminosity class V stars.

Reddening Trajectories in Two-Color Diagram (Wildey 1963)

Vega (A0 V) SED, With Reddening

Reddening Effects on SED of Vega

Extinction sufficient to produce a (B-V) color excess of 1.0 mag has a drastic distorting effect on the SED of sources at wavelengths below 1 micron.

For cases of large optical depths and broad bands, especially where the intrinsic SED in not smooth, the effect of extinction changes appreciably <u>within</u> the band. Here, it is important to actually integrate the extincted SED in order to estimate net reddening effects.

IV. REDDENING-INDEPENDENT INDICES

Because the <u>shape</u> of the extinction law (outside the UV region) does not change much in the diffuse interstellar medium, it is possible to define <u>reddening-independent</u> color combinations for the foreground screen case. These "Q" indices will be the same for an unreddened source as for a heavily extincted one. You need to measure magnitudes in at least three bands to define Q indices.
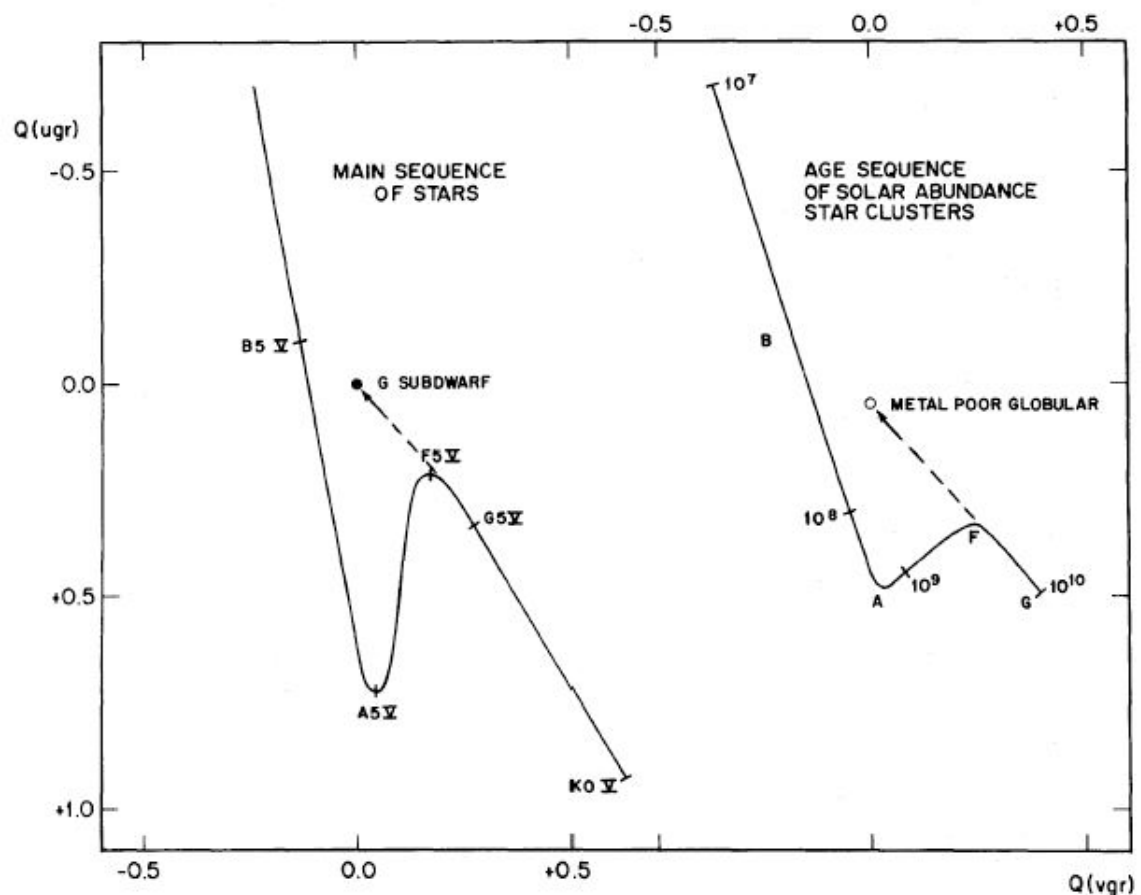
A typical Q index is defined as follows:

$$Q \equiv (m_1 - m_2) - q_{123}\,(m_2 - m_3)$$

where $q_{123} = \left[\dfrac{\zeta_1 - \zeta_2}{\zeta_2 - \zeta_3}\right]$

You can verify that this index does not change with the total extinction to the source.

Q parameters are useful, for example, in studying star clusters in other galaxies which may suffer large amounts of extinction.

Searle-Wilkinson-Bagnuolo (1980) QQ Population Diagram
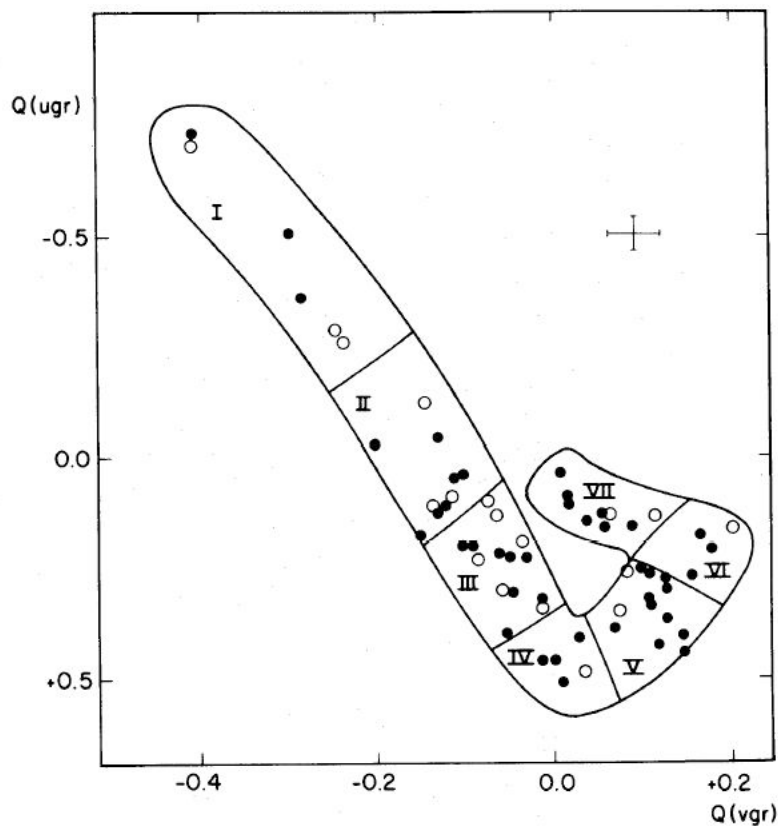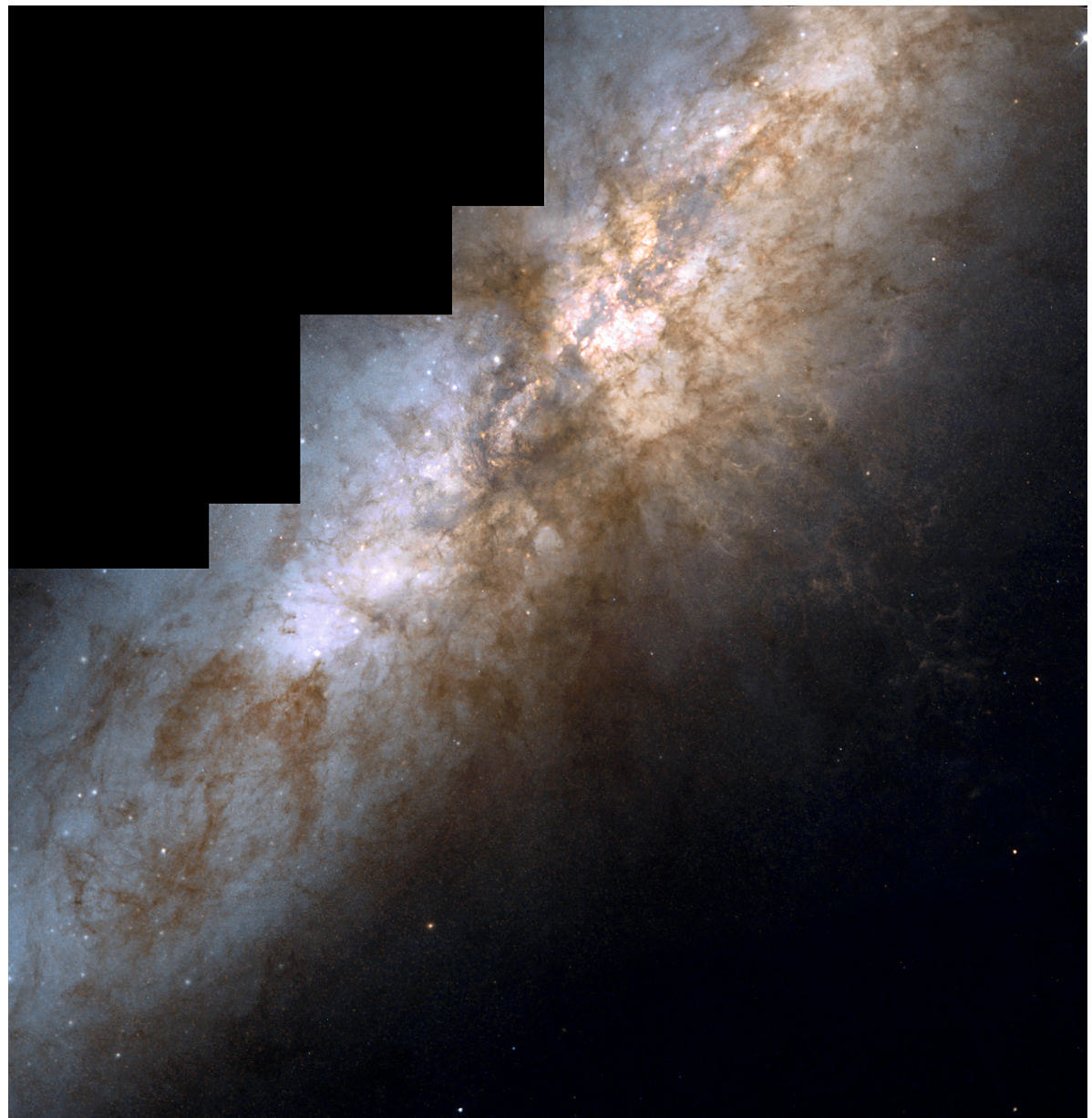
FIG. 3.—Populous clusters of the Magellanic Clouds in the *Q-Q* plane. Open and closed circles represent clusters of the SMC and LMC, respectively. The Cloud clusters form a sequence in this diagram. The sequence has been arbitrarily segmented, and the zones drawn in this figure define a classification scheme.
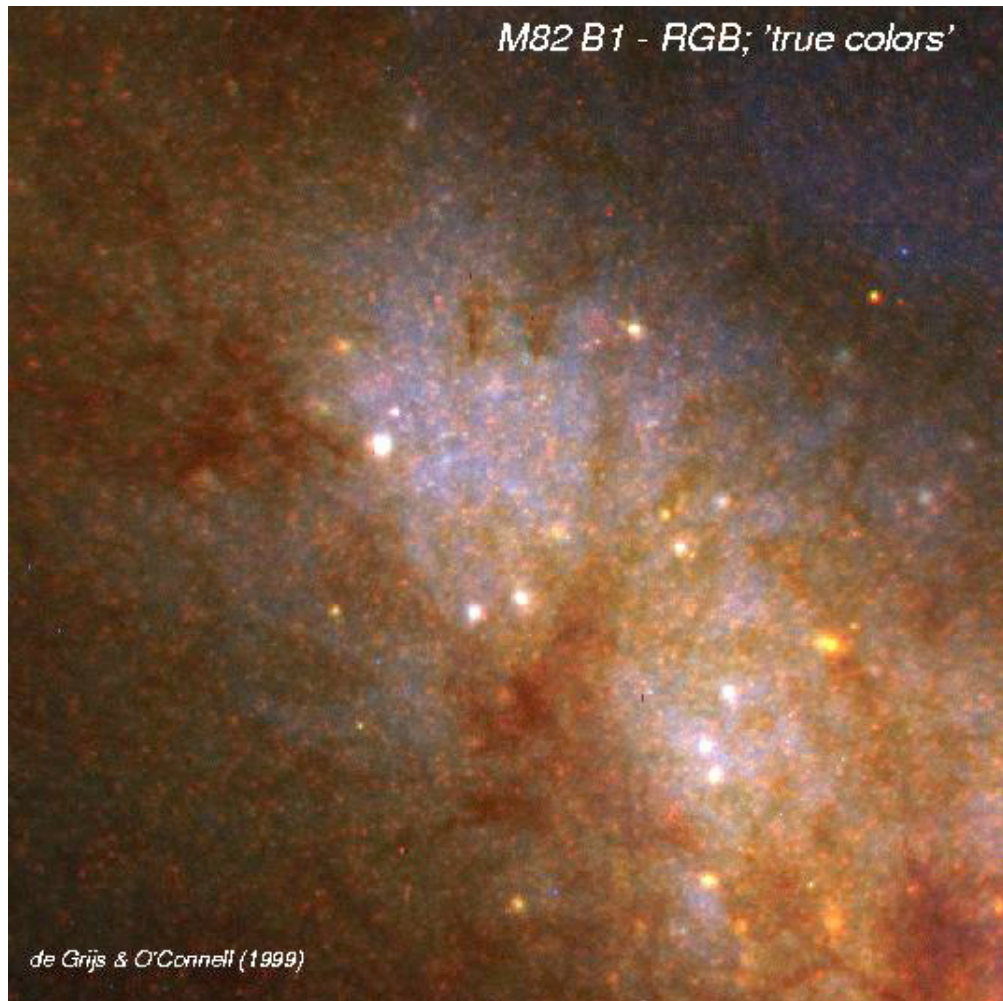
Magellanic Cloud Intrinsic Cluster Population Categories (SWB 80)

V. EXAMPLE: SUPER STAR CLUSTER AGES/EXTINCTIONS
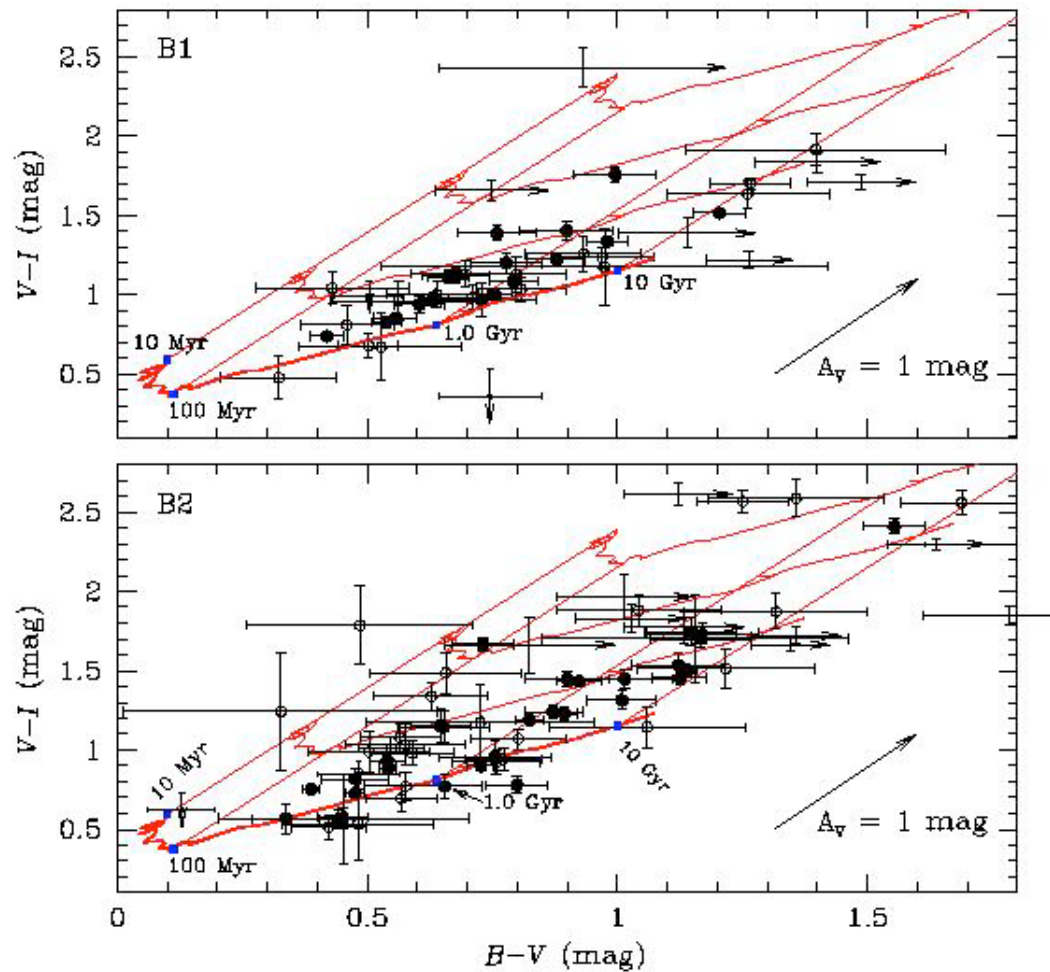
Color Composite Image of M82

Shows resolution of the starburst galaxy M82 into luminous, young star clusters with HST/WFPC2. Pinkish clumpy structures to upper right of central dark lane are the near side of the starburst region, which is mostly heavily obscured ($A_V \gtrsim 5$).
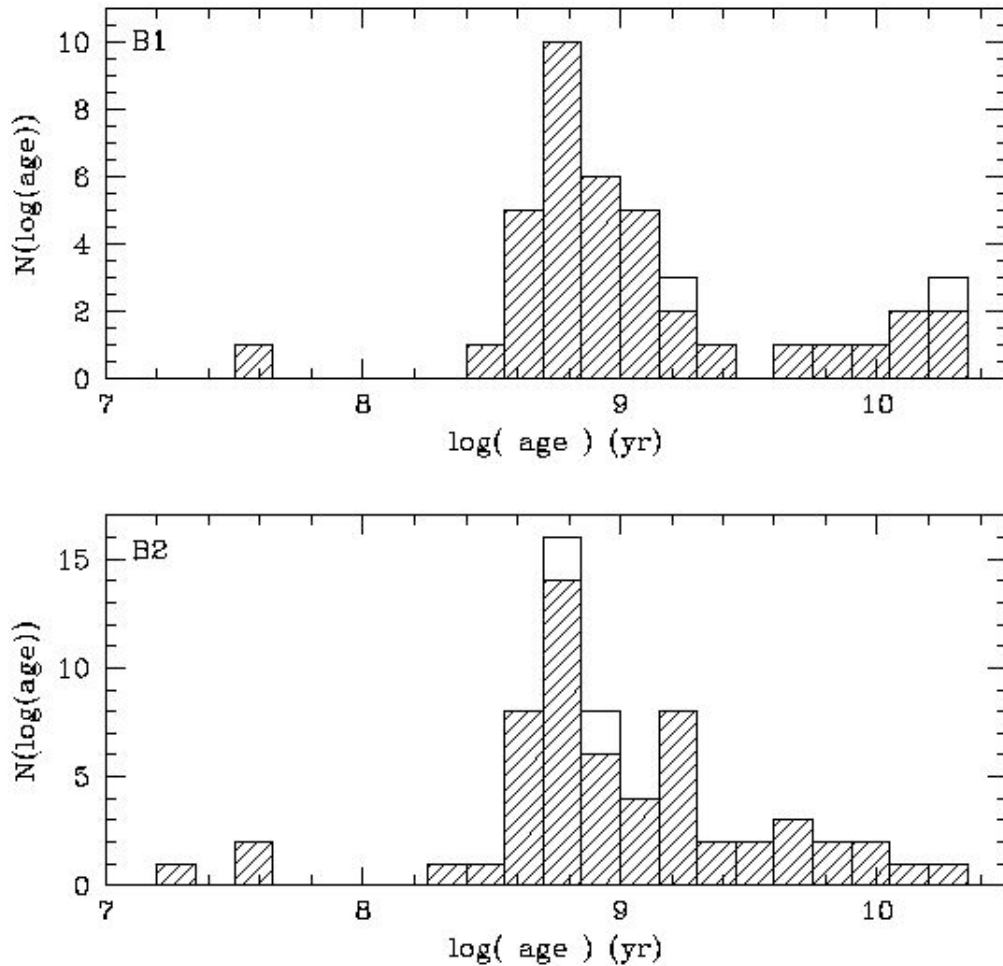
M82 Region B1 Showing Resolved Super Star Clusters

Closeup of the lower left wing of the preceding image. This region is about 1 kpc from the current starburst activity and is the site of a "fossil" starburst.

Two-Color Diagram of Clusters in M82 B1 and B2

This diagram, based on multiband images of the B1 and B2 regions, plots the BVI colors of each cluster detected. Because the "ageing" and "extinction" vectors are not parallel, it is possible to simultaneously solve for age and extinction for each cluster. There is considerable differential extinction across B1 and B2, so a common foreground dust screen model is inapplicable.

M82 Fossil Starburst: Derived Age Histogram

Histogram shows a burst of cluster formation at $\sim$ 600 Myr ago, which happens to coincide with a tidal passage of companion galaxy M81. Little SF has occurred since in this region, whereas there is a massive ongoing starburst in the galaxy's center (age $\lesssim$ 50 Myr).

VI. EXAMPLE: PHOTOMETRIC REDSHIFTS

One can use the distinctive features in broad-band spectral energy distributions of distant galaxies to obtain approximate values of their redshifts from their multi-band colors <u>alone</u>.

The main useful features are (1) the spectral slopes as a function of rest wavelength; and (2) the large <u>discontinuities</u> at rest wavelengths near 4000 Å (known the "H&K break" or the "4000 Å break"), which occurs in populations of almost all ages, and near 910 Å (the "Lyman break"), which is visible only in younger populations. There is also a sharp decline in the SED of distant younger populations below Lyα at 1216 Å caused by the intervening "forest" of hydrogen clouds.

The redshifts so determined are called <u>photometric redshifts</u> (or "photo-z's"). A large amount of effort has gone into modeling galaxy SEDs and testing the precision possible with photometric redshifts. With good data this is estimated to be $\sigma(z) \lesssim 0.03$.

The technique requires a <u>simultaneous fit</u> to the <u>intrinsic spectral shape</u> (determined by the stellar population and dust) and to the <u>shift</u> in wavelength space.

A major application is to star-forming systems at high redshift ($z \gtrsim 3$) which are detectable by their Lyman continuum and Lyα breaks. Broad-band images of such objects become dark (or "drop out") at wavelengths below the break. [This technique obviously selects against objects with large UV extinctions.]

Another is to search for high redshift analogs of low-redshift quiescent galaxies (e.g. giant E galaxies) as a means to determining the earliest epoch of massive galaxy formation. Again, these objects are dim in any filter that contains the restframe UV.

More precision is obtained (at a cost of longer exposure times or shallower surveys) by using intermediate-band filter sets, e.g. COMBO17, HST/WFC3.
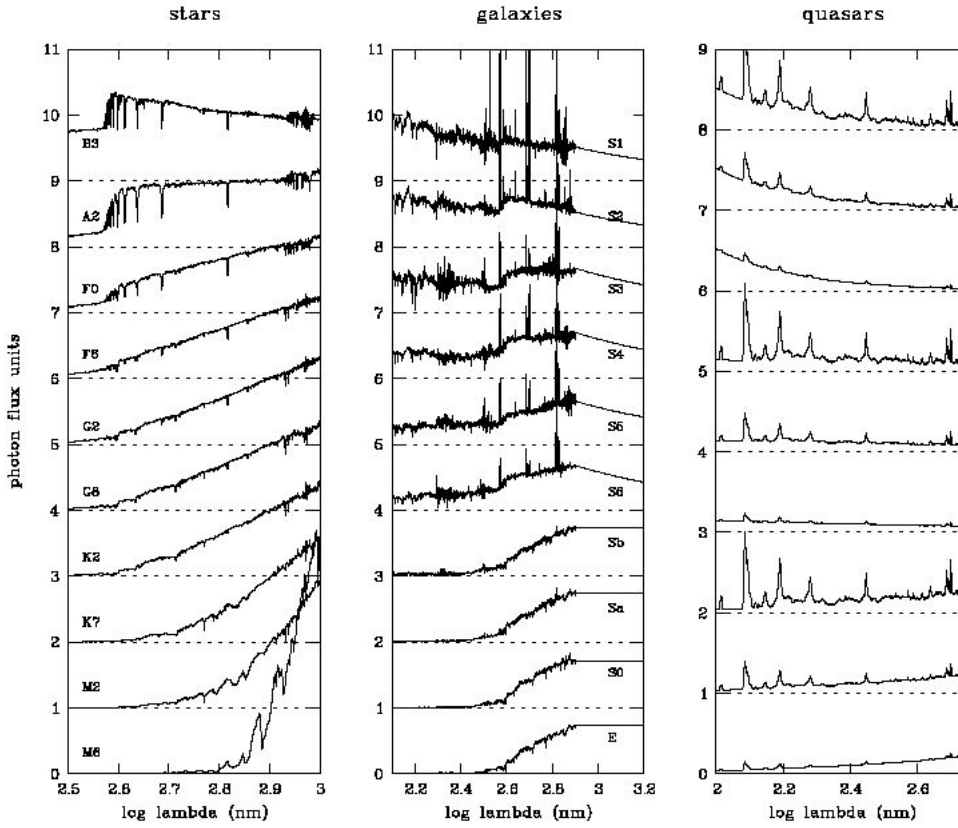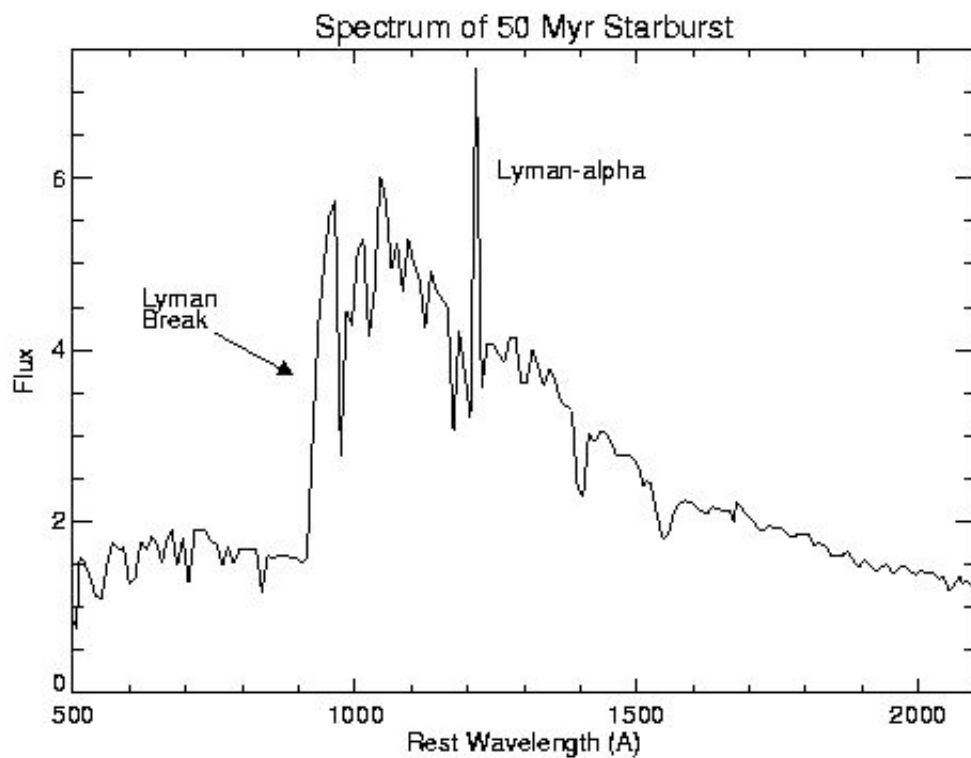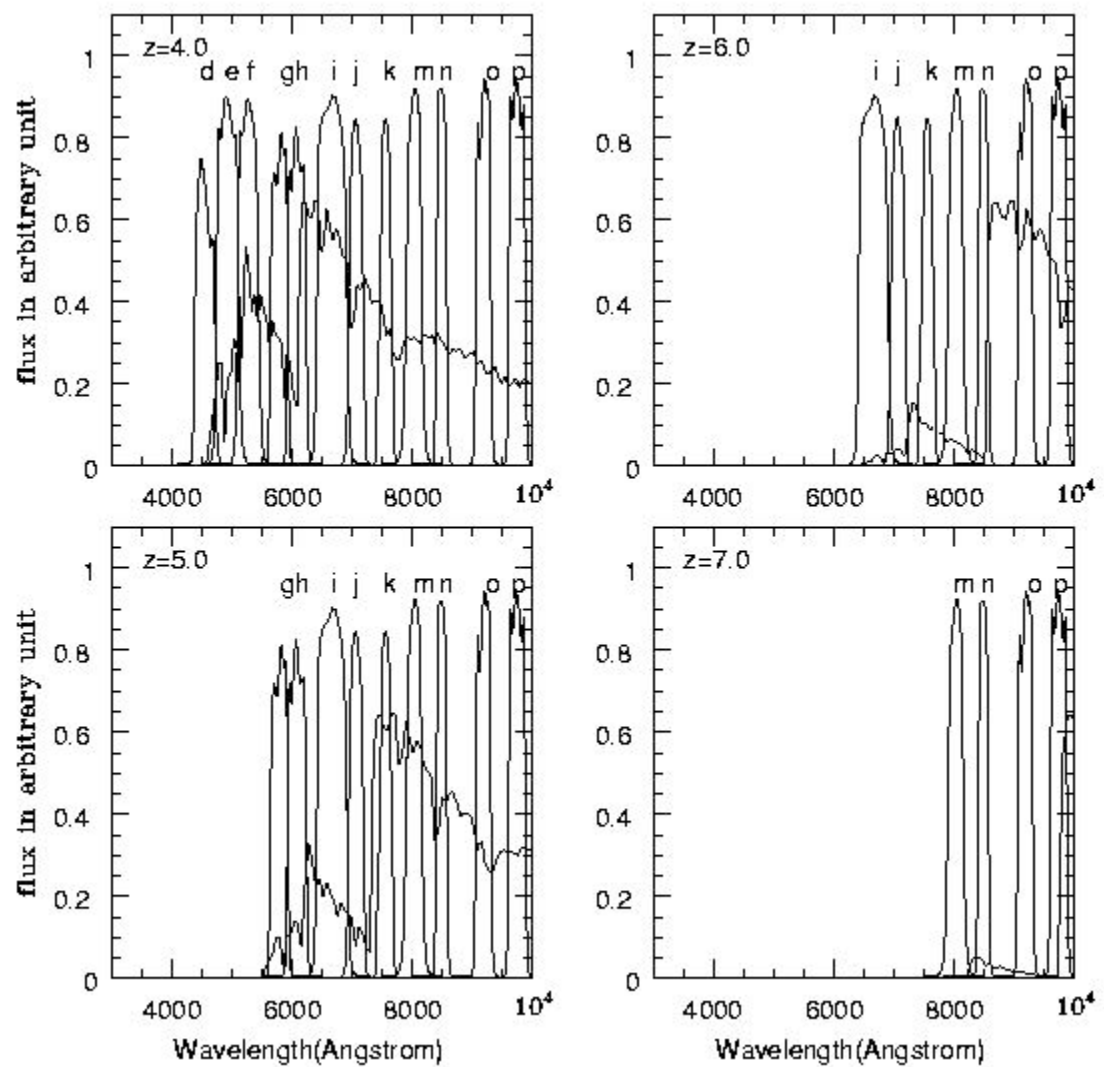
Fig. 1. This diagram shows a few selected spectra from our template libraries. The shown wavelength scale runs from 315 nm to 1000 nm for stars (left), from 125 nm to 1600 nm for galaxies (center) and from 100 nm to 550 nm for quasars (right). The flux is λf_λ in units of photons per nm, time interval and sensitive area and offset by one unit per step within a class. The flux scale is normalised to unity at 800 nm for stars, arbitrary for galaxies, and normalised to 0.2 at 250 nm for quasars. The stellar templates are taken from Pickles (1998), the galaxy templates from Kinney et al. (1996) and quasar templates are modelled after Francis et al. (1991). The quasar diagram shows nine spectra with three different spectral indices (-2.0, -0.6, +0.8) and three different relative emission-line intensities (0.6, 2.1, 5.7).

Restframe SED's of Stars, Galaxies, QSO's

Spectrum of 50 Myr Starburst
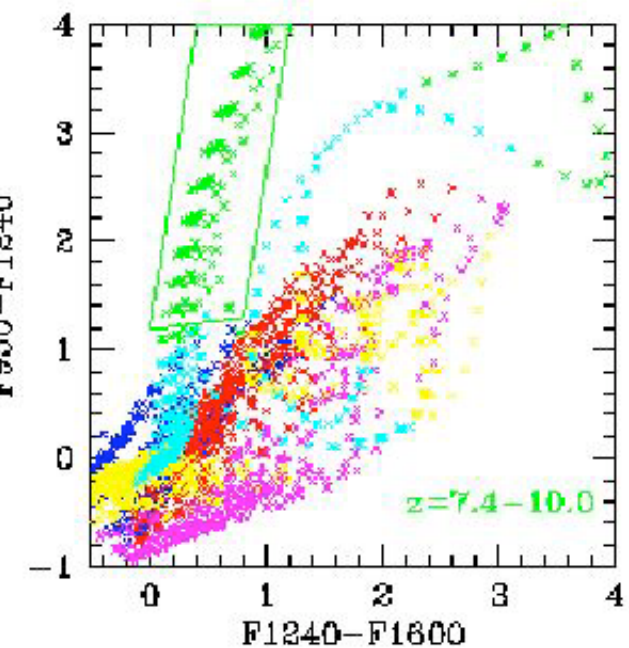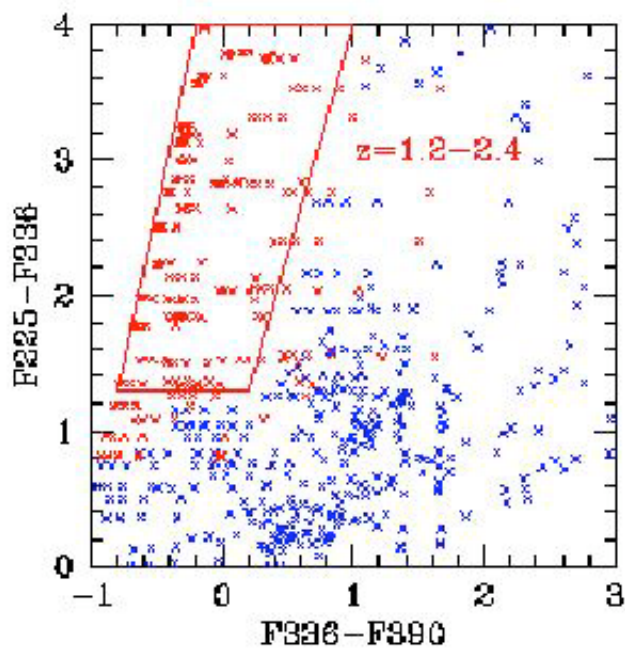
Restframe UV Energy Distribution Star Forming Galaxy

(The Lyman-α forest is not shown but would chop up the continuum shortward of 1216 Å.)
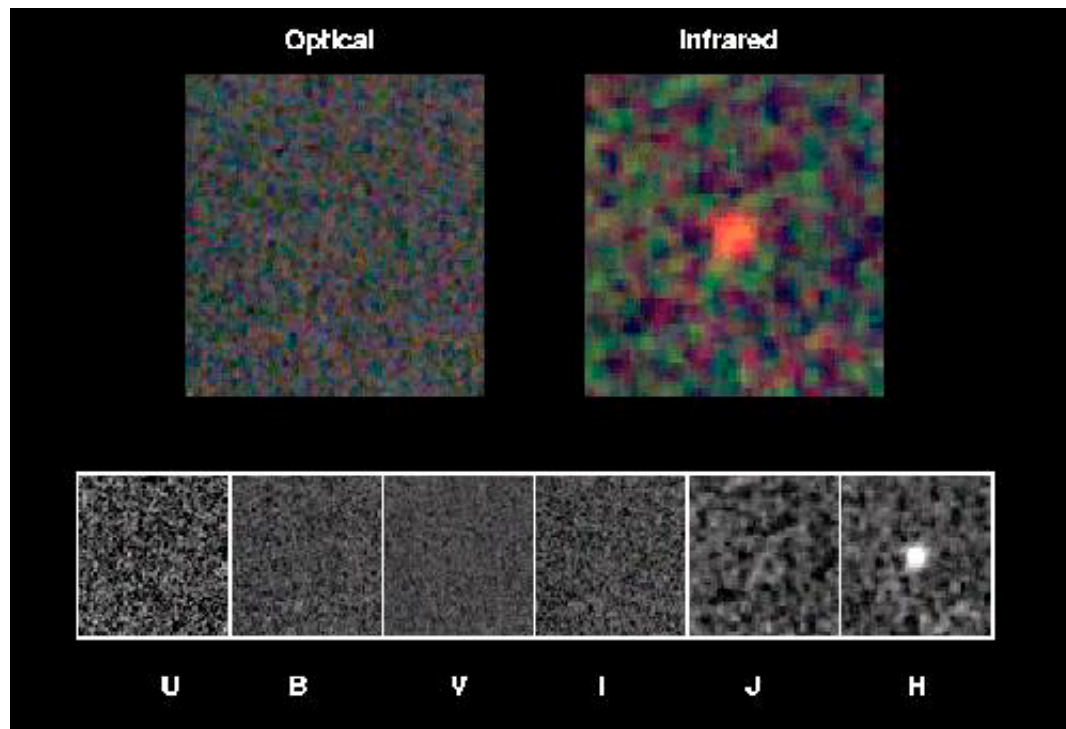
Redshifted Star Forming Galaxy SED vs Intermediate-Band Filters

Location of High Redshift Galaxies in Two-Color Diagrams

(Based on intermediate-band filters. Color coding is for different redshift regimes)

J-Band Dropout Source (Dickinson)

What redshift does this imply if the dropout is due to the Lyman break?
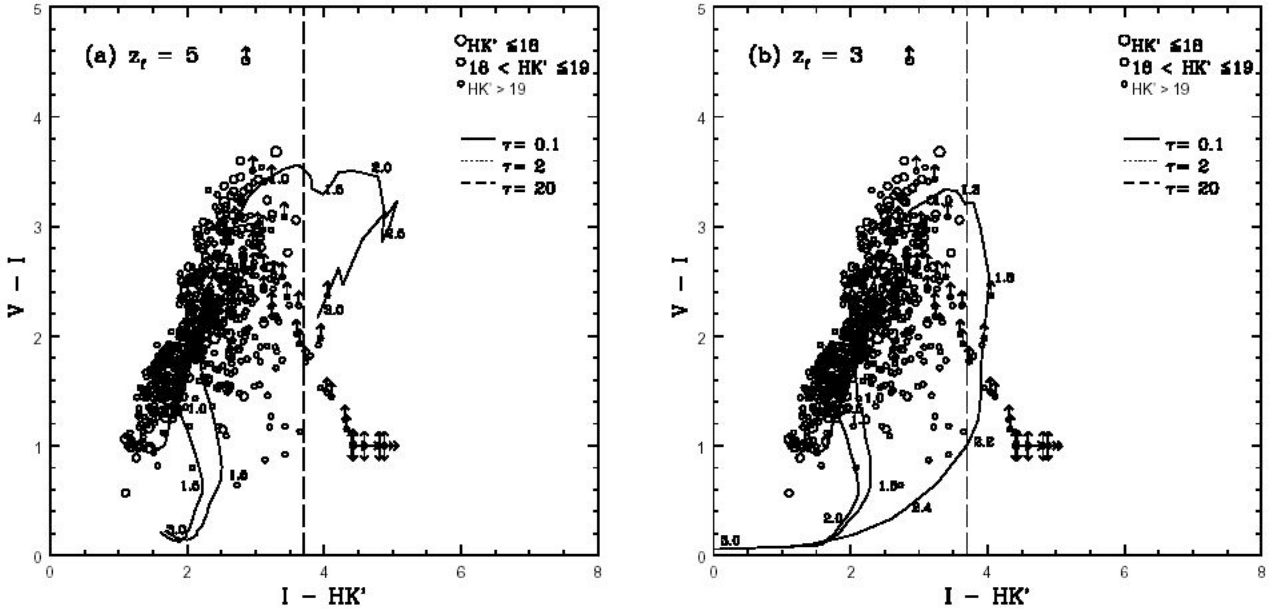
FIG. 4.—$V - I$ vs. $I - HK'$ color-color diagrams for the wide-field $HK' \leq 20.4$ sample (stars have been removed). The BC96 passively evolving model tracks folded with the appropriate V, I, and HK' filters are illustrated from $0 < z < 3$, assuming an epoch of galaxy formation of $(a) z_f = 5$ and $(b) z_f = 3$. The model tracks have been labeled with a few representative redshifts at which the various colors would be observed. The vertical dashed lines in the figures illustrate the ultrared dividing line, $I - HK' > 3.7$.

VIK search for quiescent massive galaxies at high redshift (Barger 1999)

This survey yielded few quiescent candidates (which have I-K > 3.5). More recent work by McCarthy, Glazebrook, and Abraham (2004, GDDS survey) has identified such systems with more sensitive imaging and spectroscopy over large fields. Massive quiescent galaxies reside only in denser regions.
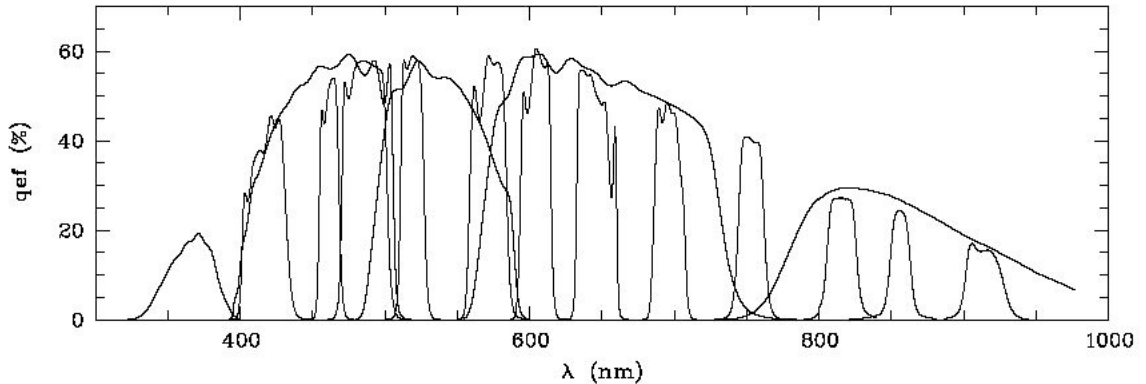
Fig. 1. COMBO-17 filter set: Total system efficiencies are shown in the COMBO-17 passbands, including two telecope mirrors, WFI instrument, CCD detector and average La Silla atmosphere. Combining all observations provides a low-resolution spectrum for all objects in the field. Photometric calibrations of such "multi"-colour datasets are best achieved with spectrophotometric standards inside the target fields.

COMBO-17 Deep Survey Interference Filter Set

VII. BROAD-BAND SKY SURVEYS

Among the most important applications of multi-band filter systems has been their use in large-scale sky surveys. Wide filters, especially when coupled to photoelectric detectors, support very deep surveys. A vast array of astrophysics has emerged from such surveys.

A. 48-in Schmidt Sky Surveys (Optical)

Prototype: Palomar Observatory Sky Survey(s)

Employ wide-field (6°) field Schmidt optics (spherical primary mirror with refractive correction lens).

Photographic: 14" plates (pressure-curved to match focal plane): <u>pairs</u> of exposures in 936 fields

POSS I: 1950-58. Sky north of -33°

103a-O: Blue (4400 Å)

103a-E: Red (6500 Å) (includes Hα)

Limit $\sim$ 20-21 for point sources

Extended to southern hemisphere 1975+ by ESO/SERC

IIIa-J: Blue (at AAO)

IIIa-F: Red (at ESO)

POSS II: 1985 –

New version of Palomar-I: deeper (to $\sim$ 22 mag) and for proper motions (40-50 year baseline)

IIIa-J (Blue), IIIa-F (Red), IV-N (Near Infrared)

Digitized

Digitized Sky Survey and Guide Star Survey (1985–)

To support HST operations, STScI digitized versions of various sets of 48-in surveys and extracted catalogues of guide stars (to $V \sim 15$). For on-line access, see: `http://www-gsss.stsci.edu/gsc/GSChome.htm`. Parts of these are available through the simpler SKYVIEW interface: `http://http://skyview.gsfc.nasa.gov/cgi-bin/titlepage.pl`.

B. Sloan Digital Sky Survey (Optical), 2000–

Special-purpose 2.5-m telescope for imaging/spectroscopy at Apache Point, NM

Imaging of about 1/4 of sky centered on N Galactic Pole

5-color imaging using drift scanning with large CCD mosaic. Limit R $\sim$ 23. Total catalogue: $\sim$ 100 million sources

Automatic morphological discrimination of stars from galaxies using SExtractor-type software. Multicolor discrimination of QSO's from stars.

Spectroscopy (3″ diameter fibers connected to aperture plug-plate) of selected targets, including about 1 million galaxies, to R $\sim$ 18.

See `http://www.sdss.org/sdss.html`

C. Other Recent Surveys

The 2dF galaxy redshift survey conducted at the Anglo-Australian Observatory is a similar undertaking on a smaller scale in the southern sky. See: `http://www.mso.anu.edu.au/2dFGRS/`

The Galaxy Evolution Explorer (GALEX) mission (`http://www.galex.caltech.edu/`) is now performing an all-sky imaging survey to m(UV)$\sim$21 that extends these ground-based surveys to the vacuum UV.

D. 2MASS Sky Survey (Near Infrared)
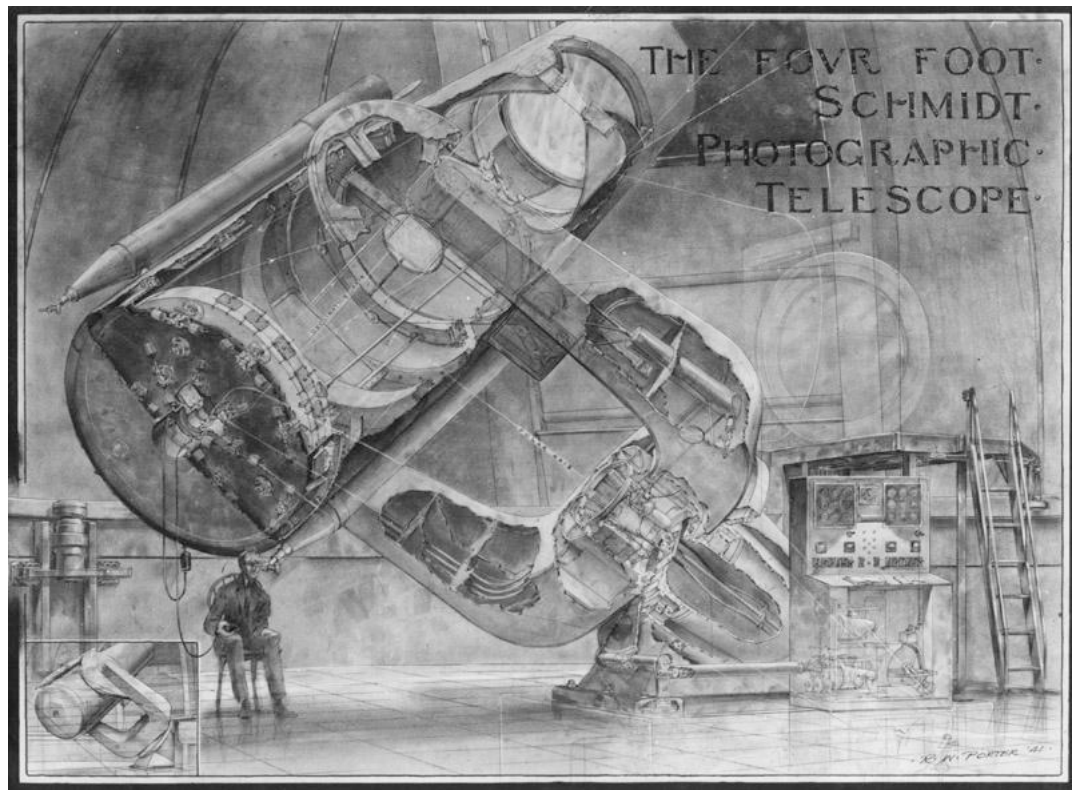
Uses two 1.3-m telescopes to do deep near-IR imaging survey of entire sky.

Bands: J (1.25 μ), H (1.65 μ), K (2.17 μ).
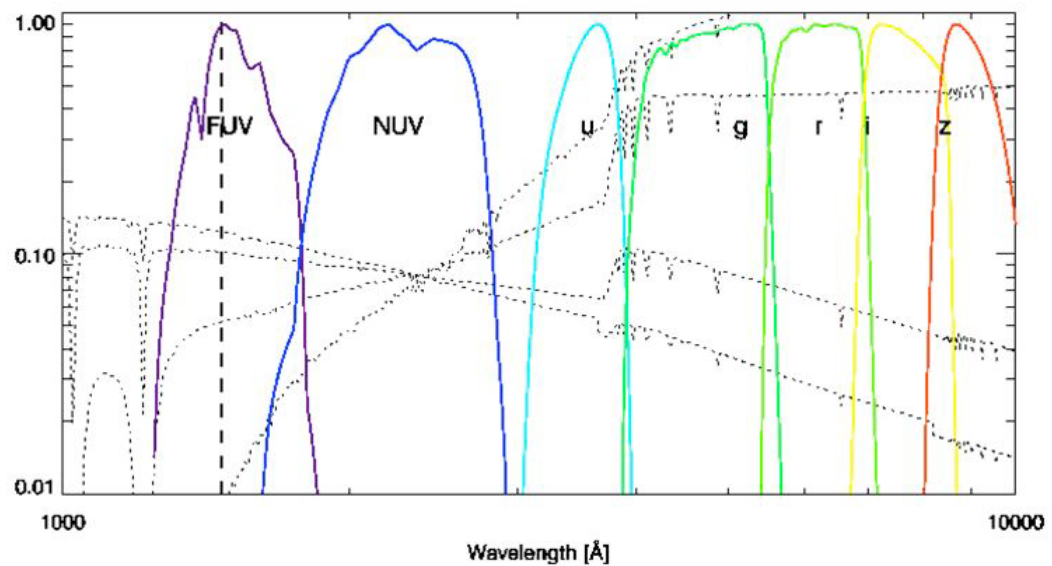
Limiting mag: $\sim$ 15-16 (J band)

Source of accurate astrometry for detected point-like targets

Final catalogue: $\sim$ 300 million point sources, $\sim$ 1 million galaxies

Palomar 48-in Schmidt (Porter)

The SDSS and GALEX Filter Bands
(with sample galaxy SEDs superposed)
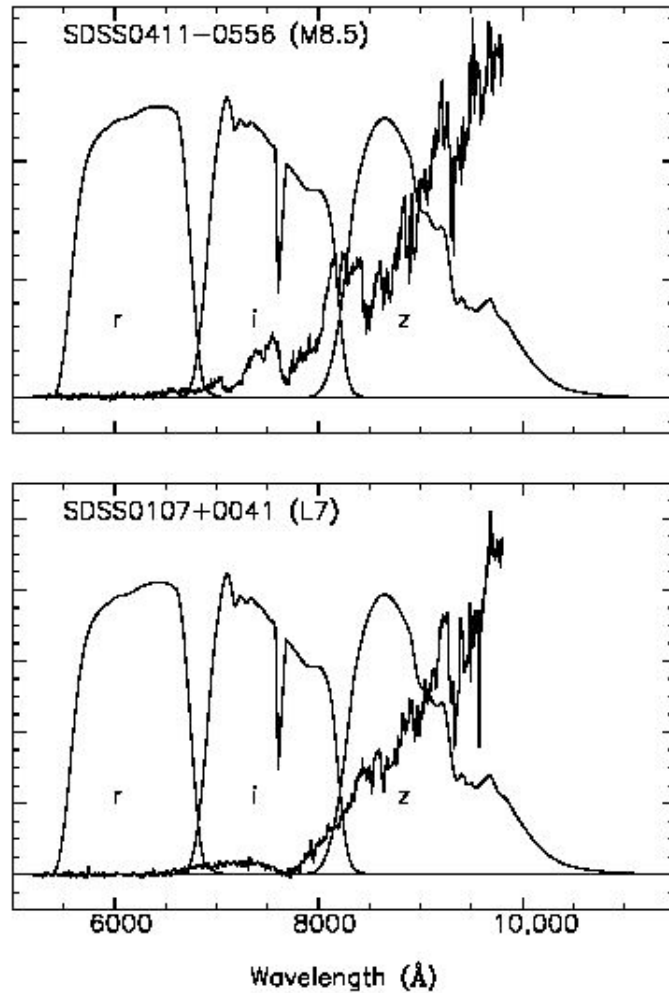
Fɪɢ. 6.—SDSS *r*, *i*, and *z* relative system responses (including 1.3 air masses) compared with HET spectra of SDSS 0411-0556 (M8.5) and SDSS 0107+0041 (L7). The strong absorption between about 8500 and 8800 Å seen in SDSS 0411-0556 is due to the 8432 and 8692 Å TiO and FeH bands, which disappear at about L3–L4 (see Fig. 4).

Cool Star SEDs in SDSS Bands
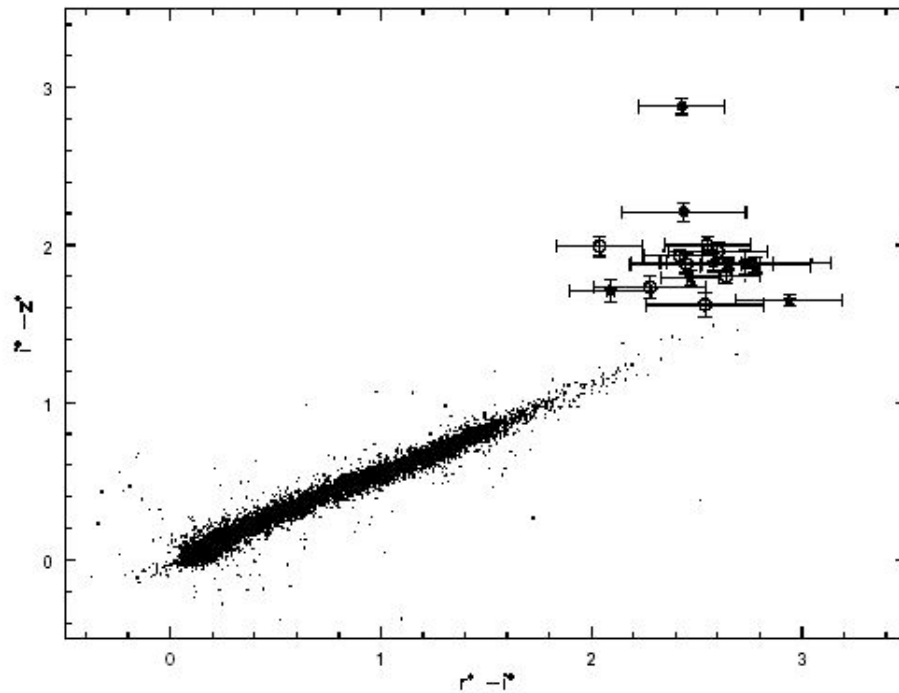
FIG. 3.—SDSS color-color plot for the 18 objects detected in all three of the *r*, *i*, and *z* bands, compared with SDSS data for 15,000 stars from Finlator et al. (2000). The symbols are the same as in Fig. 2.

Cool Star Color Separation (Brown Dwarf Candidates) in SDSS
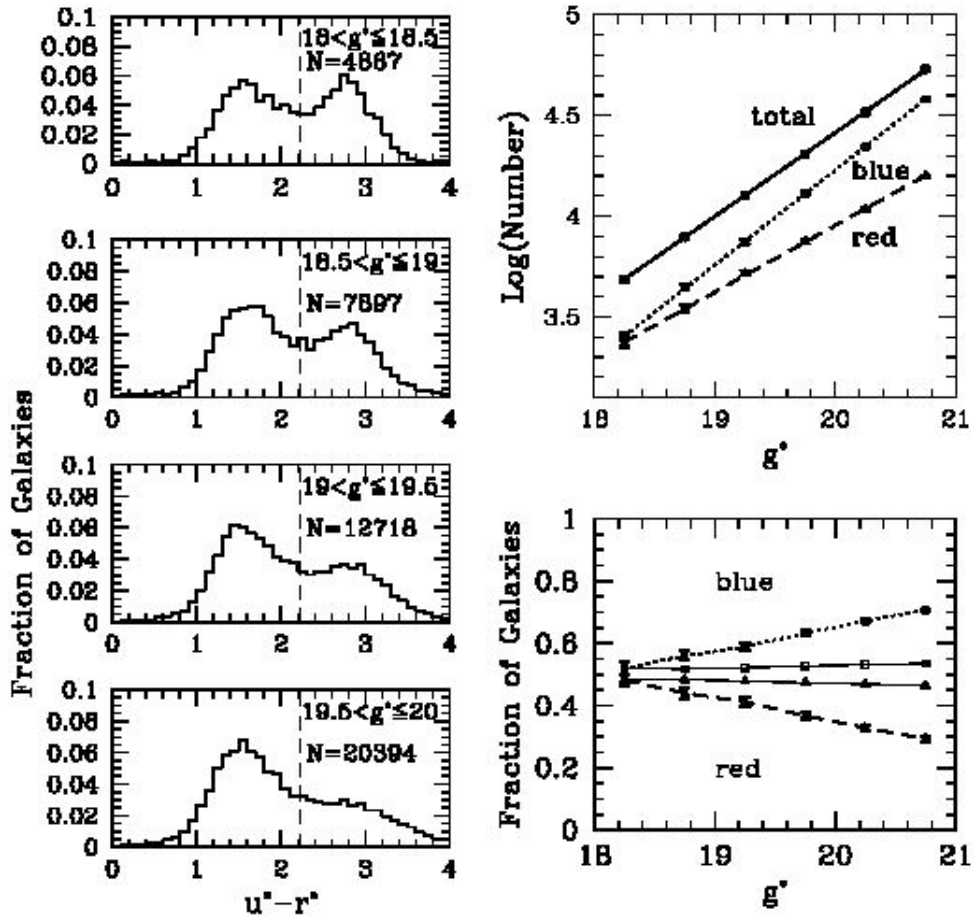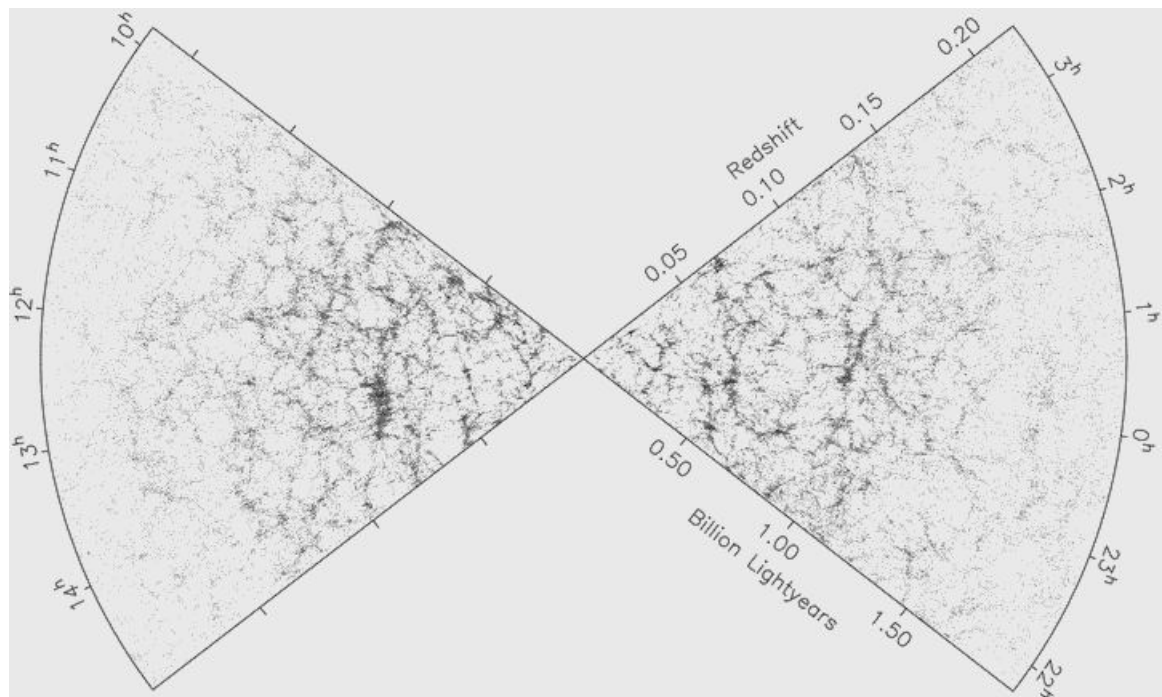
FIG. 2.—*Left*, color distribution $u^* - r^*$ as a function of g^* magnitude of the galaxy sample; *top right*, fraction of blue galaxies (*filled squares*) increasing relative to the red (*filled triangles*) for fainter g^* samples; *bottom right*, photometric errors cannot account for the dependence of the red and blue galaxy fractions on magnitude cut. The open symbols correspond to the predicted fraction (assuming only photometric errors change with magnitude), the filled symbols to the observed.

Galaxy Color Statistics (SDSS, 2001)

Although the bimodality in colors shown here was first evident in statistics from the de Vaucouleurs *Reference Catalogs*, the SDSS provides definitive evidence for a separation between star-forming (blue) and quiescent (red) galaxies.

Distribution of Galaxies in the 2dF Redshift Survey (2003)

Shows the remarkable filamentary texture that only emerges in large-scale surveys.

ASTR 511 (O'Connell) Lecture Notes

PRINCIPAL UVOIR TELESCOPES

Summit of Mauna Kea, Hawaii
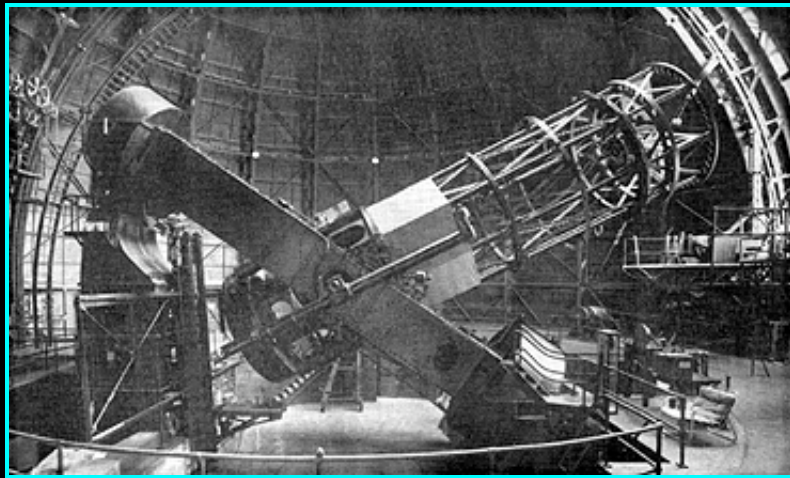
I. INTRODUCTION

The human imagination has never been a match for the universe. That is why astronomy, more than any other science, has been regularly revolutionized by new observational discoveries. Since 1610, these have depended on telescopes. When telescope technology developed slowly, as in the early 19th century, progress was slow. When technology surged, as in the late 20th century, progress was explosive.

This page surveys the principal UVOIR telescopes available in this decade together with a review of the milestones of the last 100 years. A hallmark of the major telescopes in this era is the remarkable variety of clever innovations, many of which have even more distant historical roots. There is very little in current telescope design that was not thought of long ago, though converting good ideas into realizable technologies is a different matter.

A key historical lesson is that to build an instrument at the frontier of performance is <u>always costly in terms of brains and money</u>. Thus, progress has coupled new technology, visionary astronomical pioneers, and the generosity of wealthy private donors or the financial strength of governments.

Note: we will not discuss <u>telescope optics</u> in this course. That topic and the detailed properties of detectors and instruments are covered in <u>Astronomy 512</u>.

The Mt. Wilson 100-in Reflector

II. AMERICAN OBSERVATORIES 1880-1970

A. BACKGROUND

Optical and mechanical technology in the last few decades of the 19th century had advanced to the point that the construction of large telescopes was feasible. Success with large telescopes demands that a large set of disparate requirements be met simultaneously: quality glass for optical elements, high precision shaping/polishing of optical surfaces, precision mechanical support systems, excellent control systems, excellent instrumentation, and good observing sites. Any such project is a major engineering undertaking.

Most of the large telescopes through 1960 were associated with universities. They were costly and required substantial private donations. Because of an abundance of industrial expertise, excellent observing sites, and wealthy contributors, the US became the world's leader in building large telescopes.

Refractors vs Reflectors:

- **The large telescopes of the late 1800's were mainly <u>refractors</u>. These were simple optically and featured good stability for astrometry, for instance. Through the mid-1800's, most <u>reflectors</u> had used metal mirrors and were of generally poor optical quality. However, the invention of high reflectivity thin metallic coatings for glass (initially silver) around 1850 made possible the use of glass mirrors. These were immediately competitive with refractors in terms of quality. This, together with a host of other reasons dictated that instruments larger than the Yerkes 40-in refractor were all reflectors:**

- **(1) Lenses (even achromats) produce chromatic aberration, limiting the bandwidth usable for imaging & spectroscopy. (2) Lenses must be figured on two sides (per element), whereas mirrors need be figured only on one. (3) Mirrors are easy to support accurately from behind, whereas lenses require support at their edges and will sag; it is harder to support heavy lenses mechanically at the top end of a telescope tube than a mirror at bottom end. (4) The folding action of primary and secondary mirrors means that reflector tubes are much shorter than in a "straight through" refracting design, easing mechanical design and reducing dome size.**

- **Description of standard reflector telescope designs**
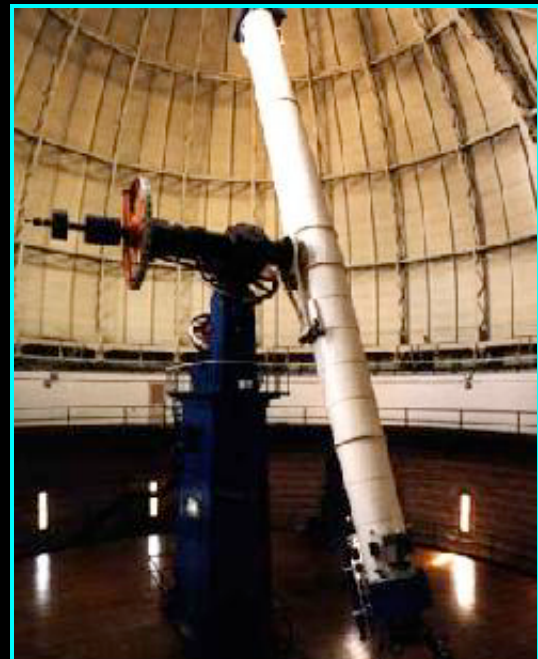
Optical Figuring Tolerance:

- **To maintain a good image, a single reflecting surface must be figured to within 1/4 wavelength of its intended design. For optical telescopes, this is 10^{-5} cm---very demanding. Good polishing/test techniques capable of reaching this precision were not developed until late 19th century. When there are several reflecting surfaces, the tolerances must be tighter. Specifications for state-of-the-art telescopes are for 1/10-1/20 wave optics. The most precise large mirror yet made was the HST 2.4-m, which was figured to about 1/50 wave (of its test wavelength of 6328 Å).**

- **Scale comparison: if a 320" (8-m) diameter telescope mirror were scaled up to the size of the continental United States, i.e. about 3000 miles diameter, then the maximum size of a ripple allowed in its polishing would be less than 2 inches! [You should be asking yourself how it is possible to determine the figure of a large mirror to that precision without the use of very expensive metrology equipment.]**
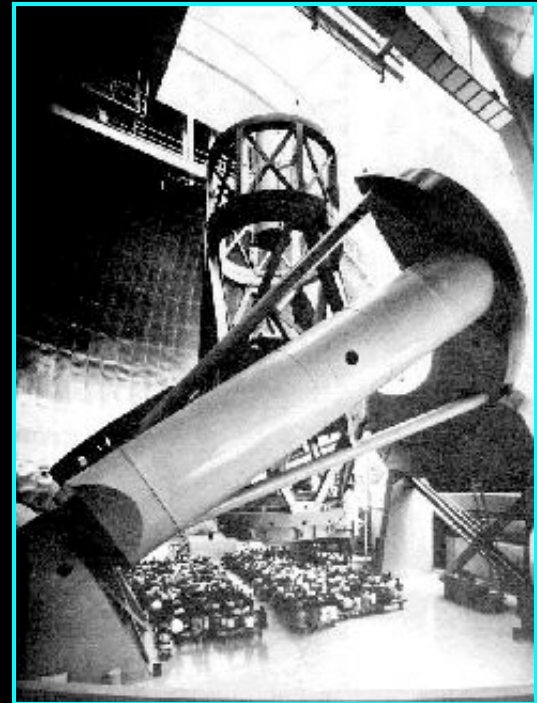
B. IMPORTANT MILESTONES

- **Leander McCormick Observatory 26-in refractor (UVa, 1885). Largest in the US when dedicated. Optics figured by Alvan Clark; 32-ft length.**

- **Lick Observatory 36-in refractor (U Calif., 1888), the first mountaintop observatory (4200 ft). Optics figured by Alvan Clark; 58-ft length.**

George Ellery Hale **was the premier American telescope founder. He planned, successively, the four largest telescopes of their era and lived to build the first three of these. He also built several major solar telescopes. Hale had a great facility for obtaining private financing, from Carnegie and Rockefeller, among others. The four major Hale telescopes were**

- **The Yerkes Observatory 40-in refractor** (Univ. of Chicago, 1897). The largest refractor ever built (picture above right). Lens originally intended by USC for a Mount Wilson site. Optics figured by Alvan Clark; f/19; 63-ft length.

- The **Mt. Wilson 60-in reflector** (1908), the **first major reflector in the US.** Fork mount. Optics figured by **George W. Ritchey**. f/5 Newtonian, bent-Cassegrain. First to have a coude focus. Early optical coatings were silver. Mt. Wilson Observatory was operated by the Carnegie Institution.

- **The Mount Wilson 100-in reflector** (1917), the most important telescope of the 20th century (**photo** at beginning of this section). Optical figuring by George Ritchey (with reluctance, because of **bubbles** in mirror blank below surface). English yoke mount on mercury flotation bearings (exclusion zone near pole). Three main foci: **Newtonian (f/5; reachable by dome-mounted platform)**, bent-Cassegrain, and coude.

- **The Palomar Observatory 200-in (5-m) reflector** (Caltech, 1948), the largest working telescope until 1992. The 20-year process of planning & building the 200-in is described in a photo-history **here.** Placed at Palomar because, even by 1920, Mt. Wilson was suffering serious **light pollution** from Los Angeles. Above right is a photo of the 200-in dedication in 1948. A diagram of the telescope is available **here**. Yoke-mounted, with a **horseshoe-shaped, oil pressure supported north bearing**. First telescope with a **prime-focus (f/3.3) "cage"** capable of carrying an astronomer. Other foci: Cassegrain, coude.

Also of note:

- At the urging of Fritz Zwicky, among others, Caltech commissioned the **48-in Schmidt telescope** as a survey instrument to support the 200-in. Based on the **design** of Bernhard Schmidt this *catadioptric* telescope uses a spherical mirror together with a thin refractive corrector lens to eliminate spherical aberration over a wide field of view (6° diameter in this case). The 14-in square focal plane is inside the body of the telescope; it is convex and requires that photographic plates be curved under pressure to match. The 48-in Schmidt made the multiband photographic "POSS" surveys.

- In the 1970's, NOAO developed a **4-m telescope design** based on the 200-in, and this has been reproduced, more or less closely, in multiple versions, sizes 3.5-4.2m, around the world (e.g. KPNO 4-m, CTIO 4-m, AAT, CFHT).

Polished & coated 8-m (315-in) mirror for the Gemini project, 1999.

III. NEW TECHNOLOGIES 1970-2000
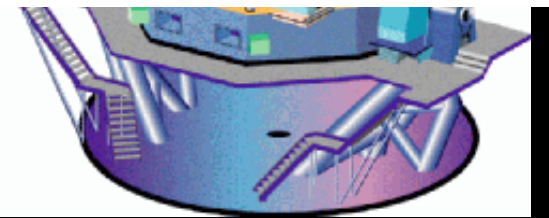
Telescope technologies steadily improved throughout the first half of the 20th century, with much progress in mechanical design (e.g. the oil pressure bearing of the 200-in), structural materials, optical figuring, electrical control systems (e.g. analog computers), and astronomical instruments to attach to telescopes. However, until about 1975, big telescope design was still based largely on the concepts used for the Mt. Wilson and Palomar telescopes (designed 1900-30). Unfortunately, the cost of extending such designs to sizes larger than 200-in was prohibitive.

In the early 1980's a series of innovations was introduced that made yet larger telescopes affordable, mainly by <u>reducing the total weight, including the dome</u>, per unit optical collecting area. These included:

- **Shorter focal length optics, < f/2 (permitting smaller domes)**
- **Lightweight structural materials**
- **Lightweight monolithic mirrors (thinner designs and/or honeycombed)**
- **Spin-cast glass mirrors (Roger Angel, UAz; method originally developed by Robert Leighton, Caltech, for mid-size IR telescopes).**
- **Multiple-mirror designs (modern implmentation by military; first large astronomical design: Jerry Nelson, UCal)**
- **Alt-azimuth mounts (simpler weight-bearing design is less costly than equatorial)**
- **Naysmith foci (light beam exits along altitude axis) allow use of massive instruments without stress on telescope tube**
- **Common azimuth bearing for both dome and telescope; <u>dome & telescope move together</u>**

- **High performance computer control for active figure correction of thin mirrors and directional control of alt-az mounts**
- **Thorough and rapid ventilation of domes and mirror cells to keep nighttime temperatures uniform (within ~1° C) and therefore improve seeing.**

Various combinations of these innovations were first incorporated in a number of 4-m class telescopes (e.g. ESO NTT, WIYN, ARC), but their main impact was on 6-m and larger telescopes.

Important related issues:

> **Site selection was recognized as critical. For best transparency at infrared wavelengths high, dry sites, most over 12,000 ft, became preferred.**
>
> **The financing yo-yo:**
>
>> **After 1950, public funding from NSF had almost completely replaced the private financing responsible for the large telescopes prior to World War II. But NSF's budget failed to keep pace with the rapidly increasing number of astronomers and the expanding observational opportunities enabled by the new technologies. By 1985, US astronomers began turning again to private benefactors to finance large ground-based telescopes.**
>>
>> **The largest individual telescopes built to date, the Keck 10-m telescopes, were supported by a private gift of $120 million to Caltech, with a comparable contribution of state funds in the form of operating costs from the University of California. Other large facilities with a significant private component include the Magellan telescopes, the MMT, and the LBT. By contrast, the European VLT was financed with public funds (about $800 million to date) secured through international treaties by the European Southern Observatory. Because of the rapidly escalating costs, US planning for telescopes in the 30-100 meter class over the next decade (e.g. the TMT) is based on hoped-for public/private partnerships.**

The US lead in state-of-the-art telescopes is now being challenged by European and Japanese astronomers.

The European Southern Observatory Very Large Telescope.

IV. STATE OF THE ART TELESCOPES
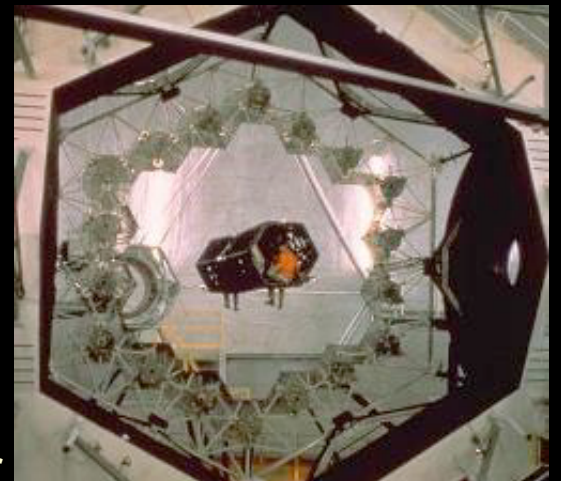
There are now 10 ground-based telescopes operating with diameters of 6.5-m or larger, with three more expected in the next two years. A list is available here.

- The European Southern Observatory Very Large Telescope: four 8.2-m telescopes on a very dry site in northern Chile, now has the largest total collecting area in the world (326,000 square inches), although the telescopes are normally operated separately. Primary mirrors are spin-cast Shott Zerodur (very low CTE) in a meniscus shape (46:1 aspect ratio). Shape is actively controlled with 150 actuators. The four telescopes can be combined to operate as an interferometer and have well developed adaptive optics (AO) systems.

- The Keck 10-m Telescopes

  The largest individual telescopes, based on a multiple-mirror design (picture at right). 36 stress-polished and cut 36" mirror segments.

  The Keck mirror figure control system is a remarkable technical achievement, although image quality is not quite as good as for a monolithic mirror. With its AO system, Keck can deliver a resolution of 0.05" at IR wavelengths. (Ground-based AO systems do not work well at wavelengths below 1 micron or

over fields larger than ~30".) Principal foci:
Naysmith, Cassegrain. Interferometric
combination of beams from the two telescopes is producing first results.

- **Hobby-Eberly Telescope**, operated by a consortium led by UTex and PennSt. An "optical Arecibo" with a large (9.2-m) mirror made of spherical segments. Fixed in altitude (55 degrees). Less successful figure control than Keck. Intended for spectroscopy of faint sources. A twin is being constructed in South Africa (SALT).

- **The Gemini Observatories**: two telescopes (Mauna Kea & Paranal, Chile) operated by an international consortium. 8.1-m, 20-cm thick Corning ULE meniscus mirrors with 120 figure control actuators. IR-optimized, using silver coatings. Total operations cost, about $33,000 per night.

- **Subaru**: 8.2-m optical/IR telescope on Mauna Kea similar to Gemini.

- 6.5-meter class: **MMT** (Mt. Hopkins, AZ), **Magellan I, Magellan II** (Las Campanas, Chile). All use Arizona Mirror Lab spin-cast, borosilicate mirrors.

- **The Hubble Space Telescope**

  First proposed by Spitzer in 1946 but launched in 1990. Long lifetime (to 2010+). Orbits at 300 mi altitude. Can be serviced by Space Shuttle crews (only such scientific satellite).

  Small (2.4-m) mirror, but very high precision. Primary mirror shape was inaccurate, however, owing to miscalibrated testing tools, with edge about 2 μ too low. This produced large spherical aberration (38 mm difference in focal length for inner and outer mirror). This was correctable, however, with small additional optical elements in each instrument. Servicing mission in 1993 carried correcting optics, and HST achieved design goals thereafter.

  Carries up to 6 instruments (imagers, spectrographs, interferometers) covering the band 1100-22500 Å. Highest UVOIR resolution images ever (0.05 arcsec). Deepest images m ~ 30 mag (4 billion times fainter than naked eye limit).

- Special Survey Telescopes: Sloan Digital Sky Survey (imaging & spectroscopy), 2MASS All-Sky Infrared Survey (imaging): see **Lecture 15**.

V. THE LARGE BINOCULAR TELESCOPE

The Large Binocular Telescope is a good example of current telescope building technology. UVa recently joined the consortium of universities which is building the LBT in southern Arizona.

- **The LBT consists of two 8.4-m diameter mirrors on a single alt-azimuth mount**

- **It can operate as two separate telescopes (pointing at the same target), or it can combine the beams of the two mirrors to act as an interferometer yielding the effective optical resolution of a 23-m diameter telescope.**

- **Spin-cast, honeycombed, lightweight borosilicate mirrors, with active ventilation thermal control system.**

- **Active control of secondary mirror for compensation of mirror figure changes and suppression of atmospheric seeing**

- ⭐**Click here** for pictures of the LBT. Assembly should be complete by 2004.

Related pages:

- **Telescope Optical Design**

- **LBT Design & Construction**

Additional References and Web links:

- **LLM text, Chapter 4**
- **Henry King, *History of the Telescope* (through 1950). Well illustrated.**
- **Allan Sandage, The First 50 Years at Palomar (ARAA, 37, 445, 1999)**
- **Daniel Schroeder, *Astronomical Optics*. Standard textbook for telescope optical design.**
- **Giant Astronomical Telescopes for the 21st Century (UCB course with full technical coverage of large telescope design)**
- **List of Largest Optical Telescopes**
- **List of Major Telescopes, All EM Bands**
- **List of Telescopes in Orbit**
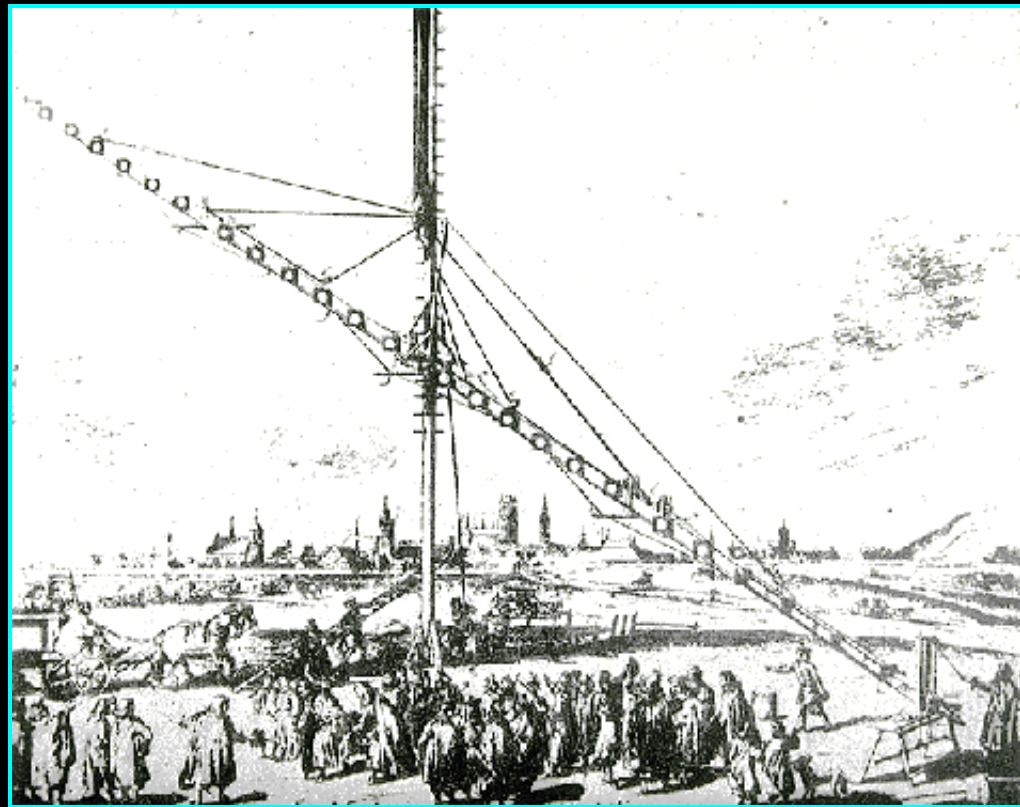
⬅ **Previous Lecture**   ⬆ **Lecture Index**   ➡ **Next Lecture**

---

*Last modified **July 2007** by rwo*

ASTR 511 (O'Connell) Lecture Notes

TELESCOPE OPTICAL DESIGN

Hevelius 140-foot Telescope (ca. 1675)

Telescope optical design is covered in detail in ASTR 512, so we give only a flavor of what is involved here.

A. Overview

The usual goal of telescope optics design is to bring all light rays, arriving at the primary element from a large range of field angles, to a sharp focus in a flat focal plane. The image should be a faithful one-to-one reproduction of the angular distribution of light in the source with minimal geometric distortion. The image representation should be independent of the wavelength of the light rays (i.e. *achromatic*).

But it is <u>not possible to accomplish this</u>. One can never build a perfect optical device. Any realized design is always a compromise because it is not possible to control for all *optical aberrations* at will.

Therefore, modern telescope design is essentially a process of successive approximations in <u>aberration control</u> in 3 dimensions. Fortunately, a number of highly capable software packages are now available to mitigate the pain of doing this.

The picture at the top of this page shows how early telescope builders tried to control for two major aberrations in crude lenses: (1) *chromatic aberration* and (2) *spherical aberration*. The effects of both of these aberrations diminish with focal length....hence the very long focal length of Hevelius' telescope.

The modern solution to chromatic aberration in refractive optics is to use <u>mirrors</u> rather than lenses, and most large telescopes employ mirrors as their primary optics. However, most optical instruments must also include refractive elements in order to achieve wavelength selection or wide-field images, so chromatic aberration is still almost always an issue.

The modern solution to spherical aberration (the fact that parallel light rays striking the surface of a sphere do not come to a single focus) is to use non-spherical optics, especially paraboloids. Rays parallel to the axis of a parabolic reflector come to a perfect focus. Unfortunately, off-axis rays do not, and this leads to a comet-shaped aberration known as *coma*, which becomes worse with field angle.

- Coma can be reduced by using a *refractive corrector* near the focal plane of a parabolic primary.

- **A widely-used alternative is the *Ritchey-Chretien* design, a Cassegrain system that employs two hyperbolic mirrors yielding zero first-order coma and spherical aberration. RC's are affected, however, by third-order coma, astigmatism, and field curvature (at larger field angles).**

- **Another famous alternative for control of spherical aberration over a wide field with a spherical primary is to use a special full-aperture refractive correcting plate called a *Schmidt corrector*. The Schmidt sky-survey telescopes employ these.**

B. Sample Ray Traces

Click below for illustrations of ray traces for spherical and parabolic reflectors. These show light paths for parallel incoming rays in a plane containing the symmetry axis of the mirror. They are for fast optical systems (small f/ ratios, where f/ = Focal Length/Diameter), so that aberrations are larger than for typical designs. You can see that, except for the case of a parabola and paraxial rays, it is not possible to find a good focal point anywhere in these systems.
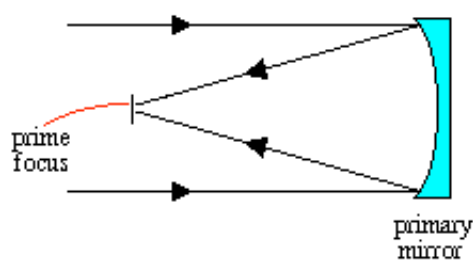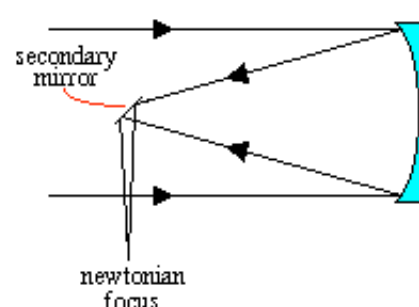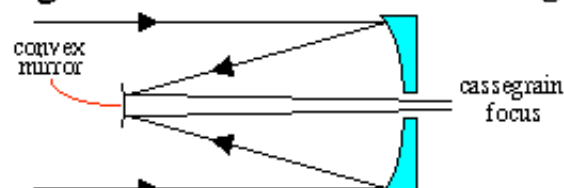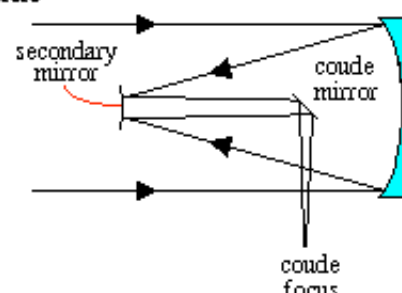
  - **Spherical mirror, paraxial rays**
  - **Spherical mirror, rays 5° off-axis**
  - **Parabolic mirror, paraxial rays**
  - **Parabolic mirror, inner/outer rays 3° off-axis**
  - **Parabolic mirror, rays 5° off-axis**

STANDARD TELESCOPE OPTICAL CONFIGURATIONS

TYPE	PRIMARY MIRROR	SECONDARY MIRROR	COMMENTS
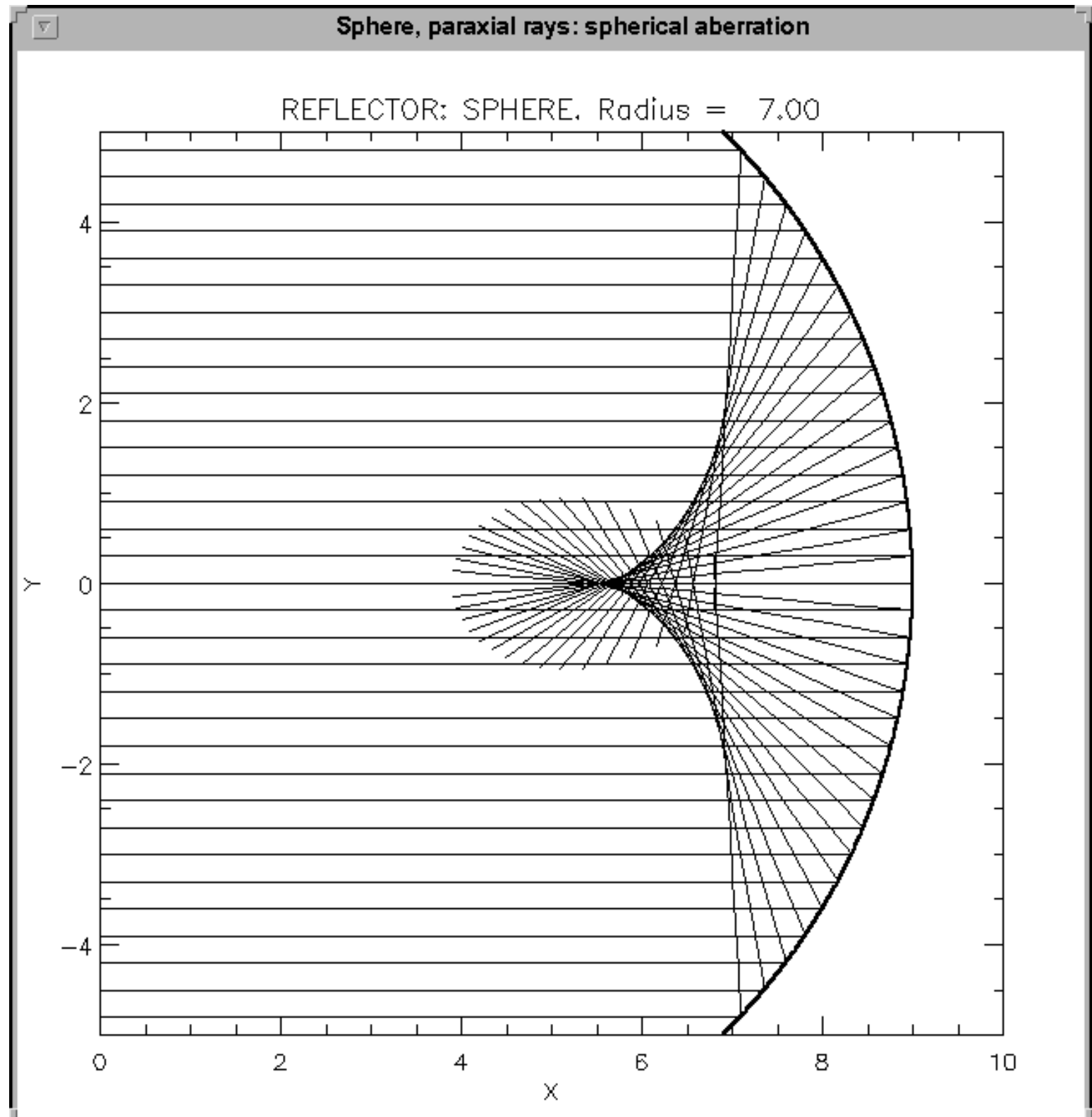
PRIME FOCUS	**Parabola**		**Focus inside telescope** **Add refractive corrector for wide field**
NEWTONIAN	**Parabola**	**Flat**	**Focus at side/top of telescope**
CASSEGRAIN	**Parabola**	**Hyperbola (convex)**	**Focus below primary**
RITCHEY-CHRETIEN	**Hyperbola**	**Hyperbola (convex)**	**Focus below primary. Zero coma & spherical aberration**
COUDE	**Various**	**Various**	**Tertiary flat directs light to fixed focus below polar axis**
NAYSMITH	**Various**	**Various**	**(Alt-Az): Tertiary flat directs light to focus outside altitude axis**
SCHMIDT	**Spherical**		**Catadioptric: Uses refractive corrector to provide wide field without spherical aberration. Focus inside telescope body**

Reflecting Telescopes

[
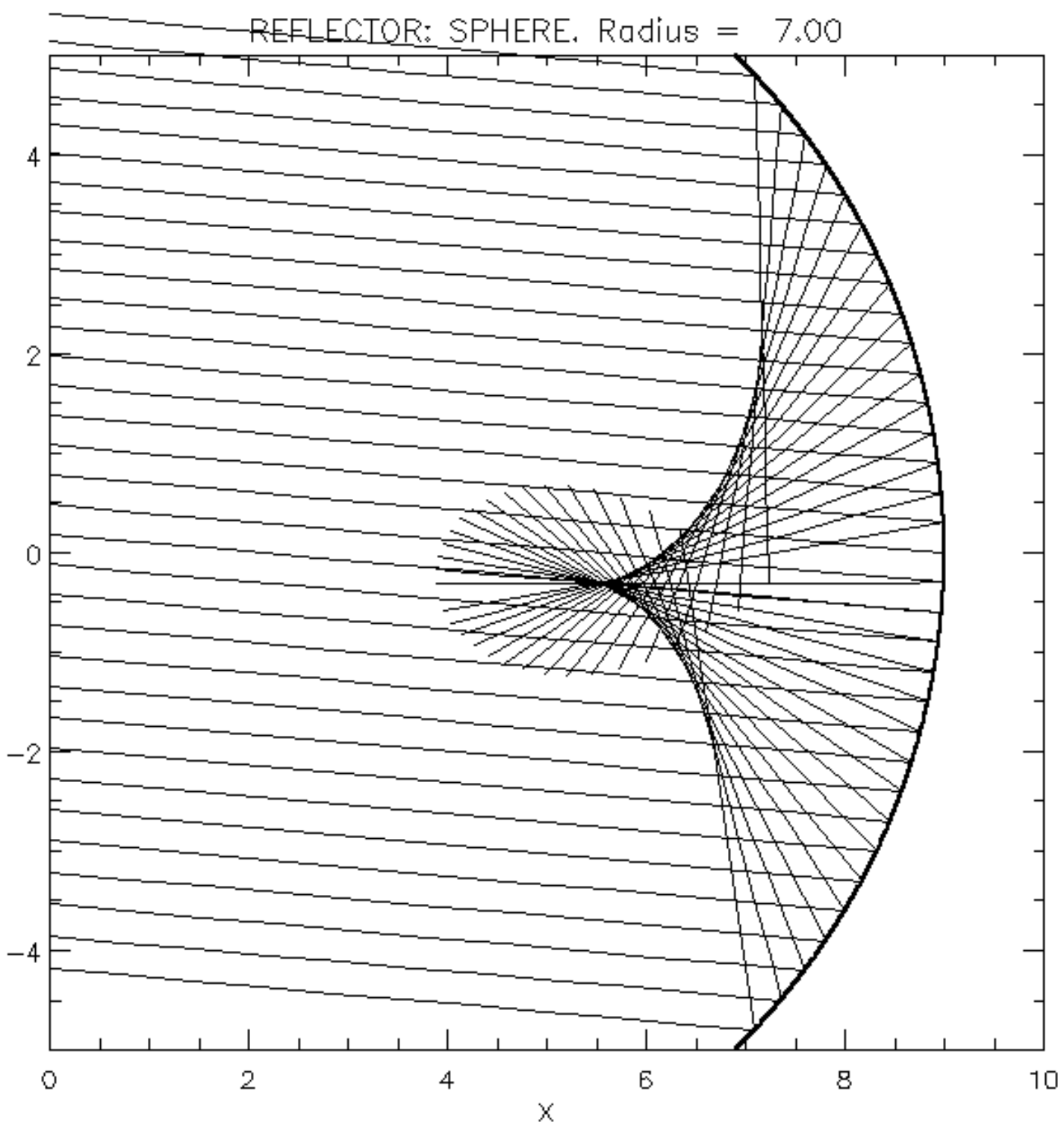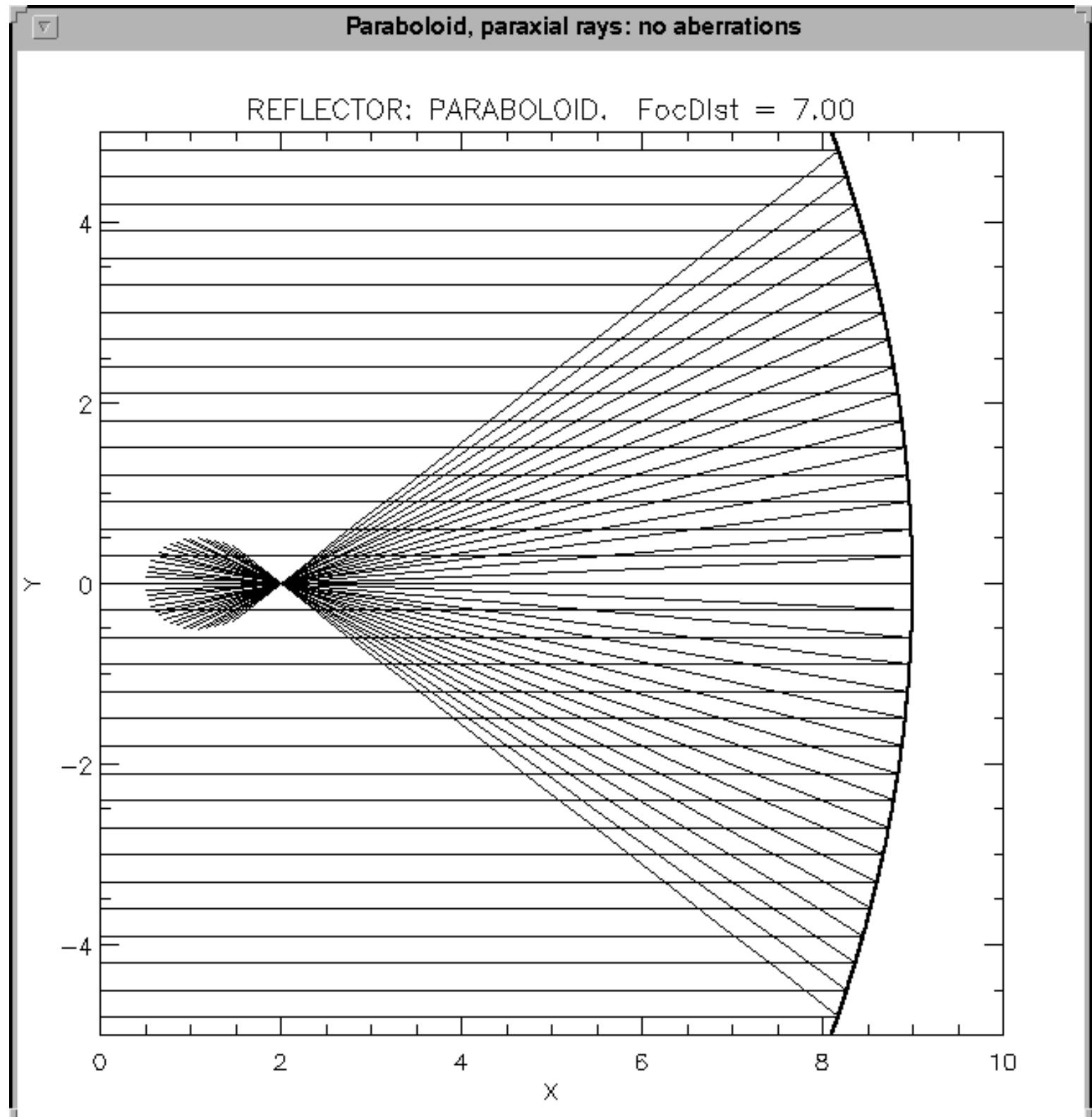
 ← **Back to Lecture 16**
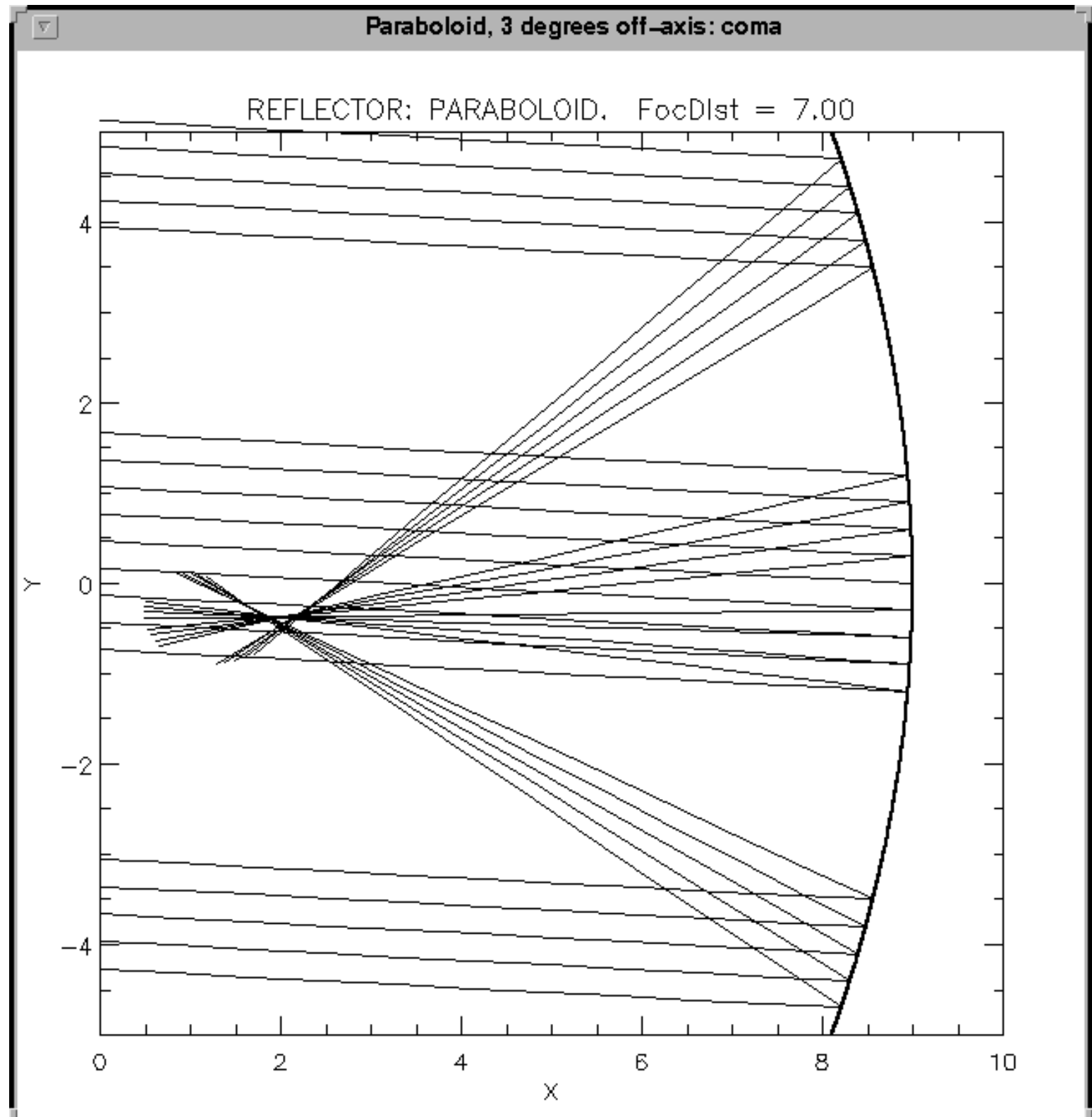
Last modified July 2007 by *rwo*
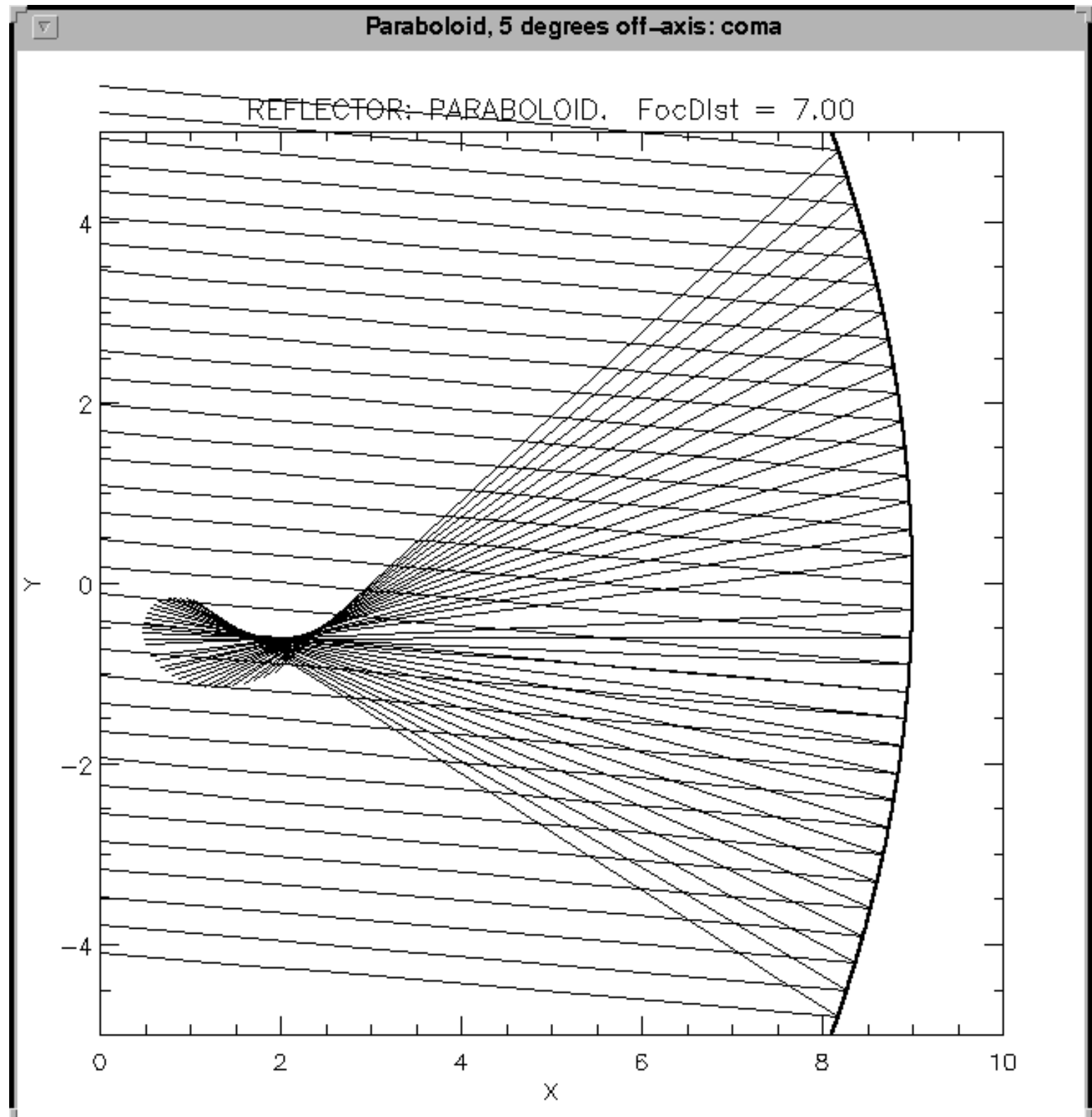
Copyright © 2000-2007 Robert W. O'Connell. All rights reserved. These notes are intended for the private, noncommercial use of students enrolled in Astronomy 511 at the University of Virginia.

Sphere, paraxial rays: spherical aberration

REFLECTOR: SPHERE. Radius = 7.00

Sphere, 5 degrees off-axis: spherical aberration

REFLECTOR: SPHERE. Radius = 7.00

Paraboloid, paraxial rays: no aberrations

REFLECTOR: PARABOLOID. FocDist = 7.00

Paraboloid, 3 degrees off-axis: coma

REFLECTOR: PARABOLOID. FocDIst = 7.00

Paraboloid, 5 degrees off–axis: coma

REFLECTOR: PARABOLOID. FocDist = 7.00

THE LARGE BINOCULAR TELESCOPE
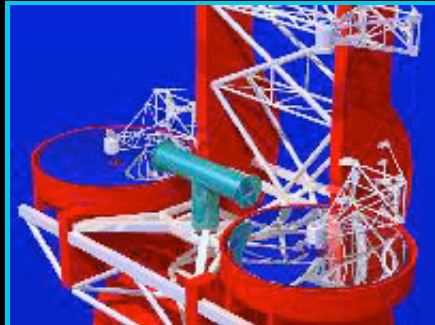
CONSTRUCTION IMAGES

One of the two 8.4-m diameter LBT mirror blanks.

ILLUSTRATIONS

[Click for Full Images]

Mechanical Design, Front

Mechanical Design, Rear

Optical Beams

Placing Cores in Casting Mold

Loading Glass

Furnace Closing

Furnace Spinning
(7 revs/min)

8.4-m Mirror Blank

Polishing Mirror

Computer Controlled
Polishing Tool

Assembled Structure
June 2001

Elevation Bearing
June 2001

Mirror Cells

Dome Interior
June 2002

Dome on Mt. Graham

Testing Mirror in Cell

Prepping Mirror for Move

Moving Mirror Cell
October 2003

Moving Mirror Cell

Moving Mirror

Moving Mirror

October 2003   October 2003   October 2003

Telescope Assembly
September 2003

LINKS

- **LBT Main Page** (Univ. of Arizona)

- **LBT Design Animation (MPEG, 8MB)**

- **Live Video of Telescope Site**

- **Arizona Mirror Laboratory**

*Last modified **March 2007** by R. W. O'Connell*

AST 511: November 17, 2003
Astronomical Polarimetry

Last modified: November 18, 2003

David McDavid
dam3ma@virginia.edu

Astro Polz

Stokes vector — 4 "Stokes parameters"

$$
\begin{bmatrix} I \\ Q \\ U \\ V \end{bmatrix} = \begin{bmatrix} I_0 + I_{90} \\ I_0 - I_{90} \\ I_{45} - I_{135} \\ I_R - I_L \end{bmatrix}
\begin{array}{l} \text{total intensity} \\ \text{linear polz intensity} \\ \text{linear polz intensity} \\ \text{circular polz intensity} \end{array}
$$

units : intensity (measured in "optical" astronomy)

normalized $\quad q = \dfrac{Q}{I}$, $u = \dfrac{U}{I}$, $v = \dfrac{V}{I}$
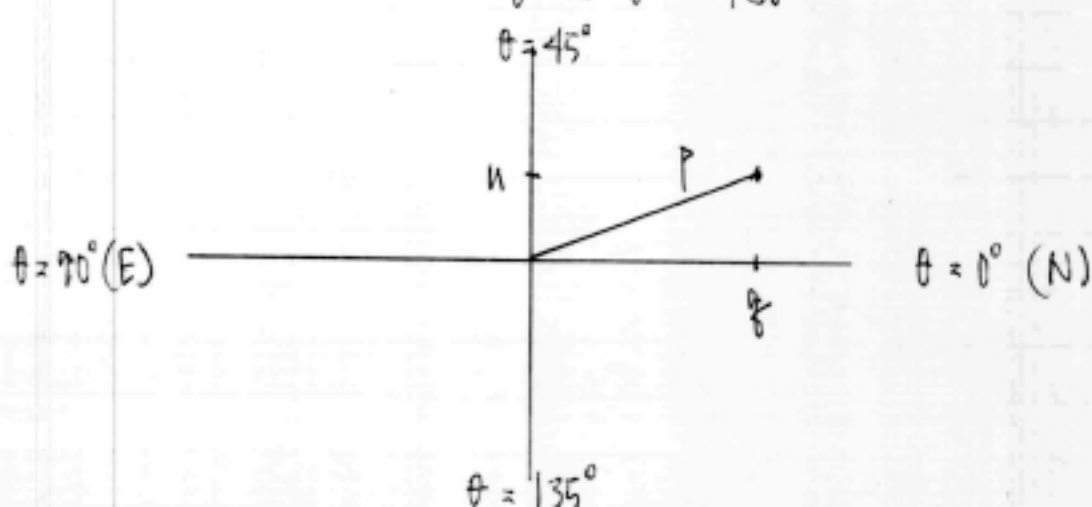
linear polz

  degree $\quad p = \sqrt{q^2 + u^2} \qquad 0 \le p \le 100\%$

position angle $\quad \theta = \frac{1}{2} \arctan\left(\dfrac{u}{q}\right) + $ quadrant fix

$$0° \le \theta < 180°$$
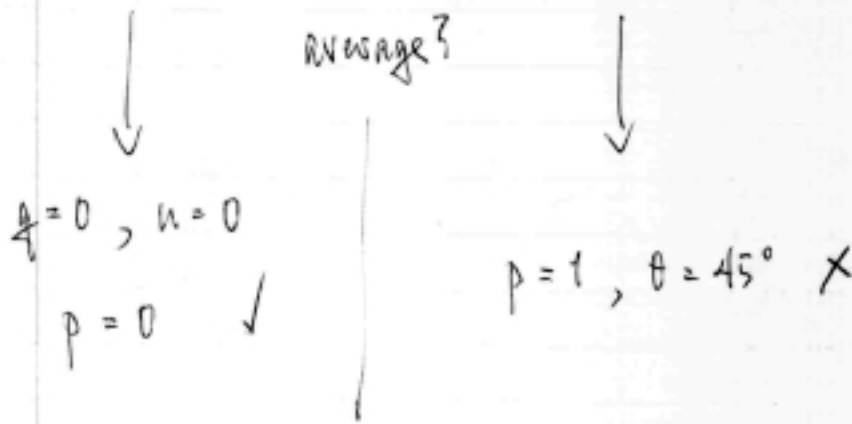
Do statistics (data reduction, averaging, error
analysis, etc.) with q & u.

p & θ are "biased" (not statistically well-behaved)

e.g.

$q = 1$, $u = 0$ $\quad \Rightarrow \quad$ $p = 1$, $\theta = 0°$
$q = -1$, $u = 0$ $\quad \Rightarrow \quad$ $p = 1$, $\theta = 90°$

$\downarrow$ $\qquad$ average? $\qquad$ $\downarrow$

$q = 0$, $u = 0$

$p = 0$ $\quad \checkmark$ $\qquad\qquad$ $p = 1$, $\theta = 45°$ $\quad ✗$

Stokes parameters combine linearly (correcting for
instrumental polz, interstellar polz, etc.),
unlike p & θ.

Mueller matrices, Mueller calculus $\quad \checkmark$

3
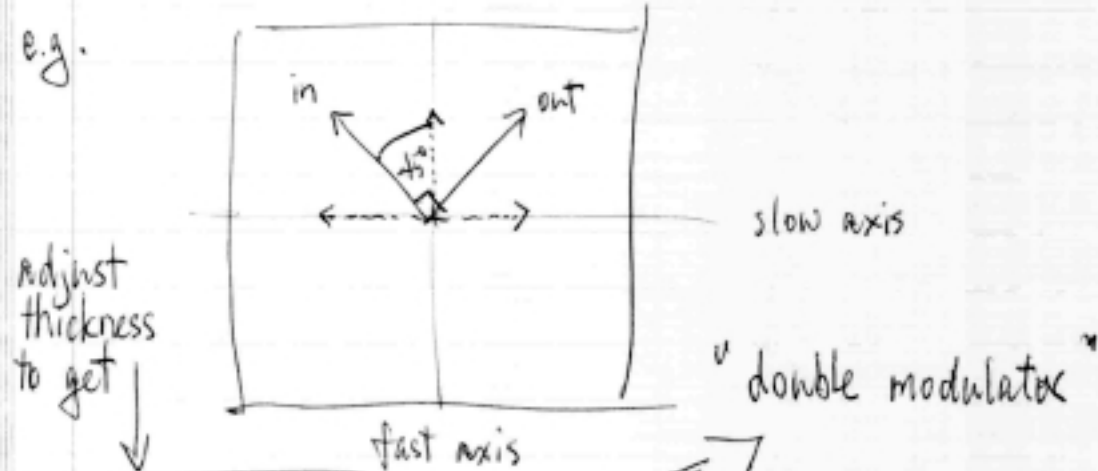
birefringence

velocities of orthogonal polz modes depend on
   direction of propagation relative to optical axis

e.g. calcite crystal

(1) neutral for light propagating along optical axis
    (plate cut ⊥ to optical axis)

(2) plate cut || to optical axis = retarder
    (modes are undeviated in direction but have
    different velocities, so emerge shifted in phase)

e.g.

slow axis

adjust
thickness
to get

fast axis

"double modulator"
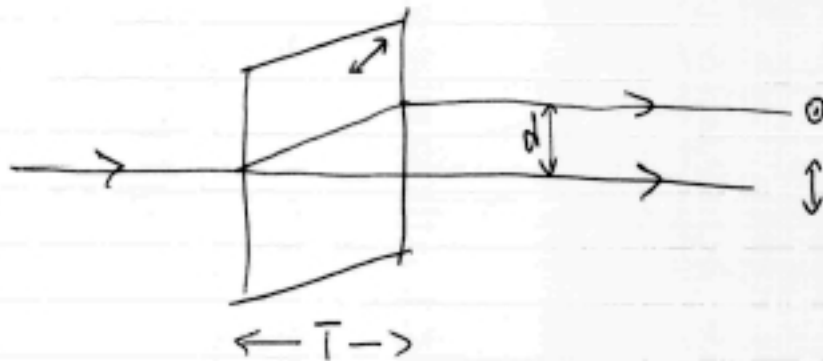
$\frac{1}{2}$ - wave plate : 180° retardation along slow axis
=> 90° rotation of linear polz. 45° from axes

(3) plate cut ~45° to optical axis
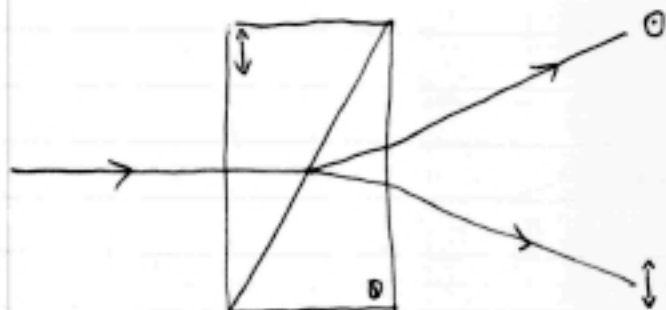
  = beam displacement prism

$$d \sim 0.1\,T \qquad (\sim 100\,\mu/mm)$$

calcite: $350 - 2300$ nm

(4) Wollaston prism
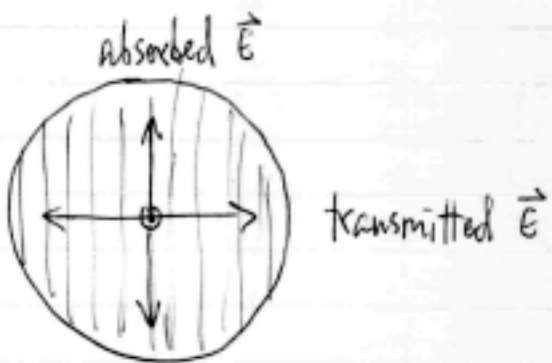
dichroism

  differential extinction of orthogonal polz modes

e.g.

(1) polaroid

absorbed $\vec{E}$

transmitted $\vec{E}$

chemical chains embedded in plastic

(2) wire grid

   wires embedded in substrate

(3) interstellar medium (aligned dust grains)

References

Methods of Experimental Physics : Volume 12 — Astrophysics, Part A : Optical and Infrared, ed. N. Carleton, (New York: Academic Press), 1974 (Ch. 8 — Polarization Techniques, K. Serkowski)

Planets, Stars and Nebulae studied with photopolarimetry, ed. T. Gehrels (Tucson: U of Arizona Press), 1974

Astronomical Polarimetry, Jaap Tinbergen (Cambridge: Cambridge), 1996

Polarization of Light and Astronomical Observation, Jean-Louis Leroy (Amsterdam: Gordon + Breach), 2000

Polarized Light, Production and Use, W.A. Shurcliff (Cambridge: Harvard U. Press), 1962

Statistical Methods of Stellar Polarimetry, Clarke, D. + Stewart, B.G. 1986, Vistas in Astronomy, Vol. 29, pp. 27-51

Astronomical Techniques -- Infrared Astronomy Overview
Mike Skrutskie -- November 18, 2003

The Infrared Wavelength Domain

- In round numbers 1.0um - 1000um (with room for argument)
  - This is largely the range from
    - silicon CCD long-wavelength cutoff (photon response) to the
    - limit of radio heterodyne sensitivity (wave response).
  - Technically 0.7-1.0um is infrared, but is better considered the "far-visible" given that it is detectable by silicon CCD's.
  - At the other extreme, radio heterodyne techniques have infringed upon the far-infrared up to 300um and to shorter wavelengths every day.

Visible/Infrared Similarites

- Astrophysics:
  - Analysis of broadband fluxes yield useful temperature and population estimates
  - Spectra reveal chemical abundances, temperature, velocity, etc.
  - Even synchrotron radiation can be important in the infrared.
- Hardware and techniques
  - Light is collected primarily by reflecting telescopes.
  - Optical components within instruments tend to be similar
    - reflective/refractive "optical" components.
    - diffraction gratings (both transmission and reflection) and prisms for spectral dispersion.
    - bandpass and narrowband filters (typically interference rather than bulk absorption)
    - Large-format (2048x2048) array detectors with high QE are available for near-infrared work.
      - Mid-infrared arrays tend to be smaller (1024x1024), but improvements are being driven by JWST.

Infrared/Optical Differences

- Astrophysics
  - Access to low-excitation energy transitions
    - Molecular vibrational and rotational lines
      - Vibrational energies correspond to wavelenths of a few microns.
        - Rotational energies are an order of magnitude or more smaller -- wavelengths of a few hundred microns.
          - The CO rotational fundamental is at 2600um (2.6mm). H_2 is at 28um. The difference arises because of the moments of inertia of the molecules.
      - Vibrational examples include
        - CO ro-vibrational bandheads at 4.6um (and overtones at 2.3 and 1.6um).
          - Seen in cool stellar atmospheres and circumstellar disks.

- Molecular hydrogen, the most common molecule in the Universe, has a vibration fundamental at 2.1um (recall the rotational fundamental is at 28um).
  - Quadrupole emission is permitted for this symmetric molecule (dipole is forbidden) -- these lines are weak.
  - Since the excitation temperature of the 2.1um vibrational lines is of order 1000K, they are only seen in fluorescence or in shock excited regions where molecular material is present -- e.g. star formation, starburst galaxies, AGN...
- Related to the molecular lines are broad absorption/emission features seen in the ISM due to silicate/carbon/ice grains (some are identified with polycyclic aromatic hydrocarbons (PAH's)).
  - These broad features originate from bends and stretches of atomic bonds in large molecules and solids.
  - They tend to be excited by UV photons and can be a good proxy for obscured star formation.
- Atomic fine structure lines
  - OI [63um] and CII [158um] are primary coolants in the ISM
  - Why so? In part, because a *typical* temperature in any galaxy is about 30K.
- Emission from warm dust
  - T=30K dust emission (i.e. most of the dust in the universe) peaks at 100um
  - Most of the energy emitted into the universe by galaxies is in the mid-and far infrared, particularly by starburst galaxies.
    - Much of the emitted starlight is *reprocessed* by dust.
    - In actively star forming galaxies or AGN-dominated galaxies the emitted infrared energy can far exceed the visible-wavelength flux.
  - Star formation occurs in dusty regions. Stellar flux is reprocessed in the circumstellar environment and in the parent molecular cloud.
  - Tenuous warm dust around normal stars, discovered in the mid-infrared, betrays the presence of mature solar systems.
- Transparency of dust
  - A_v=1 corresponds to A_K=0.1
  - There are 30 magnitudes of visual extinction toward the Galactic center.
  - Star formation occurs in dusty environments.
- Cosmological redshift
  - The peak of "visible" starlight emission in the local universe shifts to the near-infrared at z=2 and greater.
  - Conversely, the 100um peak due to warm dust in galaxies shifts into the submm regime for z=2 and greater.
  - Radio/Far-infrared observations have succeeded in revealing the values of the basic cosmological parameters (z=1000).
- Sensitivity to cool blackbodies
  - Star formation (combined with reduced extinction)
    - Circumstellar disks
  - Evolved stars
  - Brown dwarfs

- Hardware and Techniques

  - Detectors

    - The energy of an infrared photon is small compared with atomic valence/covalent bond energies.

    - Photovoltaic detector materials must be customized to respond to the feeble energy of infrared photons. Some relevant cutoff energies:

      - Silicon -- 1.05um
      - InGaAs -- 1.7um (tunable depending on "chemistry")
      - InSb -- 5.5um
      - HgCdTe >2.5um depending on "chemistry"

- - - Si:As BIB -- 28um
      - Ge:Ga -- 100um or more depending on stress!
  - Infrared arrays consist of a detector layer mechanically bonded to a silicon electronics wafer.
    - The differential expansion between these two layers has been a limiting factor in making large arrays.
    - In visible CCD's the same material, silicon, serves as detector and electronics, simplifying the requirements.
  - bolometers can take advantage of bulk thermal response to detect the longest wavelengths
- Cryogenics
  - Near-infrared detectors, particularly HgCdTe, can operate at LN_2 temperature (77K).
  - Mid/far-infrared detectors require cooling to close to liquid helium temperature (4K).
  - Bolometers work most efficiently at the lowest possible temperatures -- typically 100 mK.
    - These temperatures are obtained with He[3] refrigerators or adiabatic demagnetization coolers.
- Optical materials must be selected for appropriate infrared transmission.
  - typical glass
  - Calcium Fluoride
  - Germanium
  - Silicon
  - Zinc Selenide (refractive index 2.4!)
  - Zinc Sulfide
  - KRS-5 (Thallium Bromide)
  - Just like the combination of crown and flint glass, the appropriate combination of infrared transmissive materials can produce high-quality optics relatively free of chromatic aberation.
- Atmospheric transmission
  - Water vapor contributes substantial opacity across the infrared spectrum.
    - significant time variability and thus difficulty in calibration.
    - significant improvement with altitude
    - much of the infrared becomes accessible from aircraft altitude.
- Thermal background becomes significant beyond a wavelength of 2um at 300K.
  - Temperature changes of 0.001K can overwhelm astronomical signals.
  - Rapid chopping between a target and a comparison/blank field can significantly supress the background variations.
  - Still, Poisson statistics of the vast number of background photons produce significant background noise limiting the depth of ground-based observations.
    - A one-minute integration with an 0.5-m cryogenic space-based telescope can match the performance of a one-hour measurement with a 15-m ground-based telescope.
    - Significant effort is being put into exploiting the South Pole for infrared observations.
- Atmospheric turbulence becomes less significant at longer wavelengths.
  - The seeing disk diameter improves as $(lambda)^{-0.2}$
  - 10-meter class telescopes on good sites become diffraction limited at wavelengths of a few microns.
  - Deformable mirrors can produce high-strehl ratio (nearly diffraction limited images) in near-infrared adaptive optical systems.
    - These systems tend to sense wavefront error in the far red in order to correct the images for the near-infrared.

- Infared instrument and future project examples
  - 2MASS
  - NIRSPEC (Keck near-infrared spectrometer)
  - MIRLIN (mid-infrared camera
  - SOFIA

- SIRTF ([technical details](#))
- JWST

ASTR 511 [R. W. O'Connell]

INTRODUCTION TO ULTRAVIOLET ASTRONOMY

Astro-2 UV observatory in Shuttle payload bay.

A. THE UV BANDS

- **Earth's atmosphere is opaque below ~3200 Å.**

- **Interstellar medium is opaque below 912 Å (Lyman edge of H I)**

    But optical depth ~ (freq)$^{-3}$, so ISM becomes transparent again below 400 Å

- **Easily accessible "vacuum UV" band from space: 912-3200 Å**

    - ***"Far-UV"*: 912-2000 Å**
    - ***"Mid-UV"*: 2000-3200 Å**

- **With different technology: *"Extreme UV"* (70-912 Å)**

- ***"Near-UV":* 3200-4000 Å. Usually considered part of "optical" band, but often**

compromised by poor reflectivity or transmission of optical elements, atmospheric opacity.

B. MOTIVATION FOR UV OBSERVATIONS

Highest density (bits per unit wavelength) of astrophysical information on stars and gas

1. **Continuum sources**

   - **Stellar flux maximum (F_lam units) occurs at ~ 2900 Å/T_4.**

     Energy distributions of hot stars (over 10,000 K) peak in UV.

     Most important: massive main sequence stars over 3 M_{sun}, responsible for most element synthesis, ionization, dissociation, and kinetic energy input to galaxies.

     For cooler stars (< 8000 K), the UV is in the Wien limit, implying high sensitivity to temperature (e.g. to measure main sequence turnoff in integrated light of stellar populations)

   - **Hard nonthermal sources**

   - **"Big blue bump" in AGN = inner accretion disk?**

2. **Atomic & molecular spectral features**

   - **Many strong (often *resonance*) transitions of important species occur in UV:**

     H, D, H_2, He, C, N, O, Mg, Si, S, Fe

   - **Uniquely valuable:**

     - **Lyman series and metallic features in stars, ISM, IGM;**
     - **Atomic deuterium (offset from HI features);**
     - **O VI, C IV, N V (gas at 10^{5-6}K);**
     - **Carbon abundances from C III, C IV;**
     - **Lyman discontinuity (rest wavelength 912 Å) in high redshift galaxies;**
     - **Near-UV: [O II] and [Ne V] plasma diagnostics, Balmer jump stellar T,g diagnostic.**

3. **Low sky background**

   Deep minimum in night sky background 1600-2500 Å, <u>darkest in UV-optical-IR range</u> (40x below best ground-based sky).

4. **Sensitivity to dust**

    ○ **Dust extinction law is max in UV; local peak for Galactic dust at 2175 Å is an important & unique signature.**

    ○ **High & variable UV extinction is an advantage for studying grain types in different environments but a disadvantage for studying things behind grains.**
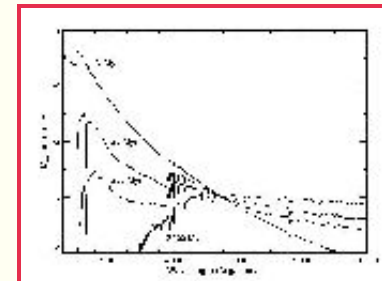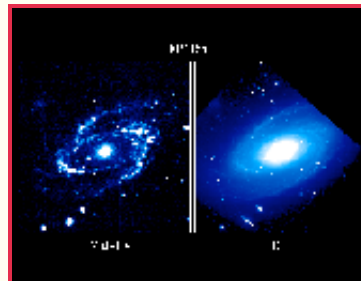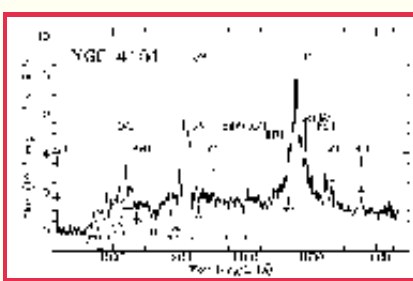
5. **Isolation of hot components in dominant cool sources: e.g. stellar chromospheres, hot stars/AGN in E galaxies**

6. **Restframe UV shifted to readily-observed optical window in high redshift (z > 1) galaxies and AGN. E.g. "Lyman-break galaxies"**

Key research areas:

- **Stellar chromospheres, winds**
- **Mass exchange and accretion in binary systems (esp. WD, NS)**
- **Abundances in stars & chemical evolution of Galaxy**
- **Advanced stellar evolution (HB and beyond)**
- **Interstellar dust grains**
- **Hot ISM, galactic halos, fountains, winds**
- **Ages and abundances of stellar populations**
- **Massive star formation and histories of galaxies**
- **AGN (accretion disks, near-nuclear plasmas, reverb mapping)**
- **Deuterium abundances & Big Bang nucleosynthesis**
- **Proto/adolescent galaxies**
- **Cosmic star formation history, background light**
- **Evolution of the intergalactic medium**

   Examples: click on thumbnails for larger view

C. MISSIONS

- **Sounding rockets, balloons (e.g. SCAP/FOCA), manned missions (Apollo, Skylab). 1960's-early 90's.**

- **PI-class satellite missions: e.g. OAO-2, Copernicus.**

- **Space Shuttle sortie missions: e.g. Astro, ORFEUS, FAUST**

- **Satellite observatories:**

  - **International Ultraviolet Explorer (IUE)**

    - **1978-1996 (a record)**
    - **Medium/high-dispersion spectroscopy 1200-3200 Å**
    - **Background information: GSFC/NSSDC; ESA, including science highlights.**
    - **Large data archive**

  - **Hubble Space Telescope (HST). Launched 1990.**

    - **1200-4000 Å (plus optical and near-IR)**
    - **High resolution (0.05 arcsec) imaging (FOC, WFPC2, STIS, ACS/SBC, ACS/HRC)**
    - **Low-med-high resolution spectroscopy (GHRS, FOS, STIS)**
    - **High speed photometry (HSP)**
    - **Data archive**

  - **Extreme Ultraviolet Explorer (EUVE): spectroscopy 70-760 Å. Launched 1992.**

  - **Far Ultraviolet Spectroscopic Explorer (FUSE): High resolution spectroscopy 900-1200 Å. Launched 1999.**

  - **The X-ray/Gamma-ray satellites XMM and Swift both carry moderate-field support telescopes which can be used for multiband UV/optical imaging.**

  - **GALEX (the Galaxy Evolution Explorer Mission), launched in April 2003, is a 50-cm, wide-field (1.2^o) telescope imaging two broad UV bands centered at 1500 and 2300 Å. Microchannel plate detectors. Grism for low-resolution spectroscopy.**

Historical Gaps:

Historical emphasis in the UV has been mainly on point-source spectroscopy, not imaging or extended faint sources (e.g. galaxies)

To 2003, only shallow all-sky surveys were available. FUV: TD-1, to 9th mag. EUV: ROSAT, EUVE, < 1000 bright sources. GALEX all-sky survey (now underway to AB ~ 21 mag) will remedy this situation.

D. UV INSTRUMENTATION

- **Optical materials: limited choices for good transmissions or reflectivities; challenge greater for shorter wavelengths.**

- **Cleanliness, contamination control are critical because many materials likely to be deposited on optics are UV-opaque**

- **FUV, MUV designs similar to optical-band, but fewer surfaces preferred**

- **Filters: require good blocking of strong geocoronal, skyglow emission lines (esp. Lyman-alpha 1216 Å, O I 1302 Å). Also require excellent long-wave blocking (see next).**

E. UV DETECTORS

- **A major problem is the requirement for *long-wavelength rejection.* Visible photon rate is ~ 10^6 higher than FUV rate in cool sources, like solar-type stars.**

- **Therefore require *"solar blind"* detection system.**

  - **Photoconductors like CCD's have broad bandwidths, *not* good for UV unless excellent "red leak" rejecting filters available. Filter rejection usually inadequate. Silicon also has large UV opacity. Some use of downconversion coatings (UV ==> visible photons), but relatively poor performance (e.g. WFPC1/2 on HST).**

  - **Photoemissive devices with large work functions preferred: photocathodes like CsI, CsTe, KrB have good UV QE, very low visible QE**

    Main technical problem: must convert single emitted photoelectron into measurable signal, maintaining image quality in 2-D case.

    Photocathode UV QE's mostly well <u>below</u> visible QE's for CCD's (20-40% instead of up to 90%).

- **2-D UV detectors: typically *hybrid* designs**

  - **Stage 1: photocathode**

    - **Manufacture of large formats with uniformity, good MTF difficult**

  - **Stage 2: amplification/acceleration and image transfer**

    - **Image Tubes: high voltage (10-30 kV) photoelectron acceleration, electric or magnetic focussing**
    - **Microchannel Plates: electron multiplication in rigid channels, proximity focussing**

  - **Stage 3: detection/readout/storage**

    - **Phosphor plus film (e.g. Astro/UIT)**
    - **Phosphor plus CCD or diode arrays (e.g. Astro/HUT)**

- TV (scanning) readout (e.g. IUE, HST/FOC)
- Electron bombarded diodes (e.g. HST/FOS, HST/GHRS)
- Electron bombarded anode arrays (e.g. HST/STIS, FUSE, GALEX)

- Key feature of most successful systems: (photoelectron-induced) *event counting,* with *centroiding* of x,y position.
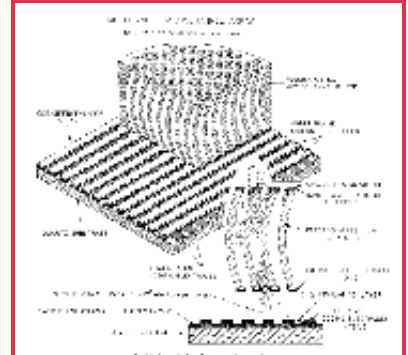
- **Current examples**

  - **STIS/ACS MAMA**: Multi Anode Microchannel Array (at right)
  - **FUSE detector**: microchannel plate plus double delay line readout

- **References:**

  Timothy, **PASP 95, 810, 1983**;
  Joseph, **UV Technology Overview**, in "From X-rays to X-Band", an STScI Workshop, 2000.

F. SPACE ASTRONOMY: SPECIAL TECHNICAL REQUIREMENTS

- **Launcher with finite payload**

  - **Space Shuttle (at right) probably most complex system ever built by humans. Total cost per launch about $400M (90% personnel).**

  - **(But Shuttle payload is 5x smaller (!) than the 1960's Saturn V).**

- **Power**

  - **Solar panels, batteries, radioactive sources, fuel cells**
  - **Explorer class experiment ~300 W; HST ~2KW**

- **Thermal control**

  - **Large temp gradients: e.g. Earth darkside: 273K from Earth, 3K on other side.**
  - **Control required for structural and electrical stability**
  - **Optics/electronics: typically maintain ~68 degrees by active heating, passive cooling to space**
  - **Detectors: usually require active cooling (thermoelectric, cryogens)**
  - **Issues: orbital dependence, materials (GEP), insulation, heat pipes, radiators**

- **Pointing control & stability**

- o **Gyros: provide 3D mechanical attitude reference**
- o **Auxiliary telescopes: star trackers, guiders: 1 arcsec-few arcmin**
- o **Focal plane trackers: e.g. HST: 0.007 arcsec RMS**

- **Scattered light rejection**

  - o **Important to enable use of sunlit orbit**
  - o **Sun, moon, bright Earth, bright stars, spacecraft structures, zodiacal light must all be considered**
  - o **Complicated baffling, special coatings & materials needed**

- **Environmental protection**

  - o **Radiation: high energy electrons, protons**

    - ▪ **"South Atlantic Anomaly" (R < 1000 mi)**
    - ▪ **Van Allen Radiation Belts (R < 25000 mi)**
    - ▪ **Shielding difficult; use rad-resistant equipment, special operations strategies instead**

  - o **Residual atmosphere (free oxygen), especially in ram direction**
  - o **Orbital debris**

- **Communications & telemetry**

  - o **Command & control**
  - o **Housekeeping/health**
  - o **Data**
  - o **Relay satellites: TDRSS 200 MBPS, but limited access**

- **Launch protection/survival: "space qualification"**

  - o **Temperature**
  - o **Acoustic vibration**
  - o **Acceleration**
  - o **Cleanliness: contamination control before launch, outgassing suppression in space**

- **Reliability**

  - o **Repair, upgrade impossible for all except HST (where it is costly)**
  - o **Must predict and mitigate all possible failure modes**
  - o **Is principal cost driver:**

    - ▪ **95% reliable: $N**
    - ▪ **98% reliable: $5N**

  - o **Complete documentation essential: "PAPER IS OUR MOST IMPORTANT PRODUCT"**

- **====> Costs!**

    - **Above list is reason that space experiments cost up to several 100x more than equivalent size ground-based facilities. Must weigh unique science return vs. cost.**

    - **"Cheaper, Faster, Better"? Pick two out of three.**

General references:

- *Exploring the Universe with the IUE Satellite*, ed. Y. Kondo et al., (Dordrecht: Reidel), 1987.
- *Astrophysics in the Extreme Ultraviolet*, ed. S. Bowyer & R. F. Malina, (Dordrecht: Kluwer), 1995.
- *The Ultraviolet Universe at Low and High Redshift*, ed. W. Waller et al., (Woodbury, NY: AIP), 1997.
- *Ultraviolet-Optical Space Astronomy Beyond HST*, eds. J. A. Morse et al., (San Francisco, ASP), 1999.
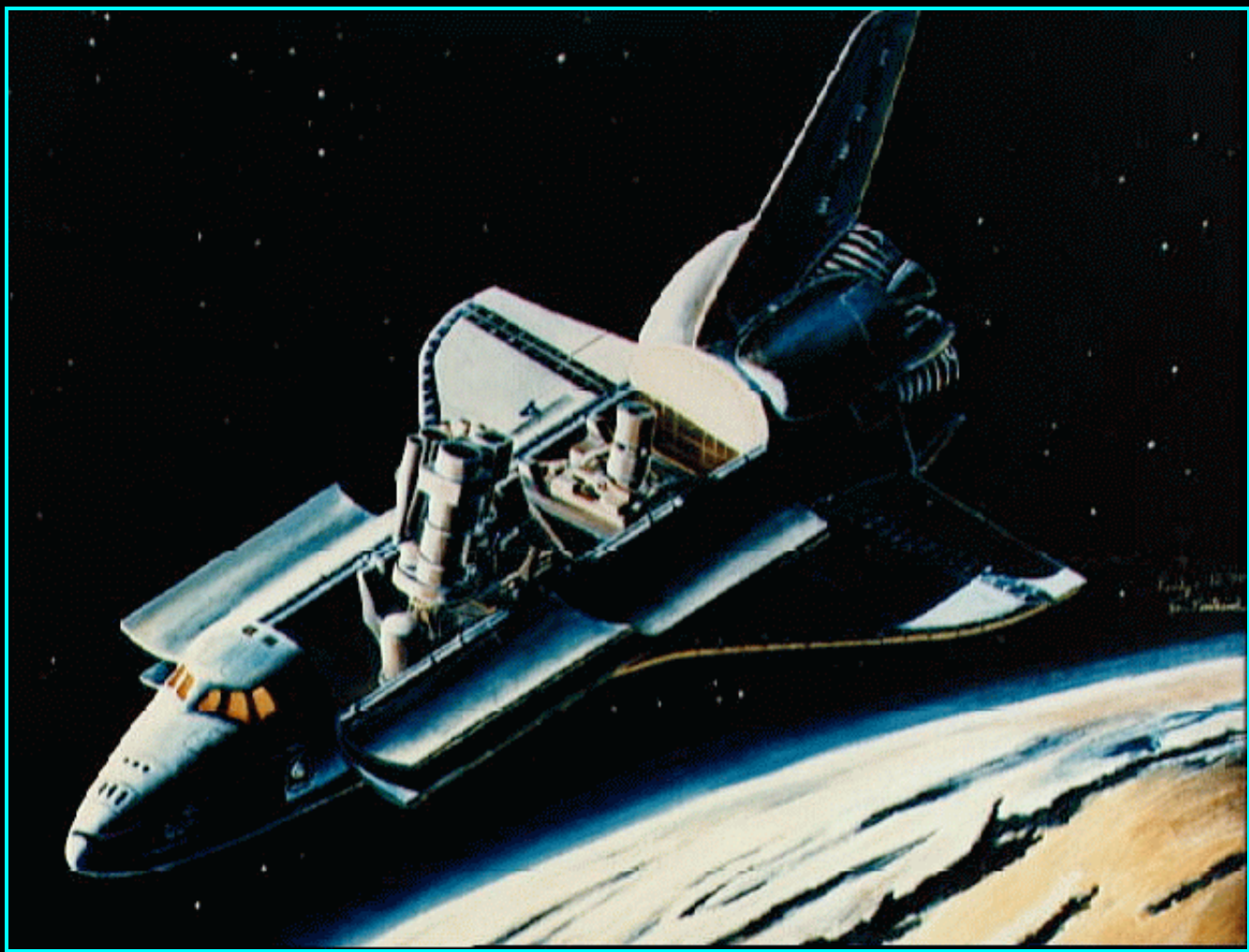
Web links:

- **Ultraviolet Imaging Telescope/Astro-1 & Astro-2 Background & Pix**

- **List of all Orbital Astronomy Missions**
- **NASA Missions** (all types)
- **Hubble Space Telescope**
- **HST Multimission Data Archive** (includes data for many UV missions)
- **International Ultraviolet Explorer (IUE)**
- **Extreme Ultraviolet Explorer (EUVE)**
- **Far Ultraviolet Spectroscopic Explorer (FUSE)**
- **GALEX**

- **ASTR 511 Home Page**

Last modified January 2006 by rwo

THE ASTRO MISSIONS ULTRAVIOLET IMAGING TELESCOPE

Astro-1 Mission on orbit (artist's concept)

BACKGROUND

The Ultraviolet Imaging Telescope, one of the three ultraviolet telescopes of the *Astro* Observatory, flew on Space Shuttle missions in December 1990 and March 1995. It was designed, built, and operated by a team led by Theodore P. Stecher at Goddard Space Flight Center.
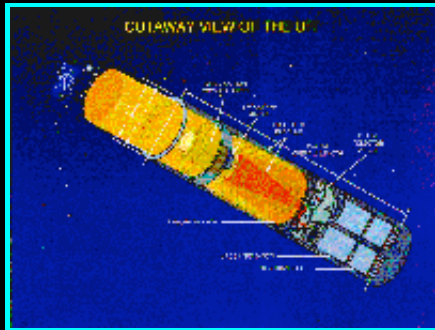
UIT was proposed in 1978 as part of a program to fly small ("university-class") scientific experiments on the Spacelab modules attached to the Space Shuttle. At that time, NASA anticipated that there would be about 3 Shuttle/Spacelab missions each year dedicated to astrophysics experiments (out of an envisioned 20 or so missions annually). By late 1985, the Astro UV telescopes had been approved for six missions. At the time of the Challenger accident in January 1986, *Astro-1* was in the Shuttle Columbia payload bay ready for the launch to follow the Challenger mission. In the aftermath of the accident and in the face of the rapidly escalating costs of the Shuttle itself, the Spacelab astrophysics program was drastically reduced. Of the 200 experiments proposed in 1978, only the four telescopes of the *Astro-1* mission were actually flown.

UIT was a 38-cm Cassegrain telescope carrying two ultraviolet cameras with 40 arc-minute diameter fields of view (150 times larger than the field of the Hubble Space Telescope). The cameras operated in the "far-UV" (120-200 nm) and "mid-UV" (200-320 nm) spectral ranges, respectively, and carried a total of 12 filters. They employed image intensifiers with very strong long-wavelength rejection to provide pure UV images. Fine guidance was accomplished with an articulated secondary mirror controlled by a signal from an externally mounted 15-cm star tracker containing a CCD detector. Final resolution for point sources was typically 2.7 arc-seconds FWHM. During the two *Astro* missions, UIT returned a total of 1570 data frames of 250 different astronomical targets.

The *Astro* UV payload consisted of UIT, the Hopkins Ultraviolet Telescope (HUT), and the Wisconsin Ultraviolet Photo-Polarimeter Experiment (WUPPE). HUT was a far-ultraviolet spectrometer (Johns Hopkins University, led by A. F. Davidsen). WUPPE was a UV spectro-polarimeter (University of Wisconsin, led by A. D. Code). These three instruments were co-aligned and mounted on the Spacelab Instrument Pointing System. They were operated simultaneously on a given target by crew members from the Shuttle aft flight deck.

For *Astro-1* (1990, Shuttle Columbia) the Broad-Band X-Ray Telescope (BBXRT, P. Serlemitsos, Goddard Space Flight Center) was operated independently on a separate pointing system. *Astro-1* compiled a NASA record for delays: 33 different assigned launch dates over 8 years, 12 complete target timelines planned (each 8 days long at 1 second resolution), and 4 scrubs within 6 hours of launch. On *Astro-2* (1995, Shuttle Endeavour), the UV telescopes flew alone. *Astro-2* was the first NASA mission to have an active Internet home page and logged over 2.5 million hits from over 200,000 people during its 15 day duration.

MISSION IMAGES

[Click for Full Size]

UIT Design

Vacuum-Tank Testing
(HUT)

UV Instruments
On Pallet

Co-Mounted UV
Telescopes

Astro-1 Payload
On Pallets
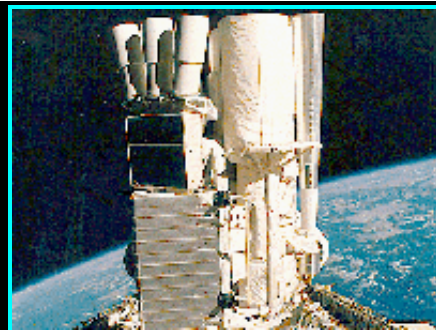
Astro-1 Patch

Rollback Of Astro
Rollout Of HST

Astro-1 & HST On
Launch Pads

On The Launch Pad

Astro-1 Launch

UIT On Orbit
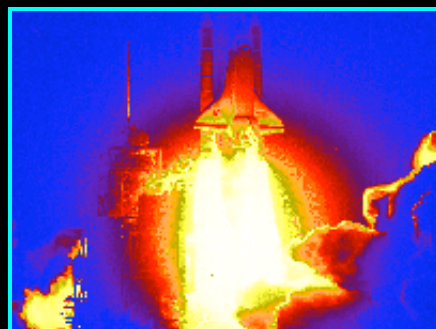
Astro-1 Crew
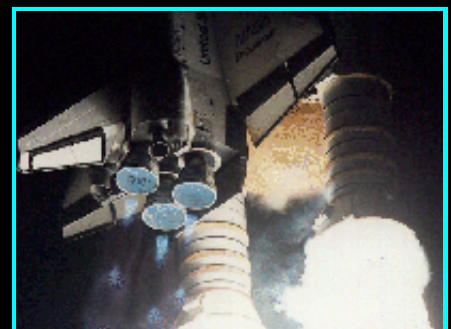
Lunch

Moon Rising Over
Earth's Limb

Orion Rising
(Daylight)

Astro-2 Patch

Astro-2 Launch

Main Engines At Launch

Astro-2 Crew

Astro-2 Payload
On Orbit

Payload Into Shadow

Stars over the Limb

Aft Flight Deck (Instrument Control)
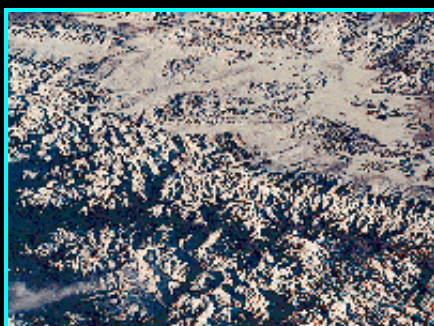
Running the Instruments

Orbiting Target Book

Payload Operations Control Center (Huntsville, AL)

Over the Andes

Disappointment Reach (Australia)

Nepal

Oahu

Low Pressure System

Sunset

The Dreaded Exercycle
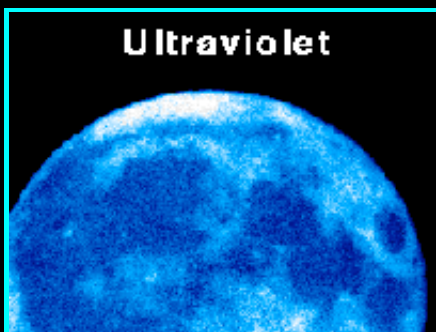
Landing Practice

Landing (Edwards
Air Force Base)
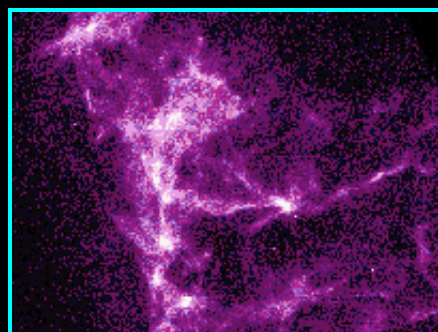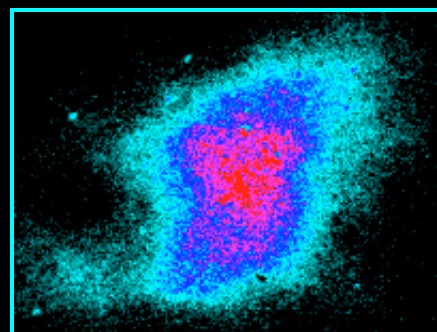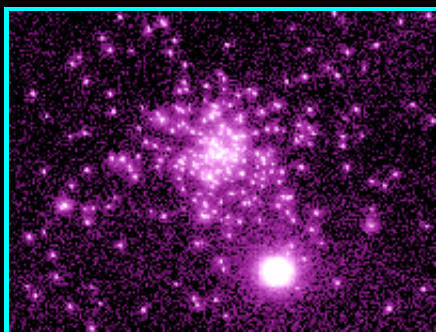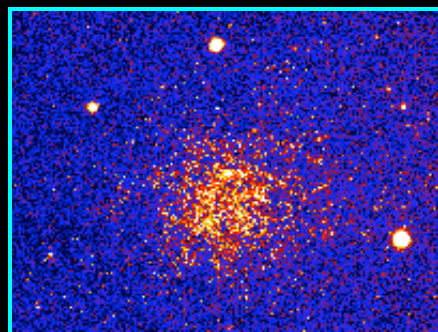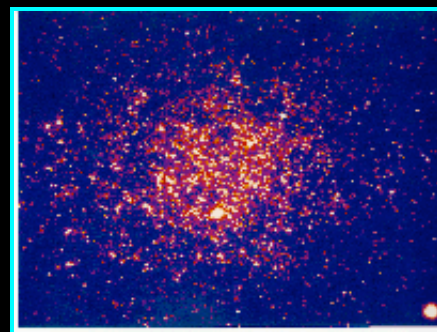
SCIENCE IMAGES
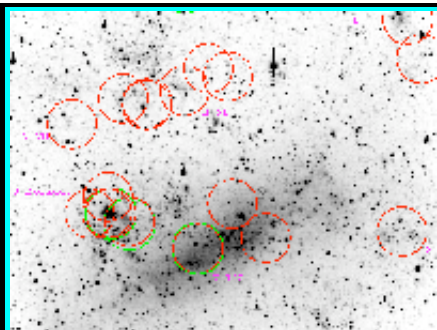
[Far-Ultraviolet Unless Noted;
Click for Full Size]
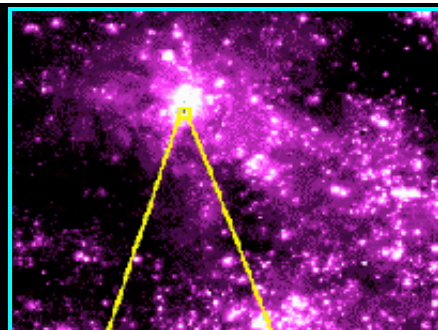
Moon (Far-UV, Optical)
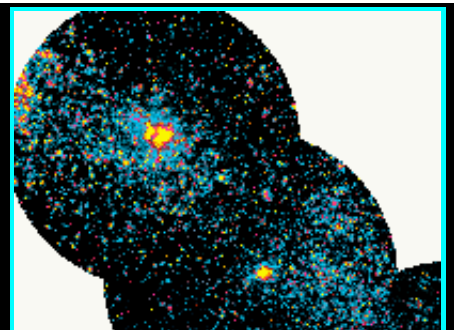
Cygnus Loop
(Supernova Remnant)

Crab Nebula 4 Bands
(Supernova Remnant)

NGC 6752
(Globular Cluster)

Omega Centauri
(Globular Cluster)

Omega Centauri
(Center)

UIT Fields in the
Large Magellanic Cloud
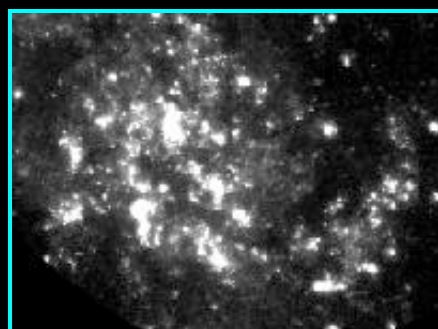
3 Views of
30 Doradus (LMC)
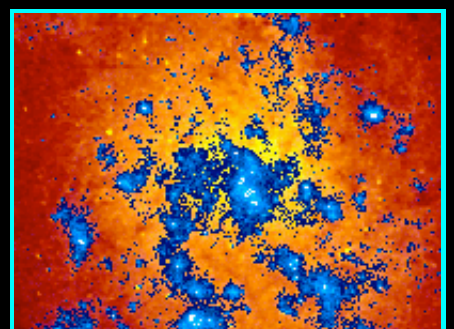
Small Magellanic Cloud
Mosaic
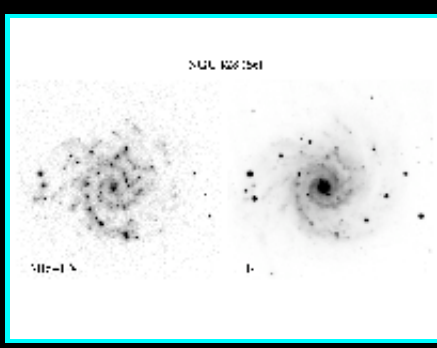
M31 (Andromeda Spiral)
Center and SW Disk
(Mid-UV Mosaic)
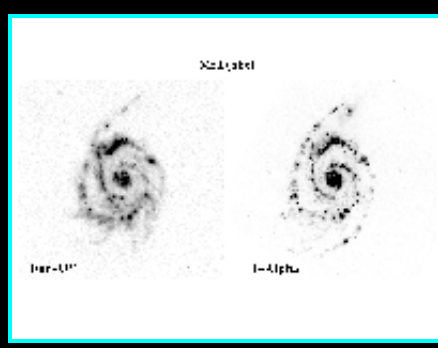
M33 (Spiral; UV/Optical
Comparison, 4 Bands)
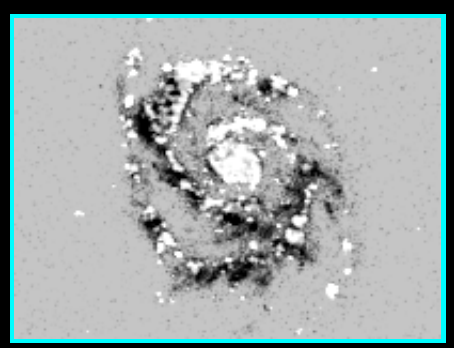
M33
UV/Optical Superposition
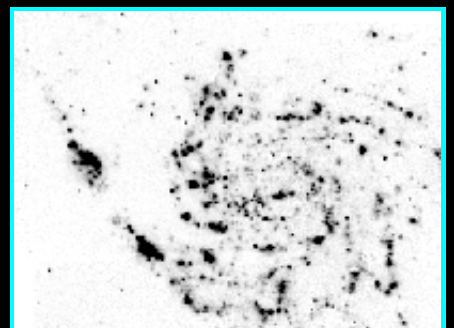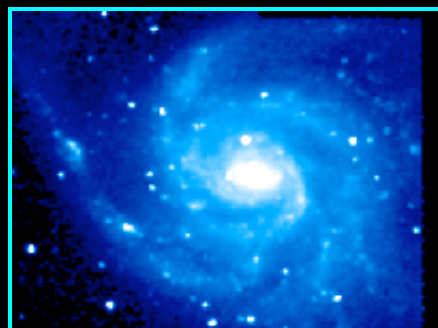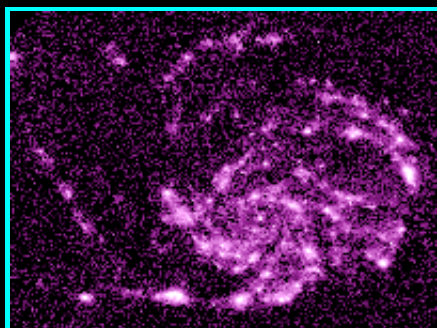
M74 (Spiral;
Mid-UV, Optical)
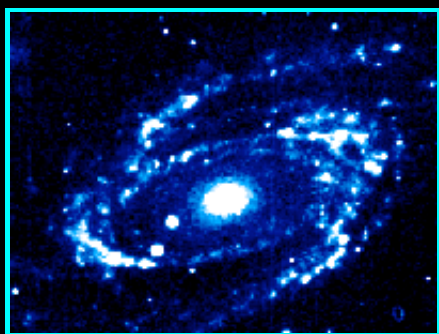
M51 (Spiral;
Far-UV, H-alpha)
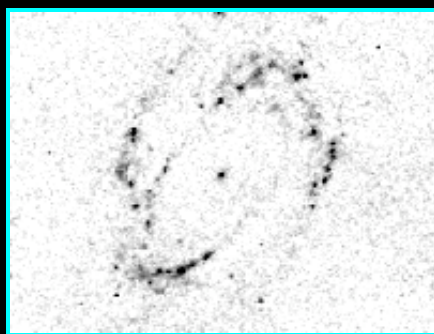
M51 (Far-UV, H-alpha
Color Map)
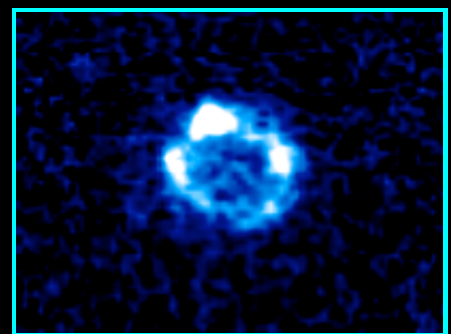
M101 (Spiral Galaxy)
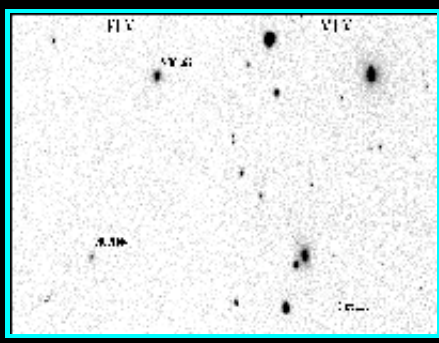
M101 (Far-UV, Optical)
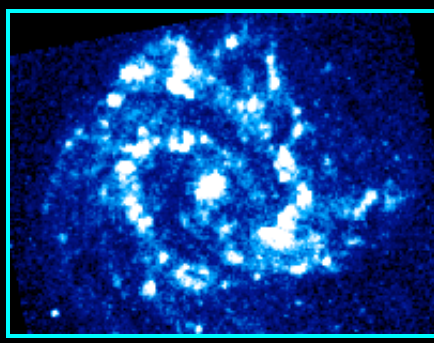
M101 (Far-UV, H-alpha)
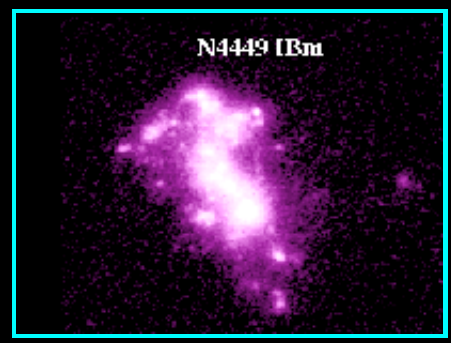
M81 (Spiral; Mid-UV, Optical)
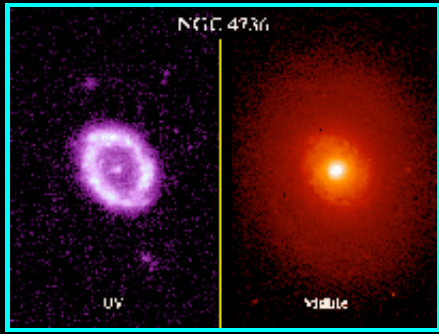
M81 (Far-UV, Mid-UV, Optical)
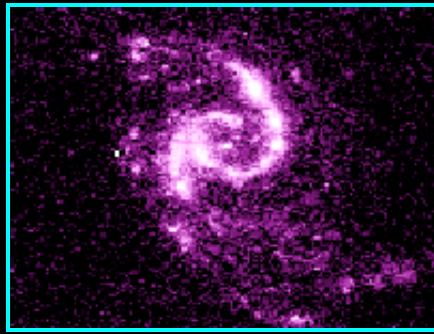
NGC 1317 (Sa Galaxy With Nuclear Ring)
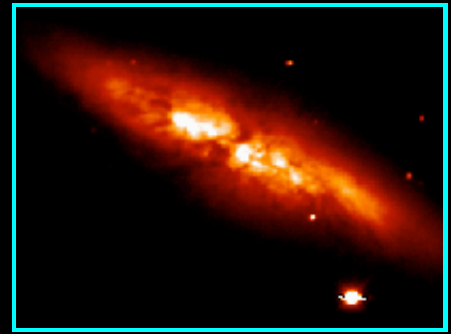
NGC 1399/1404 (E Galaxies)
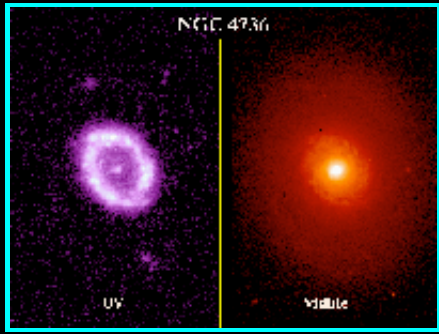
M83 (Barred Spiral; Mid-UV With UIT Rocket Prototype)
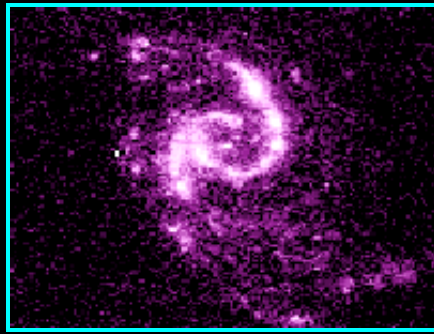
Irregular & Dwarf Galaxies
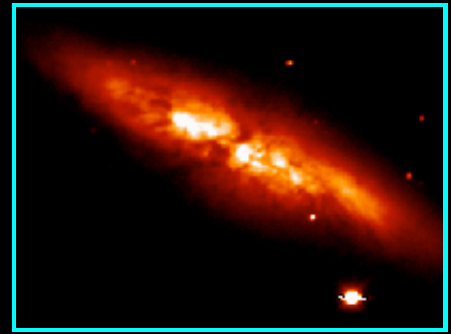
NGC 4736 (Spiral With Interior Ring)
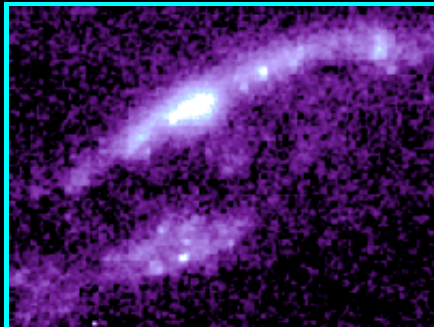
3 Spiral Galaxies

M82 (Starburst Galaxy With Galactic Wind)

Cen A: Post-Merger
Starburst Ring

LINKS
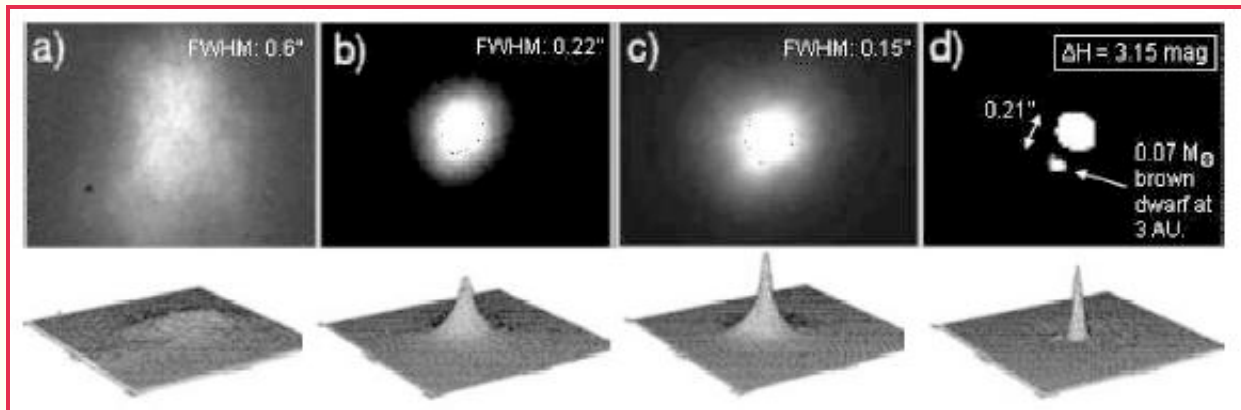
- **Astro Missions: Description & Data Archive** (STScI Multi-Mission Archive)

- **Additional Astro-2 Mission (STS-67) Information & Images** (NASA, KSC)

- **Astro-2 Mission Activities Page** (NASA, MSFC)

- **Selected Videos from Astro-2** (QuickTime)

- **Lecture on Ultraviolet Astronomy** (UVA ASTR 511, advanced undergraduate/graduate)

- **Technical Description of UIT** (Astrophysical Journal)

- **Technical Description of UIT and UIT Data Reduction** (Publications of the Astronomical Society of the Pacific)

- **HUT home page** (JHU)

- **WUPPE home page** (U. Wisconsin)

- **GALEX Mission** (long-duration, wide field, UV imaging satellite mission, launched 2003)

*Last modified **August 2007** by R. W. O'Connell*

ASTR 511 (O'Connell) Lecture Notes

ATMOSPHERIC IMAGE DEGRADATION AND COMPENSATION

- **Seeing Effects (Betelgeuse)**

- **AO System Schematic**

- **Keck AO Optical Bench**

- **Keck AO Technical Notes**

- **Keck First AO Image**

- **Keck Image of Jupiter/Io**

- **AO Laser (Lick)**

Reading:

- **LLM Section 4.4**

- **Ground-Based AO Compared to Space-Based IR Imaging**
  (8.8 Mb PDF file)

← Last Lecture   ⬆ Lecture Index

Last modified December 2003 by rwo